Neural mechanisms of decision making in the pond snail *Lymnaea stagnalis*

Michael Crossley

Submitted for the degree of Doctor of Philosophy

University of Sussex

September 2013

Declaration

The work in this thesis is entirely my own, except where references to the work of others are acknowledged. This thesis has not and will not be submitted in whole or in part to this or any other university as part of a degree.

Signature:

Michael Crossley

Acknowledgements

I would like to thank my supervisors, George Kemenes, Kevin Staras and Thomas Nowotny for their support and encouragement throughout my degree. I would like to express my appreciation to Vincenzo Marra for helping me with the confocal imaging in Chapters 3 and 6. I am also grateful to Freya Crawford, Lenzie Ford, Terri Roberts and Ian Sloss for their valuable viewpoints and discussions throughout the whole process. Finally I want to express my gratitude to my parents, sister and brother and of course Matt Linkin for their encouragement and for generally putting up with me.

University of Sussex

Michael Crossley

Neural mechanisms of decision making in the pond snail *Lymnaea stagnalis*

Abstract

The aim of this thesis was to identify key neural mechanisms underlying decision making in a model invertebrate system, the pond snail *Lymnaea stagnalis*. Specifically, this was examined with respect to two decision making processes associated with *Lymnaea's* feeding behaviour; first a stimulus present/stimulus absent perceptual decision making task for selecting between appetitive and consummatory behaviours, second a behavioural choice between ingestion and egestion.

A behavioural paradigm was designed in order to study stimulus present and stimulus absent decision making in *Lymnaea*. The switch between appetitive and consummatory behaviours was used as a read out of the decision. During stimulus absent decisions, the animal made a judgement about the absence of a sensory stimulus and entered into a period of quiescence. During stimulus present decisions the animal switched from the appetitive behaviour into the consummatory behaviour. The decision about the presence of a stimulus was reliant on the tactile cues from the potential food. Importantly the task was amenable for in vitro preparations and the identification of the decision neurons. A candidate stimulus present decision neuron, the ventral trigger neuron (vTN), was identified in the buccal ganglia. vTN received appropriate sensory input and was able to initiate fictive feeding cycles. vTN was able to initiate fictive feeding cycles via monosynaptic connections with feeding central pattern generator (CPG) interneurons. Development of an in vitro paradigm of the stimulus present and stimulus absent decision provided strong evidence that vTN was a stimulus present decision neuron. A stimulus absent decision neuron was identified as the inhibitory interneuron and member of the feeding CPG, N3t. An in vitro paradigm was used to test interactions of the stimulus present decision neuron with the stimulus absent

decision neuron. Goal directed behaviours were also shown to lower the threshold of activity needed for vTN to initiate fictive consummatory behaviours, lowering the sensory threshold needed for stimulus present decisions to be made.

The neural mechanism of behavioural choice between ingestion and egestion in *Lymnaea* was characterised using in vivo and in vitro preparations. A novel motor neuron was identified whose phase of firing activity was selectively shifted between the two behaviours. The interneuronal control of ingestion was identified and consisted of previously identified command-like neurons, whereas the interneuronal control of egestion consisted of novel interneurons located in the buccal ganglia. The two networks showed evidence of both dedicated and multifunctional interneurons.

The studies presented in this thesis demonstrate that even within the same relatively simple neural network several distinct mechanisms are utilised for different types of decision. These were identified at the level of individual neurons and their synaptic connectivity. Uniquely in these studies, distinct stimulus absent and stimulus present decision neurons were identified in the perceptual decision task and it was also shown that performing the decision making task facilitates the stimulus present decision. This provides fundamental new insights into the neural mechanisms of decision making. The studies also provide a model system for comparison between a form of decision making studied extensively in mammals (perceptual decision making in a stimulus absent/stimulus present task) and a form studied primarily in invertebrates (behavioural choice between two incompatible behaviours), bridging the gap between invertebrate and vertebrate decision making studies.

Table of contents

Abbreviations

5-CF	5(6)-carboxyfluorescein
AA	amyl acetate
AJM	anterior jugalis muscle
ANOVA	analysis of variance
BCI	buccal-cerebral interneuron
c-	contralateral
CBC	cerebral buccal connective
CBI	cerebral-buccal interneuron
CGC	cerebral giant cell
CNS	central nervous system
CPG	central pattern generator
CV	cerebral ventral
DBN	dorsal buccal nerve
e	excitatory
EGTA	ethane glycol-bis (*β*-aminoethylether)-N, N, N',N'-tetracetic acid
EPSP	excitatory post synaptic potential
HEPES	N-2-hydroxyethylpiperazine-N'-2-ethanesulphonic acid
HiDi	Hi Mg^{2+} Hi Ca^{2+}HEPES buffered saline
HiLo	Hi Mg^{2+} Low Ca^{2+} HEPES buffered saline
i	inhibitory
i-	ipsilateral
IPSPS	inhibitory post synaptic potential
LBN	lateral buccal nerve

LJ	lettuce juice
LJNA	lettuce juice no appetitive
MLN	medial lip nerve
ms	milliseconds
mV	millivolts
N1L	N1 lateral
N1M	N1 medial
N2d	N2 dorsal
N2v	N2 ventral
N3p	N3 phasic
N3t	N3 tonic
nA	nanoamps
NS	not significant
NSS	no sensory stimulus
OC	octopamine cell
P	protraction
PBN	post buccal nerve
PIR	post inhibitory rebound
PJM	posterior jugalis muscle
Q	quiescence
R	rasp
RM	radula mechanosensory neuron
RMP	resting membrane potential
s	seconds

S	swallow
SEM	standard error of the mean
SL	solid lettuce
SLN	superior lip nerve
SLRT	supralateral radula tensor muscle
SO	slow oscillator
TN	tentacle nerve
TS	tactile stimulus
VBN	ventral buccal nerve
vTN	ventral trigger neuron

Publications

The following published abstracts contain a selection of results from Chapters 3, 4, 5 and 7:

Crossley M, Staras K, Kemenes G (2011) A mechanosensory activated trigger neuron in the feeding system of *Lymnaea*. Soc. Neurosci. Abstracts Washington D.C. Programme number 918.09

Crossley M, Staras K, Kemenes G (2012) The switch from appetitive to consummatory behavior by a trigger interneuron in the feeding system of *Lymnaea*. Soc. Neurosci. Abstracts New Orleans. Programme number 86.01

Crossley M, Staras K, Kemenes G (2013) Cellular mechanisms of behavioral switching in the feeding system of *Lymnaea*. Soc. Neurosci. Abstracts San Diego. Programme number 169.08

1 General introduction

1.1 Decision making

Animals are presented with a barrage of sensory information in their day to day lives which they use to make decisions. Decisions can include whether to respond to a stimulus or to ignore it. If choosing to respond to a stimulus, the animal must then choose an optimal behaviour from a large repertoire of possible alternatives. In general there are two forms of decision making: perceptual decision making and value based decision making. Perceptual decisions are choices between behaviours based on sensory information (Merten and Nieder, 2012). Perceptual decisions are relatively simple forms of decision making such as judgements about the presence or absence of a sensory stimulus or the choice between two incompatible behaviours based on simultaneous exposure to two stimuli. Value-based decisions are more complex decisions which rely not only on sensory information but also on other variables. These variables include the animal's prior experience of the sensory stimulus, expectations about the stimulus or the animal's behavioural state when encountering the stimulus (Gold and Shadlen, 2007).

1.1.1 Neural mechanisms of decision making

A recent goal in neuroscience has been to identify the neural mechanisms involved in decision making. Two major experimental strategies have been used to study decision making. The first uses highly trained monkeys performing complex tasks. Single unit recordings can be achieved from regions of the brain whilst the monkey performs a decision making task. These tasks often involve the monkey making a perceptual decision about the presence or absence of a stimulus, or choosing which of two stimuli are of greater amplitude. The advantage of this approach is that the decisions studied and mechanisms used are probably more similar to the mechanisms used in humans. The disadvantage is that the complexity of the nervous system being studied inevitably prevents a complete characterization. Specifically, the neural networks for the behaviours being studied are never fully characterised and the studies typically rely heavily on correlating activity in single neurons with the behavioural report of the decision, rather than manipulating neurons to test their role in decision making.

The second approach exploits invertebrate preparations, which, while not performing such complex behaviours as vertebrates, carry out simple, readily observable decisions, which are highly suitable for the detailed investigation of underlying mechanisms. Studies on decision making in invertebrates have focused on behavioural choices between competing behaviours. Intracellular electrodes or voltage sensitive dyes are often used to record from neurons and classify their roles in decision making. The advantage of this approach is that the behaviours are simple and the neural networks underlying them often well characterised. Typically, circuits are comprised of large, highly accessible and identified neurons, which can be specifically targeted from one animal to the next. This allows for the identification of candidate decision neurons, and for directly testing their role in decision making by ablating these relevant target neurons or transiently removing them from the network (i.e. via hyperpolarising them). They can also be characterised in the context of both their connectivity and anatomical organization with respect to other neurons. Of course, such a simple system approach has disadvantages; a key concern is that mechanisms of decision making in invertebrates may not be broadly applicable to mechanisms operating in vertebrates (Kristan, 2008).

The neural mechanisms of decision making have been studied in four major types of studies: sensory discrimination, choice variability, choice competition and cost/benefit decisions. Sensory discrimination tasks have been successfully utilised in monkeys (Gold and Shadlen, 2007). In sensory discrimination studies, animals are presented with a near threshold level stimulus and must make a decision based on the animal's perception of whether the stimulus is present or absent. A separate method involves applying two stimuli of different amplitude and making the animal decide which stimulus is greater. In choice variability studies, a stimulus is used that can elicit two competing behaviours on different trials. The advantage of this method is that it allows for the focus on decision making neurons downstream from sensory discrimination neurons (Briggman et al., 2005). Choice competition involves the application of two stimuli to the animal which when presented alone elicit two incompatible behaviours (Gaudry and Kristan, 2009). Since only one of the behaviours can be elicited at a time, a choice must be made about which behaviour to express. Most behaviours are ranked in a behavioural hierarchy, as some behaviours are dominant over others (Davis et al., 1974). Cost/benefit decisions are value-based decisions which involve the animal making a decision based on the sensory stimulus as well as other factors, such as internal state, previous experience or environmental context (Gillette et al., 2000). Davis and Mpitsos (1971) proposed a simple mechanism for decision making. They

hypothesised that there were dedicated decision neurons within the network of each behaviour. During a choice between behaviours, decision neurons from the dominant behaviour inhibited decision neurons from hierarchically lower behaviours, thus suppressing their activity and the behaviour they activate. Evidence for inhibition between decision neurons has been identified in some networks; however this mechanism is not used in all systems. Indeed, in the systems where it has been shown to be used, separate mechanisms have been identified for other decision making tasks investigated. Studies of decision making have used different experimental designs and focused on different types of decision depending on the system being used. Below, several model systems used to study decision making and the mechanisms identified are discussed.

1.1.2 Invertebrate models of decision making

Pleurobranchaea

Behavioural hierarchies were first described in the marine mollusc *Pleurobranchaea* (Davis, 1979). This animal was simultaneously presented with two stimuli. Presentation of each stimulus in isolation of the other elicited a different behaviour. The two behaviours elicited were incompatible with each other. When the two stimuli were presented together, only a single behaviour could be elicited, therefore the animal had to make a choice between the two. In *Pleurobranchaea* a behavioural hierarchy was identified (Davis, 1979). Certain behaviours were found to be dominant over other behaviours. At the top of the hierarchy was escape swimming, which was dominant over all behaviours. Next was egg-laying then feeding, local withdrawal and righting behaviours (Davis, 1979). Davis and Mpitsos (1971) proposed that there were dedicated decision neurons in each network and those in the dominant behaviour inhibited those in lower behaviours. This was supported by findings of Kovac and Davis (1980) that showed that a feeding neuron inhibited the withdrawal network. It was proposed that this was achieved via inhibition of an unidentified withdrawal network decision neuron; however such a neuron was never identified.

Later work in *Pleurobranchaea* found a separate mechanism for decision making. Jing and Gillette (1995, 2000) found that activation of swim network interneurons strongly inhibited feeding initiating interneurons. However, this was achieved via excitation of a member of the feeding network, the I1 interneuron. I1 fired in bursts during feeding, aiding in the biphasic protraction-retraction movements necessary to move food into the buccal cavity. During swimming, I1 fired tonically, providing inhibition to the feeding

initiator interneurons. Therefore, I1 was not dedicated to feeding behaviours, but was multifunctional since it was also active in escape swimming. Therefore the previously proposed mechanism of inhibition between decision neurons of the two networks was found to be over simplified. Gillette et al. (2000) showed that *Pleurobranchaea* can perform a cost/benefit analysis during decision making. An appetitive stimulus was shown to elicit withdrawal behaviours if the animal was satiated and an aversive stimulus could elicit feeding behaviours if the animal was hungry. Interestingly, they found that the same stimulus could elicit different behaviours in the same animal if the animal's behavioural state was altered. It was proposed that the animal made a judgement about the cost of attacking a prey based on the benefits, i.e. its need for food. Using an in vitro preparation, Hirayama and Gillette (2012) showed that the same stimulus could elicit either orienting turns (orienting towards food) or avoidance turns (withdrawing away from the stimulus) depending on the behavioural state of the animal. Importantly, a stimulus which elicited avoidance in a preparation could elicit orienting if the behavioural state of the animal was artificially altered via activation of the feeding network. These experiments confirmed earlier findings by Gillette et al. (2000) that decision making was dependent on internal cues as well as sensory stimuli.

Medicinal leech

Experiments by Shaw and Kristan (1997) examined the choice between swimming and whole-body shortening in the medicinal leech. Both behaviours use the same set of motor neurons and shortening is dominant over swimming. The swim circuit is organised hierarchically and consists of three interneuronal levels, the top two levels consist of swim decision neurons and the third swim oscillator interneurons. Activation of the swim decision neurons was sufficient to elicit swimming behaviour in vitro. Shaw and Kristan (1997) tested each of the swim decision interneurons response to a stimulus which elicited shortening. The first cell type tested, cell 204, was strongly hyperpolarised by the stimulus, supporting the hypothesis of Davis and Mpitsos (1971) that decision neurons of a subordinate behaviour are inhibited by stimuli which elicit the dominant behaviour. However, four other swim decision neurons were all excited by the shortening stimulus. Therefore during this decision, simple inhibition between the two networks was not the mechanisms by which a choice was made between the two behaviours. These results suggest that most of the swim decision neurons were not dedicated to a single behaviour, but instead aided in the initiation of at least one other behaviour, making them multifunctional. It has been proposed that behaviours in the

leech are chosen due to a combinatorial code, whereby the behaviour selected is due to the combination of different neurons active or inactive (Kristan and Gillette, 2007).

Esch et al. (2002) described a multifunctional interneuron, R3b1, which was active in both swimming and crawling behaviours. The neuron was sufficient to drive both swimming and crawling if activated during quiescence. The neuron did not specify which behaviour to elicit, but only to locomote away from a stimulus. The decision about which behaviour to perform was made downstream from the neuron, relying on cues from the animal's environment (Esch et al., 2002). It was therefore hypothesised that leech perform sequential decision making. This study provided evidence that decision making is also dependent on the context that the stimulus is encountered in. Briggman et al. (2005) studied the decision between crawling and swimming using voltage-sensitive dyes, allowing for the simultaneous recording of ~140 neurons. A choice variability paradigm was developed, whereby the same stimulus was used to elicit swimming in half the trials and crawling in the other half. They found that 6-8 individual neurons showed a significant difference in their activity between swimming and crawling trials before the fictive behaviour began, suggesting that these neurons were important for the decision about which behaviour to generate. However, artificial depolarisation or hyperpolarisation of each of these neurons had no biasing effect on which behaviour was generated, suggesting that these neurons were not involved in the decision making process. Briggman et al. (2005) next analysed activity of all the neurons and identified a population of neurons which responded earlier than the previously mentioned 6-8 neurons. One neuron within this group was found to be able to bias the evoked behaviour towards crawling or swimming if it was hyperpolarised or depolarised respectively. Therefore, the decision to swim or crawl involved a population of neurons, and within this population was a single neuron which was able to bias the decision.

Gaudry and Kristan (2009) described a separate mechanism for choice competition, presynaptic inhibition. Feeding behaviours in the leech are dominant over all other behaviours, including local bend behaviours and swimming. Rather than inhibiting local bend interneurons, feeding reduces the size of EPSPs from the mechanosensory cells (which respond to aversive stimuli) to local bend interneurons and swim interneurons. Activation of swim interneurons was still sufficient to elicit fictive swimming during feeding, suggesting that the decision neurons themselves were not affected, rather the inputs to these cells from the sensory neurons were reduced via presynaptic inhibition. Experiments using the leech preparation therefore have provided several different mechanisms of decision making within the same preparation.

Aplysia

The sea slug, *Aplysia*, has been used as a model for studying the neural mechanisms involved in the choice between the two competing behaviours ingestion and egestion. Activation of an interneuron in the feeding network (CBI-2) was found to be able to initiate either ingestion or egestion (Morgan et al., 2002), suggesting that it was a multifunctional interneuron. This was supported by experiments showing that CBI-2 responded to stimuli which elicit both ingestive and egestive motor programs. A number of dedicated interneurons were also identified in the two networks (Morgan et al., 2002, Jing and Weiss, 2001, 2002). A decision neuron involved in ingestion was shown to inhibit two egestion interneurons, whereas stimuli which elicit egestive behaviours inhibit the ingestive decision neuron, therefore biasing CBI-2 driven cycles towards egestion (Morgan et al., 2002). Therefore, in the choice between ingestion and egestion in *Aplysia*, there is evidence of dedicated decision interneurons which monosynaptically inhibit decision neurons for the competing behaviour, as hypothesised by Davis and Mpitsos (1971). However, there was also evidence of multifunctional interneurons which responded to both ingestive and egestive stimuli. It is possible that CBI-2, like R3b1 in the leech, initiates a behaviour, but the decision about specifically which behaviour is made downstream. Jing et al. (2008) showed that command-like interneurons in the locomotor network excited rather than inhibited several elements of the incompatible feeding circuitry. They proposed that stimuli which can elicit escape behaviours create a state of arousal in the feeding network, increasing the likelihood of the animal to respond to the presence of food in the future.

Lymnaea

In *Lymnaea* the whole-body withdrawal response and aerial respiration are two incompatible behaviours. The whole-body withdrawal response is a defensive behaviour elicited in response to aversive stimuli and is thought to be hierarchically higher than aerial respiration (Inoue et al., 1996). The central pattern generator (CPG) for aerial respiration is well characterised in *Lymnaea* (Syed et al., 1991, Syed and Winlow, 1991a). The whole-body withdrawal response is coordinated by the interneuron RPeD11 (Syed and Winlow, 1991b). Stimuli which elicit whole-body withdrawal inhibited the aerial respiration network (Inoue et al., 1996). RPeD11 was shown to monosynaptically inhibit several of the respiration CPG interneurons and motor neurons. These experiments provide an example of simple inhibition between competing behaviours for decision making.

Kemenes et al. (2001) studied the decision to feed in response to food in *Lymnaea*. The two decision interneurons which were previously hypothesised to initiate feeding in response to food were found to be active after the CPG interneuron N1M. Further work by Staras et al. (2003) found that an inhibitory neuron and member of the feeding CPG was itself inhibited prior to N1M activation, suggesting that the decision to feed was distributed in the CPG itself, rather than due to activation of the command-like interneurons. These experiments provided evidence that although a neuron may be sufficient to elicit behaviour, it may not be necessary for the decision to elicit the behaviour in response to a stimulus.

Clione

In the pteropod mollusc *Clione limacine* whole-body withdrawal interneurons have been identified which directly inhibit the hierarchically lower slow swimming behaviour (Norekian and Satterlie, 1996). The whole-body withdrawal neurons were found to inhibit swim interneurons, whereas there was no reciprocal connection from the swim network to the withdrawal network. However, sensory stimuli which elicited swimming inhibited withdrawal neurons. Therefore it is possible that the withdrawal network is inhibited directly by stimuli which elicit swimming, or that the network is inhibited by a decision neuron which has not yet been identified.

Other invertebrate models for studying decision making

The fruit-fly *Drosophila* was used by Yang et al. (2008) to study egg-laying site selection decisions. They observed a characteristic “search-like” behaviour which preceded egg-laying, indicative of sampling the environment for the most suitable substrate to lay their eggs on. Yang et al. (2008) presented *Drosophila* with a choice between two substrates, one sweet (an attractive stimulus for *Drosophila*) and one bitter (an aversive stimulus for *Drosophila*). *Drosophila* preferentially laid eggs on the bitter substrate. When placed on either a sweet or a bitter only substrate, *Drosophila* laid a comparable number of eggs on each, suggesting that when given no choice, *Drosophila* will lay eggs on both substrates. Thus both were suitable egg-laying substrates, but a value was assigned to each when a choice was given between the two and the bitter substrate was higher than the sweet. Therefore *Drosophila* were able to make comparisons between two substrates and make a simple decision between one and the other.

The worm *C.elegans* was used by Shinkai et al. (2011), who designed a choice assay where the worm was simultaneously presented with an aversive and an attractive stimulus. To reach the attractive stimulus, the worm had to cross the aversive stimulus. The decision about whether to cross the aversive stimulus or to move away from it was based on the relative strength of the aversive and attractive stimuli. Therefore, *C.elegans* placed a value on the attractive stimulus and weighed it against the aversive stimulus, performing a cost/benefit analysis. An interneuron was identified as important for integrating the two stimuli and making a decision about whether to approach or avoid. The interneuron was electrotonically coupled with sensory cells responsive to the attractive stimulus and inhibited by sensory cells responsive to the aversive stimulus, providing a site for sensory integration and decision making.

Summary of invertebrate decision making studies

Derived from early work on *Pleurobranchaea,* it was hypothesised that the mechanism by which decisions between two incompatible behaviours were made was via direct inhibition between dedicated decision neurons (Davis and Mpitsos, 1971). However, later work using invertebrate preparations has identified several different mechanisms for decision making. These include the previously proposed monosynaptic inhibition between decision neurons (Inoue et al., 1996), presynaptic inhibition of sensory neurons of a lower behaviour (Gaudry and Kristan 2009) and the use of multifunctional interneurons and the reconfiguration of neural networks to produce incompatible behaviours (Jing and Gillette, 1995, 2000, Shaw and Kristan, 1997, Briggman et al., 2005, Jing and Weiss, 2001, Morgan et al., 2002). The latter mechanism is the most widely observed and Kristan and Gillette (2007) have proposed that this is a common mechanism of decision making between competing behaviours.

1.1.3 Mammalian decision making

Decision making studies in mammals have focused on the use of highly trained monkeys performing sensory discrimination tasks. Single-unit recordings are made from specific regions of the brain whilst these tasks are being performed. Regions of the brain whose activity correlates with the decision, rather than with the strength of the stimulus or production of the motor output, are deemed to be involved in the decision making process. de Lafuente and Romo (2005, 2006) used the somatosensory system as a model to study stimulus detection. During the task, a vibrotactile stimulus was

either applied to the fingertip of the animal or no stimulus was applied. The animal had to make a decision about the presence or absence of the stimulus. Importantly, the stimulus used varied in strength, and was near the animal's sensory threshold point. Therefore there were four possible outcomes of the task: a "hit trial" represented a correct judgement about the presence of the stimulus, a "rejection trial" represented a correct judgement about the absence of a stimulus, a "false alarm" represented a false judgement about the presence of the stimulus and a "miss trial" represented the false judgement about the absence of a stimulus. The animal indicated its decision about the presence or absence of the stimulus by pressing a button and was rewarded for hit and rejection trials only. Whilst the task was performed, single-unit recordings were made from regions of the somatosensory system. de Lafuente and Romo (2005) showed that the primary somatosensory cortex (S1) faithfully co-varied with the strength of the stimulus but their activity did not correlate with the perceptual decision about the presence or absence of the stimulus. Neurons in the medial premotor cortex (MPC) did not co-vary with the strength of the stimulus but did with the animal's decision about the presence or absence of the stimulus. Importantly, artificial activation of MPC neurons in stimulus present trials increased the number of hit responses, suggesting that MPC is important for the stimulus present decision. This was further supported by experiments where the vibrotactile stimulus was replaced with artificial activation of MPC neurons with varying current strengths. This elicited a similar response to varying vibrotactile stimuli. MPC neurons activity only increased during hit trials or false alarm trials, therefore only in trials in which the animal judged the presence of the stimulus. During rejection and miss trials, MPC neuron activity remained at baseline levels. The stimulus absent decision was hypothesised to be the default response which must be overridden by the stimulus present response, accounting for lack of neurons changing their activity in the stimulus absent decision. Carnevale et al (2012) performed similar vibrotactile stimuli experiments and found that the decision about the presence or absence of the stimulus was heavily reliant on the state of cortical networks before the stimulus onset.

Merten and Nieder (2012) also studied a stimulus present/absent decision, but in an abstract decision visual detection task. The task was considered an abstract decision, rather than action-based as in the above experiments by de Lafuente and Romo (2005, 2006) and Carnevale et al. (2012), since the animal made a decision about the presence or absence of the stimulus without knowing the behavioural response needed to report its decision. Therefore, the decision could be fully dissociated from motor planning. Single-unit recordings were carried out throughout the trials from the

prefrontal cortex (PFC). Stimulus present decision neurons were found that co-varied their activity in stimulus present decisions and stimulus absent decision neurons were found that co-varied their activity in stimulus absent decisions. The stimulus present decision neurons activity remained at baseline levels during stimulus absent decisions as did the stimulus absent decision neurons during stimulus present decisions. However, Merten and Nieder (2012) were not able to test the sufficiency of the two groups of neurons via artificial activation since both were located in the same brain region.

Hernandez et al. (2002) and Romo et al. (2004) used a vibrotactile frequency discrimination task to study decision making. The monkey was presented with a vibrotactile stimulus followed by a delay period followed by a second vibrotactile stimulus. The monkey made a decision about whether the second stimulus was of a higher or lower frequency than the first and received a reward if it was correct. Neurons in S1 were found to co-vary their activity with the stimulus, but show little activity in the delay period. Activity in neurons in the MPC and the ventral premotor cortex persisted in the delay period between the stimuli, and activity during the second stimulus reflected a comparison between the two stimuli. Therefore, it appears that in both type of decision making task the decision was made by neurons in the premotor cortices.

1.2 Feeding behaviour in *Lymnaea*

1.2.1 *Lymnaea* as a model system for studying decision making

To study the neural mechanisms of decision making, a suitable model system is necessary. The system should produce readily observable behaviours and the neural networks controlling them should be well characterised. The pond snail, *Lymnaea stagnalis*, has successfully been used to study decision making (see above). *Lymnaea* have a relatively simple central nervous system which consists of around 20,000 neurons. The neurons are relatively large and reidentifiable from preparation to preparation allowing for the testing of individual neurons' role in decision making. Semi-intact preparations can also be utilised for applying sensory stimuli to sensory structures, aiding in the design of in vitro preparations of decision making tasks. The feeding behaviours and its neural control are well characterised in *Lymnaea* making it an ideal model to study decision making.

1.2.2 Feeding in *Lymnaea*

Feeding behaviours in molluscs can be separated into appetitive and consummatory phases (Kupfermann, 1974a, 1974b). Appetitive behaviours are goal-directed behaviours performed with the aim of locating food. Consummatory behaviours are performed when food is located with the aim of ingesting the food. *Lymnaea* use the same motor output for both appetitive and consummatory behaviours (Tuersley and McCrohan, 1987). This consists or protraction and retraction of the toothed radula into and out of the mouth (see Section below for further description) which is referred to as either rasping or biting. Carricker (1946b) and Runham (1975) argue that *Lymnaea* only perform true rasping on a flat substrate, whereas when feeding on a three-dimensional solid, like lettuce, the animal “bites” the lettuce with its radula. During bites the radula is often brought into apposition with the dorsal mandible in a shearing motion. In this study, both the appetitive and consummatory behaviour are referred to as bites. The appetitive bite program is an internally generated behaviour, occurring in the absence of sensory stimuli (Tuersley and McCrohan, 1987) whereas the consummatory bite program is generated in the presence of a sensory stimulus. The function of the appetitive bite program is to locate a palatable food for ingestion. *Lymnaea* have poor distance chemoreception (Bjorverg 1969), therefore appetitive bites serve as a major mechanism for locating food.

Feeding in *Lymnaea* consists of four major synchronous movements: 1. opening and closing of the mouth, 2. rotations of the entire buccal mass, 3. rotations of the odontophore within the buccal mass, and 4. movements of the radula over the odontophore (Carriker, 1946b). Movements of the radula during feeding have been most extensively studied in the closely related *Helisoma* (Smith, 1988), and will therefore be discussed here. **Figure 1.1** shows a schematic of the movements of the odontophore with respect to the mouth.

Feeding movements are often described in relation to movements of the odontophore into and out of the mouth. Using these criteria, feeding cycles can be divided into three phases: a protraction phase, and a retraction phase, which can be split into two phases, a rasp phase and a swallow phase (Carriker, 1946a, 1946b, Rose and Benjamin, 1979). A rest/quiescent phase is sometimes considered as a distinct fourth phase. Before a feeding cycle occurs, the odontophore is positioned upright in the rear of the buccal cavity (Carriker, 1946b).

Protraction phase. During the protraction phase, the mouth is opened to permit the protraction of the odontophore out of the mouth. The buccal mass is rotated

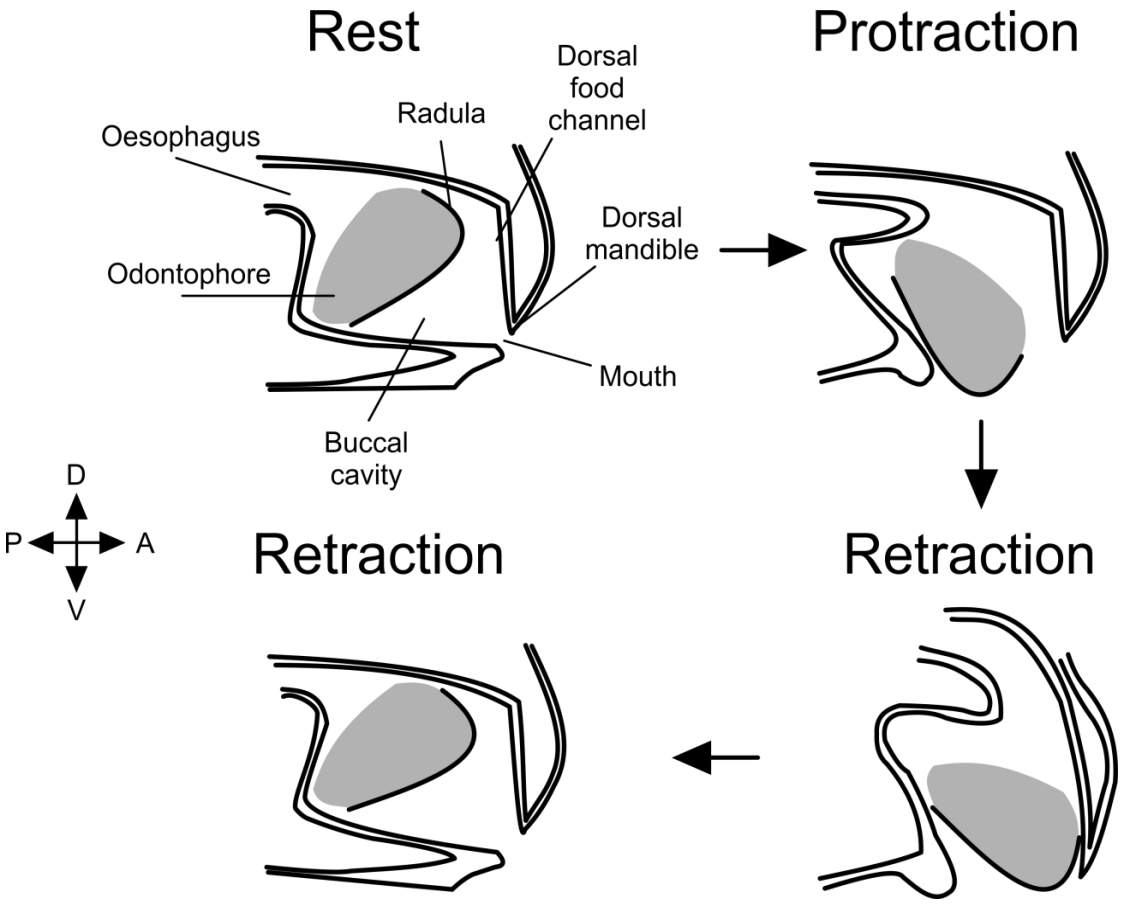

Figure 1.1 A schematic of a single feeding cycle showing the movements of the odontophore and radula with respect to the mouth. At rest the odontophore is located within the buccal cavity at an almost dorsal/ventral position and the mouth is closed. In the protraction phase, the mouth is opened and the odontophore is rotated towards the posterior region of the mouth. In the retraction phase, the odontophore is moved towards the dorsal mandible in the power stroke. The radula often comes into contact with the dorsal mandible in a shearing motion referred to as a 'bite'. The mouth closes as the odontophore is further retracted into the mouth and any food particles moved into the oesophagus. Adapted from Benjamin (2012). Abbreviations: D - dorsal, V - ventral, A - anterior, P - posterior.

anteroventrally. Simultaneously, the odontophore within the buccal mass also undergoes rotations. Muscles pull the odontophore from its vertical position at rest, to a horizontal position within the buccal mass. The distal end of the odontophore is then moved forward, resulting in the odontophore being moved towards the opening of the mouth (Runham, 1975). The entire rotation of the odontophore can be between 125-170° (Runham, 1975). During protraction, the radula is drawn over the tip of the odontophore and down its anterior face (Smith, 1988). The odontophore is then further contracted and elongated causing the radula to protrude out of the mouth at the end of the protraction phase (Carriker, 1946b).

Rasp phase. The odontophore is drawn towards the dorsal mandible, and the distal tip is accelerated across the substrate (Carriker, 1946b). The dorsal mandible is turned partly forward, with the consequence that as the odontophore is drawn past it, the two pass each other in a shearing motion. Carriker (1946b) describes this as a biting motion. During the rasp stroke, the radula is retracted back across the odontophore.

Swallow phase. During the swallow phase, the odontophore is rotated back to and past its original resting position, pushing food into the oesophagus (Rose and Benjamin, 1979).

The buccal mass complex consists of 46 muscles and has been extensively studied (Carriker, 1946a, 1946b, Goldschmeding and De Vlieger, 1975, Rose and Benjamin, 1979). A brief summary of the major muscles involved in movements of the buccal mass and its internal structures are given. During protraction, the posterior jugalis muscle (PJM) is involved in rotation of the buccal mass (Carriker, 1946a, 1946b, Rose and Benjamin, 1979). Odontophore rotation is thought to arise via contraction of the dorsal odontophoral flexor muscle (Carriker, 1946a, 1946b, Rose and Benjamin, 1979). Retraction of the buccal mass and odontophore is due to contraction of the anterior jugalis muscle (AJM) and postventral protractor muscles (Rose and Benjamin, 1979). Contraction of the odontophore and movements of the radula across the odontophore are due to the three tensor muscles; the supralateral tensor muscles (SLRT), supramedian tensor muscles and inframedian radula tensor muscle (Carriker, 1946a, 1946b, Goldschmeding and De Vlieger, 1975, Rose and Benjamin, 1979, Smith, 1988).

1.3 The neural control of feeding in *Lymnaea*

Feeding in *Lymnaea* is produced by a well characterised CPG (Rose and Benjamin, 1981b, Elliott and Benjamin, 1985a, Brierley et al., 1997c). Many of the CPG

interneurons, modulatory interneurons and motor neurons have been identified and will be discussed below. The majority of feeding neurons are located in the buccal ganglia. **Figure 1.2** shows the location of identified buccal neurons.

1.3.1 CPG interneurons

A schematic of the connections and firing activity of key feeding CPG and buccal modulatory interneurons are shown in **Figure 1.3**. The feeding behaviour in *Lymnaea* consists of three phases: protraction, rasp and swallow. The feeding CPG is made up of three types of CPG interneurons: N1, N2 and N3. The N1 interneurons produce the protraction phase of the feeding cycle, the N2 interneuron the rasp phase and the N3 interneurons the swallow phase. Each of the N1, N2 and N3 groups are made up of two types of interneuron.

N1 medial (N1M)

The N1Ms are protraction phase CPG interneurons located between the B1 and B2 motor neurons (Rose and Benjamin, 1981b). They have a single projection down the contralateral cerebral buccal connective (CBC) (Elliott and Benjamin, 1985a). It was previously thought that there was a cluster of N1Ms in each ganglion, however back-filling the CBCs revealed that there is only one N1M per buccal ganglion (Kemenes and Elliott, 1994). N1M produces plateau potentials both in the CNS and when isolated in cell culture (Straub et al., 2002), confirming that this is an endogenous property of the cell. N1M makes cholinergic synapses with many of the buccal motor neurons and interneurons (Elliott and Kemenes, 1992). Activation of N1M is able to drive a fictive feeding rhythm via its connections with the N2 interneurons (Elliott and Benjamin, 1985a, Brierley et al., 1997c). N1M has been shown to be necessary for both command-like interneuron and sucrose driven fictive feeding rhythms (Kemenes and Elliott, 1994, Kemenes et al., 2001). N1M was also shown to be active in sucrose driven fictive feeding cycles before the command-like interneurons SO and CV1a, suggesting that N1M plays a role in the decision to initiate feeding as well as being a member of the CPG (Kemenes et al., 2001).

N1 lateral (N1L)

The N1Ls are a pair of bilaterally symmetrical interneurons on the dorsal surface of the buccal ganglia, lateral from the B1 motor neuron (Yeoman et al., 1995). The N1Ls are buccal interneurons as their projections do not leave the buccal ganglia. The N1Ls, like the N1Ms, are protraction phase interneurons. Activation of an N1L can drive fast

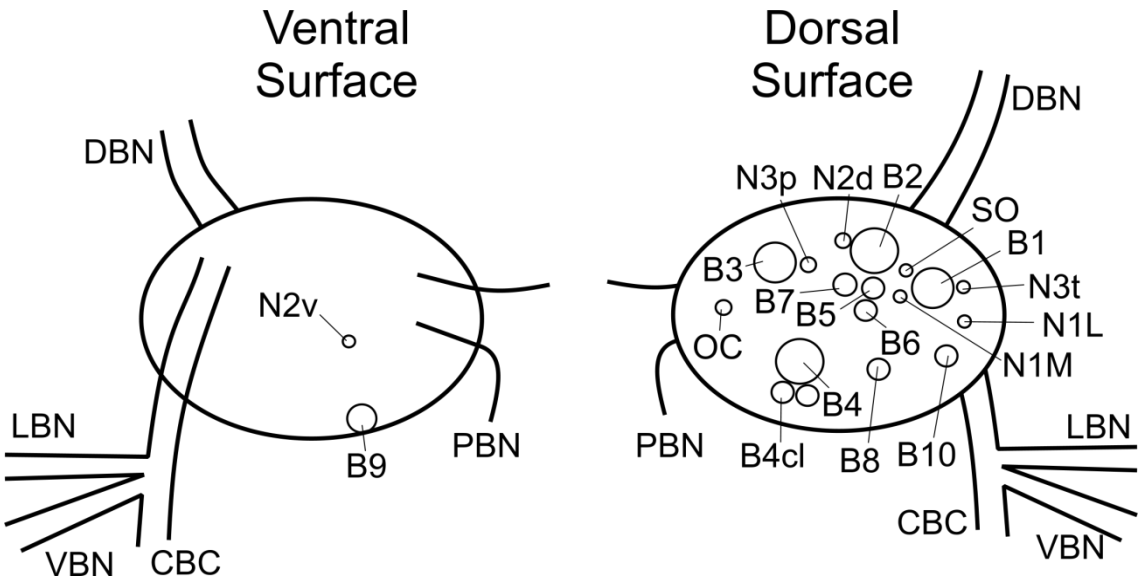

Figure 1.2 Diagram of the locations of identified neurons in the buccal ganglia. The dorsal (right side of figure) and ventral (left side of figure) surface of the right buccal ganglion is shown. All of the neurons are thought to have bilaterally symmetrical homologues in the other buccal ganglion apart from the SO which appears as a single neuron in either the left of right buccal ganglion. Diagram adapted from Staras et al. (1998b). Abbreviations: CBC – cerebral buccal connective, DBN – dorsal buccal nerve, LBN, lateral buccal nerve, PBN, post buccal nerve, VBN, ventral buccal nerve.

fictive feeding rhythms, partly due to a monosynaptic excitatory chemical synapse with the N1Ms (Yeoman et al., 1995). Similar to N1M, the N1Ls are cholinergic (Vehovszky and Elliott, 1995).

N2 dorsal (N2d)

The N2ds are a cluster of neurons located on the dorsal surface of each buccal ganglion anteriorly of the B2 motor neuron (Elliott and Benjamin, 1985a). The N2ds have a projection down the post-buccal nerve (PBN) and the ipsilateral dorsal-buccal nerve (DBN). They are excited by both N1M and N1L in the protraction phase, and fire large somatic spikes in the rasp phase. The N2ds inhibit N1M, N1L and the N3 phase interneurons. The N2ds excite the B3 motor neuron, inhibit the B4cl, B7 and B8 motor neurons (Brierley et al., 1997a) and are electrotonically coupled with the B10 motor neurons (Staras et al., 1998b).

N2 ventral (N2v)

The N2vs are a pair of bilaterally symmetrical neurons located medially on the ventral surface of each buccal ganglion (Brierley et al., 1997a). They have extensive neuritic processes within the ipsi- and contralateral buccal ganglia and a single projection which exits the buccal ganglion via the PBN. The N2vs are excited by the N1Ms and inhibited by the N1Ls. They are active throughout the entire rasp phase. N2vs do not fire large somatic spikes, but small spikelets riding on a large depolarisation. The N2vs are electrotonically coupled with the N2ds (Brierley et al., 1997a). N2v produces plateau potentials in the CNS (Brierley et al., 1997a), but not when isolated from the CNS (Straub et al., 2002). N2v activation inhibits both N1M and N1L (Brierley et al., 1997c), excites the B3 and B9 motor neurons and inhibits the B7 and B8 motor neurons (Brierley et al., 1997a). They are also electrotonically coupled with the B10 motor neurons (Staras et al., 1998b). There is evidence that the N2vs use glutamate as their main neurotransmitter (Brierley et al., 1997b) and that they are immunoreactive to small cardioactive peptide (SCP) and myomodulin (Santama et al., 1994).

N3 phasic (N3p)

The N3ps are a cluster of swallow-phase neurons located on the dorsal surface of each buccal ganglion between the B2 and B3 motor neurons (Elliott and Benjamin, 1985a). They have extensive neuritic processes in both the ipsi- and contralateral buccal ganglia and have projections into both the ipsi- and contralateral DBN. The N3ps are inhibited in the protraction phase by the N1Ms and N1Ls and in the rasp phase by the N2ds. They often fire in the late rasp/early swallow phase (Yeoman et al., 1995). It was

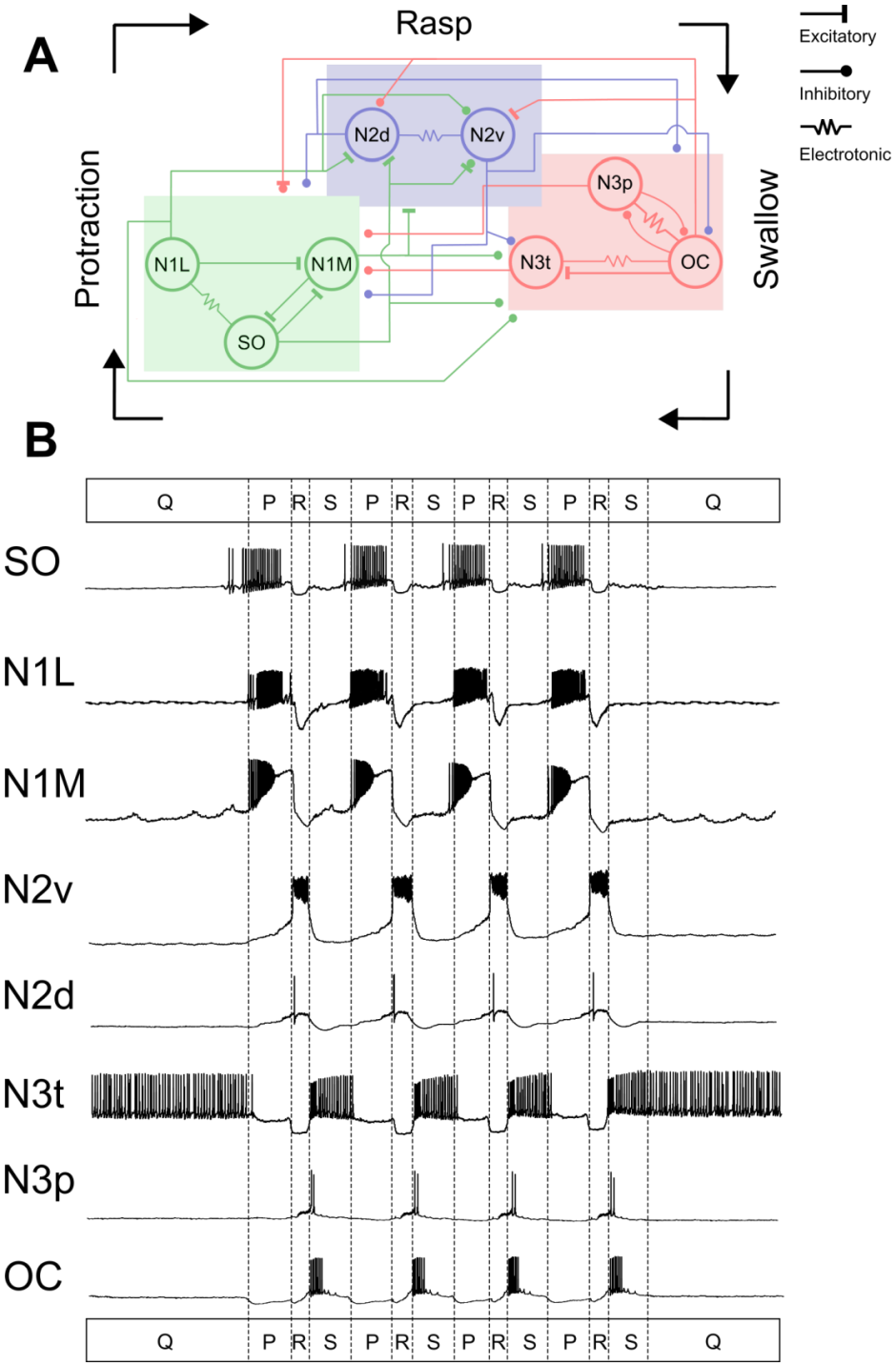

Figure 1.3 Summary schematic of connections between feeding buccal interneurons and their phase of activity. **A.** Circuit diagram of connections between buccal interneurons. Each interneuron is categorised into boxes by which phase it is active in: protraction (green), rasp (blue) or swallow (red). Connections which touch a box rather than a single interneuron have the same connection with all interneurons within that box. **B.** The phase of activity of the buccal interneurons is shown in four fictive feeding cycles. Each interneuron is active in a single phase only apart from N3t which is active in the swallow phase and the quiescent phase. Firing activity of interneurons from Rose and Benjamin (1981a, 1981b), Elliott and Benjamin (1985a, 1985b), Brierley et al. (1997c), Yeoman et al. (1995), Vehovszky and Elliott (2001). Abbreviations: Q – quiescent phase, P – protraction phase, R – rasp phase, S – swallow phase.

originally thought that the N3ps fired due to post-inhibitory rebound (PIR), however N3ps show no evidence of PIR when isolated from the CNS (Straub et al., 2002). The N3ps inhibit the B4 motor neurons and excite the B3 motor neurons.

N3 tonic (N3t)

The N3ts are a pair of bilaterally symmetrical interneurons located laterally of the B1 motor neuron on the dorsal surface of each buccal ganglion (Elliott and Benjamin, 1985a). The N3ts have a single projection to the contralateral buccal ganglion, therefore are classified as buccal interneurons, similar to the N1Ls. They are inhibited in the protraction phase and throughout the rasp phase and then fire via PIR in the swallow phase (Elliott and Benjamin, 1985a). The N3ts are inhibited by the N1Ms (Elliott and Benjamin, 1985a), N1Ls (Yeoman et al., 1995), N2ds and N2vs (Brierley et al., 1997c). They provide inhibitory inputs to the N1Ms and N1Ls. During periods of quiescence, the N3ts fire tonically, preventing activity in the N1 interneurons (Staras et al., 2003). N3ts excite the B3 motor neurons and are coupled with the B4 motor neurons (Staras et al., 1998b).

1.3.2 Generation of the basic feeding pattern

Fictive feeding cycles can be generated by activation of the N1 phase interneurons (N1M, N1L, SO, CV1a or CV1b), application of a feeding stimulant to a sensory structure (Lips or oesophagus) or can occur spontaneously. **Figure 1.4** shows an example of a single spontaneous cycle recorded on the interneurons N1M, N2v and N3t. This allows for the visualisation of all three levels of the CPG within a fictive feeding cycle.

During periods of quiescence, the N3ts fire tonically (Staras et al., 2003). The N3ts prevent the generation of feeding cycles via monosynaptic inhibition of the N1Ms, N1Ls and the SO (Elliott and Benjamin, 1985a, Elliott and Benjamin, 1985b, Yeoman et al., 1995). Activation of any one of these protraction phase interneurons, or release from inhibition by a reduction in N3t firing, initiates a feeding cycle. N1M depolarisation triggers an endogenous plateau potential (Straub et al., 2002). N1M monosynaptically excites the N2v and N2d interneurons (Elliott and Benjamin, 1985a, Brierley et al., 1997c). The N1Ls provide further excitation to the N1Ms and also to the N2ds (Yeoman et al., 1995). Once the N2vs are sufficiently depolarised, a plateau potential is initiated. Due to strong coupling between N2v and N2d, N2v activation often elicits activity in the N2ds (Brierley et al., 1997a). The two N2 interneurons strongly inhibit the N1Ms, N1Ls

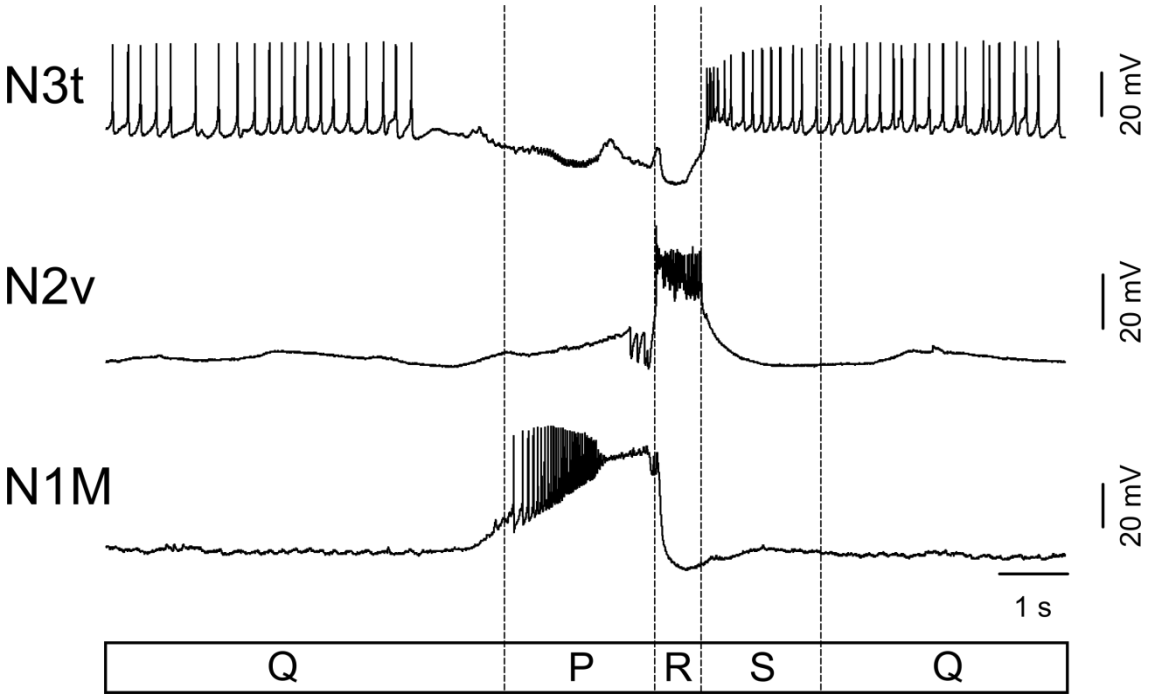

Figure 1.4 Activity of the three CPG interneurons in a fictive feeding cycle. A spontaneous fictive feeding cycle was recorded on an N1M, N2v and N3t interneuron. There was a period of quiescence before a spontaneous fictive feeding cycle. During the period of quiescence (Q), N3t fired tonically, inhibiting N1M. N3t spontaneously stopped firing, releasing N1M from inhibition. N1M rapidly depolarises. Once N1M reaches threshold, it inhibits N3t, preventing further inhibition, and excites N2v. This is the start of the protraction (P) phase. N1M activity is sustained as it enters a plateau potential. Once N2v is sufficiently depolarised, it generates a plateau potential which terminates N1M's plateau. This is the start of the rasp (R) phase. N3t is also strongly inhibited by N2v activity. N2v's plateau terminates due to an endogenous mechanism, and N3t fires a burst of spikes via post inhibitory rebound in the swallow phase. This is the start of the swallow (S) phase. N3t then returns to firing tonically as prior to the onset of the cycle. In the protraction phase, N2v receives several large inhibitory inputs. These most likely arose from inputs from the SO or N1L protraction phase interneurons.

and the SO. This terminates N1M's plateau potential and activity in the N1Ls and the SO. The N2 interneurons fire throughout the rasp phase. The N3 interneurons receive inhibition during both the protraction and rasp phases (Elliott and Benjamin, 1985a, Elliott and Benjamin, 1985b, Brierley et al., 1997c). Both N3t and N3p are monosynaptically inhibited by N1M, N1L, SO and N2d (Elliott and Benjamin, 1985a, Elliott and Benjamin, 1985b, Yeoman et al., 1995). N3t is also inhibited by the N2vs (Brierley et al., 1997c). The N3ps fire in the late rasp/early swallow phase and the N3ts in the swallow phase via PIR. Neither of the N3 interneurons have connections with the N2 interneurons; therefore it is likely that the N2 phase ends due to an endogenous termination of N2v's plateau potential.

1.3.3 Modulatory neurons

Several modulatory neurons have been identified in the feeding system of *Lymnaea*. Sufficient activation of each of these interneurons is able to initiate fictive feeding cycles. Historically, interneurons with this capability were termed command neurons, however Kupfermann and Weiss (1978) argued that for a neuron to be classified a command neuron it must be shown to be active in the behaviour it commands, be sufficient to elicit the behaviour and necessary for the behaviour to occur. None of these neurons fulfil all three criteria, in fact only a few examples of command neurons which fulfil these strict criteria have been identified. The dorsal ramp interneuron in *Tritonia* (Frost and Katz, 1996), the lateral giant fibre of the crayfish (Edwards et al., 1999) and the Fdg interneurons in *Drosophila* (Flood et al., 2013) are three examples of command neurons. Neurons which are sufficient to drive a fictive behaviour alone are often referred to as command-like interneurons (Shaw and Kristan, 1997) or decision neurons (Kristan, 2008). In this study, the term command-like neuron is used to refer to neurons which have the ability to drive a fictive behaviour whereas decision neuron is used to refer to neurons involved in a specific decision making process.

Slow oscillator (SO)

The SO is a single interneuron located in either the left of the right buccal ganglion between the B1 and B2 motor neurons (Elliott and Benjamin, 1985b). The SO projects into the contralateral buccal ganglion via the buccal commissure and then loops back into the ipsilateral buccal ganglion. The SO has extensive neuritic processes in both buccal ganglia, but does not have projections which leave any of the peripheral nerves nor project down the CBC, therefore, like the N1Ls and N3ts, SO is a buccal interneuron. Activation of the SO is able to drive fast fictive feeding cycles (Elliott and

Benjamin, 1985b) at a similar rate to N1L (Yeoman et al., 1995). Kemenes et al. (2001) found that although the SO was active in some sucrose driven rhythms, it was not necessary for the generation of fictive feeding cycles. The SO is thought to drive fictive feeding cycles via a monosynaptic facilitating excitatory chemical synaptic connection with the N1Ms (Elliott and Benjamin, 1985b). SO excites the N2ds (Elliott and Benjamin, 1985b) and has a biphasic (i/e) connection with the N2vs (Brierley et al, 1997c). Both N3 interneurons are inhibited by the SO. The SO receives excitatory inputs from N1M (Elliott and Benjamin, 1985b), is electrotonically coupled with N1L (Yeoman et al, 1995) and inhibited by the N2 (Elliott and Benjamin, 1985b, Brierley et al, 1997c) and N3 interneurons (Elliott and Benjamin, 1985b). The SO, similar to the N1Ms and N1Ls, is cholinergic (Yeoman et al., 1993).

Octopamine cells (OC)

The OCs are a pair of interneurons located on the dorsal surface of the buccal ganglia near the buccal commissure (Vehovszky et al., 1998). The OCs project across the buccal commissure and enter the contralateral buccal ganglion. They have projections into the initial section of both the ipsi- and contralateral CBC, but the processes terminate well before reaching the cerebral ganglia. The OCs are inhibited in the protraction and rasp phases and fire spikes in the swallow phase therefore are considered swallow phase interneurons. Short duration activation of a single OC is able to trigger fictive feeding cycles that outlast the duration of the stimulus to the neuron (Vehovszky and Elliott, 2001). The OCs have biphasic (i/e) connections with the N1Ms, N1Ls and SO, excite N2v and are electrotonically coupled with the N3 interneurons (Vehovszky and Elliott, 2001). The OCs are able to modulate feeding in two ways, they can increase the frequency of an SO driven rhythm and selectively prevent B3 spiking activity in cycles (Vehovszky and Elliott, 2001). As their name suggests, the OCs are octopamine immunoreactive (Vehovszky et al., 1998) and use octopamine as a neurotransmitter (Vehovszky et al., 2000).

Cerebral ventral 1a (CV1a) cells

The CV1a cells are a pair of bilaterally symmetrical interneurons located on the ventral surface of the cerebral ganglia between the medial lip nerve (MLN) and the superior lip nerve (SLN) (McCrohan, 1984a). The CV1as each have a single projection up the ipsilateral CBC where it enters the buccal ganglia. CV1a projects to the contralateral buccal ganglion via the buccal commissure. Activation of CV1a is able to drive fictive feeding cycles (McCrohan, 1984a, McCrohan and Kyriakides, 1989). The CV1as show greater activity in sucrose driven fictive feeding cycles than the SO, but are not

necessary for the generation of sucrose driven cycles (Kemenes et al., 2001). The CV1a cells are thought to drive fictive feeding via a monosynaptic facilitating excitatory chemical synaptic connection with the N1Ms (McCrohan and Kyriakides, 1989). Neither CV1a nor SO recruit the other into their driven rhythms (McCrohan, 1984a). The CV1as receive inhibition in the rasp phase of fictive feeding cycles; however the source of this inhibition remains unknown. During periods of quiescence, unitary IPSPs are present on CV1a, which arise from the pleural-to-buccal interneuron (Alania et al., 2004).

Cerebral ventral 1b (CV1b) cells

The CV1b interneurons are located on the ventral surface of the cerebral ganglia between the MLN and the SLN near to the CV1a interneuron (McCrohan and Kyriakides, 1989). There are thought to be two CV1bs per cerebral ganglion. Similar to CV1a, CV1b projects up the ipsilateral CBC and enters the ipsilateral buccal ganglion and then crosses the buccal commissure and enters the contralateral buccal ganglion. Activation of CV1b is able to drive fictive feeding cycles (McCrohan and Kyriakides, 1989, McCrohan and Croll, 1997), however less reliably than CV1a. CV1b differs from CV1a in that it does not receive large inhibitory inputs in the rasp phase of cycles and does not receive large unitary IPSPs during quiescence. One of the CV1bs is immunoreactive to the neuropeptide APGWamide (McCrohan and Croll, 1997), and is named the cerebral buccal white cell (CBWC) due to its white colour.

Cerebral giant cell (CGC)

The CGCs are a pair of large serotonergic bilaterally symmetrical interneurons located in the anterior lobe of each cerebral ganglion. The CGCs have projections out of the labial artery nerve (LBN) and the CBC of the cerebral ganglion (McCrohan and Benjamin, 1980a). The projection up the CBC enters the ipsilateral buccal ganglion and projects to the contralateral buccal ganglion via the buccal commissure. The CGCs have projections out of the ipsilateral DBN, posterior jugalis nerve (PJN), lateral buccal nerve (LBN), ventral buccal nerve (VBN) and PBN. The CGCs fire tonically and often synchronously with each other due to strong electrotonic coupling between the two (McCrohan and Benjamin, 1980a). Activation of a CGC is sufficient to activate fictive feeding cycles (McCrohan and Audesirk, 1987). In vivo recordings of the CGCs show that firing rates in the isolated CNS (60-120 spikes/min) are much higher than in vivo (1-20 spikes/min) (Yeoman et al., 1994b), therefore the firing rates necessary to activate fictive feeding are not physiological. The CGCs, instead, have a gating function

on the feeding network. A minimum firing rate is necessary for the SO to drive fictive feeding cycles (Yeoman et al., 1994a). The CGCs have connections with all feeding interneurons (Yeoman et al., 1996) and many of the motor neurons (McCrohan and Benjamin, 1980b).

1.3.4 Motor neurons

Fifteen motor neurons have been identified in the feeding network. B1-B10 are located in the buccal ganglia and CV3-7 are located in the cerebral ganglia. The motor neurons fire in either one or two of the phases of feeding, or during periods of quiescence. The motor neurons innervate the buccal mass, oesophagus, salivary glands and the mouth. Six buccal mass motor neurons have been identified. The B4, B4cl and B8 motor neurons innervate the AJM, The B6 and B7 motor neurons innervate the PJM and the B4cl and B10 motor neurons innervate the tensor muscles (Rose and Benjamin, 1979, Staras et al., 1998b). The B1s are thought to be salivary gland motor neurons (Benjamin et al., 1979) and the B2s are oesophageal motor neurons (Perry et al., 1998). The CV motor neurons are thought to innervate the lip and mouth muscles (McCrohan, 1984b). A summary of the firing activity of the B1-10 motor neurons is given in **Figure 1.5**.

From the above it is clear that the feeding system of *Lymnaea* has been extensively characterised, both on the behavioural and the neuronal level. The fact that *Lymnaea* perform readily observable behaviours which can be observed in vivo, recorded in semi-intact preparations and persist in a fictive form in the CNS makes it an ideal system to study decision making.

1.4 Thesis Outline

The most detailed studies of the neural mechanisms of decision making have been performed using invertebrate preparations. However most studies have focused on how two incompatible action based behaviours are chosen between based on sensory information. A behavioural paradigm was designed in order to study stimulus present and stimulus absent decision making in *Lymnaea*. Similar decision making tasks have been used in vertebrate systems, thus allowing for the comparison of invertebrate and vertebrate decision making. *Lymnaea's* internally generated food searching behaviour was used as a method to determine the animal's decision making process in response to a sensory stimulus or no sensory stimulus. *Lymnaea* were shown to be able to

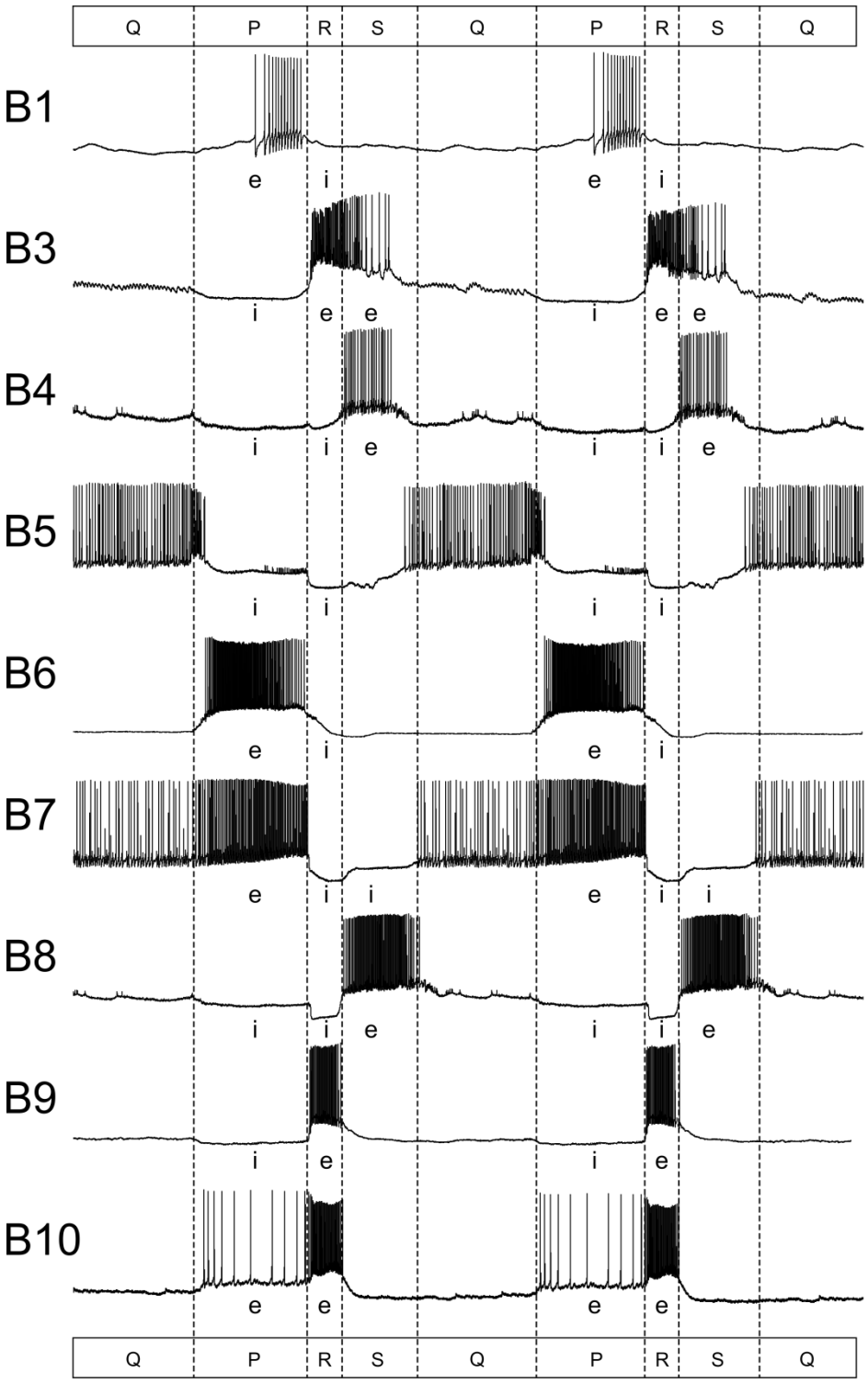

Figure 1.5 Summary diagram of firing activity of buccal motor neurons. Two fictive feeding cycles are shown. Each cycle is preceded by a period of quiescence. Each motor neuron receives either excitatory (e) or inhibitory (i) inputs during the protraction (P), rasp (R) or swallow (S) phases. The B5 motor neuron is almost exclusively active in the quiescent phase. Firing times of motor neurons from Benjamin and Rose (1979), Rose and Benjamin (1981a), Brierley et al. (1997a), Staras et al. (1998b).

reliably perform a stimulus absent and stimulus present decision. A novel interneuron, vTN, was identified as a candidate stimulus present decision neuron in Chapter 3. vTN fulfilled the two criteria necessary to be considered a stimulus present decision neuron: vTN received the appropriate input from sensory stimuli and was sufficient to activate fictive feeding. In Chapter 4 it was further investigated how vTN was able to initiate fictive feeding cycles. vTN was classified as a trigger neuron as it was able to initiate fictive feeding cycles which outlasted the duration of the stimulus to the neuron. vTN relied on activation of the CPG interneuron N1M to trigger the first fictive feeding cycle and then via a reduction in inhibition on the system for the subsequent triggered cycles. This was a novel method for initiating cycles in the feeding system of *Lymnaea*. In Chapter 5 an in vitro paradigm of the stimulus present and stimulus absent decision seen in vivo was designed. Experiments using the in vitro paradigm showed that vTN was a stimulus present decision neuron. A member of the feeding CPG, N3t, was identified as a stimulus absent decision neuron. During stimulus absent decisions, N3t activity increased and prevented the generation of further fictive feeding cycles. At the decision point of a stimulus present decision, both vTN (stimulus present neuron) and N3t (stimulus absent neuron) were simultaneously active, providing contradictory information to the system. vTN activity overcame N3t inhibition and a stimulus present decision was made. The presence of the appetitive behaviour reduced the level of vTN activity needed to trigger fictive feeding cycles. In Chapter 6, it was shown that vTN had diverse synaptic connections with all levels of the feeding network.

In Chapter 7 the neural mechanisms of the choice between two distinct rhythmic movements which use the same muscles was investigated. The two behaviours were ingestion and egestion. The egestive behaviour and its neural control have not been well studied in *Lymnaea*. A combination of behavioural experiments and semi-intact preparations was used to identify features by which they could be distinguished. A novel motor neuron was identified whose activity was a critical determinant of the motor program generated. The interneuronal control of the two behaviours was extensively studied and involved the characterisation of several new interneurons. The mechanisms underlying the choice between the two behaviours were studied by testing interactions between the two networks. Finally, vTN's role in the choice between ingestion and egestion was examined. These results provide fundamental new insights into the mechanisms of decision making.

2 Materials and methods

2.1 Animal maintenance

All experiments were carried out on adult (4–5 month old) pond snails, *Lymnaea stagnalis.* The animals were bred at the University of Sussex, where they were maintained in large holding tanks containing Cu^{2+}-free water at 18−20°C with a 12 h light-dark cycle. The snails were fed three times a week with lettuce and twice a week with vegetable fish food (Tetra-Phyll; TETRA Werke). The animals were moved to smaller holding tanks one to four days prior to experimenting. Animals used to make the whole-lip CNS preparation in Chapter 7 were starved for three days prior to experiments as this enhanced the response of the preparation to chemical stimuli (Marra, V., personal communication); all other animals were starved for one day prior to experiments. This level of satiety was chosen as animals typically produced unitary appetitive bites in the absence of sensory stimuli (see Section 3.2.1).

2.2 Electrophysiological preparations

2.2.1 Dissection of preparations

Animals were dissected under a light microscope in a Sylgard-lined dish containing normal saline (**Table 2.1**). In all preparations used, a cut was made under the mantle to remove the shell and viscera. The preparation was pinned dorsal side-up and all internal organs apart from the buccal mass were removed. For all experiments where intracellular recordings were made, the outer ganglionic sheath covering the buccal and cerebral ganglia was removed using a pair of fine forceps. The second, inner sheath was softened by application of a non-specific solid protease (Sigma, XIV) on the surface of the saline above the preparation for one minute. The preparation was then washed three times using normal saline. A description of the dissection procedure is given for each preparation below.

2.2.1.1 Isolated CNS

The CNS was isolated by severing all nerves connecting the CNS to the periphery. A short length of oesophagus was kept attached to the dorsal buccal nerve (DBN) to aid in pinning the preparation. The CNS was transferred to a recording chamber and pinned so that the ventral surface of the buccal ganglia was accessible. The pedal

commissure was cut and the ganglionic ring was pinned flat so as to expose the ventral surface of the cerebral ganglia. When it was necessary to record from neurons on both the ventral and dorsal surface of the buccal ganglia, one of the buccal ganglia was twisted 180° as described by Brierley et al. (1997a).

2.2.1.2 Radula-CNS preparation

All nerves linking the CNS to the periphery were severed apart from the post buccal nerve (PBN) connecting to the buccal mass. The buccal mass was cut away from the mouth and the buccal mass and CNS transferred to a recording chamber. The CNS was pinned as in the isolated CNS preparation, except the buccal ganglia were never twisted 180°. An incision was made anteriorly from the oesophagus to the dorsal mandible, exposing the odontophore and radula. The external muscles of the buccal mass were pinned flat to stabilise the preparation, allowing for the application of tactile stimuli to regions of the radula whilst recording intracellularly from neurons in the buccal ganglia. A photo of the Radula-CNS preparation is shown in **Figure 2.1A**.

2.2.1.3 SLRT-CNS preparation

The supralateral radula tensor-CNS (SLRT-CNS) preparation was similar to the Radula-CNS preparation; however the ventral buccal nerve (VBN) was left connecting the CNS to the buccal mass rather than the PBN. This allowed for extracellular suction electrode recordings of the SLRT muscle and intracellular recordings from neurons in the buccal ganglia.

2.2.1.4 Whole-lip CNS preparation

The whole-lip CNS preparation consisted of the CNS attached to the lips, tentacles and an anterior section of the foot via the medial lip nerves (MLNs), superior lip nerves (SLNs) and tentacle nerves (TNs). All peripheral projections from the CNS to the buccal mass were severed and the buccal mass removed. The preparation was transferred to a recording chamber where the anterior foot was pinned down. The buccal ganglia were pinned ventral surface up on a raised Sylgard block. This preparation allowed for the perfusion of chemical stimuli to the lips and tentacles whilst recording intracellularly from neurons in the buccal ganglia. In some experiments, the whole-lip CNS preparation was prepared and pinned in the recording chamber as above, but once pinned the MLNs, SLNs and TNs were severed. This was to test

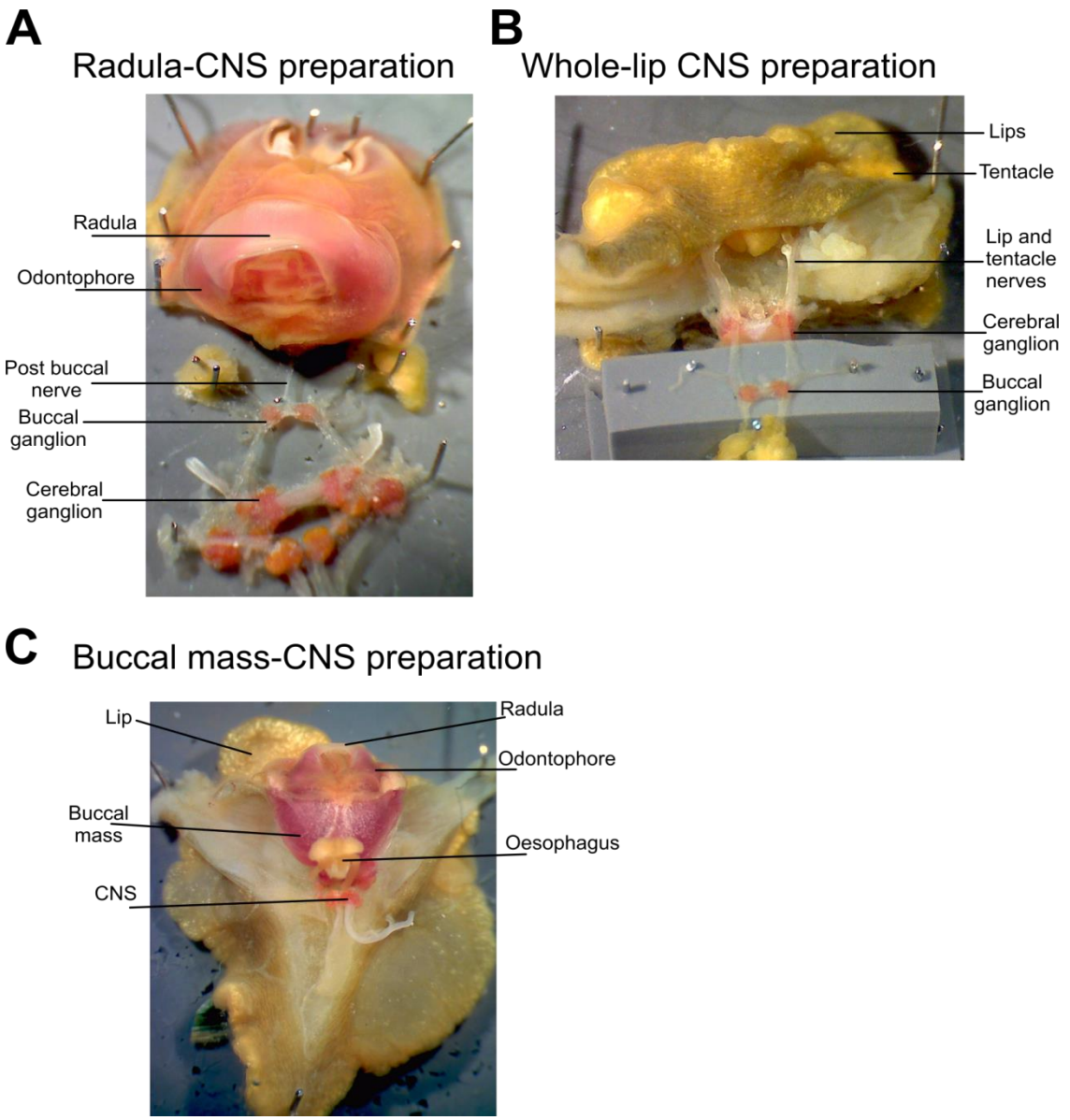

Figure 2.1 Preparations used for electrophysiology and observations of movements of the odontophore/radula complex. **A.** The Radula-CNS preparation consists of the CNS attached to the odontophore and radula via the PBN. The external muscles of the buccal mass are pinned to the Sylgard dish as are the other buccal nerves. This preparation allowed for intracellular recordings of neurons within the buccal ganglia whilst applying a tactile stimulus to regions of the radula. **B.** The whole-lip CNS preparation consists of the CNS attached to the lips and tentacles via the SLNs, MLNs and TNs. A portion of the anterior foot was also kept attached which was pinned to the Sylgard to anchor the preparation. The buccal ganglia were pinned on a raised Sylgard platform ventral surface up. This preparation allowed for intracellular recordings from buccal neurons whilst chemical sensory stimuli were applied to the lips. **C.** Buccal mass-CNS preparation. This preparation was used to observe movements of the buccal mass and odontophore during the application of chemical sensory stimuli to the lips. It was not possible to record intracellularly from neurons in this preparation. All peripheral nerves were left intact apart from those leaving the visceral and parietal ganglia. The oesophagus was cut away from the buccal mass and an incision made from the opening towards the mouth, exposing the odontophore and radula.

whether the chemical stimuli used in Chapter 7 were activating chemosensory neurons in the lips or having a direct effect on the CNS. A photo of the Whole lip-CNS preparation is shown in **Figure 2.1B**.

2.2.1.5 Buccal mass-CNS preparation

The buccal mass-CNS preparation consisted of the CNS, lips and buccal mass and the entire foot. The oesophagus was cut away from the buccal mass but left attached to the buccal ganglia via the dorsal buccal nerve (DBN). An incision was made from the start of the oesophagus anteriorly towards the dorsal mandible, exposing the odontophore and radula. Many of the nerves connecting the cerebral and pedal ganglia to the periphery were left intact. This preparation allowed for the application of chemical stimuli to the lips and tentacles whilst observing movements of the odontophore and radula. A photo of the Buccal mass-CNS preparation is shown in **Figure 2.1C**.

2.3 Identification of neurons

Several identified feeding motor neurons and interneurons were routinely recorded in the buccal and cerebral ganglia. The large buccal motor neurons B1, B2, B3 and B4 could often be identified by their size and location. Other neurons had to be identified by their characteristic endogenous properties, firing patterns and synaptic connections (Rose and Benjamin, 1981a, 1981b, McCrohan, 1984a, Elliott and Benjamin, 1985a, 1985b, McCrohan and Kyriakides, 1989, Yeoman et al., 1995, Brierley et al., 1997a, 1997c, Vehovszky and Elliott, 2001). A single N1M interneuron is located in each buccal ganglion beneath the surface between the B1 and B2 motor neurons (Kemenes and Elliott, 1994). N1M could be distinguished by its characteristic plateau potential when injected with positive current. Activation of N1M was sufficient to drive fictive feeding cycles. The SO is a single interneuron located in either the left or right buccal ganglion (Elliott and Benjamin, 1985b). Similarly to N1M, SO was located between the B1 and B2 motor neurons, however SO was located more superficially than N1M. N1L interneurons are located laterally of the B1 motor neuron (Yeoman et al., 1995). Activation of either SO or N1L was able to drive fictive feeding cycles.

The rasp phase interneurons N2d are located anteriorly of the B2 motor neuron and could be identified by their activity and large spikes in the rasp phase (Elliott and Benjamin, 1985a). The N2v interneurons are located medially on the ventral surface (Brierley et al., 1997a). Depolarising N2v caused a characteristic plateau potential as

well as wide spread synaptic inputs on many follower neurons. The N3p interneurons are located between the B2 and B3 motor neurons (Elliott and Benjamin, 1985a). Action potentials in N3p interneurons caused large unitary IPSPs on the B4 motor neuron and a large depolarisation of B3. The N3t interneurons are located anterior to the B1 motor neuron (Elliott and Benjamin, 1985a). They were often identified via their unitary 1:1 EPSPs on the B3 motor neurons. The OC interneurons are located near the buccal commissure (Vehovszky et al., 1998). They fired in the swallow phase of fictive feeding cycles and activation of an OC caused a large inhibitory input to the B3 motor neuron. The smaller motor neurons, B5, B7, B9 and B10 were identified based on their firing patterns in fictive feeding cycles and synaptic inputs they received from CPG interneurons.

The CV1a interneurons are located on the ventral surface of the cerebral ganglia in the CV region (McCrohan, 1984a). Activation of CV1a was able to drive fictive feeding cycles. CV1a could be distinguished from other cells in the CV region by large unitary IPSPs which occurred during periods of quiescence. The CV1bs are located more posteriorly in the CV region than CV1a (McCrohan and Croll, 1997). There are thought to be two CV1bs per cerebral ganglion, however no distinction was made between the two in this study. One of the CV1bs has a characteristic white colour. Activation of CV1b was often able to drive fictive feeding cycles. The CV3 motor neurons are located adjacent to CV1b and were identified by their firing pattern. The CGCs are a pair of large bilaterally symmetrical CBIs located in the anterior lobe of the cerebral ganglia. They can often be visually identified via their size and location.

2.4 Intracellular recording and data acquisition

Microelectrodes were pulled from borosilicate glass capillaries with filaments (Harvard Apparatus, 1.16 mm inner diameter, 2 mm outer diameter) using a vertical puller (Narishige) to a resistance of between 10-40 MΩ when filled with 4M potassium acetate. To aid in impalement, the tips of the electrodes were dipped in black drawing ink (Rotring). The electrodes were attached to headstage preamplifiers (Axoclamp and Neurolog) which were mounted on micromanipulators. Four micromanipulators were positioned around the preparation, allowing for up to four neurons to be simultaneously recorded. Signals were fed into amplifiers. The amplifiers used were Axoclamp 2B (Axon Instruments) and Neurolog NL 102 (Digitimer Ltd). The signal from the amplifiers was digitalized using a MICRO 1401 mk II (CED) analogue to digital converter. The signal from the second channel of the Axoclamp was amplified before digitalisation

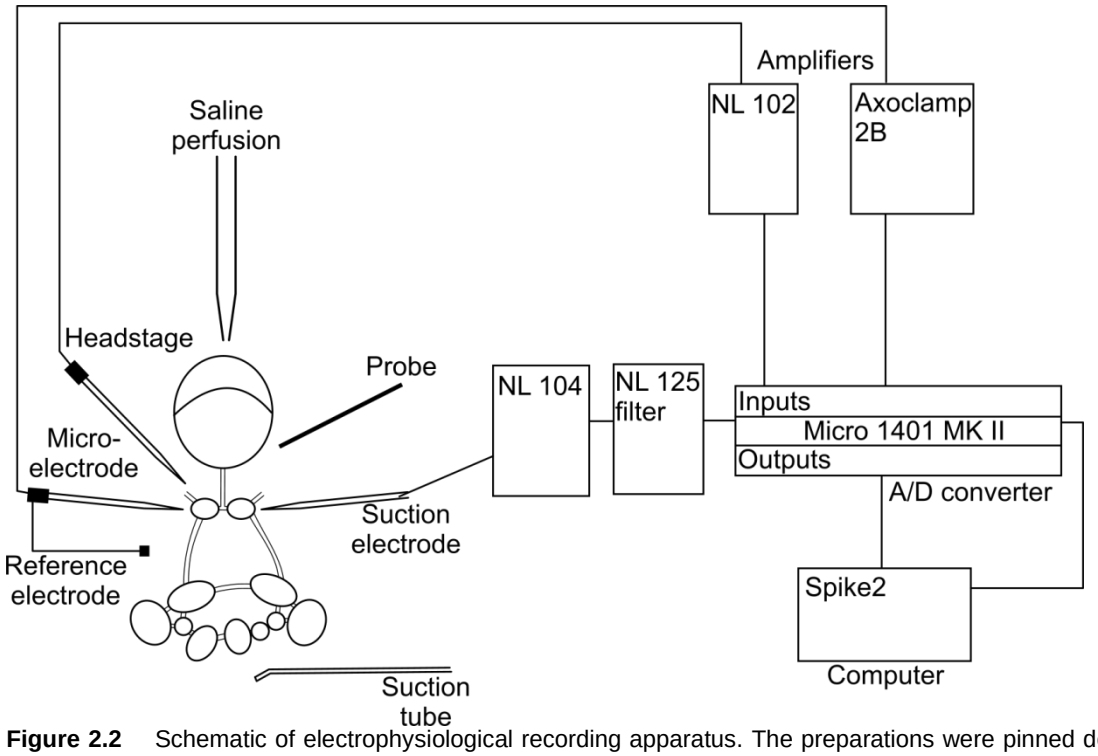

Figure 2.2 Schematic of electrophysiological recording apparatus. The preparations were pinned down in a recording chamber and perfused with saline using a gravity fed perfusion system. The microelectrodes containing 4M potassium acetate were mounted in headstages which were held by micromanipulators. The headstages were connected to the amplifiers. The amplifiers connected to an analogue to digital converter, which digitalised the signal. This was visualised and stored using a computer. A silver chloride pellet was immersed in the saline and was connected to the ground plug of one of the headstages and was the reference electrode. Suction electrodes used for muscle recordings were connected to an amplifier and the signal from this was filtered before being fed into the A/D converter and then into the computer. A probe was attached to one of the micromanipultors in order to apply tactile stimulation to the radula.

using a non-inverting operational amplifier circuit with a gain of 10. The digital signals were fed into a PC running Spike2 version 5.14 software (CED). The preparation was illuminated using a cold light source and viewed under a binocular microscope (Wild Heerbrugg). A schematic of the electrophysiological recording apparatus is shown in **Figure 2.2**.

2.5 Extracellular muscle recording

The SLRT muscle was recorded in the SLRT-CNS preparation (Section 2.2.1.3). A suction electrode was made by pulling a glass pipette using a vertical puller. The tip was cut off with a diamond tipped cutter and fire polished to smooth the edges. The electrode was filled with normal saline and a region of the SLRT muscle sucked into it using a 50 ml syringe attached to the other end of the electrode. A silver wire was inserted into the electrode and this was connected to one input of a Neurolog 104 A.C difference amplifier with 10K gain (Digitimer). The other input was connected to a silver wire in contact with the saline in the recording chamber. The amplifier was connected to a Neurolog 125 (Digitmer) high frequency filter at 10kHz and a 50Hz notch. The signal was digitised and visualised similarly to the intracellular recording signal. Extracellular muscle recordings were performed synchronously with intracellular neuron recordings.

2.6 Iontophoretic dye-filling of neurons

Neurons were filled with a fluorescent dye allowing for the morphology of the cell to be determined. Microelectrodes were made as in Section 2.4. The electrode was placed blunt end first in either 5(6)-carboxyfluorescein (5-CF) or AlexaFluor 568 (Molecular probes), which passed up the capillary to fill the tip of the electrode. The electrode was then filled with 4M potassium acetate and a chlorinated silver wire immersed in the solution. This was then connected as in Section 2.4. Once the neuron of interest was impaled, a pulse generator was used to apply regular interval negative current pulses into the neuron for >30 minutes. The preparation was then left over night at 4°C. Images of the neurons were taken using a digital camera (Andor Ixon EMCCD) mounted on a Leica stereomicroscope using 470 nm excitation (CoolLED) and 520/10 emission or by using a laser-scanning confocal microscope (Olympus BX51WI, FV300) with 488 nm Argon or 543 nm HeNe laser for excitation and 520/10 nm or 600LP nm for emission.

2.7 Modified salines

The majority of experiments were performed in normal HEPES-buffered saline (**Table 2.1**). Two modified salines were used to confirm synaptic connections. High divalent (HiDi) saline contained a higher concentration of the divalent cations calcium and magnesium than normal saline (**Table 2.1**). HiDi saline reduces polysynaptic connections by raising the spike threshold in intermediate cells. In general, only monosynaptic connections persist after perfusion of HiDi saline for >30 minutes. High Magnesium Zero calcium saline (HiLo) + EGTA is used to block chemical synaptic transmission (**Table 2.1**). Chemical synaptic transmission relies on the presence of calcium, therefore, in the absence of calcium, only electrotonic connections persist. Therefore any connections which persist after perfusion with HiLo saline for >40 minutes are likely to be mediated by electrotonic synapses. Salines were perfused onto the CNS via an inlet tube near the buccal ganglia. A suction tube connected to a Gilson peristaltic pump was positioned towards the visceral ganglion to remove excess saline.

Compound	Normal (mM)	HiDi (mM)	HiLo + EGTA (mM)
NaCl	50.0	35.0	35.0
KCl	1.6	2.0	1.6
$MgCl_2.6H_2O$	2.0	8.0	18.0
$CaCl_2.2H_2O$	3.5	14.0	0.0
HEPES	10.0	10.0	10.0
EGTA	0.0	0.0	2.0

Table 2.1 Composition of salines. Normal saline was used for most of the electrophysiological experiments. HiDi saline, which contains high concentrations of both Ca^{2+} and Mg^{2+}, reduces the excitability of polysynaptic connections and is used to test for monosynaptic connections. HiLo saline contains high concentration of Mg^{2+} and zero Ca^{2+} and the calcium chelator EGTA. The absence of Ca^{2+} blocks chemical synaptic transmission and the saline is used to test for electrotonic synaptic connections.

2.8 Tactile and chemical stimulation

To determine the response of neurons to tactile stimulation of the radula, a fire polished pipette was used as a probe. The probe was mounted on a micromanipulator allowing for tactile stimulation of specific regions of the radula.

Chemical stimuli and normal saline were applied to the lips of the whole-lip CNS preparation via an inlet tube placed next to the lips. Normal saline was perfused onto the CNS throughout via a separate inlet tube near the buccal ganglia. Two suction tubes were placed on either side of the lips to ensure rapid removal of the chemical stimuli from the preparation after application. A 0.69% sucrose solution was used to initiate ingestive motor programs in Chapter 7. Previous work has shown this concentration is sufficient to elicit ingestive motor programs in vivo and in vitro (Kemenes et al., 2006). A 0.1% amyl acetate (AA) solution was used to elicit egestive motor programs in Chapter 7. Previous work has shown that 0.02% concentration AA is able to inhibit spontaneous fictive feeding cycles in vitro (Straub et al., 2006). A higher concentration was used in Chapter 7 as it was found to be reliable at eliciting egestive motor programs in vivo. The same concentration was used in vitro. Sucrose and AA were dissolved in Cu^{2+} free water for in vivo experiments and in normal saline for in vitro experiments.

2.9 Perceptual decision making behavioural trials

In the perceptual decision making behaviour trials, animals to be tested were removed from holding tanks and kept in smaller containers in Cu^{2+} free water. Three snails were kept per container and each was numbered in order to compare responses to different stimuli. Animals were tested in five trials. Before each trial, the animals were starved for a single day as *Lymnaea* produce fewer appetitive bites under these conditions (Tuersley, 1989, Staras et al., 2003). During a trial the animal was removed from the container and placed in a custom built chamber (**Figure 2.3**). The chamber consisted of three Sylgard platforms glued to a plastic dish. The snail was placed between the platforms with its foot facing upwards. The dish was then filled with Cu^{2+} free water sufficiently so as to just submerge the snail. A length of tube was used to hold the snails shell in place and prevent the snail from moving. This set up allowed for the application of sensory stimuli to the mouth of the snail whilst being able to fully observe movements of the feeding structures. *Lymnaea* often feed whilst floating across the surface of the water, therefore the experimental design allowed for them to feed in a behaviourally relevant manner. The snails were left to acclimatise for 10 minutes after being placed in the dish. Within this time period, all animals fully extended out of their shell. The trial lasted up to 50 minutes from the end of the 10 minute acclimatisation. The snails were tested under five conditions. In the first condition the snails received no sensory stimuli throughout the 50 minutes and the number of appetitive bites that each

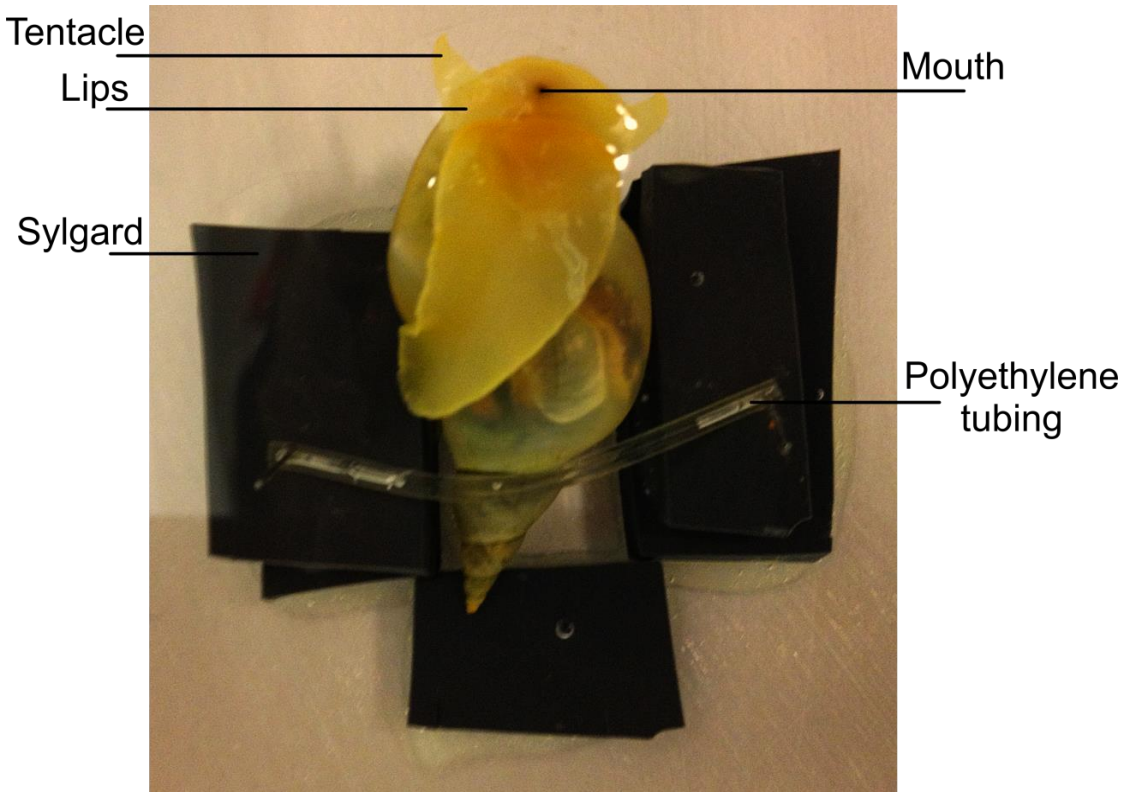

Figure 2.3 Chamber used for observing feeding behaviours in *Lymnaea*. Snails were place between three pieces of sylgard upside down so as that their mouth was accessible for observation and application of sensory stimuli. The snail was held in place by a loop of polyethylene tubing across the shell. The chamber was filled with Cu^{2+} free water so as that the head and foot of the animal were covered. All experiments were recorded by a camera which was mounted above the chamber.

animal performed was counted. In the second trial, during an appetitive bite, a piece of solid lettuce (2 mm by 1 mm) was placed in the animal's mouth. This was repeated again after ~20 minutes. In the third trial, the solid lettuce was replaced by a tactile probe. The tactile probe consisted of a 1 ml syringe whose tip had been heated and pulled into a fine point. The tactile probe was placed in the animal's mouth as in the solid lettuce trial. The tactile probe trial was repeated up to 5 times in 50 minutes. In the fourth trial a drop of lettuce juice was applied to the animal's mouth during an appetitive bite. In the fifth trial a drop of lettuce juice was applied to the animal's mouth but in the absence of an appetitive bite. The lettuce juice was presented up to two times in the 50 minute trial.

After each trial, the snail was placed in a fresh container of Cu^{2+} free water with lettuces leaves in it. Snails were allowed to eat *ad libitum* for a day after each trial. They were then starved for a single day before the next trial. To ensure that the order of the trials did not affect the results, each group of three snails performed a different trial on each test day. Therefore on the first test day, Group 1 received the no sensory stimuli trial, Group 2 the solid lettuce trial, Group 3 the tactile stimulus trial, Group 4 the lettuce juice trial and Group 5 the lettuce juice no appetitive bite trial. All behavioural experiments were videoed using a Kodak digital camera. The videos were analysed using ImageJ software (ImageJ) and Spike2 software (CED). During the behavioural experiments, bites which occurred within 6 s of the previous bite were considered associated with the previous bite. *Lymnaea* can perform a bite every 3-5 s in the presence of a sensory stimulus (Dawkins, 1974, Kemenes et al., 1986, Large et al., 2006). A value 1 s longer than the rates previously reported was chosen in this study to ensure that no associated bites were missed. The number of associated bites which occurred after an appetitive bite were counted in all of the behavioural trials. The first appetitive bite was always discounted, and only the number of subsequent related bites counted. The duration from the onset of the appetitive bite until the onset of the consummatory bite was measured in the solid lettuce, tactile stimulus and lettuce juice trial, whereas in the lettuce juice in the absence of appetitive bite trial the onset of a consummatory bite was measured from the application of the stimulus.

2.10 Analysis of data

Data was analysed using GraphPad Prism 5 (Graphpad Software) and expressed as means ± SEM. Each 'N' represents an individual preparation unless stated otherwise. Normality was tested using the D'Agostino and Pearson omnibus normality test. Non-

parametric tests were used when the distribution was found to be not normal or when there was insufficient information on the nature of the population distribution. Two group statistical comparisons were performed using t-test statistics (either paired or unpaired as stated in the text). Data with more than two groups were first analysed using either a One-way ANOVA for unpaired samples or One-way Repeated-measures ANOVA or a Friedman test for paired samples. Subsequent comparisons were performed using Dunnett's or Tukey's multiple comparison tests or Dunns test. Pearson's correlation was used in Chapter 4 to examine whether a statistical relation could be found between the number of cycles triggered by vTN and the duration of the stimulus applied to vTN. The significance level was set at $P < 0.05$ (*** $P < 0.001$; ** $P < 0.01$; * $P < 0.05$; NS $P > 0.05$). All graphs show mean and SEM.

3 Stimulus absent and stimulus present decision making in *Lymnaea*

3.1 Introduction

The aim of this chapter was to design a simple decision making task which was amenable for in vitro experiments in order to identify the neural mechanisms of decision making in a well characterised neural network. In order to gain effective insights into the neural mechanisms of decision making, an appropriate system and behaviour needs to be selected. Ideally the decision being made should be readily observable and, for ease of quantification, have only two easily distinguishable possible outcomes, Decision 1 or Decision 2. One of the simplest forms of decision making is decision making about the presence or absence of a stimulus (see Section 1.1.3). This involves the subject receiving either a stimulus or no stimulus. A report must then be made about whether a stimulus is perceived to be present (decision 1) or absent (decision 2).

The feeding behaviour in *Lymnaea* consists of both appetitive and consummatory behaviours. Both consist of the same motor program, or bite, during which the toothed radula is protracted and retracted out of and subsequently back into the mouth. Consummatory programs consist of a bout of high frequency bites in the presence of the food stimulus. Their function is to bring food into the buccal cavity to be ingested. They can be initiated from quiescence by the application of food to the mouth region. Appetitive bites occur in the absence of a sensory stimulus and are goal-directed behaviours performed with the aim of locating a food source (Tuersley and McCrohan, 1987).

A number of studies have examined how a chemical stimulus is able to initiate the consummatory behaviour from quiescence, and the neural mechanisms are well characterised (Kemenes et al., 1986, 2001, Staras et al., 2003). However, how the switch from the appetitive bite program to the consummatory bite program in the presence of a sensory stimulus is made has not been examined. As the appetitive bite program is performed with the aim of locating food, a mechanism must exist by which the animal judges the presence or absence of food and performs the appropriate action. This represents a perceptual decision about the presence or absence of a sensory stimulus. Therefore a simple behavioural paradigm was designed to investigate the mechanisms of this decision. This allowed for the development of a

novel semi-intact preparation and the identification of candidate decision neurons for the stimulus present decision.

3.2 Results

3.2.1 Perceptual decision making about the presence or absence of a stimulus in *Lymnaea*

To characterise the decision to switch from the appetitive to the consummatory bite program, behavioural experiments were designed in which the two could be separated, and the switch between them clearly distinguished. Preliminary experiments were carried out where animals were starved for a single day before testing. They were found to produce unitary appetitive bite programs in the absence of sensory stimuli, as seen in **Figure 3.1**. In this trace two appetitive bite programs were produced in the absence of any sensory stimuli. The animal enters back into a period of quiescence after each appetitive bite before a subsequent appetitive bite is performed. This represented a stimulus absent trial. Therefore *Lymnaea* could correctly judge the absence of a sensory stimulus. Placing a piece of solid lettuce into the animal's mouth during an appetitive bite program resulted in a switch to the consummatory bite program, which consisted of high frequency bites in the presence of the food (**Figure 3.1**). This represented the stimulus present trial. Therefore *Lymnaea* could correctly judge the presence of a sensory stimulus and convert the single appetitive bite into consummatory bites. The expression of the appetitive bite program as unitary behaviours facilitated the distinction of the appetitive and consummatory bites. This simple behavioural paradigm provided evidence that *Lymnaea* can successfully perform a perceptual decision about the presence or absence of a sensory stimulus.

A series of experiments were carried out to further test and characterise the decision process involved. One important question was which sensory modality of the solid lettuce was important for the animal to make the judgement about the presence of the food. Identifying the sensory pathway would aid in later identification of candidate decision neurons.

Fifteen animals were starved for one day before each trial. In the first trial the animals were placed in a testing chamber for ~one hour where they received no sensory stimulus (NSS) (**Figure 3.2Ai**). This represented the stimulus absent trial. They were left to acclimatize to the new surrounding for 10 minutes and then the number of appetitive bites produced was counted. *Lymnaea* can perform a bite every 3-5 s in the

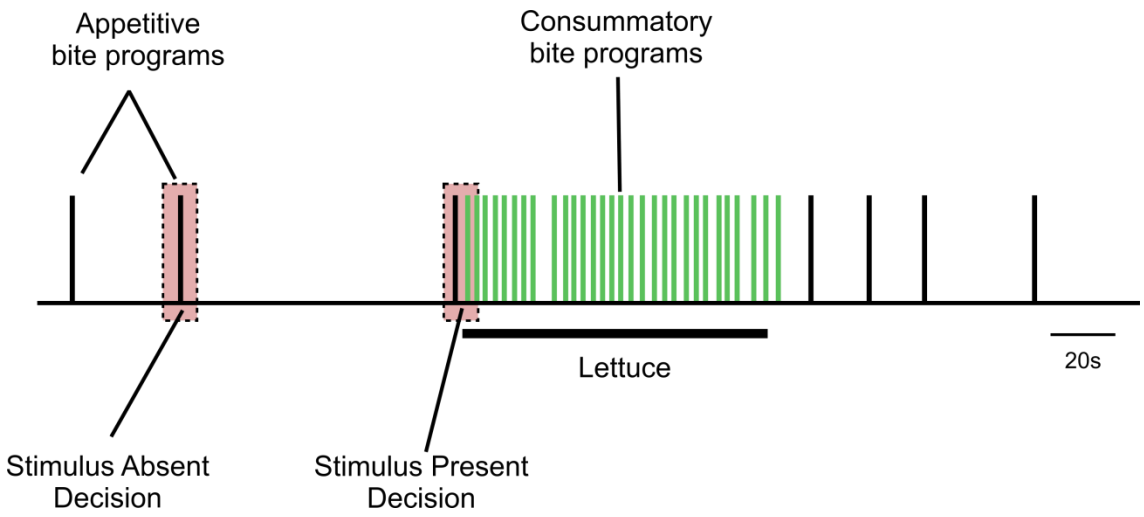

Figure 3.1 *Lymnaea* performing a perceptual decision about the presence or absence of a sensory stimulus. A behavioural trace showing both the appetitive and consummatory behaviours in *Lymnaea*. Two appetitive bites are elicited. During the appetitive bite no sensory stimulus was encountered and the animal enters back into a period of quiescence. This represents the stimulus absent trial and the correct decision about the absence of a sensory stimulus. During the third appetitive bite, a piece of solid lettuce was placed in the animal's mouth. The animal switched into the consummatory bite program, which occurred at a high frequency. This represents the stimulus present trial and the correct decision about the presence of a sensory stimulus. Appetitive bites are represented by black lines. Consummatory bites are represented by green lines. Each line represents the start of a bite only, not the entire duration of the bite.

presence of a sensory stimulus (Dawkins, 1974, Kemenes et al., 1986, Large et al., 2006). In these experiments, if a bite occurred within 6 s of the previous bite then it was considered to be associated with it. This value was used to ensure no associated bites were missed. The average number of bites within 50 minutes was 17.4 (±4.0). We looked at whether or not an associated bite occurred after the appetitive bite in a binary manner, where 0 represented no associated bites and 1 represented an associated bite. This quantification was used to determine whether appetitive bites occurred in isolation in the absence of a sensory stimulus. On average, 24% (±4) of appetitive bites had a bite which was associated with them in the absence of a sensory stimulus. The average total number of associated bites after the first appetitive bite was 0.47 (±0.1). Therefore at this level of satiety, *Lymnaea* typically produced unitary appetitive bite programs during the stimulus absent trials. This was in agreement with the results seen in the pilot studies. Therefore, in the presence of a sensory stimulus, bites performed after an appetitive bite can be considered consummatory bites.

In the second trial, during an appetitive bite, a piece of solid lettuce (SL) (2mm by 1mm) was placed in the animal's mouth (**Figure 3.2Aii**). This represented a stimulus present trial. As the radula was brought forward in the rasp stroke, the SL was bitten upon. The animal switched into an on-going consummatory behaviour. 100% of appetitive bites had an associated bite in the presence of the SL. The average number of consummatory bites elicited within 40 seconds of the appetitive bite was 13.07 (±0.7).

It was next tested which sensory modality was important for the stimulus present decision which brought about the switch of behaviours. The lettuce contains both a chemical and a tactile cue. The contribution of the two was separated by applying either a purely chemical stimulus or a purely tactile stimulus during the appetitive bite of separate trials. The chemical stimulus consisted of lettuce juice (LJ). A single drop was applied to the mouth during an appetitive bite, at a similar time point as the SL was applied. Only 49% (±10) of appetitive bites had an associated bite which followed within 6 s. However, the application of LJ to the lips always caused a high frequency bout of consummatory bites, even if there was a delay from the appetitive bite until the first consummatory (**Figure 3.2Aiii**). The average number of associated consummatory bites elicited within 40 seconds of the appetitive bite was 12.03 (±0.6). A tactile stimulus (TS) was placed in the animal's mouth during an appetitive bite, to mimic the tactile properties of the lettuce (**Figure 3.2Aiv**). It was removed when the next bite was produced. This was also able to initiate consummatory bite programs. 100% of

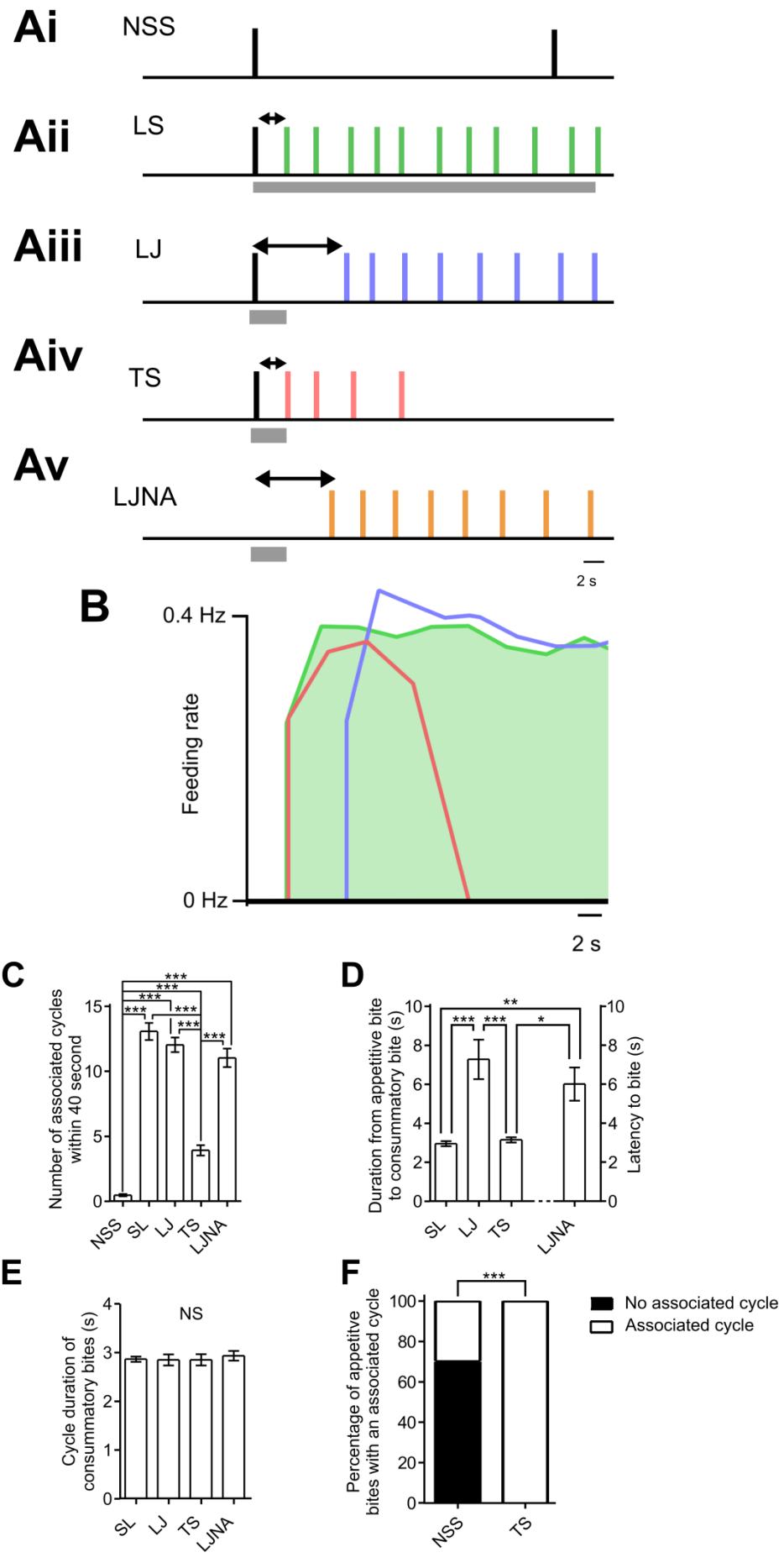
Ai
NSS
Aii
LS
Aiii
LJ
Aiv
TS
Av
LJNA
2 s
B
0.4 Hz
Feeding rate
0 Hz
2 s
C
Number of associated cycles within 40 second
NSS
SL
LJ
TS
LJNA
D
Duration from appetitive bite to consummatory bite (s)
Latency to bite (s)
SL
LJ
TS
LJNA
E
Cycle duration of consummatory bites (s)
NS
SL
LJ
TS
LJNA
F
Percentage of appetitive bites with an associated cycle
No associated cycle
Associated cycle
NSS
TS

Figure 3.2 Perceptual decision making in a goal-directed behaviour. **Ai**. In the absence of sensory stimuli, *Lymnaea* perform unitary appetitive bites. Appetitive bites are represented by a black line on the behavioural trace. **Aii**. During an appetitive bite, SL was placed in the animal's mouth. This caused the animal to switch into on-going high frequency consummatory bite programs. The latency of the decision about the presence of a sensory stimulus is the time from the appetitive bite until the onset of the next bite program. Green lines represent consummatory bites elicited by SL. **Aiii**. During an appetitive bite, a drop of LJ was applied to the mouth region. This caused a switch into the consummatory behaviour. Blue lines represent consummatory bites due to LJ application. **Aiv**. During an appetitive bite, TS was placed in the animal's mouth. This was removed when the next bite was initiated. This initiated consummatory bites. Red lines represent consummatory bites elicited by the TS. **Av**. In the absence of an appetitive bite LJ (LJNA) was applied to the mouth region. This initiated consummatory bite programs. Orange lines represent consummatory bites elicited by LJNA. Each line in the behavioural traces represents the start of a bite only, not the entire duration of the bite. **B**. The frequency of consummatory bites elicited by the SL, LJ and TS were plotted together. The onset of the first consummatory bite, which represents the time course of the decision about the presence of a sensory stimulus, is closely matched in the SL and TS trials. The LJ, although able to initiate consummatory bites, is characterised by a delayed onset from the appetitive bite. Data grouped into bins of 3.5 s. **C**. Mean number of associated cycles within 40 seconds of the appetitive bite, or after application of the stimulus in LJNA trail, under each condition. Significantly more cycles were initiated by all sensory stimuli over NSS trials. SL, LJ and LJNA produced significantly more consummatory bites than TS. **D**. Mean duration from appetitive bite to consummatory bite, or latency to first consummatory bite in LJNA trial. No difference was found between the SL and TS trials, or LJ and LJNA trials. There was a significant increase in duration of the LJ vs. the SL and TS and the LJNA vs. the SL and TS. **E**. Mean cycle duration of consummatory bites showing that no difference was present between the feeding rates of the different conditions. **F.** Percentage of appetitive bites which occurred in isolation or had an associated bite in the NSS trial and the TS trial. A significant difference was present between the two indicating that the animals were able to make a judgement about the presence or absence of a sensory stimulus. Abbreviations: NSS, no sensory stimulus; SL, solid lettuce; LJ, lettuce juice; TS, tactile stimulus; LJNA, lettuce juice no appetitive. * $P < 0.05$, ** $P < 0.01$, *** $P < 0.001$, NS not significant.

appetitive bites were followed by an associated bite due to the TS. The average number of associated consummatory bites produced was 4.00 (±0.4).

As a chemical stimulus has previously been shown to be able to initiate consummatory bites in the absence of an appetitive bite, it was tested whether the lettuce juice was sufficient to do this. Lettuce juice was applied to the mouth region of the animal during a period of quiescence (**Figure 3.2Av**). Lettuce juice in the absence of an appetitive bite ('Lettuce juice – no appetitive' LJNA) was able to initiate consummatory bites. The average number of associated consummatory bites was 11.03 (±0.7). A Repeated-measures ANOVA showed that there was a significant difference in the number of bites produced between the conditions (**Figure 3.2C**) (Repeated-measures ANOVA: $F[4,14] = 107.1$, $P < 0.0001$). Post-hoc analysis using a Tukey's Multiple Comparison Test revealed that all stimulus conditions produced significantly more bites than the NSS ($P < 0.001$ for all comparisons). There were also significantly more consummatory bites elicited in the SL, LJ and LJNA trials over the TS trial ($P < 0.001$ for all comparisons). There was no significant difference between the SL, LJ and LJNA trials ($P > 0.05$ for all comparisons).

These experiments therefore provide evidence that both the chemical and tactile cues are able to initiate consummatory bites independently of each other. The temporal characteristics of the decision to switch from appetitive to consummatory bites were next analysed by measuring the duration from the appetitive bite until the first consummatory bite. This represents the 'decision point' at which the animal makes the judgement about the presence of food. The duration from the appetitive to the consummatory bite occurs within 3.00 (±0.1) seconds in the SL trial. The switch occurred within 7.29 (±1.0) seconds in the LJ trail and within 3.15 (±0.1) seconds in the TS trial. In the LJNA trial, the latency to bite from the application of the stimulus to the mouth was measured. The latency to bite was 6.00 (±0.9) seconds. A significant difference between the durations was present (**Figure 3.2D**) (Repeated-measures ANOVA: $F [3,14] = 12.03$, $P < 0.0001$). Post hoc analysis using a Tukey's Multiple Comparison Test revealed that the switch from appetitive to consummatory bite was significantly longer in the LJ trial vs. the SL and the TS (LJ vs. SL $P < 0.001$, LJ vs. TS $P < 0.001$). No difference was found in the duration to switch between the SL and the TS (SL vs. TS $P > 0.05$). There was also a significant increase in the latency to bite in the LJNA trial compared with the duration to switch behaviour in both the SL and the TS trials, whereas no difference was found with the LJ (LJNA vs. SL $P < 0.01$, LJNA vs. TS $P < 0.05$, LJNA vs. LJ $P > 0.05$). It was possible that LJ simply produced a much slower consummatory bite rate, which could account for the delayed consummatory

bite initiation. However this was an unlikely explanation due to the high number of associated consummatory bites produced within 40 seconds. This was shown to not be the cause of the delay as there was no significant difference between the cycle duration of the consummatory bites of the different stimulus conditions (**Figure 3.2E**) (Repeated-measures ANOVA: $F [3,14] = 0.17$, $P > 0.05$). The cycle duration was measured as the time from the onset of the protraction phase until the onset of the subsequent protraction phase. This result suggests that all stimuli are eliciting a similar type of consummatory bite program.

It seems therefore that the temporal characteristics of the decision made in the SL trial are most faithfully mimicked by the TS. This is most evident in the frequency plot of the averaged data from all 15 animals in the SL, LJ and TS trials (**Figure 3.2B**). Although LJ was able to elicit consummatory bites, there was a significant delay until the onset of the consummatory bites. This delay, on average, exceeded the time limit (see earlier) for considering it to be associated with the appetitive bite, and this is evidenced by the low percentage of appetitive bites which had an associated bite due to the LJ. This suggests these bites were in fact not related to the appetitive bite. This was confirmed in the LJNA trial. A similar delay from the application of the stimulus until the onset of the consummatory bites was also present. Therefore the chemical stimulus is able to initiate consummatory bites independently of appetitive bites. However, it is not important for the early judgement about the presence of food which brings about the switch from appetitive to consummatory bites seen in the SL trials. These results suggest that the animal uses the tactile properties of food during an appetitive bite to make the judgment about the presence of food and switch into the consummatory behaviour.

Lymnaea's reliability at performing the stimulus absent/stimulus present task was further analysed by performing a Fisher's exact test on the pooled data to establish whether an appetitive bite occurred in isolation or was followed by an associated bite for the NSS trial (115 appetitive bites in isolation, 50 appetitive bites followed by an associated bite) compared with the TS trial (0 appetitive bites in isolation, 51 appetitive bites followed by an associated bite). A significant difference between the two was revealed ($P < 0.0001$) (**Figure 3.2F**). This result, combined with the finding showing that the TS elicited significantly more associated bites than the NSS trial (**Figure 3.2C**), confirmed that *Lymnaea* was reliably able to make a judgement about the absence or presence of a sensory stimulus based on no stimulus or a tactile stimulus respectively.

These experiments provided a simple behavioural paradigm in which to study perceptual decision making about the presence or absence of a sensory stimulus in *Lymnaea*. Stimulus absent decisions are made in the absence of a sensory stimulus and reported by the animal entering back into quiescence. During stimulus present decisions, tactile cues are used to make the judgement about the presence of the stimulus and are reported by the switch from the appetitive bite to consummatory bites. This facilitated the identification of the sensory pathway and candidate decision neurons involved in the decision making process.

3.2.2 Identification of candidate stimulus present neurons

The behavioural experiments demonstrated that the main sensory modality in the decision to switch from appetitive to consummatory bite programs was the tactile properties of the food. It was therefore necessary to identify the sensory structures which received the most stimulation from the TS in the behavioural experiments. Close analysis of the TS application revealed that the radula was the feeding structure which consistently came into contact with the probe. This occurred in the retraction phase of the appetitive bite, when the radula is brought back into the mouth. The dorsal mandible was often brought into apposition with the radula. However in several trials, no clear contact was made with the dorsal mandible. In these trials, the TS was still able to bring about the switch to consummatory bites. **Figure 3.3A-C** show a cartoon of where and when the TS was placed in the mouth and the structures it most likely comes into contact with. The black arrows signal the two points in the retraction phase at which the most pressure is likely to be applied to the radula by the TS.

A semi-intact preparation was developed consisting of the radula connected to the CNS via the PBN in order to identify stimulus present decision neurons. A set of criteria were established from the behavioural experiments for which a neuron had to meet to be considered a stimulus present decision neuron. The first criterion a cell had to fulfil was to respond correctly to the appropriate sensory stimulus. In this case the cell must be excited by a tactile stimulus to the radula. The second criterion was that the cell had to be able to activate the feeding network and drive a rhythmic motor output. Specifically it should be capable of converting a relatively short duration stimulus into an on-going motor output as the TS could in vivo. The radula-CNS preparation allowed for intracellular recordings to be made from candidate neurons whilst a tactile stimulus was applied to regions of the radula in order to identify neurons which fulfilled the first

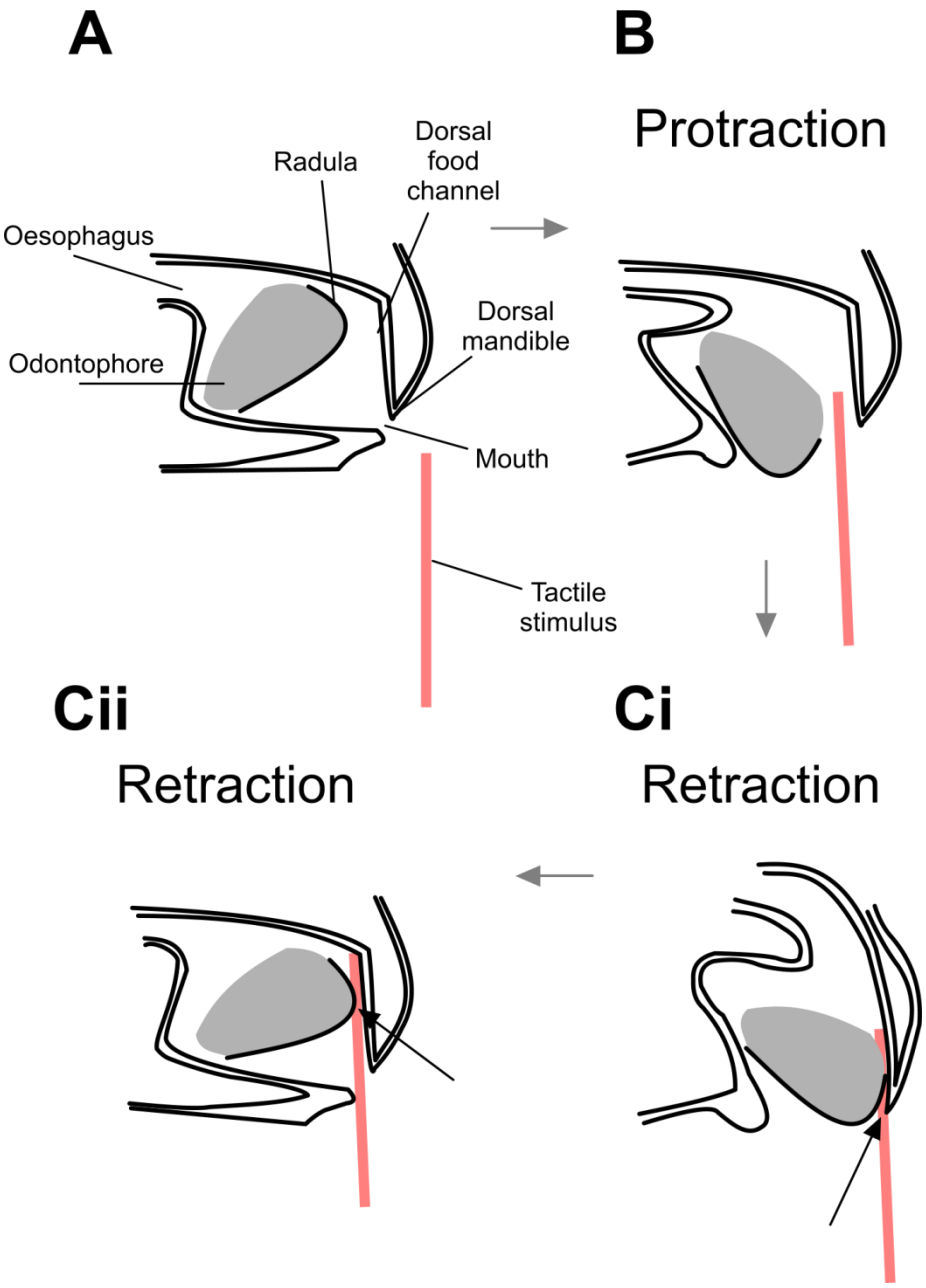

Figure 3.3 Identification of feeding structures receiving the most innervation from the tactile probe **A.** Side view of the feeding structures at rest and the tactile stimulus outside the mouth. **B.** During the protraction phase, the mouth is opened and the odontophore rotated ventrally and protracted out of the mouth. The tactile stimulus is placed into the open mouth. **Ci.** During the retraction phase, the odontophore is rotated dorso-anteriorly and often brought into apposition with the dorsal mandible. The tactile probe is bitten upon in a shearing motion between the radula and the dorsal mandible. **Cii.** The odontophore is rotated dorso-ventrally along the dorsal food channel. In some instance no contact is made between the dorsal mandible and the tactile probe. The radula however always came into contact with the tactile probe. The black arrows represent points at which the tactile probe comes into contact with the radula.

of the criteria. Two pairs of cells were identified which consistently responded to tactile stimuli to the radula.

3.2.2.1 Radula mechanosensory neurons

This neuron type was a pair of bilaterally symmetrical cells located on the ventral surface of the buccal ganglia (**Figure 3.4A**). Each cell responded to a tactile stimulus to the ipsilateral side of the radula with somatic action potentials that arose from baseline (**Figure 3.4B**). Presynaptic potentials were rarely present. The cell was injected with a fluorescent dye (5(6)-carboxyfluorescein) to reveal its morphology (n=5). The cell body was ~30 µm. It had a single projection from the cell body. This left the buccal ganglia via the PBN towards the buccal mass. A side branch left the main process within the ipsilateral ganglion and crossed the buccal commissure and entered the contralateral ganglion but few arborisations were seen (**Figure 3.4Ci**). The axon leaving the buccal ganglia could be traced to the tissue underlying the chitinous toothed radula. Each cell projected only to the ipsilateral side of the radula. Numerous processes could be seen projecting under the radula (**Figure 3.4Cii**). This combined with the response to tactile stimuli to the radula suggested that it was a mechanosensory cell, thus was named a radula mechanosensory cell (RM). Further evidence that RM was a sensory cell came from bathing the preparation in HiLo saline, effectively blocking chemical synaptic transmission. In these conditions a tactile stimulus to the radula still elicited somatic action potentials (n=4) (**Figure 3.4D**), confirming that the response was not due to a third party neuron.

When the stimulus was applied to the contralateral lateral edge of the radula, RM was depolarised but somatic spikes were rarely elicited. This is in agreement with the projections of the cell (processes are only present under the ipsilateral side of radula) and implies that it receives input from other mechanosensory cells projecting to that contralateral side of the radula, possibly from the contralateral RM. Longer duration stimulation of the radula produced longer responses in RM. If the stimulus remained then RM showed evidence of adaptation (**Figure 3.4E**). **Figure 3.4F** provides evidence that tactile stimulation to the radula does not cause spiking in every cell. An N2v interneuron and the newly characterised SLRT motor neuron B11 (see Section 7.2.2) were not activated by the tactile stimulation, whereas RM fired a burst of spikes.

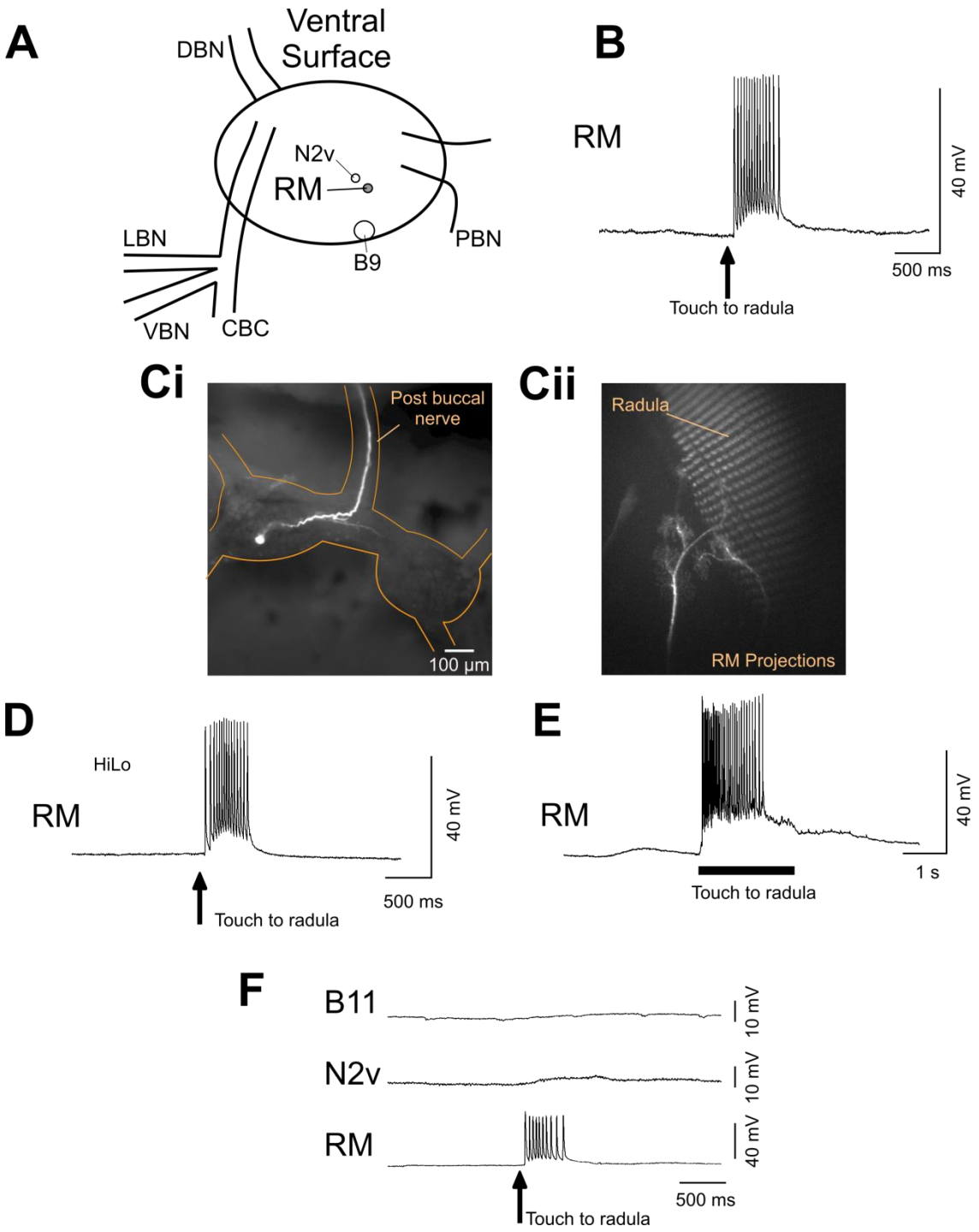

Figure 3.4 Morphology and Characterisation of RM. **A**. One RM is located in each buccal ganglion on the ventral surface, near the N2v interneuron. **B**. Tactile stimulus applied to the ipsilateral dorsolateral edge of the radula elicited somatic spikes in an RM. The spikes arose from baseline. **Ci**. Soma dye fill of RM revealed that it has a projection towards the contralateral buccal ganglion which often terminates in the buccal commissure. The main axonal projection leaves the buccal ganglia via the PBN. **Cii**. RM's projection can be traced to the ipsilateral dorsolateral edge of the odontophore, where it projected under the radula into the subradular tissue. **D**. Bath application of HiLo saline for an hour did not prevent somatic spikes in RM from tactile stimulation of the radula. **E**. Long duration tactile stimulation of the radula caused a longer duration response in RM. If the stimulus was maintained, then RM showed evidence of adaptation. **F**. Tactile stimulation did not activate all neurons within the buccal ganglia. N2v (an interneuron) and B11 (a motor neuron) show a small depolarization in response to the tactile stimulus, but no spiking. RM produces several somatic action potentials.

3.2.2.2 Ventral trigger neuron

The second class of cell identified which consistently responded to tactile stimuli were a pair of bilaterally symmetrical cells located on the ventral surface of the buccal ganglia (**Figure 3.5A**). A tactile stimulus to the radula caused a large depolarization of the cell, which was often sufficient to elicit action potentials (**Figure 3.5B**). Large unitary EPSPs were often evident throughout the stimulus.

The cell was injected with a fluorescent dye to characterise its morphology. The cell body was ~40-50 µm (n=11). It had projections within the ipsi- and contralateral buccal ganglia where numerous arborisations were present. These were often seen to project into the initial segment of both CBCs; however they never projected down to the cerebral ganglia. A single projection left the buccal ganglia via the PBN and projected towards the buccal mass (**Figure 3.5C**). This was never seen to leave the PBN and enter any surrounding muscle, or reach the radula. It was therefore classified as an interneuron and was named the ventral trigger neuron (vTN – see Section 3.2.4 and results in Section 4.2.1 for rationale for the name). vTN received excitation from tactile stimuli from either side of the radula, but a stronger input was consistently seen from tactile stimulation of the ipsilateral side. vTN was seen to fire at a maximum rate of 38 Hz in response to a tactile stimulus to the radula.

3.2.3 RM and vTN connections

Pairwise recordings of RM and vTN revealed that both cells were most strongly activated by tactile stimulation of the ipsilateral dorsolateral edge of the radula (**Figure 3.6A** and **3.6B**). There was also strong activation via touch to the dorsomedial edge. Both were depolarised by touch to the contralateral edge of the radula, but RM did not fire spikes, whereas vTN was sometimes sufficiently depolarised to fire actions potentials. No response was seen when the tactile stimulus was applied to the medial ventral surface of the radula (**Figure 3.6A** and **3.6B**). The dorsolateral and dorsomedial regions of the radula are the regions at which the earliest and most pressure will be applied throughout a bite on a solid, especially if the radula is brought into contact with the dorsal mandible.

Since vTN had no processes under the radula, it was important to establish the source of excitation to vTN occurring in response to tactile stimulation of the radula. Pairwise recordings of RM and vTN within a semi-intact preparation revealed that the majority of the input to vTN from a tactile stimulus arose directly from RM activity. A long tactile stimulus to the radula caused a high firing rate in both the ipsilateral RM and vTN and

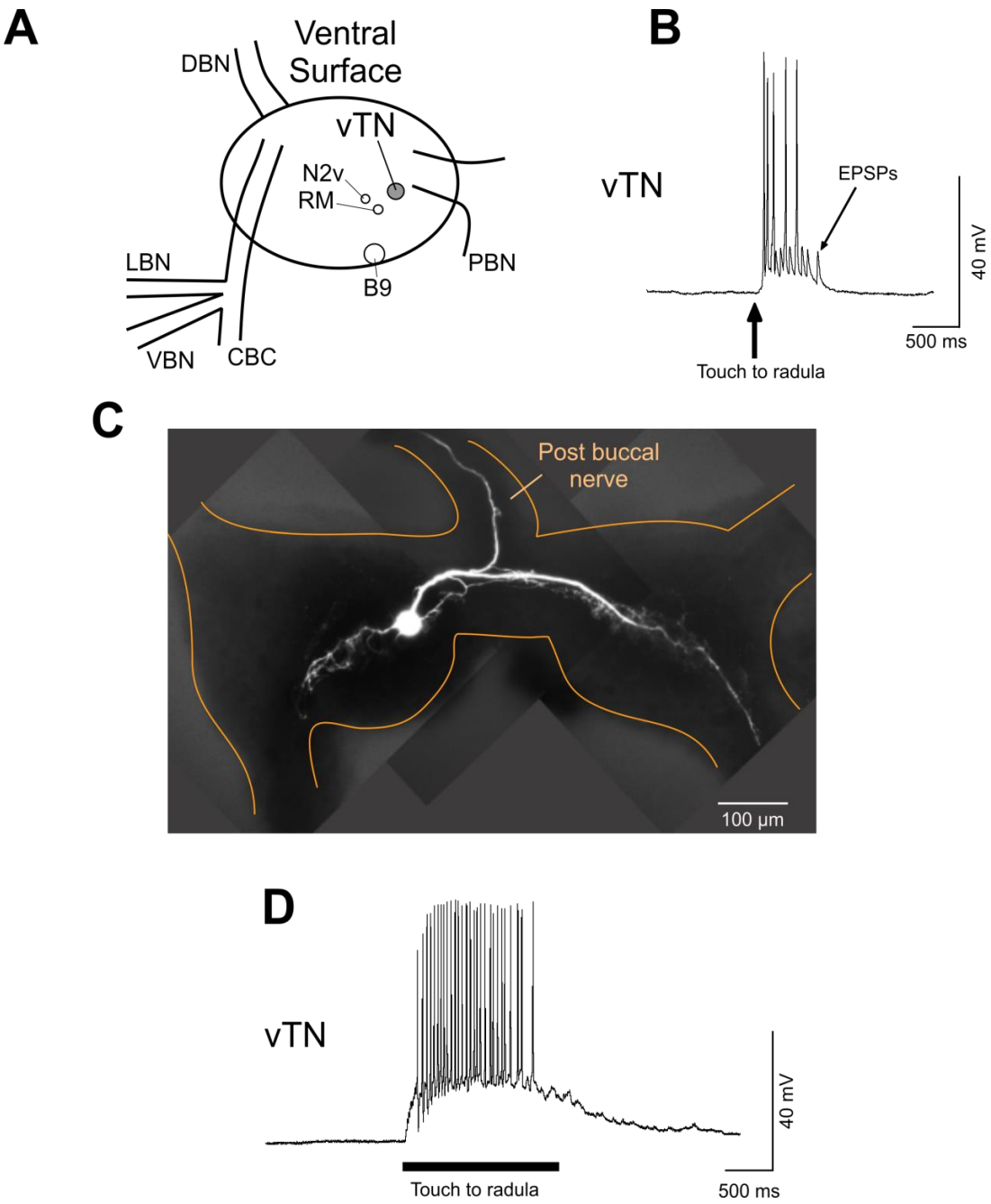

Figure 3.5 Morphology and Characterisation of vTN. **A**. One vTN is located in each buccal ganglion on the ventral surface, near to the buccal commissure. **B**. Tactile stimulation to the ipsilateral dorsolateral edge of the radula depolarises vTN sufficiently to elicit action potentials. A number of EPSPs can be seen on vTN throughout the response. **C**. Soma dye fill of a vTN reveals its morphology. vTN has numerous arborisations within both the ipsi- and contralateral buccal ganglia. These project into the initial segment of both CBCs, but never project down to the cerebral ganglia. A single small process leaves the buccal ganglia via the PBN. It was never seen to leave the PBN. **D**. Longer duration stimulation of the radula caused a larger and longer lasting response in vTN.

some activity in the contralateral vTN (**Figure 3.7Ai**). Hyperpolarising vTN before the tactile stimulus revealed that vTN received a number of large unitary EPSPs which followed 1:1 from somatic action potentials in the ipsilateral RM (**Figure 3.7Aii**). Artificially depolarising RM to fire action potentials elicited similar size and shape EPSPs on vTN as those seen from a tactile stimulus (**Figure 3.7Bi** and **3.7Bii**). RM activated the ipsilateral vTN more than the contralateral vTN, analogous to the stronger activation of vTN achieved by stimulating the ipsilateral side of the radula (compare **Figure3.7Ai** with **Figure 3.7Bi**). At resting membrane potential (RMP), artificially depolarising RM to fire action potentials often activated the ipsilateral vTN sufficiently to elicit 1:1 action potentials (**Figure 3.7C**).

Injecting the presynaptic cell with a square pulse elicited a similar but attenuated response in the postsynaptic cell (**Figure 3.7Di** and **3.7Dii**); suggesting that an electrotonic synapse exists between the two cells. Impaling both cells with two electrodes permitted a reliable readout of the coupling coefficients between the two cells. The average coupling coefficient from RM to the ipsilateral vTN for depolarising current pulses was 0.46 (±0.02) and for hyperpolarising current pulses 0.45 (±0.03) (n=5). From vTN to RM the coupling coefficient for depolarising current pulses was 0.31 (±0.01) and for hyperpolarising current pulses 0.3 (±0.02) (n=3). The coupling coefficient from RM to the contralateral vTN for depolarising current pulses was 0.15 (±0.001) and for hyperpolarising current pulses 0.13 (±0.006) (n=2). The connection persisted in HiLo saline, providing strong evidence that the connection was electrotonic in nature (n=3).

These results provide evidence that RM is a primary mechanosensory cell, whereas vTN is a putative interneuron. However the large coupling coefficient between the two cells ensures that the vTN is reliably activated by tactile stimuli to the radula via activation of RM.

3.2.4 RM and vTN's ability to initiate fictive feeding cycles

As both RM and vTN fulfilled the first of the two criteria for a stimulus present decision neuron, both were tested with respect to the second criterion namely, their ability to initiate fictive feeding. A single RM or vTN was impaled, as well as up to 3 other feeding network cells. The cell being tested was then stimulated and it was determined whether fictive feeding was initiated or not by the presence or absence of the standard triphasic feeding rhythm on the feeding network cells recorded.

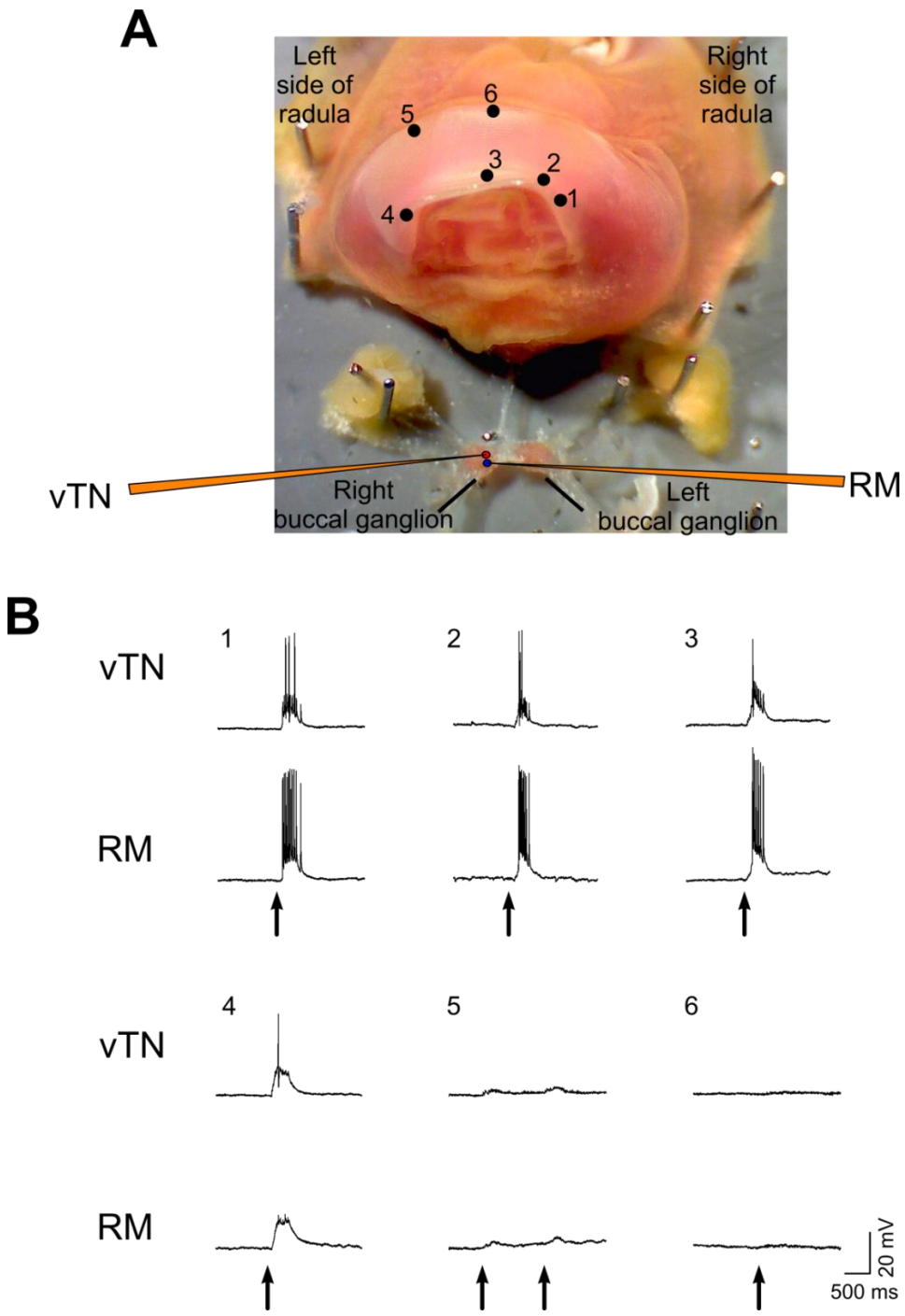

Figure 3.6 RM and vTN responses to tactile stimulation of different regions of the radula. **A**. Picture of the semi-intact preparation. A single RM and ipsilateral vTN were recorded. Tactile stimulation was applied to 6 different regions of the radula and responses recorded on the two cells. Since both RM and vTN are located on the ventral surface of the buccal ganglia, the buccal ganglia has been flipped so as the left side is on the right. **B**. Responses of RM and vTN to tactile stimulation. Both RM and vTN respond strongest to tactile stimulation of the ipsilateral dorsolateral edge of the radula. As the tactile stimulus is applied more dorsomedially, both cells still produce action potentials. At the contralateral dorsolateral edge, the stimulus causes a large depolarization of both RM and vTN, however this is only sufficient to elicit an action potential in vTN, but not RM. Tactile stimuli to the ventromedial and ventrolateral regions of the radula failed to produce a strong response in either RM or vTN.

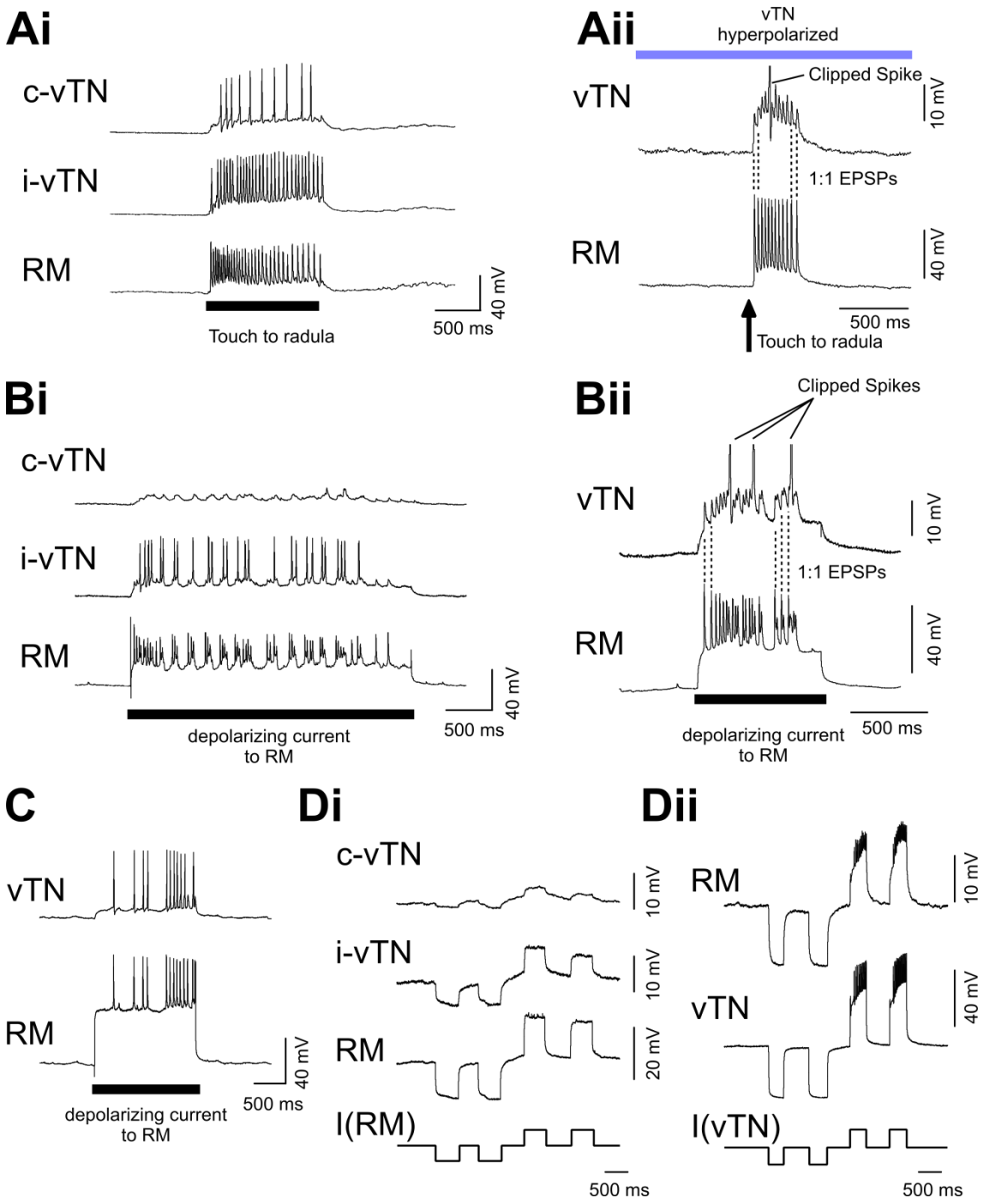

Figure 3.7 Connection between RM and vTN. **Ai**. Tactile stimulation of the dorsolateral edge of the radula causes high frequency activity in both the ipsilateral RM and vTN and depolarization of the contralateral vTN which resulted in low frequency spiking. **Aii**. Tactile stimulation to the radula causes large unitary EPSPs on vTN which follow 1:1 from RM somatic action potentials. vTN has been hyperpolarized prior to the tactile stimulus to reduce spiking and facilitate identification of the EPSPs. **Bi**. Injecting RM with positive current sufficient to elicit a series of action potentials causes the ipsilateral vTN to fire a number of action potentials. The contralateral vTN is depolarised but not sufficiently to reach threshold. **Bii**. A short duration positive current injection into RM results in large unitary EPSPs on vTN which follow 1:1 from RM spikes. These are similar to those elicited by tactile stimulation of the radula, strongly suggesting that they originate from the ipsilateral RM. **C**. At RMP, spikes in RM can result in 1:1 spikes in vTN. **Di**. Square pulse current injections into RM cause a similar but attenuated shift in membrane potential of both ipsilateral and contralateral vTN, revealing an electrical synapse between the two. Coupling between RM and ipsilateral vTN is much stronger than to contralateral vTN. **Dii**. Current injection into vTN caused a similar yet attenuated response in the ipsilateral RM.

Either a continuous depolarising current or a series of short duration (20 ms) high frequency depolarising pulses was injected into the cell. In the latter protocol, this allowed for a single action potential to be elicited per pulse, allowing the number and frequency of action potentials to be controlled. The tactile stimulus in the behavioural experiments was only present for a short duration, yet was able to initiate a number of cycles. Therefore the decision neuron had to be able to initiate a number of fictive feeding cycles after only a short duration stimulus to the cell. Relatively short duration stimuli of between 1-4 seconds were therefore used.

Both RM and vTN were able to initiate fictive feeding cycles following this level of stimulation. **Figure 3.8A** shows an example of RM initiating fictive feeding cycles. RM was injected with positive current for 2 s eliciting high frequency spiking in the neuron. This initiated four fictive feeding cycles, as seen by the standard triphasic inputs on the B3 and B4 motor neurons. Each grey line represents the rasp phase of a cycle. **Figure 3.8B** shows an example of vTN activating a fictive feeding rhythm. vTN was injected with positive current for 1.5 s eliciting high frequency spiking in the neuron. This initiated four fictive feeding cycles as seen by the standard triphasic inputs on N1M, B3 and B4.

Interestingly, no further activity was necessary in either cell for the generation of the subsequent cycles. Both RM and vTN showed rhythmic inputs during the fictive feeding cycles; however RM only fired two spikes in the third and the fourth cycle whereas vTN fired no spikes in any of the cycles. The short duration stimulus did not cause a prolonged activation of either RM or vTN which drove the on-going cycles, rather the activity in both cells stopped once the stimulus was removed and the activity started after this and persisted in the absence of any further activity in the cells. The ability to initiate an on-going rhythmic motor output via a short duration stimulus is a characteristic of a trigger neuron (Marder et al., 2005). Therefore the cycles initiated by a short duration stimulus to either cell were referred to as “triggered cycles”.

It was next tested whether either RM or vTN could trigger cycles independently of the other. To do this an RM and ipsilateral vTN were impaled and each tested for their trigger ability. First it was found that both cells often activated the other during the period of stimulation (**Figure 3.9Ai** and **Bi**), presumably due to their strong electrotonic coupling. RM activated vTN more than vTN activate RM. This too was explained by the relative coupling coefficients (stronger from RM to vTN). This made it difficult to determine the relative contributions of each cell in triggering cycles. Therefore RM’s trigger ability was tested whilst the ipsilateral vTN was hyperpolarised to prevent

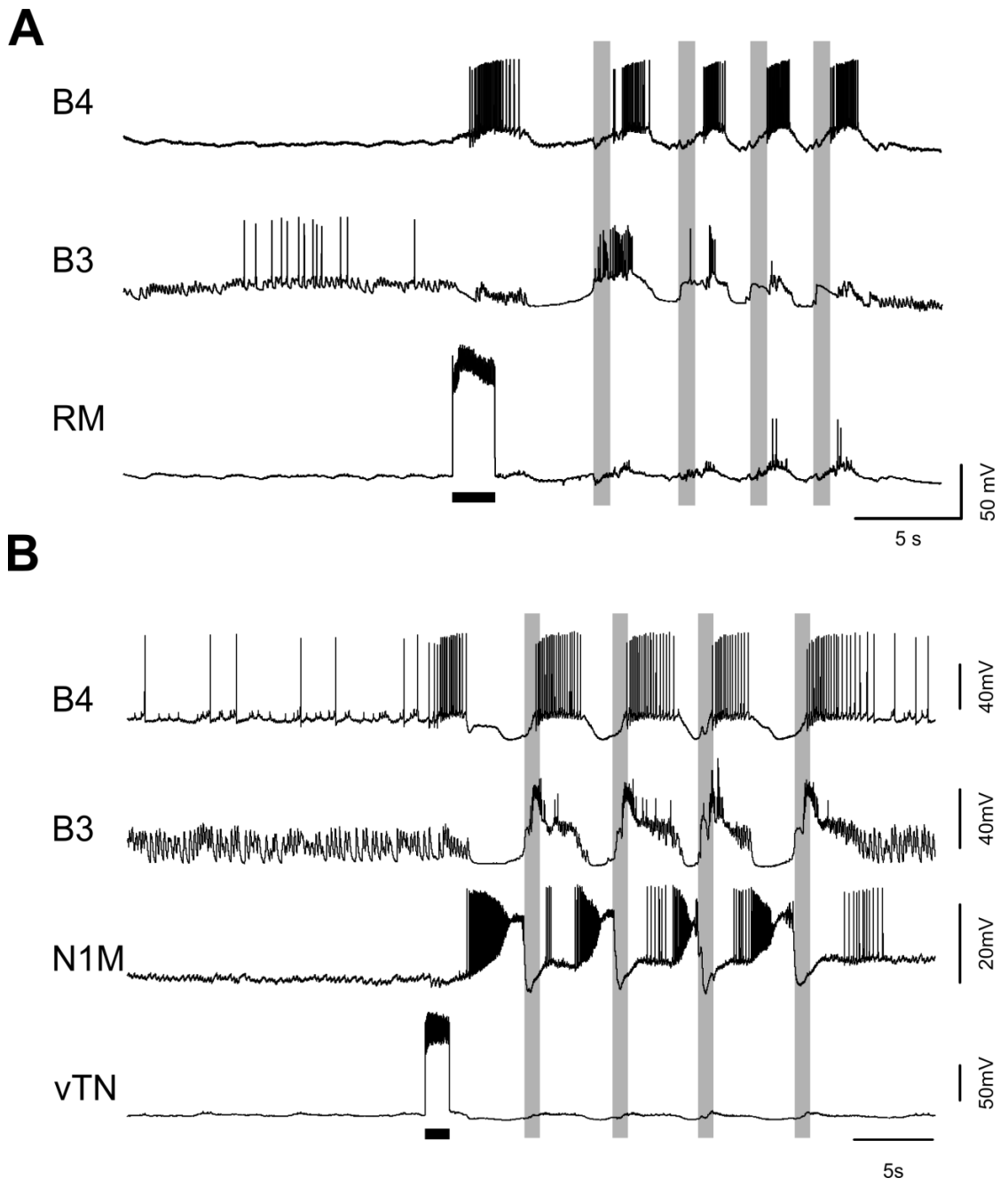

Figure 3.8 RM and vTN's ability to initiate fictive feeding cycles. **A**. RM's ability to initiate fictive feeding cycles recorded on a B3 and B4 motor neuron. Before RM stimulation, no rhythmic activity was occurring. A short duration positive current to RM was sufficient to elicit high frequency spiking in the cell. Once the stimulus was removed, four fictive feeding cycles were initiated. Each grey line marks a single N2 phase. RM shows minimal rhythmic activity and does not spike during the first two cycles. In the third and fourth cycle RM fires two spikes. **B**. vTN's ability to initiate fictive feeding cycles recorded on an N1M interneuron and a B3 and B4 motor neuron. Before vTN stimulation no rhythmic activity was occurring. A short duration stimulus to vTN was sufficient to elicit four fictive feeding cycles. vTN shows no activity within the cycles. Black lines represent duration of positive current to neuron.

somatic spikes, and vTN's trigger ability tested whilst the ipsilateral RM was hyperpolarised to prevent somatic spikes. When vTN was hyperpolarised, stimulating RM was insufficient to trigger cycles (**Figure 3.9Aii**). The blue rectangle in **Figure 3.9Aii** represents continuous injection of negative current into vTN. RM activation with vTN hyperpolarised caused no rhythmic activity on the B3 and B4 motor neurons recorded. When vTN was returned to RMP then RM was able to trigger cycles. When RM was hyperpolarised, vTN stimulation was still sufficient to trigger cycles. In **Figure 3.9Bi** and **3.9Bii** vTN stimulation caused a large amount of activity in RM in one trial but only elicited 3 spikes in RM in the second trial even though RM was not hyperpolarised. However vTN was able to trigger fictive feeding cycles in both trials, as seen by the rhythmic inputs seen on the B4 and B10 motor neurons in **Figure 3.9Bi** and B4 and N3p in **Figure 3.9Bii**. The low level of activity in RM indicates that it was not necessary for vTN to trigger cycles. These results provide evidence that in order for RM to trigger fictive feeding cycles it must sufficiently activate vTN. In contrast vTN is able to initiate fictive feeding in the absence of RM activity. A proposed simplified circuit is presented in **Figure 3.9C**. The tactile stimulus is applied to the radula, which activates RM. This drives vTN activity, which in turn activates the feeding CPG, producing a motor output.

The above experiments show that both RM and vTN fulfil the two criteria to be considered a decision neuron. They both receive excitation from tactile stimulation of the radula (vTN relies on RM for this) and are both able to initiate a fictive feeding rhythm (RM relies on vTN for this). Due to vTN's ability to trigger fictive feeding independently of RM, vTN became the main candidate for the stimulus present decision neuron.

3.3 Discussion

3.3.1 Perceptual decision making about the presence or absence of a sensory stimulus

In this chapter a decision making paradigm was designed that could be amenable for in vitro preparations to identify the neural correlates of decision making. The decision about the presence or absence of a sensory stimulus during an appetitive bite program was used as a task to be studied. The animal was either presented with a sensory stimulus or no stimulus during an appetitive bite. The animal reported the presence or

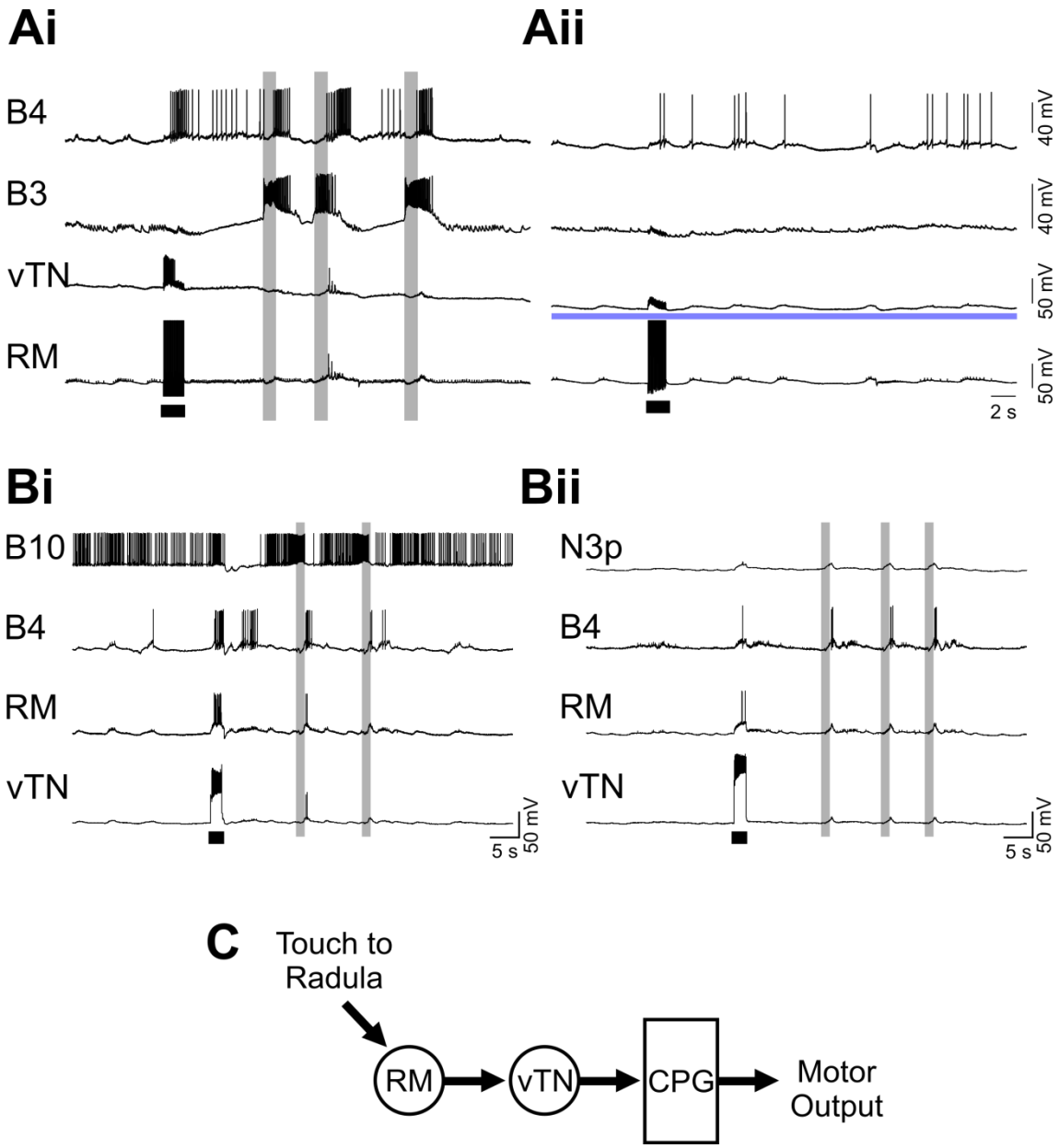

Figure 3.9 RM vs. vTN trigger ability. **Ai**. RM's trigger ability tested with a vTN and a B3 and B4 motor neuron. RM stimulation triggers three cycles of fictive feeding. This level of stimulation strongly recruits vTN. Both RM and vTN are only active in one of the cycles, firing two and one spike respectively. **Aii**. Hyperpolarising vTN before the same level of RM stimulation prevents spiking in vTN and no fictive feeding cycles are triggered. **Bi**. vTN's trigger ability tested with an RM and a B4 and B10 motor neuron. Stimulating vTN strongly activates RM and triggers two fictive feeding cycles. **Bii**. The same stimulus to vTN does not strongly activate RM. RM was not hyperpolarised but only fired three action potentials in response to vTN stimulation. vTN was still able to trigger three fictive feeding cycles. An N3p was recorded instead of a B10. **C**. Circuit diagram showing proposed sensory pathway from tactile stimulation to motor output. Notice that vTN relies on RM for information from the radula, whereas RM relies on vTN activation to initiate the CPG. Black bars represent duration of positive current stimulus or pulses to neuron. Blue bar represents duration of negative current stimulus to neuron.

absence of the stimulus by switching into the consummatory behaviour or entering back into quiescence respectively; effectively making a simple perceptual decision.

It was found that animals that had been deprived of food for a single day reliably produced appetitive bite programs in the search for food. Under these conditions, in the absence of a sensory stimulus the animal typically entered back into a period of quiescence before further appetitive bite programs were produced. This provided evidence that the animal was able to make a correct judgement about the absence of a sensory stimulus, preventing any further appetitive behaviours. Previous studies have shown that the number of appetitive bites which occur within a feeding bout is dependent on the level of satiety of the animal (Tuersley, 1989). At increased levels of hunger, more related bites occur. At the level of satiety used in this Chapter, only single appetitive bites were elicited. This is potentially due to a form of cost/benefit analysis: the energetic cost of performing numerous appetitive bites vs. the benefit of locating food during one of the bites. At this level of satiety the cost appears to outweigh the benefit and no further cycles are generated in the absence of a stimulus. Cost/benefit studies have been performed in *Pleurobranchaea* (Gillette et al., 2000), where changes in levels of satiety alter the responsiveness of the animal to food and noxious stimuli. However, in the experiments of this Chapter, the satiety level was carefully controlled and not altered between trials; therefore this was unlikely to alter the animal's decision making process in each trial. The expression of single appetitive bites also allowed for the dissociation of the appetitive bite program from the consummatory bite programs. When the animal was presented with a solid piece of food (SL) during an appetitive bite, it switched into an on-going consummatory behaviour. The switch to the consummatory behaviour occurred within 3 s of the appetitive behaviour. This is within the range of the fastest rate at which the animal can produce another feeding cycle (Dawkins, 1974, Kemenes et al., 1986, Large et al., 2006). Therefore the animal is able to make an early judgement about the presence of a sensory stimulus and switch into the consummatory behaviour.

An important finding of this Chapter was that the animal used the tactile properties of the food as the main cue about the presence of the SL during appetitive bites. Application of a tactile probe alone most faithfully mimicked the latency of the decision about the presence of SL. The TS was removed from the mouth after the first bite since the decision point between the appetitive and the consummatory bite was of most interest. However, without further stimulation from the TS, on average 4.00 (±0.4) further associated bites were elicited, indicating that the short duration of the stimulus was able to initiate on-going biting in the absence of any further stimulation. The

chemical component of the SL was found to be able to initiate consummatory bites too; however the delayed nature of the onset of the consummatory bites indicated that it was not important for the decision about the presence of food seen with SL. It had previously been shown that a chemical stimulus alone in the absence of appetitive behaviours was reliable at initiating consummatory bites (Sucrose and Maltose (Kemenes et al., 1986) and Sucrose (Kemenes et al., 2001)). Therefore it was possible that the LJ in the presence of the appetitive bite was simply initiating consummatory bites independently of the appetitive bite. This was confirmed in the LJNA trial. Applying the LJ in the absence of an appetitive bite caused a similarly delayed onset of consummatory bites as the LJ presented in an appetitive bite. This implies that the chemical cue, although sufficient to elicit consummatory bites, was not important for the decision about the presence of food in an appetitive bite and the switch from appetitive to consummatory bites seen in SL trials. This provided evidence that the tactile properties of food during an appetitive bite are important for the decision to switch to consummatory bites.

This simple behavioural paradigm provides a valuable system for exploring the neuronal mechanisms underlying a perceptual decision. The most extensive work on perceptual decision making has been carried out in monkeys in the somatosensory or visual system (de Lafuente and Romo, 2005, de Lafuente and Romo, 2006, Merten and Nieder, 2012) looking at detection tasks. In these studies monkeys were either presented with a near-threshold stimulus or no stimulus and had to report its presence or absence correctly to receive a reward. The use of a near-threshold stimulus allowed for neurons which encode the decision to be dissociated from neurons which encode the sensory stimulus. However, the decision made by the monkey was a simple stimulus present or stimulus absent decision similar to the decision made by *Lymnaea* in the experiments of this Chapter. These studies have successfully identified regions of the brain involved in decision making for these tasks by correlating activity in certain regions with the decision rather than the sensory stimulus or the motor output. However the complexity of the system is a limitation. Due to the large number of neurons participating in the decision, testing the necessity or sufficiency of these neurons is difficult. The perceptual decision used in this Chapter uses a simple stimulus present or stimulus absent task which takes advantage of *Lymnaea's* natural food-searching behaviour. This facilitated the study of perceptual decision making in a behaviourally-relevant task. The extensive characterisation of the neural circuitry of the behaviours involved in the decision and the ease of developing semi-intact preparations will aid in the identification of decision neurons and testing hypotheses

about decision making in an in vitro preparation. Decision making studies in invertebrates have historically focused on behavioural choice between two different sensory stimuli rather than decisions about the presence or absence of a stimulus (Kovac and Davis, 1980, Esch et al., 2002, Gaudry and Kristan, 2009, Hirayama and Gillette, 2012). However many preparations have successfully been utilised to design simple behavioural experiments to study decision making and successfully identify decision neurons (Esch et al., 2002, Briggman et al., 2005). Therefore the development of this behavioural paradigm and identification of decision neurons will allow for the comparison of mechanisms of decision making with both invertebrate and vertebrate studies.

3.3.2 Identification of candidate stimulus present decision neurons

To identify the decision neurons involved during the stimulus present task, a set of criteria were established from the behavioural experiments which cells had to fulfil in order to be considered as candidates. First, cells had to be excited by the correct sensory stimulus. The main cues about the presence of a stimulus were found to be from the tactile properties of the food. The radula was identified as the feeding structure which received the most innervation from both the SL and TS during the behavioural experiments. The other structure that also received stimulation from both cues was the dorsal mandible. During feeding this moves in the opposite direction to the radula during the retraction phase, and the two are brought into contact with each other in a shearing motion. Therefore equal pressure may be applied to both the radula and dorsal mandible. However in some bites, the radula was retracted strongly into the mouth, whereas there was no strong movement of the dorsal mandible, and little or no contact was made with the TS. In these bites, the TS was still able to switch the appetitive bite into a consummatory bite. This suggests that the dorsal mandible may play a role, but that the radula is the key sensory structure in relaying the information about food. Therefore a stimulus present decision neuron had to be activated by tactile stimulation of the feeding structure, the radula. The second criterion was that the decision neuron must be able to initiate fictive feeding cycles, similarly to the TS in the behavioural experiments.

Two candidate decision making neurons were identified, RM and vTN. Both received the correct sensory input, excitation from tactile stimulation of the radula. RM was classified as a mechanosensory cell due to its response to tactile stimuli and its morphology whereas vTN was classified as an interneuron due to its lack of projections

to the sensory structure. The two cells were tightly coupled to each other via a strong electrotonic synapse. This ensured that vTN was strongly activated by tactile stimuli to the radula, even though it had no projections to the structure. Radula mechanosensory neurons have been identified in a number of molluscs. They have similar characteristics to the RMs identified in this Chapter. The RMs in *Aplysia* are all located on the ventral surface (called the rostral surface in *Aplysia*) of the Buccal ganglia (Miller et al., 1994, Rosen et al., 2000, Evans et al., 2007). They have projections down the PBN (Radula Nerve in *Aplysia*) towards the radula where they have numerous projections in the subradula tissue. RM neurons in *Helisoma* are also located on the ventral surface (called the rostral surface in *Helisoma*) in a similar location to the RMs in *Lymnaea* and have a similar morphology (Murphy et al., 1985, Wentzell et al., 2009). RMs in the terrestrial slug *Incilaria fruhstorferi* are located on the dorsal surface but have a similar morphology to the RMs in *Lymnaea* (Kawahara et al., 1994). Both the *Aplysia* and *Incilaria* RMs response to stimulation of the radula persists in low Ca^{2+}, supporting their role as primary mechanosensory cells. Both the *Aplysia* and *Helisoma* RMs are immunoreactive to SCPb (Miller et al., 1994, Wentzell et al., 2009), and one of each contains Glutamate (B21 in *Aplysia* (Klein et al., 2000), B102 in *Helisoma* (Wentzell et al., 2009). The morphological similarities suggest that the RMs discovered in *Lymnaea* may be homologous to those in *Aplysia*, *Helisoma* and possibly *Incilaria*. vTN appears morphologically similar to neuron B51 in *Aplysia* (Plummer and Kirk, 1990, Evans and Cropper, 1998). Both have projections within the ipsi- and contralateral buccal ganglia and a single projection down the PBN (RN in *Aplysia*). B51 is also electrotonically coupled with radula mechanosensory neuron B21 (Shetreat-Klein and Cropper, 2004). However there is no evidence that B51 can trigger fictive feeding similarly to vTN. B51 also produces characteristic plateau potentials (Plummer and Kirk, 1990, Evans and Cropper, 1998, Nargeot et al., 1999, Brembs et al., 2002), which vTN does not. Therefore the two are unlikely to be homologous neurons. No other known neurons in other molluscs appear to be homologous with vTN.

Since both RM and vTN fulfilled the first of the two criteria, both were tested for the second criterion. In the TS trials, the TS was only applied for a short duration (~1-3 seconds as it was removed when next cycle initiated and this occurred within 3.15 s) and then removed so as no further stimulation was present. This was sufficient to initiate on average 4.00 (+0.4) more cycles. Both RM and vTN were tested for their ability to initiate fictive feeding. A short duration stimulus (between 1-4 seconds) was therefore used to mimic the application of the TS. Both RM and vTN were able to initiate the feeding network and produce rhythmic motor output that outlasted the

duration of the stimulus to the cell. No further activity in either cell within the generated cycles was necessary. The ability to initiate a fictive motor-output after only a short duration stimulus is a characteristic of a trigger neuron (Stein, 1978, Brodfuehrer and Friesen, 1986a, Marder et al., 2005), therefore the cycles initiated by this protocol were referred to as triggered cycles. By hyperpolarising either RM or vTN and testing the others ability to trigger fictive feeding, it was determined that RM was only able to trigger cycles if it sufficiently activated vTN, whereas vTN was able to trigger cycles in the absence of activating RM. Therefore RM relies on vTN to initiate the feeding network whereas vTN relies on RM for information about the stimulus to the radula. Due to vTN's strong effect on the feeding network, it became the main candidate as a stimulus present decision neuron. Decision neurons in both vertebrates and invertebrates have been found to be downstream from sensory neurons (Esch et al., 2002, Briggman et al., 2005, de Lafuente and Romo, 2005).

In conclusion, a suitable behavioural paradigm was designed in order to study the neural correlates of a perceptual decision. *Lymnaea* were found to be able to accurately make judgements about the presence or absence of a sensory stimulus. The stimulus present decision was based on the tactile properties of a potential food and switches the appetitive bite into an on-going consummatory behaviour. vTN was identified as a candidate stimulus present decision neuron since it received the correct input from a tactile stimulus and was able to initiate the feeding network after a short duration stimulus to the cell. How vTN was able to trigger fictive feeding was an important question for understanding the mechanisms involved in the switch between behaviours.

4 Mechanisms of vTN's trigger ability

4.1 Introduction

In the previous chapter a novel neuron, vTN, was identified as a strong candidate for being a stimulus present decision neuron. vTN had the ability to initiate fictive feeding cycles after a high frequency but relatively short duration stimulus to the cell. The fictive behaviour outlasted the duration of the stimulus. As mentioned in Chapter 3, these are important defining features of a trigger neuron (Stein, 1978, Brodfuehrer and Friesen, 1986a, Marder et al., 2005). However, a number of other criteria also have to be met before a neuron can be classified as a trigger neuron. These are as follows:

i) The neuron must be able to reliably initiate the fictive behaviour that outlasts the duration of the stimulus to the cell.
ii) The stimulus used to activate the neuron must be in the physiological range.
iii) The number of cycles triggered by the neuron must be independent of the duration of the stimulus to the cell.
iv) No further activity in the cell is necessary for the initiation of each subsequent cycle.

This Chapter aimed to test whether vTN fulfilled these criteria and could be classified as a trigger neuron and describe the mechanisms by which vTN was able to initiate fictive feeding.

4.2 Results

4.2.1 Is vTN a trigger neuron?

Experiments in Section 3.2.4 had already established that vTN had the capacity to trigger fictive feeding. It was next necessary to test whether the trigger ability was a reliable feature of the neuron. A single vTN was stimulated to fire action potentials at between 25-35 Hz in 29 preparations. This activity level was selected because it was within the frequency range seen in response to a tactile stimulus to the radula (see Section 3.2.2.2). vTN activity at this rate was sufficient to trigger at least one full fictive feeding cycle in 86% of preparations tested (n=25). Within the preparations in which vTN could trigger a full triphasic cycle, vTN's reliability to trigger cycles was 67% (successful triggers n=67, number of attempts n=100). The high percentage of

preparations and the high reliability within preparations in which vTN can trigger fictive feeding suggests that the trigger ability is a key function of vTN.

The average number of cycles triggered in successful attempts was 4.0 cycles (± 0.7). There was no significant difference between the number of cycles initiated by vTN or by the TS in the behavioural experiments in Section 3.2.1 (4.00 cycles (+0.4)) (unpaired t-test, P > 0.05) (**Figure 4.1A**). The onset of the first protraction phase from the end of the vTN pulse was 4.2 s (±0.3). The average cycle period of triggered cycles was 6.8 s (±0.4).

A range of vTN stimulus durations were used to test whether the number of cycles triggered was a function of the stimulus duration. Stimulus durations between 1 and 6 seconds were tested. No correlation was found between stimulus duration and number of cycles triggered (Pearson's correlation r = 0.21) (**Figure 4.1B**).

No further activity from vTN was necessary for the triggered cycles to continue (**Figure 4.1Ci** and **4.1Cii**). However, in 30% of successful triggers, vTN was active within the subsequent triggered cycles (**Figure 4.1Di**). vTN activity occurred in the early swallow phase (**Figure 4.1Dii**). The average number of spikes produced in these cycles was 9.9 (±1.3). The average spike frequency was 7.5 Hz (±0.8). The average spike frequency of vTN within the entire swallow phase was 4.1 Hz (±2.5).

Therefore vTN was able to initiate a fictive behaviour after a short, physiologically relevant stimulus. The fictive behaviour outlasted the duration of the stimulus and there was no correlation between stimulus duration and number of cycles triggered. vTN activity was not necessary for the subsequent cycles to be generated, however it could be recruited into its own triggered cycles. Other characterised trigger neurons (e.g. Tr1 in the Leech and Tr1 in *Tritonia*) do not typically show much activity within the triggered cycles (Brodfuehrer and Friesen, 1986a, Frost et al., 2001). However, as vTN's activity is not necessary for the subsequent cycles to be generated and this neuron fulfils all other criteria, vTN was classified as a trigger neuron.

4.2.2 Activity of command-like neurons within vTN triggered cycles

To better understand how vTN was able to trigger fictive feeding, next I looked at which command-like cells the vTN recruited in triggered cycles. To do this, particular attention was focussed on the first of the triggered cycles to establish which target neurons were consistently activated in this phase and which, if any, was activated first. This would provide us with an insight into the mechanisms of vTN's trigger ability.

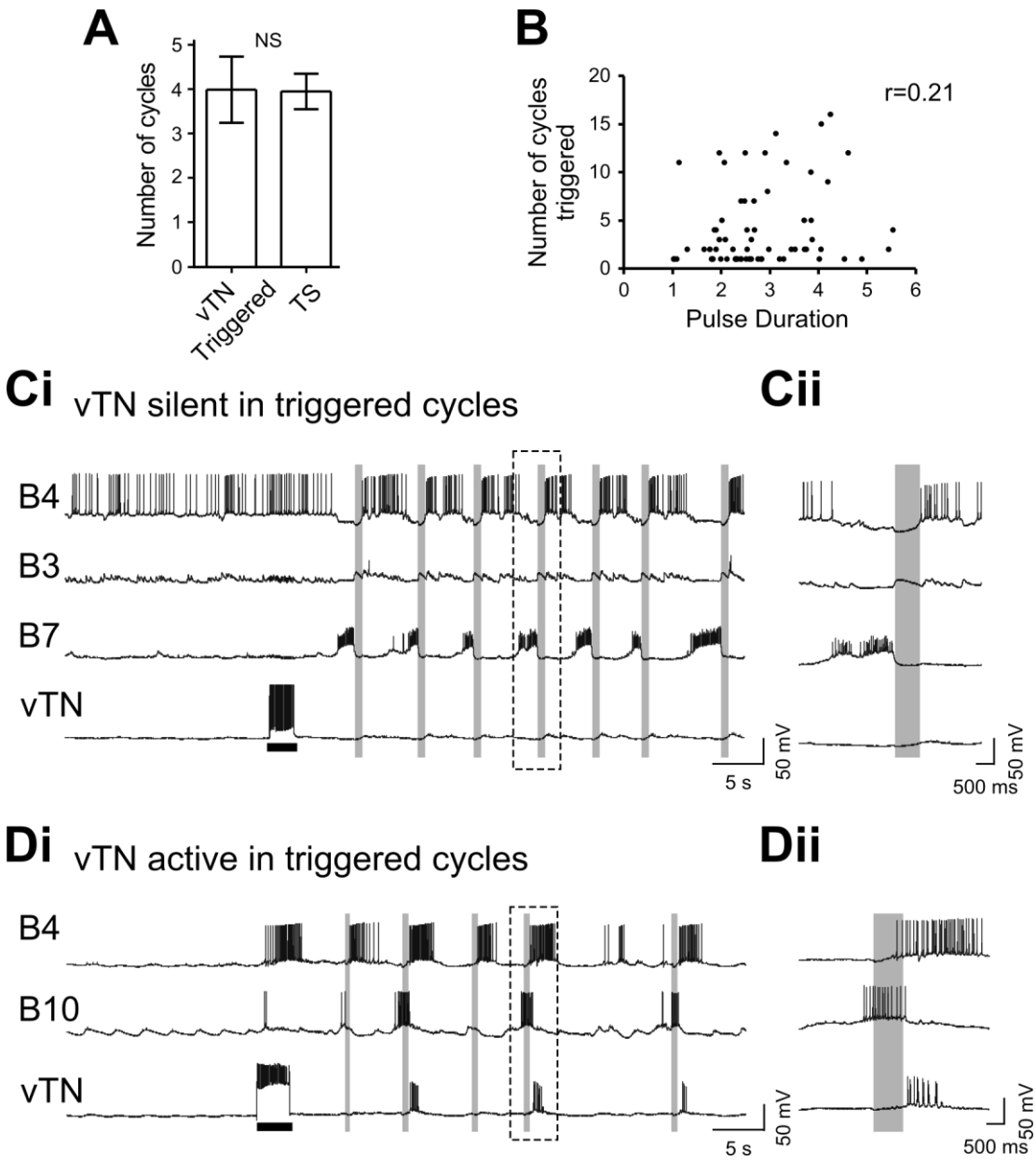

Figure 4.1 Trigger neuron characteristics of vTN **A.** The number of cycles initiated by TS in vivo is not significantly different from the number of cycles triggered by vTN. **B.** No correlation exists between the duration of the stimulus to vTN and the number of cycles triggered. **Ci.** vTN triggers fictive feeding cycles via a short duration stimulus to the cell. No further activity is necessary from vTN for the generation of the subsequent cycles. **Cii.** Single cycle at a faster timebase of Ci showing no activity in vTN. **Di.** vTN could be recruited into its own triggered cycles. vTN shows no activity in the first of the triggered cycles, but fires a number of action potentials in the swallow phase of the second, fourth and fifth cycles. **Dii.** Single cycle at a faster timebase of Dii showing vTN activity in the early swallow phase. B4 activity outlasts vTN activity, indicating that vTN is not active throughout the entire swallow phase. NS not significant.

There are a number of cells with the ability to drive a rhythmic motor output in the feeding system of *Lymnaea* – these are referred to as command-like cells. These include buccal interneurons (SO and N1L), cerebral to buccal interneurons (CV1a, CV1b) and buccal to cerebral interneurons (N1M and the newly identified Buccal-Cerebral Interneuron 1 (BCI1) – see Section 7.2.4.2 for further characterisation of BCI1). Each of these cell types was recorded within vTN triggered cycles to establish which of them were recruited into the rhythm and if any could explain vTN's trigger ability.

4.2.2.1 N1M activity in triggered cycles

The first cell type tested was the N1M interneuron. N1M is a CPG interneuron and has been shown to be necessary for fictive feeding to occur (Kemenes and Elliott, 1994, Kemenes et al., 2001). N1M was active in every vTN triggered cycle (vTN triggers = 39, preparations = 21). Therefore N1M always participates in vTN triggered cycles. **Figure 4.2A** shows an example of N1M activity in a triggered rhythm. N1M fires a burst of spikes within the protraction phase of all six triggered cycles. The necessity of N1M for vTN to trigger fictive feeding was next tested. To do this, N1M was hyperpolarised just after vTN stimulation. This was sufficient to block any cycles being triggered by vTN (n=2) (**Figure 4.2Bi** and **4.2Bii**). Therefore N1M is necessary for vTN to trigger cycles. This supports previous findings (Kemenes and Elliott, 1994, Kemenes et al., 2001) about N1M's key role within the feeding circuitry.

The N1M is known to receive many synaptic inputs from the other command-like cells (**Figure 4.2C**). In most cases the main mechanism by which they are able to drive fictive feeding is via monosynaptic excitatory connections with the N1M. It was therefore tested if any other command-like cells were active during vTN triggered cycles and whether their activity could account for N1M activation.

4.2.2.2 CBI activity in triggered cycles

The CV1a interneurons are located in the cerebral ganglia and send a projection down the ipsilateral CBC into the buccal ganglia. They are able to initiate fictive feeding via a facilitating excitatory connection with N1M (McCrohan and Kyriakides, 1989). During vTN triggered cycles, CV1a showed some activity in 75% of trials (n=36) and in 78.5% of preparations (n=14). **Figure 4.3A** shows an example of CV1a active in a triggered rhythm. CV1a fires a burst of spikes in the protraction phase of each of the four

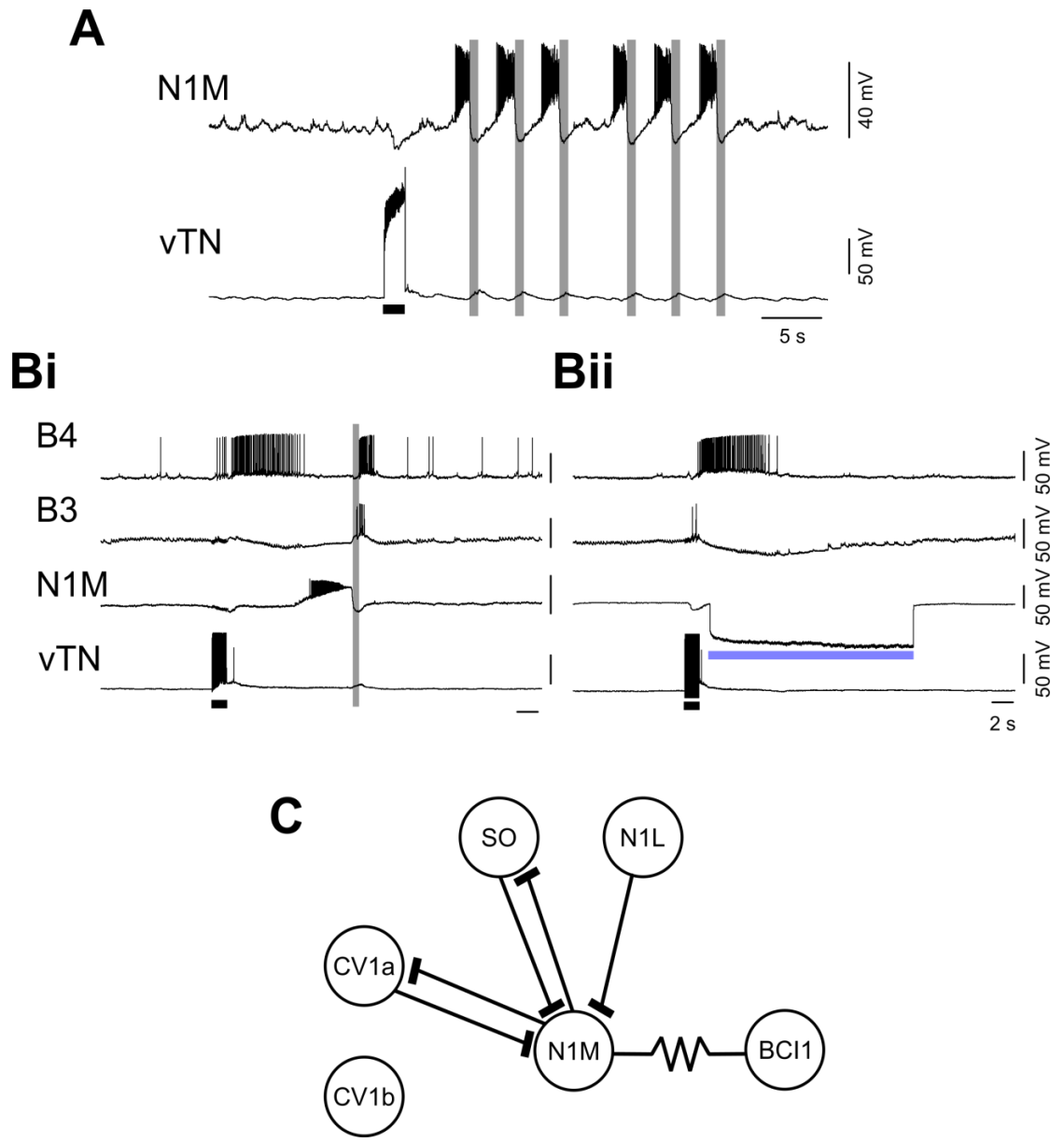

Figure 4.2 N1M activity in vTN triggered cycles. **A.** vTN triggered six full fictive feeding cycles. N1M was active in every cycle. **Bi.** vTN triggered a single full fictive feeding cycle, and recruited N1M into it. **Bii.** The same stimulus was applied to vTN, but N1M was hyperpolarised just after the end of the stimulus. This blocked any cycles being triggered by vTN, indicating the necessity of N1M activity for vTN triggered cycles. **C.** Known synaptic connections with N1M from other command-like neurons. CV1a and SO have reciprocal excitatory connections with N1M. N1L has an excitatory connection with N1M, but no connection exists from N1M to N1L. BCI1 is electrically coupled with N1M. CV1b has no known monosynaptic connection with N1M. Black horizontal lines represent depolarising current. Blue horizontal lines represent hyperpolarising current. Grey vertical lines represent the rasp phase of a cycle.

triggered cycles. The average spike frequency per cycle within the protraction phase was 9.14 Hz. Facilitation of EPSPs on N1M from CV1a depend on CV1a spike frequency. In two preparations tested, CV1a spike frequency had to be ~20 Hz or above in order for facilitation to occur on N1M (**Figure 4.3B**). The highest CV1a firing frequency seen in a triggered rhythm was 23.8 Hz, which is high enough for facilitation on N1M to occur. Therefore CV1a may be responsible for some of the drive on N1M in triggered cycles. However, the fact that CV1a was not active in every preparation, or in every triggered cycle, demonstrates that it is not necessary for vTN to trigger fictive feeding. **Figure 4.3C** shows an example of CV1a not active in triggered cycles. CV1a shows sub-threshold depolarising inputs in the protraction phase and inhibitory inputs in the rasp phase, but does not participate in the rhythm. In 69.4% of the vTN triggered cycles CV1a was active in the first cycle (**Figure 4.3A** and **4.3D**). To determine whether CV1a activation occurred before N1M activity, both cells were recorded during vTN triggered cycles (**Figure 4.3D**). In four preparations where this was tested, N1M was always active before CV1a during the first triggered cycles (trigger attempts = 5). Therefore CV1a was not the source of the excitation to N1M during the first cycle.

The next cell type tested was the CV1b interneurons. Like CV1a neurons, these are also located in the cerebral ganglia and project to the buccal ganglia via the CBC. Previous evidence indicates there are two CV1b neurons in each cerebral ganglion (McCrohan 1989). One of these contains the neuropeptide APGWamide and is called the CBWC (McCrohan and Croll, 1997). Since no functional difference is known by which the two CV1bs can be differentiated, here, no distinction was made between the two CV1bs. CV1b is able to initiate fictive feeding, although less reliably than CV1a. How it is able to do this is unknown, since it has no monosynaptic connection with N1M (McCrohan and Croll, 1997).

CV1b was active in 76.5% of vTN triggered cycles (n=17) and in 83% of preparations tested (n=6). **Figure 4.4A** shows an example of CV1b activity in a triggered rhythm. CV1b is active in the protraction phase of each of the five triggered cycles. **Figure 4.4B** shows an example of CV1b not active in a triggered rhythm. The average spike frequency per cycle within the protraction phase was 4.89 Hz. In 76.5% of vTN triggered cycles CV1b was active in the first cycle (**Figure 4.4A** and **4.4C**). In one preparation CV1b was recorded with N1M in a triggered rhythm. N1M was shown to be active before CV1b in two triggered cycles out of three (**Figure 4.4C**). Therefore CV1b could play a role during vTN triggered cycles. However, CV1b's low firing rate when it was active in triggered cycles and the fact that it was not active in every trigger attempt show that it was not necessary for vTN to trigger cycles. A modulatory role has

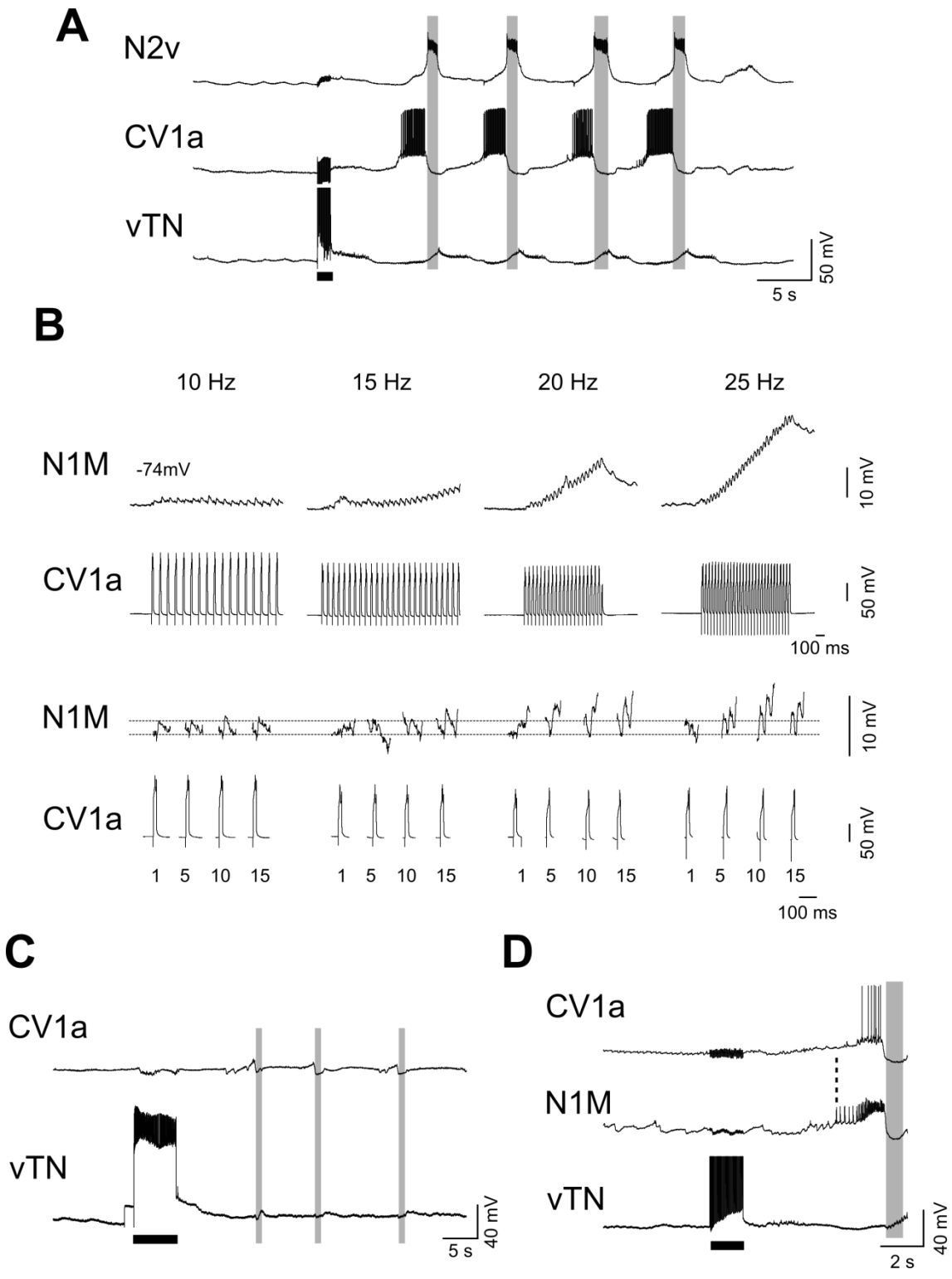

Figure 4.3 CV1a activity in vTN triggered cycles. **A.** vTN triggered four fictive feeding cycles. CV1a was strongly active in the protraction phase of all of the cycles. **B.** Facilitating EPSPs from CV1a to N1M. CV1a produces EPSPs on N1M which facilitate depending on CV1a spike frequency. Facilitation of the EPSP on N1M from CV1a was most evident when CV1a was firing at 20 Hz and above. Bottom traces shows expanded single spikes and corresponding EPSPs. **C.** CV1a activity was not necessary for vTN to trigger fictive feeding. **D.** N1M was always seen to be active before CV1a in the first triggered cycle. The dotted line represents N1M's first spike. Black horizontal lines represent depolarising current. Grey vertical lines represent the rasp phase of a cycle.

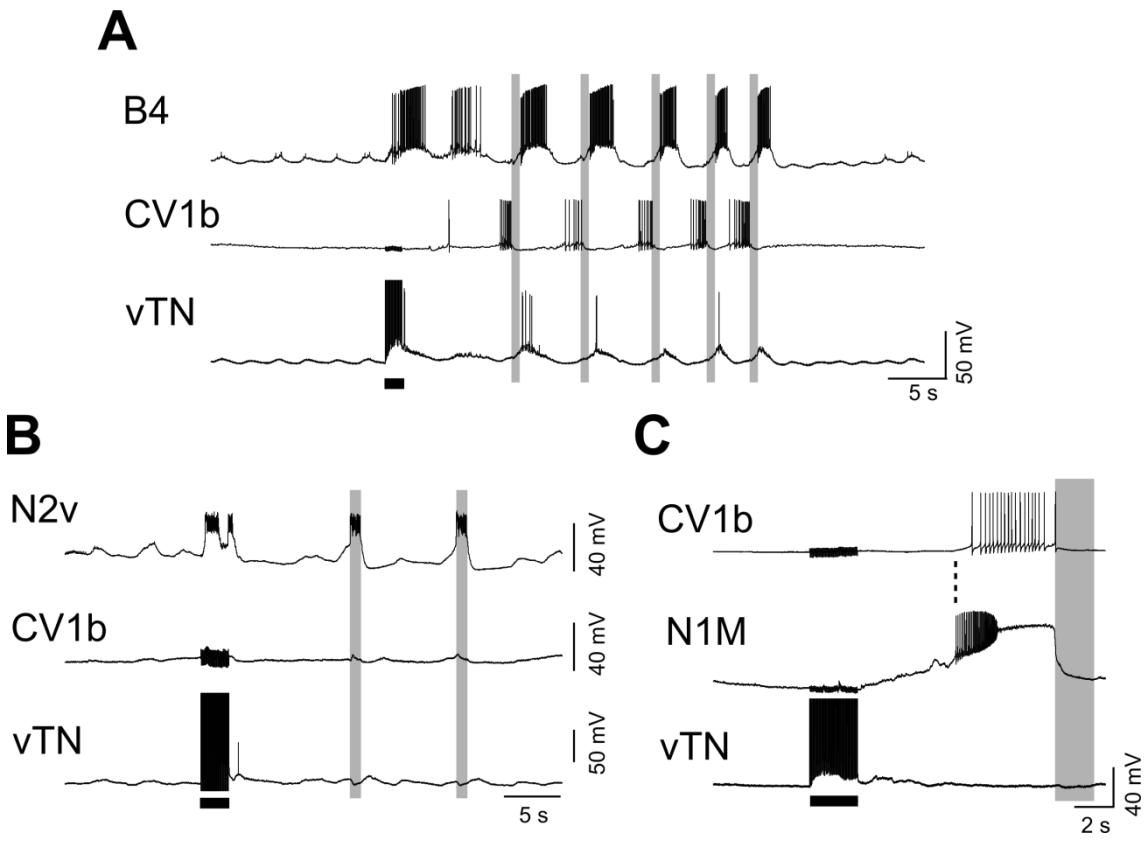

Figure 4.4 CV1b activity in vTN triggered cycles. **A.** vTN triggered five fictive feeding cycles. CV1b was active in the protraction phase of all cycles. **B.** CV1b was not necessary for vTN to trigger fictive feeding. Two full fictive feeding cycles are generated, as seen by N2v activity, but CV1b fires no action potentials. **C.** N1M was shown to be active before CV1b in 2 of 3 trigger attempts in one preparation. The dotted line indicates N1M's first spike, which occurs before CV1b activity. Black horizontal bars represent depolarising current. Grey vertical bars represent the rasp phase of a fictive feeding cycle.

previously been suggested for CV1b (McCrohan and Croll, 1997), which supports the results showing that it is not necessary for triggered cycles.

4.2.2.3 SO and N1L activity in triggered cycles

There are two protraction phase interneurons which have their processes located purely within the buccal ganglia: the SO and the N1L. The SO is a single cell located on either the left or the right buccal ganglion. It is able to drive a strong fictive feeding rhythm, mainly via its facilitating excitatory connection with N1M (Elliott and Benjamin, 1985b). The SO showed activity in 45% of vTN triggered cycles (n=11) and in 42.9% of preparations (n=7). However, the SO's average spike frequency within the protraction phase of the cycles was 0.44 Hz and the average number of spikes initiated per cycle was low (1.27 spikes (±0.2)). **Figure 4.5A** provides an example where SO showed no activity in either of the two triggered cycles. In **Figure 4.5B**, SO fires a single action potential in the second triggered protraction phase. Therefore it is very unlikely that SO plays any role in vTN triggered cycles. This was supported by the fact that in only 18.2% of trials did SO show any activity in the first cycle, and in one preparation where N1M was shown to be active without any SO activity.

The N1Ls have a large excitatory non-facilitating connection with the N1Ms (Yeoman et al., 1995) and are electrotonically coupled with the SO. N1L was active in 40% of vTN triggered cycles (n=10) and in 16.7% of preparations (n=6). The average spike frequency during the protraction phase was 3.83 Hz and it was active in 40% of trials during the first cycle. In **Figure 4.6A** N1L shows its typical response in a vTN triggered rhythm. It receives a small excitation in the protraction phase which fails to reach threshold, and is inhibited in the rasp phase. In one preparation N1L was strongly recruited into vTN triggered rhythms (**Figure 4.6B**). Given its very low rate of activation, it is therefore unlikely that N1L plays an important role in vTN triggered cycles.

4.2.2.4 BCI1 activity in triggered cycles

The newly identified BCI1 interneuron is located in the buccal ganglia and sends projections down both ipsi- and contralateral CBCs. It is able to initiate fictive feeding via an electrotonic connection with the N1M. A detailed characterisation of this neuron and its function in feeding will be discussed in Chapter 7. Due to BCI1's ability to initiate fictive feeding, its role in vTN-triggered cycles was tested. BCI1 was active in 48% of vTN triggered cycles (n=25) and in 56.3% of preparations (n=16). **Figures**

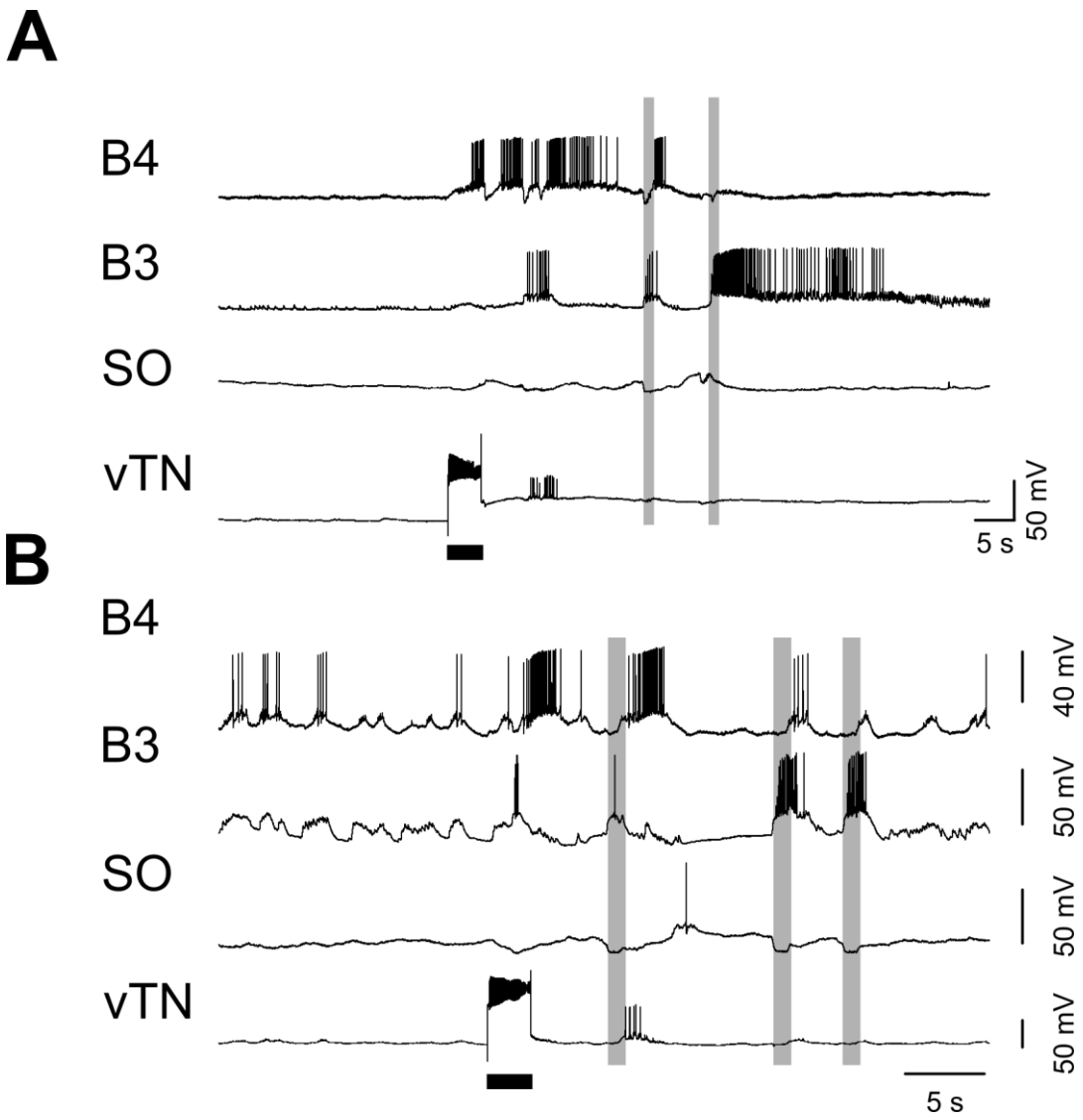

Figure 4.5 SO activity in vTN triggered cycles. **A.** vTN triggered two fictive feeding cycles. SO showed no activity in the protraction phase during either cycle, indicating that it is not necessary for vTN to trigger cycles. **B.** vTN triggered three fictive feeding cycles. SO showed activity in the protraction phase of the second cycle. However it only fired a single action potential, indicating that it plays very little role in vTN triggered cycles. Black horizontal bars represent depolarising current. Grey vertical bars represent the rasp phase of a fictive feeding cycle.

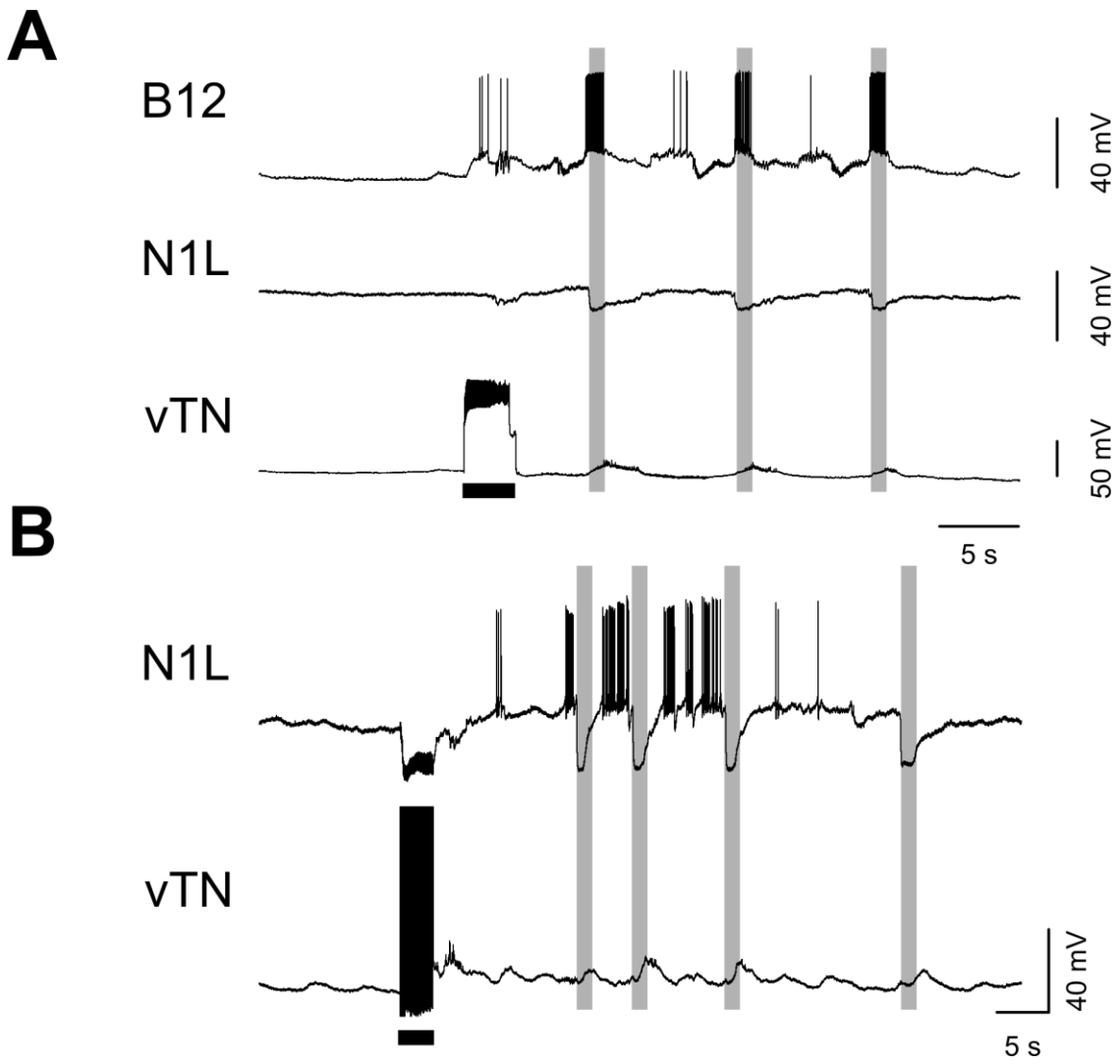

Figure 4.6 N1L activity in vTN triggered cycles. **A.** vTN triggered three fictive feeding cycles. N1L showed no activity in the protraction phase during any of the cycles, indicating that it is not necessary for vTN to trigger cycles. **B.** N1L showed activity in vTN triggered cycles in one preparation. vTN triggered four fictive feeding cycles. N1L was active in all four cycles at a high frequency. Black horizontal bars represent depolarising current. Grey vertical bars represent the rasp phase of a fictive feeding cycle.

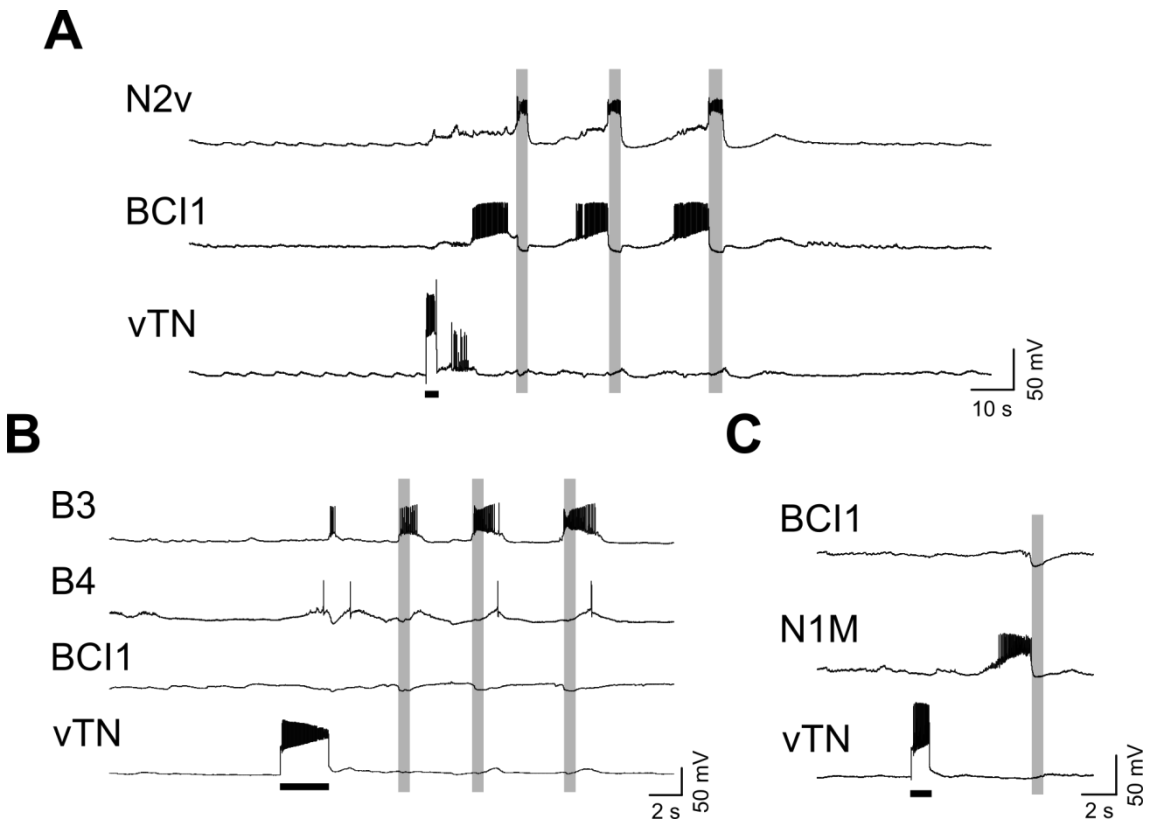

Figure 4.7 BCI1 activity in vTN triggered cycles. **A.** vTN triggered three fictive feeding cycles. BCI1 was strongly active in all three cycles. **B.** BCI1 activity was not necessary for vTN to trigger cycles. vTN triggered three fictive feeding cycles whilst BCI1 showed no activity. **C.** vTN triggered rhythm showing N1M activity in the absence of BCI1 activity. Black horizontal bars represent depolarising current. Grey vertical bars represent the rasp phase of a fictive feeding cycle.

4.7A and **4.7B** provide examples of BCI1 active and not active in vTN triggered rhythms respectively. BCI1's average spike frequency in the protraction phase was 7.39 Hz. BCI1 was active in the first triggered cycle in 36% of trials. The high firing rate of BCI1 implies that it may play a role in the triggered cycles, but it is not necessary for vTN to trigger cycles. In **Figures 4.7C** N1M was active in the absence of any BCI1 activity.

Therefore the only protraction phase interneuron always activated by vTN is the N1M. The fact that N1M was always active is in accordance with previous data showing that it is necessary for fictive feeding to occur. N1M is also active before the other command-like cells. It was therefore necessary to test how vTN was able to initiate N1M activity.

4.2.3 Testing vTN's synaptic connection with N1M

As N1M was active in every triggered cycle and before other command-like cells, it was tested whether vTN had any monosynaptic connections with N1M. In normal saline the connection from vTN to N1M was often difficult to analyse. This was due to there being several different inputs arising on the N1M at the time of vTN stimulation (**Figure 4.8A**).

To remove any polysynaptic inputs the preparation was bathed in HiDi saline for 30 minutes and the stimulus was applied to vTN again. At RMP in HiDi saline (-74.4 ±1.3 mV) N1M showed a delayed depolarization after vTN stimulation (n=15) (**Figure 4.8B**). The average amplitude of this depolarization was 6.6 mV (±0.8). When N1M was depolarised, vTN stimulation caused an early inhibition followed by a delayed excitation (**Figure 4.8Ci**) which could elicit spiking in N1M (**Figure 4.8Cii**). No unitary PSPs following 1:1 from vTN spikes were evident; however the persistence in HiDi saline does not allow us to rule outthat a component of the connection was may be monosynaptic. The average duration to the end of the excitatory input to N1M from the end of the vTN stimulation was 10.5 s (±1.4).

The excitatory input from vTN persisted on N1M even after inhibitory inputs from an N2v interneuron (n=1) (**Figure 4.8D**). This also provides evidence that N1M has no PIR properties, since the N2v input to N1M is purely inhibitory. The vTN input in contrast consists of an early inhibition followed by a delayed excitation which suggests that this is a biphasic connection. This long lasting depolarization of N1M which persisted after polysynaptic inhibitory inputs was a possible candidate for explaining vTN's trigger ability. The excitation could drive N1M to reach threshold in the first cycle

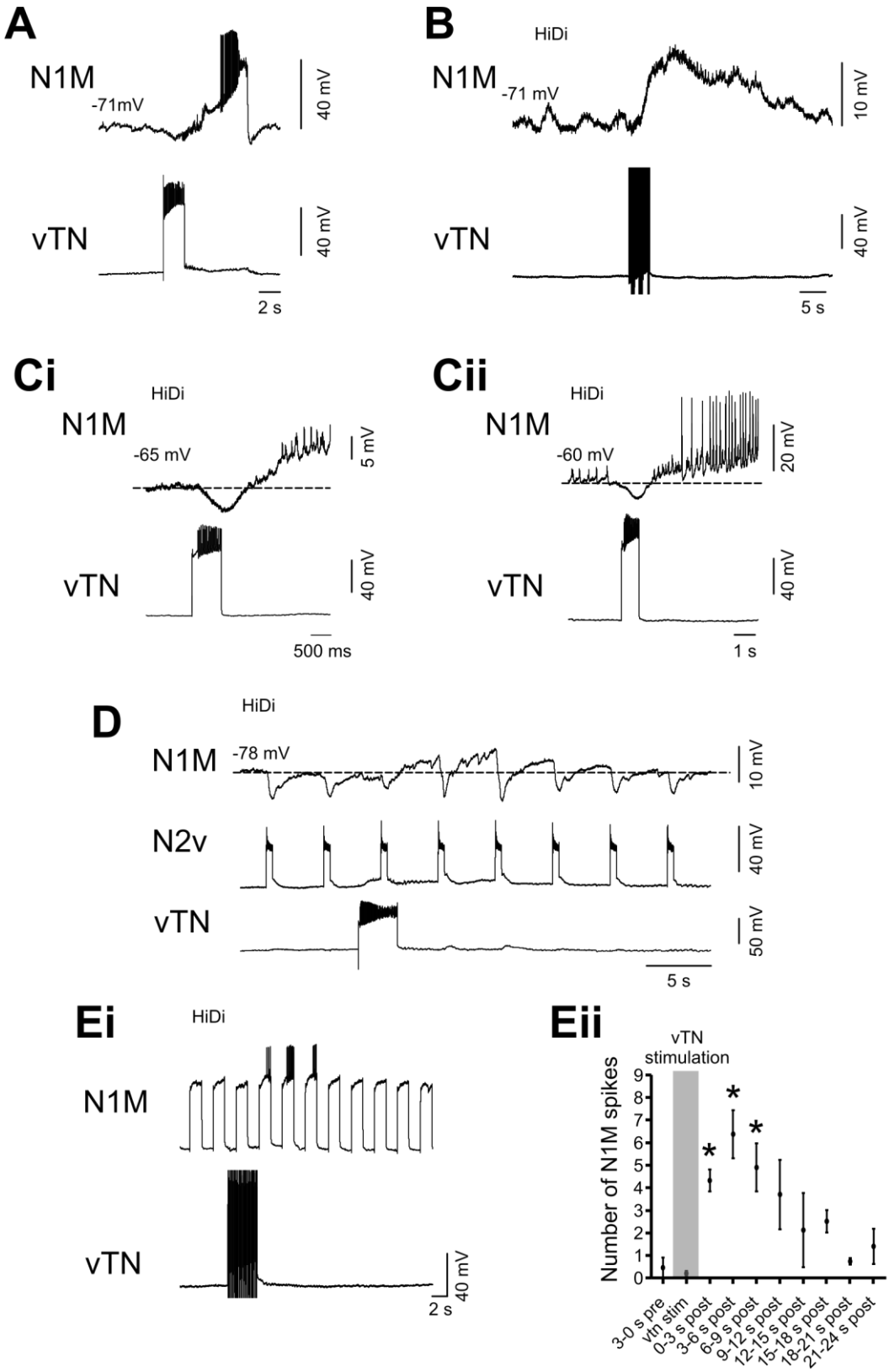
A
N1M
-71mV
40 mV
vTN
40 mV
2 s
B
HiDi
N1M
-71 mV
10 mV
vTN
40 mV
5 s
Ci
HiDi
N1M
-65 mV
5 mV
vTN
40 mV
500 ms
Cii
HiDi
N1M
-60 mV
20 mV
vTN
40 mV
1 s
D
HiDi
N1M
-78 mV
10 mV
N2v
40 mV
vTN
50 mV
5 s
Ei
HiDi
N1M
vTN
40 mV
2 s
Eii
vTN
stimulation
Number of N1M spikes
0
1
2
3
4
5
6
7
8
9
*
*
*
3-0 s pre vtn stim
0-3 s post
3-6 s post
6-9 s post
9-12 s post
12-15 s post
15-18 s post
18-21 s post
21-24 s post

Figure 4.8 vTN's synaptic connections with N1M **A.** vTN stimulation caused a variable inhibitory input followed by a delayed excitation in normal saline. **B.** In HiDi saline at RMP vTN stimulation caused a delayed depolarization of N1M. The persistence in HiDi saline suggests that a component of the connection may be monosynaptic. **Ci.** When N1M was more depolarised, vTN stimulation caused a fast inhibition followed by a delayed excitation. No 1:1 PSPs were ever evident; however the persistence in HiDi saline suggests that a component of the connection may be monosynaptic. **Cii.** The excitatory component was sufficient to elicit action potentials in N1M. **D.** N2v stimulation causes large inhibition on N1M. No delayed excitation was present after N2v stimulation. This suggests that N1M has no PIR which could account for vTN's biphasic input. vTN excitation to N1M persisted after several N2v inhibitory inputs. N1M continues to depolarise even after the N2v inhibition. **Ei.** vTN stimulation increased N1M's excitability after the end of the stimulus. Subthreshold pulses become suprathreshold after vTN stimulation. **Eii.** N1M excitability is significantly increased 0-3, 3-6 and 6-9 seconds after vTN stimulation. * $P < 0.05$.

and persist in subsequent cycles after periods of inhibition from other CPG interneurons. However the average duration of the onset of N1M activity in triggered cycles was 3.6 s (±0.3) and the average cycle period was 6.9 s (±0.5) (Data from vTN triggered cycles whilst recording an N1M). Therefore N1M depolarization is unlikely to persist until the generation of the second cycle.

During the period of depolarization on N1M from vTN activation, N1M excitability was increased. This was tested by applying depolarising current pulses to N1M which were either sub-threshold or elicited very few spikes per pulse. vTN was then activated during one of the pulses (**Figure 4.8Ei**). The number of spikes elicited per pulse before, during and after vTN activation were counted (n=4). There was a significant increase in the number of spikes elicited 0-3 s, 3-6 s and 6-9 s after vTN activation compared with the number of spikes from a control pulse before vTN activation (Number of N1M spikes per pulse before vTN stimulus = 0.3 (±0.3), during vTN stimulus = 0.4 (±0.2), 0-3 s after vTN stimulus = 4.3 (±0.3), 3-6 s after vTN stimulus = 5.5 (±1.1), 6-9 s after vTN stimulus = 4.2 (±1.0), 9-12 s after vTN stimulus = 3.0 (±1.3), 12-15 s after vTN stimulus = 1.6 (±1.3), 15-18 s after vTN stimulus = 1.9 (±0.7), 18-21 s after vTN stimulus = 0.5 (±0.2). Friedman test: df = 3, $\chi^2 = 26.48$, $P < 0.01$, Dunns Test 0-3 s after vTN stimulus $P < 0.05$, 3-6 s after vTN stimulus $P < 0.05$, 6-9 s after vTN stimulus $P < 0.05$, all other conditions $P > 0.05$.) (**Figure 4.8Eii)**

This data suggests that the excitatory drive to N1M in the first of the triggered cycles originates directly from vTN. This was sufficient to explain the initiation of the first of the triggered cycles. It was next tested whether this was also sufficient to account for the subsequent triggered cycles. To test this, a single N1M was depolarised sufficiently to initiate a full fictive feeding cycle, mimicking vTN's activation of N1M. The stimulus was removed from N1M at the onset of the rasp phase and the total number of fictive feeding cycles that were elicited was counted (**Figure 4.9A**). The average number of cycles initiated by N1M stimulation alone was 1.1 (±0.1) (trigger attempts = 38, preps = 12). Therefore vTN activation of N1M is not sufficient to account for subsequent triggered cycles, but only the initiation of the first cycle. This also provides evidence that vTN's trigger ability is not a feature shared by all neurons with the ability to drive cycles within the feeding network. The trigger ability of several other command-like neurons was next tested. All neurons were stimulated until a full fictive feeding cycle was initiated and then the stimulus was removed. The total number of cycles initiated was then counted. BCI1 initiated 1 (±0) cycle (trigger attempts = 16, preps = 10) (**Figure 4.9B**), CV1a initiated 1.2 (±0.1) cycles (trigger attempts = 56, preps = 14) (**Figure 4.9C**) and CV1b initiated 1.0 (±0.04) cycle (trigger attempts = 16, preps = 7)

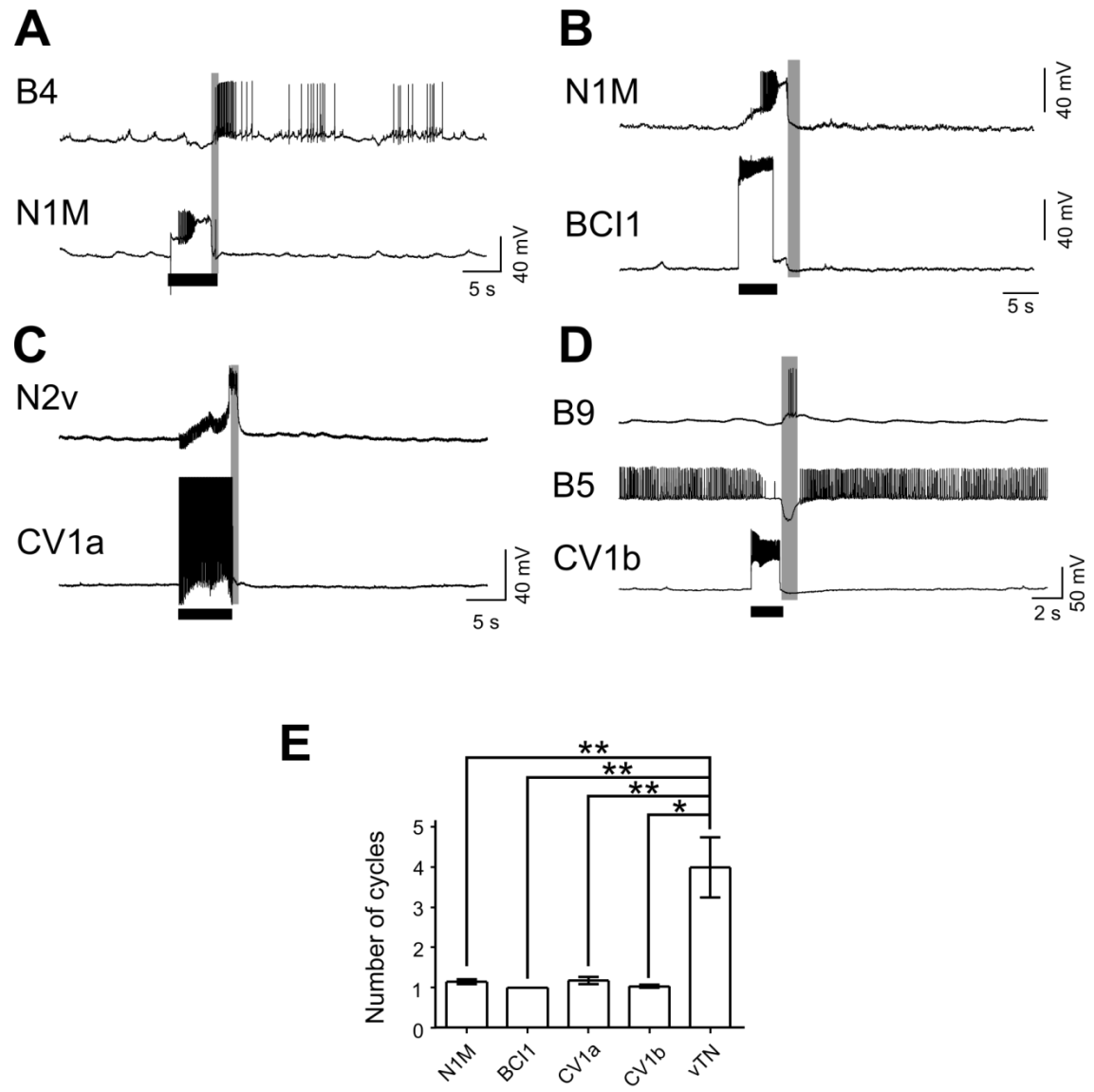

Figure 4.9 Trigger ability of command-like neurons within the feeding network **A.** An N1M was depolarised until the onset of the rasp phase and then the stimulus was removed from the cell, resulting in a full fictive feeding cycle, as seen by the inhibitory input to both N1M and B4, and the activation of B4 in the swallow phase. No further cycles were generated once the stimulus was removed from the cell. **B.** Depolarising BCI1 triggers a full fictive feeding cycle, as seen by the activation of N1M and subsequent inhibition from the N2 interneurons. No further cycles were generated. **C.** CV1a stimulation elicits a fictive feeding cycle, as seen by the activation of the rasp phase interneuron N2v. No further cycles were generated. **D.** CV1b stimulation initiates a fictive feeding cycle. B5 is inhibited in the protraction and rasp phase, and B9 excited in the rasp phase. No further cycles were generated. **E.** vTN stimulation was able to trigger significantly more cycles than any of the command-like neurons in the feeding network. Black horizontal bars indicate depolarising current. Grey vertical bars indicate the rasp phase of a fictive feeding cycle. * $P < 0.05$, ** $P < 0.01$.

(**Figure 4.9D**). vTN was able to trigger significantly more cycles than all command-like neurons tested, whereas there was no significant difference between each of the command-like neurons (vTN number of cycles in successful triggers = 4.0 ±0.7) (One-way ANOVA: $F[4,65] = 6.512$, $P < 0.0001$, Tukey's Multiple Comparison Tests: vTN vs. N1M, $P < 0.01$. vTN vs. BCI1, $P < 0.01$. vTN vs. CV1a, $P < 0.01$. vTN vs. CV1b, $P < 0.05$. All other conditions, $P > 0.05$) (**Figure 4.9E**). This confirms that all of these neurons are sufficient to activate fictive feeding, but are not able to trigger cycles in the same manner as vTN. Therefore the biphasic connection from vTN to N1M is sufficient to explain the first triggered cycle, but not the subsequently generated cycles in the absence of further vTN activity.

4.2.4 N3t activity in triggered cycles

It was therefore important to identify the mechanism by which vTN was able to trigger on-going cycles but which prevented the generation of further cycles in command-like neuron driven cycles. A candidate for providing this mechanism was the N3t cell. N3t is a swallow phase CPG interneuron (Elliott and Benjamin, 1985a). It also fires tonically during periods of quiescence, providing inhibition to N1M (**Figure 4.10A**). Staras et al. (2003) showed that by hyperpolarising N3t, N1M was released from inhibition and a fictive feeding cycle was generated. It was tested whether levels of N3t activity within the swallow phase of single command-like initiated or spontaneously generated cycles were different to levels in vTN triggered cycles.

N3t receives inhibition during the protraction and retraction phases and then fires due to PIR in the swallow phase. In triggered cycles I examined N3t frequency from the start of the swallow phase until the beginning of the next protraction phase and the initiation of the next cycle. This was compared with N3t spike frequency during spontaneous or command-like neuron initiated single cycles (n=6) (**Figure 4.10B**). Since there was no subsequent protraction phase in single cycles, the average duration of N3t activity in the swallow phase of triggered cycles was measured within preparations and used as a measure of N3t activity in single cycles. There was a significant reduction in N3t firing rate in triggered cycles (6.7 Hz ±0.8) vs. single cycles (8.9 Hz ±0.9) (Paired t-test $df = 5$, $t = 9.8$, $P < 0.001$) (**Figure 4.10Ci**). N3t fires both via PIR, acting as a CPG interneuron, and tonically, acting as a suppressor of N1M activity. Therefore N3t activity within triggered and single cycles was separated into a PIR phase and a tonic phase to examine whether the reduction seen in triggered cycles was present in both phases (**Figure 4.10B**).

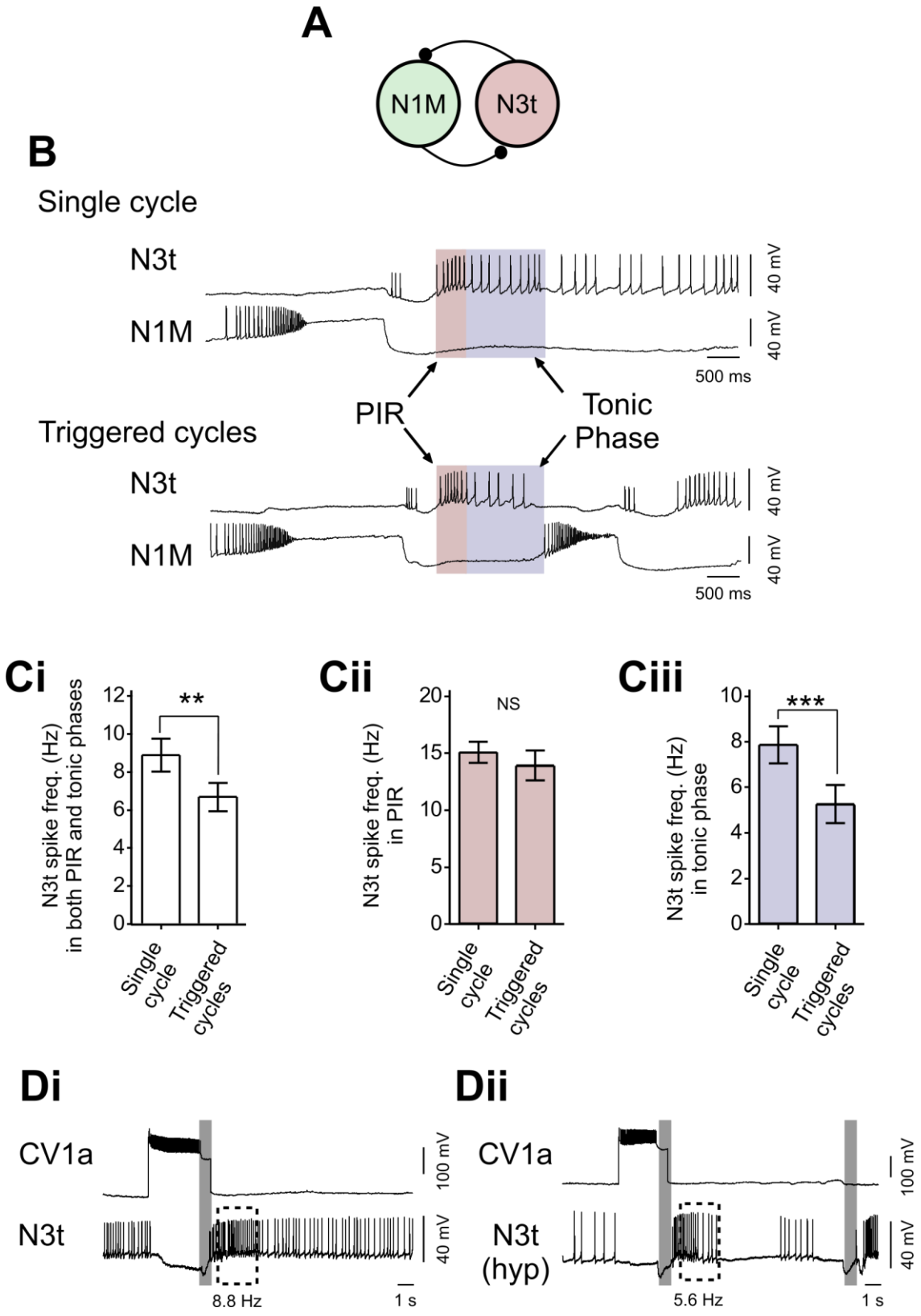
A
N1M
N3t
B
Single cycle
N3t
N1M
40 mV
40 mV
500 ms
PIR
Tonic
Phase
Triggered cycles
N3t
N1M
40 mV
40 mV
500 ms
Ci
N3t spike freq. (Hz)
in both PIR and tonic phases
**
Single cycle
Triggered cycles
Cii
N3t spike freq. (Hz)
in PIR
NS
Single cycle
Triggered cycles
Ciii
N3t spike freq. (Hz)
in tonic phase
***
Single cycle
Triggered cycles
Di
CV1a
N3t
100 mV
40 mV
8.8 Hz
1 s
Dii
CV1a
N3t
(hyp)
100 mV
40 mV
5.6 Hz
1 s

Figure 4.10 N3t activity in triggered cycles **A.** Circuit showing mutual inhibitory connections between N1M and N3t **B.** N3t activity was compared in the period after a cycle between single cycles and triggered cycles. The duration from the start of the swallow phase until the onset of the next protraction phase was measured in triggered cycles and used as a value to measure from the start of the swallow phase in single cycles (since no subsequent protraction phase was present in these trials). N3t fires via PIR after inhibition and tonically in the absence of inputs. Therefore N3t activity was also separated into a PIR phase (red rectangle) (500 ms from the end of the rasp/N2 phase) and a tonic phase (blue rectangle). The tonic phase was measured in triggered cycles from the end of the PIR phase until the onset of the next protraction phase. This duration was averaged per preparation and the value used to measure the tonic phase in single cycles. N3t firing frequency was unchanged in the PIR phase between the two conditions. N3t firing frequency was reduced in the tonic phase in triggered cycles compared with single cycles. N1M was recorded simultaneously to determine whether any changes in N3t rate were due to active inhibition from N1M. The reduction in N3t firing rate in the tonic phase occurred before the onset of N1M. **Ci.** There was a significantly reduced level of N3 firing in triggered cycles compared with single cycles. **Cii.** No significant difference was found between the triggered and single cycle in the PIR phase. **Ciii.** A significant reduction in N3t firing frequency was present in the tonic phase of triggered cycles compared with single cycles. **Di.** Stimulating a single CV1a interneuron was sufficient to elicit a single fictive feeding cycle. N3t firing rate in the tonic phase was similar to those seen in the previous experiment. **Dii.** To test whether the reduction in N3t firing rate seen in vTN triggered cycles was sufficient to explain the on-going nature of triggered cycles vs. single cycles, N3t firing rate was artificially manipulated. Reducing N3t firing rates in the tonic phase of a CV1a driven cycle to those seen in vTN triggered cycles was sufficient to initiate another fictive feeding cycle. This provides evidence that the reduction in rate is sufficient to explain vTN's trigger ability. Completely preventing N3t from firing during periods of quiescence is sufficient to initiate a fictive feeding cycle via removal of tonic inhibition on N1M. In these experiments N3t was hyperpolarised prior to CV1a stimulation. The firing rate was reduced, not completely prevented; therefore this reduction alone was not sufficient to elicit a fictive feeding cycle. Interestingly this suggests that a reduction in rate after a feeding cycle has occurred is more likely to initiate another cycle than simply reducing the rates in a period of quiescence. Circles represent inhibitory synaptic connections in the circuit diagram. Black horizontal lines represent depolarising current. Blue horizontal lines represent hyperpolarising current. Grey vertical lines represent the rasp phase of a cycle. * $P < 0.05$, ** $P < 0.01$, *** $P < 0.001$, NS not significant.

In a previous study, the PIR of N3t was modelled (Vavoulis et al., 2007). The PIR was hypothesised to be due to a low-threshold calcium current, i_T, which was de-inactivated due to the protraction and rasp phase inhibition and had a 400 ms inactivation rate. Therefore, here, the PIR phase of both triggered and single cycles was measured from the beginning of the swallow phase (when N3t is released from inhibition from rasp phase interneurons) until 500 ms later, ensuring that the majority of PIR activity was measured. The tonic phase was measured from the end of the PIR phase until the onset of the next protraction phase in triggered cycles. The average duration of the tonic phase within preparations was measured and used as a measure of the tonic phase in single cycles. No difference was found between the PIR phases in single cycles vs. triggered cycles (single cycles PIR phase = 15.08 Hz ±0.9, triggered cycles PIR phase = 13.91 Hz ±1.3, paired t-test df = 5, t = 1, P > 0.05) (**Figure 4.10Cii**). There was a significantly higher rate of N3t activity during the tonic phase of single cycles vs. triggered cycles (single cycles tonic phase = 7.86 Hz ±0.8, triggered cycles tonic phase = 5.26 ±0.84, paired t-test df = 5, t = 13.4 P < 0.001) (**Figure 4.10Ciii**).

The fact that there was no change in the PIR phase suggests that N3t's role as a CPG interneuron is unaffected. The reduction in N3t firing rate in the tonic phase was not due to inhibition from N1M (n=3). In **Figure 4.10B** the reduction in N3t firing rate occurs before N1M becomes active and provides inhibition to N3t. Therefore it is possible that this reduction in rate allows N1M to reach threshold and initiate a further cycle.

It was next tested whether the reduction in N3t activity was sufficient to allow further cycles to be generated and explain vTN's trigger ability. To test this, N3t rates were artificially manipulated during cycles to mimic levels seen in triggered cycles. Cycles were initiated by a CBI. These initiated single cycles similarly to N1M stimulation or single spontaneous cycles, with comparable N3t levels (8.8 Hz in the tonic phase) (**Figure 4.10Di**). When N3t levels were reduced to those seen in triggered cycles (5.6 Hz in the tonic phase), further cycles were generated (n=3) (**Figure 4.10Dii**). This shows that the reduction in N3t rate seen in triggered cycles is sufficient to explain vTN's on-going trigger ability.

4.2.5 Testing vTN's synaptic connection with N3t

vTN's synaptic connections with N3t were tested to determine how vTN reduced N3t's firing rate in the tonic phase. HiDi saline was used to reduce polysynaptic connections and prevent N3t from firing tonically. vTN stimulation caused a depolarization of N3t which was often sufficient to elicit action potentials (n=12). **Figure 4.11Ai** provides an

example of vTN stimulation exciting N3t which in turn causes unitary EPSPs on the B3 motor neuron. The excitation from vTN to N3t persisted in HiLo saline suggesting that the connection was electrotonic in nature (n=3). **Figure 4.11Aii** shows an example from the same preparation as **Figure 4.11Ai**. Notice how the vTN to N3t connection persists, but the N3t to B3 chemical EPSPs are now absent. Square pulses in either direction to vTN (**Figure 4.11Bi**) or N3t (**Figure 4.11Bii**) produced a similar but attenuated response in the postsynaptic cell. vTN activation caused no inhibition of N3t in HiDi saline. When N3t was depolarised to fire at a steady rate, vTN stimulation caused no long term reduction in firing rate (n=9) (**Figure 4.11C**). It was next tested whether vTN caused any long term changes in N3t excitability. N3t was stimulated with regular interval suprathreshold depolarising pulses and the number of spikes per pulse counted. vTN was then stimulated to fire at a high rate and N3t spike numbers were counted in the post vTN activity pulses.

vTN activity caused no significant increase in N3t excitability (n=4) (pre-vTN activation = 6.3 spikes (±1.0), 0-5 s = 8.3 spikes (±0.8), 5-10 s = 6.5 spikes (±1.2), 10-15 s = 6.3 spikes (±0.9), Friedman test: df = 3, χ^2 = 7.37, P > 0.05) (**Figure 4.11D**).

4.2.6 Search for mechanisms by which vTN reduces N3t activity

Whilst looking for a possible mechanism by which vTN could reduce N3t's activity during triggered cycles, a previously unidentified connection was found. The N3t to B3 excitatory connection has been reported previously (Elliott and Benjamin, 1985a) (see **Figure 4.11Ai**) and is often used as a readout of N3t's activity (also see Section 5.2.4). In HiDi saline it was found here that B3 had a previously unidentified inhibitory connection with N3t (n=3). This was a slow but consistent effect. **Figure 4.12A** shows high frequency spiking in B3 causes a hyperpolarization of N3t. However, no unitary IPSPs were ever evident. In one preparation B3's effect on N3t was tested further. In HiDi saline, N3t was stimulated for 1 s with +0.2 nA at 2 s intervals. When B3 was stimulated to fire at a high rate, it reduced the firing rate of N3t whilst B3 was active and for the first pulse after B3 activity had ended (**Figure 4.12B**). This was also looked at with respect to N3t's PIR in the same preparation. Stimulating a CV1a caused a large hyperpolarization in N3t. Once CV1a activity had ceased, N3t recovered and fired spikes by PIR (**Figure 4.12Ci**). Activation of B3 prior to and throughout CV1a activation caused a reduction in the number of spikes N3t fired via PIR, but did not completely block the effect (**Figure 4.12Cii**). This is in agreement with the effects seen during vTN triggered cycles: the PIR phase remains unaffected whilst the tonic phase is reduced. B3 has also been shown to have a weak excitatory effect on N1M in normal saline

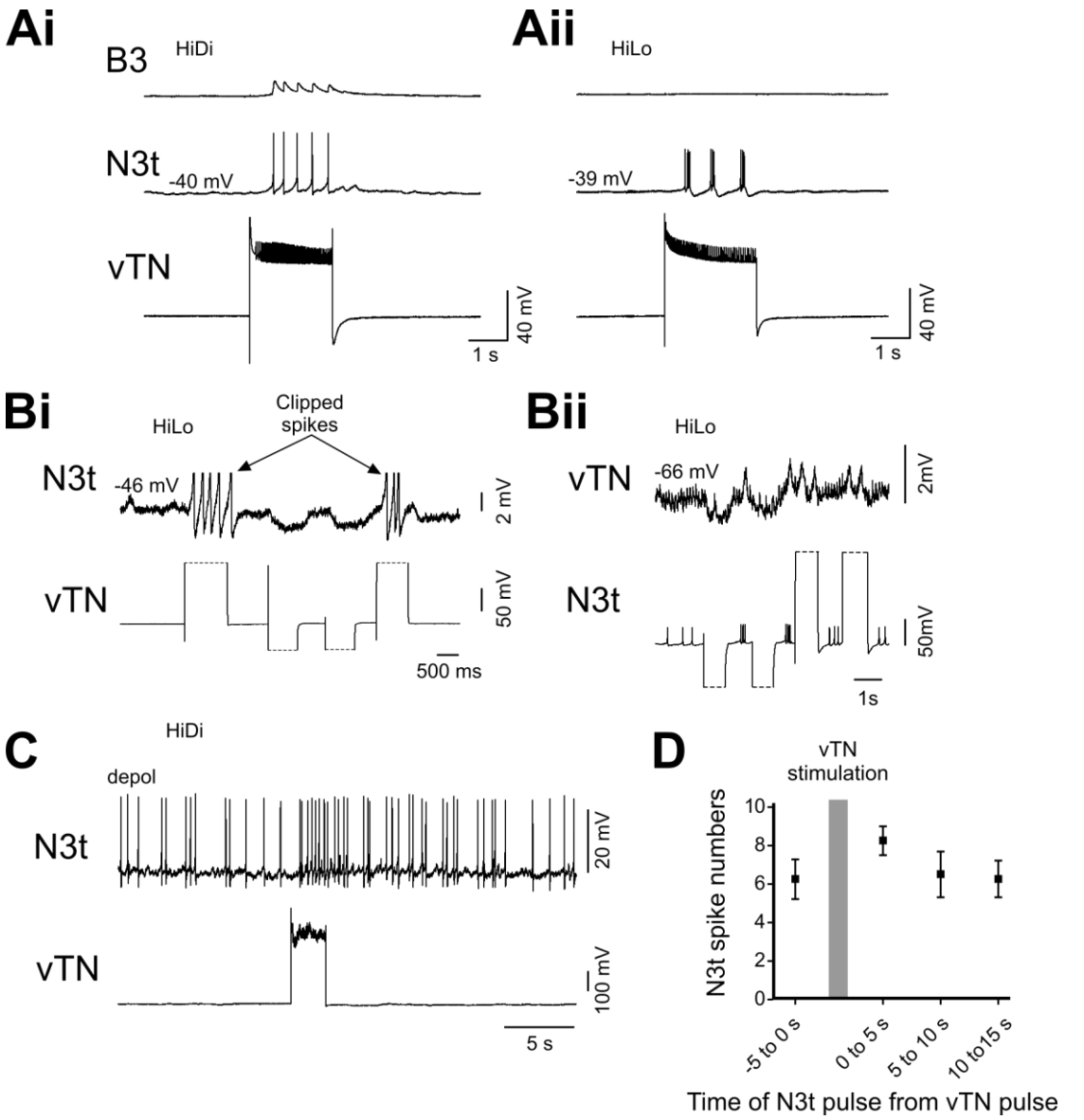

Figure 4.11 vTN's synaptic connections with N3t **Ai.** vTN stimulation depolarised a silent N3t in HiDi saline. This caused unitary EPSPs on the B3 motor neuron originating from N3t. **Aii.** This connection persisted in HiLo saline which effectively blocks chemical synaptic transmission. This suggests that the connection from vTN to N3t is electrical in nature. The N3t to B3 excitatory chemical connection is no longer present, but the vTN to N3t connection persists. **Bi.** Injecting vTN with depolarising and hyperpolarising square pulses produced similar yet attenuated responses in N3t in HiLo saline strongly suggesting that an electrical synapse is present. Several spikes are elicited in N3t in response to the depolarising steps in vTN. These are clipped in the trace. **Bii.** Injecting N3t with depolarising and hyperpolarising square pulses caused a similar yet attenuated response in vTN in HiLo saline. **C.** vTN causes no long term reduction of N3t spiking in HiDi saline. N3t was injected with continuous positive current to elicit spiking. vTN stimulation increases N3t's firing rate throughout the duration of the stimulus but no long term effect was seen on the firing rate. **D.** N3t excitability was not significantly increased by vTN stimulation. The grey bar represents vTN stimulation. Numbers above traces indicate the membrane potential of the neuron before another neuron was activated. Depol above a neuron indicates that the neuron was injected with positive current throughout the trace.

(Staras, 1997). This connection was confirmed in HiDi saline here, however no unitary PSPs were present on N1M following B3 spikes 1:1 (n=2) (**Figure 4.12D**). This would increase the likelihood of a subsequent cycle. B3 is a rasp phase neuron which often continues to fire in the swallow phase. This would mean it was active before N3t and could start to exert its effects on N3t earlier. **Figure 4.12E** provides a summary of known B3 connections with N1M and N3t and the newly identified ones from B3 to the interneurons. However, several preparations showed that vTN's trigger ability remained intact when there was little or no activity in B3 (see **Figure 4.1Ci**). Only one B3 could be recorded in triggered cycles since a twisted buccal preparation was used. However the two B3s are electrotonically coupled (Benjamin et al., 1979), making it unlikely that the contralateral B3 was very active in the cycles. Therefore, although B3 can affect N3t firing rates, it is unlikely to be the mechanism by which vTN can trigger fictive feeding.

Another possible mechanism by which vTN reduces N3t firing frequency was that vTN stimulation alters the strength of electrotonic synaptic connections with N3t. A number of neurons are known to have electrotonic synapses with N3t, including B4 (Staras et al., 1998b) and vTN itself. vTN and B4 have lower membrane potentials than N3t (N3t = -47.16 mV (±0.98) (n=11), vTN = -69.19 mV (±0.29) (n=232), B4 = between -53.9mV and -56.1 mV (Patel et al., 2006)). Therefore if vTN were to strengthen the electrotonic connection between N3t and itself or B4 it would effectively act as a shunt to N3t, reducing N3t activity. Changes in the B4-N3t electrotonic synapse was tested in one preparation. N3t was stimulated with regular negative current pulses which caused similar yet attenuated responses on a B4. vTN was then stimulated and any long term changes in the strength of the electrotonic synapse with B4 were monitored. No change was present in the connection from N3t to B4 in the hyperpolarising direction (**Figure 4.13A**). The connection from B4 to N3t was next tested in a similar manner (**Figure 4.13B**). Here too no change was observed. The connection was also tested in the depolarising direction, but no long term changes were present (**Figure 4.13C**).

4.3 Discussion

This chapter aimed to determine whether vTN was a true trigger neuron and identify the mechanisms by which vTN activated the feeding network. vTN fulfilled all the criteria to be classified as a trigger neuron (Stein, 1978, Brodfuehrer and Friesen, 1986a, Marder et al., 2005). vTN stimulation was able to reliably trigger fictive feeding which outlasted the duration of the stimulus to the cell. The stimulus levels used were

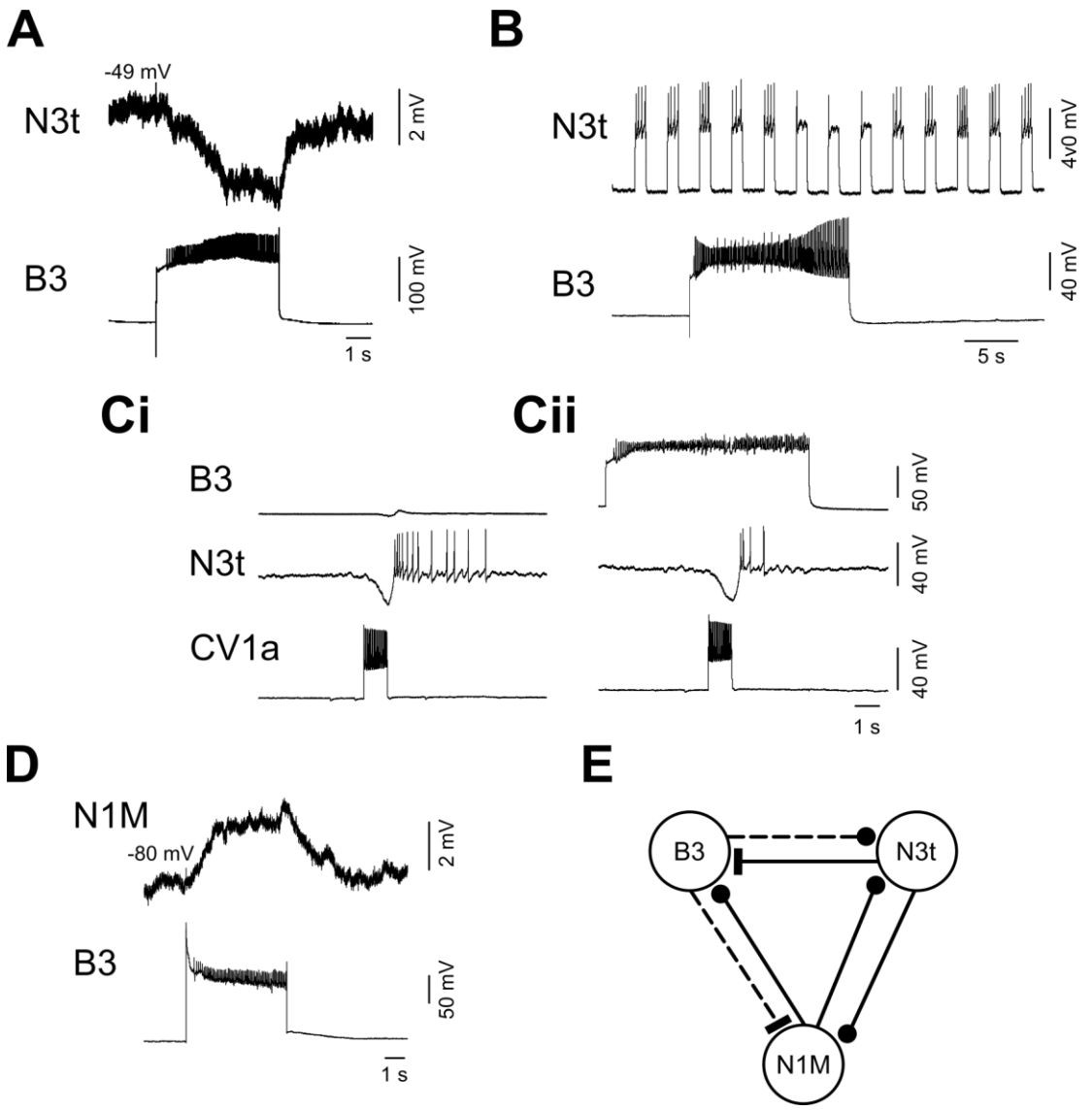

Figure 4.12 Effects of B3 on N3t and N1M **A.** A previously unidentified inhibitory connection from B3 to N3t exists. B3 activation hyperpolarised N3t. This was present in HiDi saline, however no 1:1 IPSPs were ever evident, suggesting that a component of the connection may be monosynaptic. **B.** N3t was stimulated with the same positive current injection at regular intervals. High frequency B3 activity reduced N3t activity. This reduction in N3t excitability persisted for a short duration after B3 activity. **Ci.** B3 activity reduces N3t firing after PIR. CV1a activity inhibited N3t. Once the stimulus to CV1a had been removed, N3t fired a number of action potentials via PIR. Notice how this persists for several seconds after the PIR. **Cii.** When this was repeated whilst B3 was stimulated throughout, N3t fired fewer action potentials after CV1a stimulation had ended. N3t's PIR persisted, however the number of spikes initiated and the duration of spiking was greatly reduced. **D.** B3 stimulation depolarized N1M in HiDi saline. No 1:1 EPSPs were ever present but the persistence in HiDi saline suggests that a component of the connection may be monosynaptic. This connection had previously been reported in normal saline (Staras 1997). **E.** Summary of known synaptic connections between B3, N1M and N3t. Black lines represent connections which persist in HiDi saline and there is evidence of unitary PSPs on the postsynaptic neuron following presynaptic spikes 1:1. Dotted lines represent connections which persist in HiDi saline but there is no evidence of unitary PSPs. Numbers above traces indicates the membrane potential of the neuron before another neuron was activated. All experiments performed in HiDi saline.

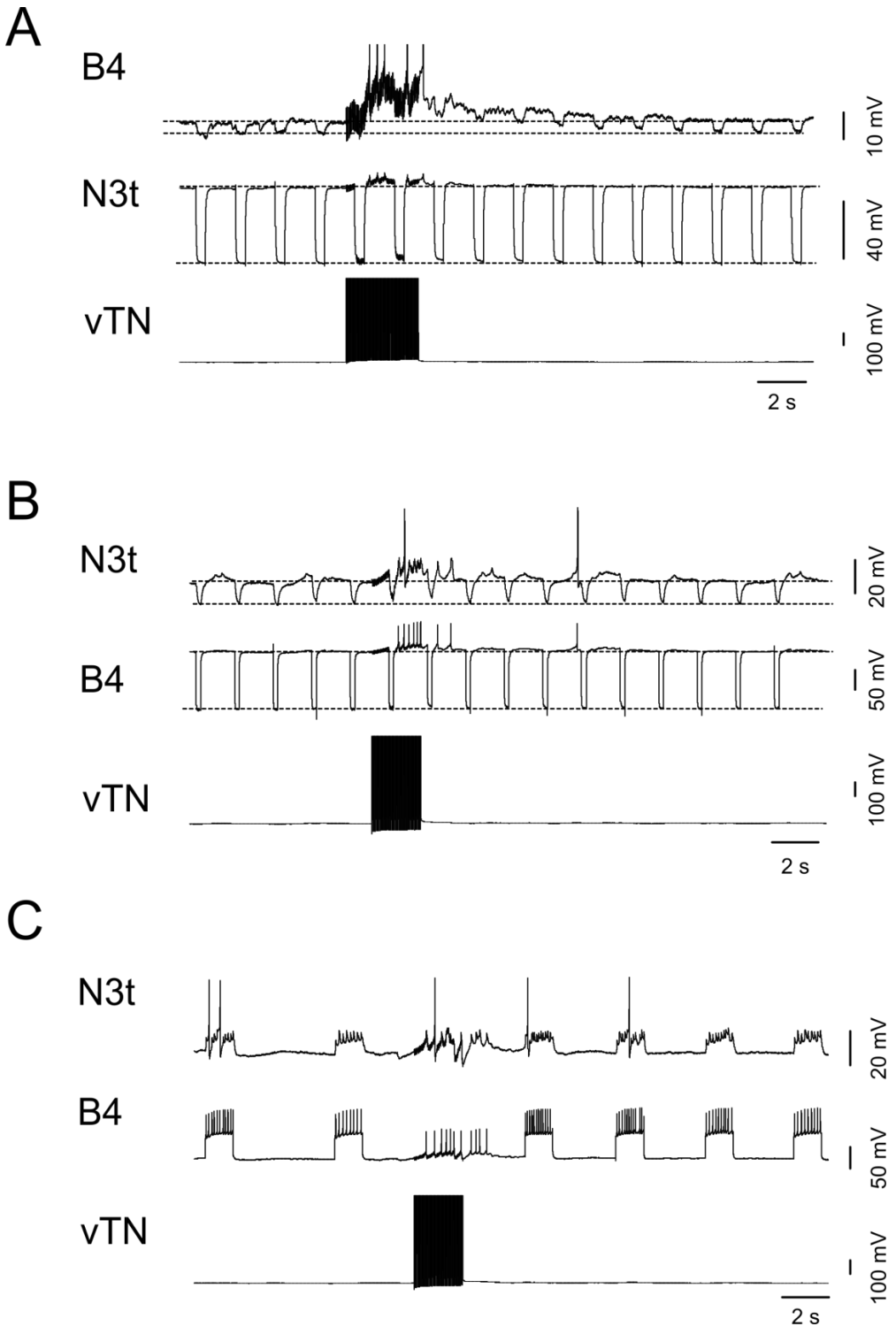

Figure 4.13 vTN effects on N3t-B4 electrical coupling **A.** vTN stimulation caused no noticeable change in the strength of the N3t-B4 electrical synapse. N3t was injected with negative square current pulses at regular intervals and the response recorded on B4. vTN stimulation caused a depolarization of both N3t and B4. There were no long term changes in the strength of the coupling between the two cells. Accurate coupling coefficients could not be gained due to the use of a single high resistance electrode in each neuron. N3t's membrane resistance also appears to remain unchanged after vTN stimulation. **B.** Changes in the B4-N3t direction electrical synapse were tested in a similar manner. B4 was injected with negative current and the response recorded on N3t. vTN caused no noticeable change in the strength of the connection. **C.** No changes were present in the strength of the connection from B4-N3t in the positive direction either after vTN stimulation. All experiments performed in HiDi saline.

also physiologically relevant, since similar firing rates were seen when the radula was simulated using a physiologically-relevant tactile input. No correlation was present between the number of cycles triggered and the duration of the stimulus either. Finally, further activity from vTN was not necessary for the cycles to be generated. These properties meant that vTN could be classified as a trigger neuron.

Previous trigger neurons have all been identified in escape behaviours (Brodfuehrer and Friesen, 1986a, Brodfuehrer and Friesen, 1986b, Soffe, 1997, Frost et al., 2001, Buhl et al., 2012). The role of these neurons is to convert an aversive stimulus into on-going escape behaviours. Trigger neurons have not previously been classified in any feeding behaviours. There is however some evidence that they may exist. In both *Tritonia* and *Aplysia* tactile stimulation of a sensory structure (Oral tube and buccal mass in *Tritonia*, buccal mass and perioral zone in *Aplysia*) activates identified mechanosensory neurons (Audesirk and Audesirk, 1979, Rosen et al., 1982). A short duration stimulus to these cells can elicit a number of fictive feeding cycles. However the reliability of these cells, and their role in initiating feeding were not examined. Stimulating a single RM in *Incilaria* can cause buccal motor programs (Kawahara et al., 1995). However the cell was stimulated at a high frequency for durations between 5-20 seconds. Although these studies suggest that similar trigger mechanisms may exist in the feeding system of other molluscs, no comprehensive experimental evidence has yet been provided for them.

The cycles triggered by vTN were on average 6.8 s long. This is longer than the cycle period recorded in vivo in the TS trials. Only the SO and N1L can reliably drive fictive feeding at a rate seen in vivo (Elliott and Benjamin, 1985a, Yeoman et al., 1995). CV1a can drive cycles of duration between 4-9 seconds long and CV1b can drive cycles which are 6.5 seconds long on average (McCrohan and Kyriakides, 1989). N1M drives the slowest feeding cycles (9 second duration) (Yeoman et al., 1995). Interestingly, N1M was the only interneuron always recruited into triggered cycles, yet triggered cycles were faster than N1M driven cycles, and closer in range to CBI driven cycles. By using in vitro preparations, it has been found that a chemical stimulus (sucrose) which is able to drive a high feeding rate in vivo produces a much slower fictive feeding rate in vitro (Kemenes et al., 1986, Staras et al., 1998a). Sucrose driven fictive feeding cycles ranged from 4-6 seconds in one study (Vehovszky et al., 2004) and 7-14 seconds in another (Kemenes et al., 2001). Therefore it appears that feeding can occur faster in vivo than in vitro.

One other neuron type within the feeding network of *Lymnaea* has been found to have some characteristics of a trigger neuron, the OCs. The OC interneurons in the buccal ganglia were shown to be able to initiate the feeding CPG after a short duration pulse at a physiological rate. This was found to be an unreliable characteristic of the neuron though, with only 28% of preparations successfully triggering cycles (Vehovszky and Elliott, 2001). If the cell was pulsed several times at regular intervals then the reliability increased to 41% (Vehovszky and Elliott, 2001). The poor reliability and need for repeated stimulations suggested that this was not OC's function within the feeding network and instead a modulatory role was suggested for the cell. Interestingly, the mechanism by which OC initiated feeding cycles was via a biphasic (i/e) connection with SO, N1L and N1M. It was not explored whether the depolarization to these neurons was sufficient to explain the on-going nature of the cycles triggered. However the excitatory input does not appear to last for a prolonged period (Vehovszky and Elliott, 2001). Therefore both vTN and OC appear to initiate at least the first cycle via a biphasic input to protraction phase interneurons (N1M only by vTN, SO, N1L and N1M by OC). Activation of the OCs also increases excitability in the SO and N1L interneurons, thereby increasing the excitatory drive on the N1Ms (Vehovszky and Elliott, 2002). None of the protraction phase command-like neurons tested here were able to trigger fictive feeding in a similar manner as vTN. All were sufficient to drive at least one full cycle, but removal of their activity usually resulted in the cessation of fictive feeding. Therefore vTN's reliable trigger ability is unique within the feeding network of *Lymnaea*.

vTN's connection with N1M was only sufficient to explain the initiation of the first cycle. The excitatory input to N1M did not persist long enough to account for the subsequent cycles, and no other command-like neurons were consistently activated by vTN, or active before N1M. Instead, vTN was found to trigger the subsequent cycles via a reduction in inhibition on the system during the swallow phase. N3t is both a swallow phase CPG interneuron and a modulatory neuron (Elliott and Benjamin, 1985a, Staras et al., 2003). It fires tonically during periods of quiescence, providing inhibition to N1M and preventing the generation of cycles. Hyperpolarising N3t in periods of quiescence has been shown to be sufficient to allow N1M to recover from inhibition and reach threshold and generate a fictive feeding cycle (Staras et al., 2003). During single fictive feeding cycles, N3t fired at a high rate during the 'tonic phase'. There was a significant reduction in N3t firing rates within this phase in vTN triggered cycles. This was not due to active inhibition by N1M on N3t, since the reduction in firing rate occurred before N1M was active. By artificially manipulating N3t firing rates in CBI driven cycles, it was

shown that the reduction in N3t firing rate was sufficient to explain vTN's trigger ability. vTN had no monosynaptic inhibitory connection with N3t. A weak electrotonic synapse existed between the two cells, which was unable to account for the reduction in N3t firing seen in triggered cycles. vTN activity resulted in no long term reduction in N3t excitability in HiDi saline either. In fact a small significant increase in N3t's excitability occurred immediately after vTN stimulation. Although N3t's membrane resistance could not accurately be recorded in these experiments, due to the small size of the neuron (<10µm) and need for high resistance electrodes, preliminary data suggest that vTN caused no long term changes in N3t's membrane resistance (n=4) (see **Figure 4.13A**).

There are a number of possibilities for how vTN reduces N3t firing rates within triggered cycles. The newly identified B3 to N3t slow inhibitory connection was a possible candidate for the mechanism by which N3t rates in the tonic phase were reduced in triggered cycles. B3→N3t inhibition had a slow onset, however as B3 is active in the rasp and the swallow phase, it could provide inhibition to N3t from the start of the rasp phase into the swallow phase. However, B3 activity was not necessary for vTN triggered cycles, indicating that this was not the mechanism by which N3t rates were reduced. It is possible that an unidentified neuron is activated during triggered cycles but not in single cycles, which provides inhibition to N3t in the tonic phase in a similar manner as B3. Another possibility is that an unidentified neuron is active in both triggered and single cycles, but vTN activity results in heterosynaptic facilitation of its inhibitory connection to N3t. Heterosynaptic facilitation has been found in a number of molluscan preparations (Hawkins et al., 1981, Katz and Frost, 1995) and in the feeding system of *Lymnaea* (Vehovszky and Elliott, 2002). There are many other examples of neurons having long term modulatory effects after a short duration of activity (Nagy and Dickinson, 1983, McCrohan and Audesirk, 1987, Blitz and Nusbaum, 1997, Straub and Benjamin, 2001).

Electrotonic synapses are also a site for synaptic plasticity. One possibility was that vTN alters the strength of electrotonic synapses between N3t and other neurons. Since N3t has a relatively high RMP, increasing the strength of electrotonic synapses with a neuron with a lower RMP could potentially reduce N3t's firing rate. This has been observed in *C.elegans* (Kawano et al., 2011) and long-term plasticity in electrotonic synapses is present in rats (Haas et al., 2011) and the pyloric network of the lobster (*Panulirus interruptus*) (Johnson et al., 1993a, 1993b). In *Aplysia*, plasticity of electrotonic synapses is a proposed mechanism of operant conditioning (Nargeot et al., 2009). Patel et al. (2006) showed that the synchronous activity of the two CGCs in *Lymnaea* reduced with age. It was hypothesised that the strength of the electrical

coupling between the two neurons decreased with age. However, the preliminary experiments show no long-term changes in the B4-N3t electrotonic synapse after vTN stimulation.

As mentioned, trigger neurons have been identified in a number of other species. The mechanisms by which the short duration stimulus is able to produce a long duration motor-output have been addressed in most detail in the leech. Tr1 neurons cause a fast excitation followed by a prolonged excitation of the swim initiation interneurons (SIIs) (Brodfuehrer and Friesen, 1986b). This can partly account for the on-going nature of Tr1's trigger ability, since the SIIs provide excitation to the oscillatory neurons. In failed Tr1 triggers, a high level of inhibition is present on neuron 208 (a decision neuron and member of the swim CPG). Brodfuehrer and Friesen (1986b) propose that in order for Tr1 to trigger swimming it must overcome this inhibition. This appears to be a similar process as vTN's trigger ability.

In conclusion, vTN can be classified as a trigger neuron as it fulfils the necessary criteria. It was able to reliably trigger fictive feeding cycles when stimulated to fire at a physiologically-relevant rate and its activity within triggered cycles was not necessary. Experimental evidence showed that the mechanism accounting for vTN triggered fictive feeding involved a monosynaptic biphasic connection with N1M and a delayed inhibition of N3t activity within cycles. Having identified the mechanisms by which vTN activated the feeding network it was next necessary to test whether vTN was a stimulus present decision neuron by developing an in vitro analogue of the detection task.

5 An in vitro analogue of decision making

5.1 Introduction

Results in Chapter 3 and 4 provided strong evidence that vTN is a stimulus present decision neuron in the behavioural paradigm designed in Section 3.2.1. The objective of the work in this chapter is to provide direct confirmation for this idea by developing an in vitro analogue of the task from Section 3.2.1. Sections 3.2.2, 3.2.3 and 4.2.1 provided evidence that vTN not only receives the correct sensory inputs but is also able to trigger fictive feeding. However, vTN's ability to trigger fictive feeding was only tested during periods of quiescence in the previous two Chapters. In the behavioural experiments the tactile stimulus is presented to the animal during an appetitive bite, which is able to convert it to consummatory bites. Therefore it was necessary to examine whether vTN was able to trigger the switch from an appetitive bite to a consummatory bite in a similar manner to that evoked by the tactile stimulus in vivo. To fully characterise the neural mechanisms of the decision in the behavioural experiments it was important to identify how the stimulus absent decision was made. Results in Section 3.2.1 provided evidence that, at this level of satiety, *Lymnaea* can reliably judge the absence of a sensory stimulus during an appetitive bite, resulting in the animal entering back into quiescence. There are two likely mechanisms that could be responsible for this. First, the lack of activity in stimulus present neurons could simply result in no further cycles being generated. Alternatively, a stimulus absent neuron could actively prevent any further cycles from being generated. Distinguishing between these two possibilities is an important issue to address, as it would provide direct understanding about how the two competing behavioural outcomes are processed.

5.2 Results

5.2.1 Does vTN represent the stimulus present decision in vitro?

To develop an in vitro analogue of the decision in Chapter 3, a suitable method to induce single appetitive bites similar to those seen in vivo was necessary. Results from Section 4.2.3 provided a suitable method to reliably achieve this. Stimulating a single protraction phase command-like interneuron to generate a full cycle on average elicited no further cycles. In the in vitro analogue, activating a single CBI or N1M in an isolated CNS preparation (see Section 2.2.1.1) was used to represent the appetitive bites seen

in vivo (**Figure 5.1Ai**). These were therefore referred to as fictive appetitive bites. A cycle was considered associated with the fictive appetitive bite if it occurred within 10 seconds from the start of the fictive appetitive bite. N1M driven cycles have previously been reported as ~9 seconds in duration (Yeoman et al., 1995), therefore a value of 1 second longer was chosen to ensure that no associated cycles were missed. The average number of cycles generated by this protocol was 1.2 (±0.1) (n=15). However, in the behavioural experiments in Section 3.2.1 the first appetitive bite was not counted, only the subsequently generated cycles; for consistency, therefore, the first cycle in CBI driven fictive appetitive bites was not counted. Using this protocol 0.2 (±0.1) cycles were generated. vTN's trigger ability was then tested during a period of quiescence. vTN was stimulated in a similar manner as in Section 3.2.4 and 4.2.1 and the number of cycles that were triggered was counted (**Figure 5.1Aii**). The average number of cycles triggered in successful triggers was 3.4 (±0.5) (n=15). vTN was next stimulated to fire during a fictive appetitive bite to test whether vTN could initiate the switch into consummatory bites when active at a physiologically-relevant time. vTN was stimulated during the early swallow phase. This was the point in the behavioural experiments when the most pressure is applied to the radula, as it makes a shearing motion against either the dorsal mandible or dorsal food channel (See **Figure3.3B**). This was also the phase in which vTN received the greatest excitation within triggered cycles (Section 4.2.1). Therefore a fictive appetitive bite was initiated via CBI stimulation and the same vTN stimulation applied during quiescence was then applied during the cycle (**Figure 5.1Aiii**). The number of cycles triggered was on average 3.7 (±0.5) (similarly to the fictive appetitive bite alone trials, the fictive appetitive bite itself was not counted). There was no significant difference between number of cycles triggered between vTN stimulation in quiescence and vTN stimulation within a fictive appetitive bite, but both initiated more cycles than the fictive appetitive bite alone (Repeated-measures ANOVA: $F[2,14] = 20.61$, $P < 0.0001$ – Tukey's multiple comparison test – vTN stimulation in quiescence vs. vTN stimulation within fictive appetitive bite = $P > 0.05$, vTN stimulation in quiescence vs. fictive appetitive bite only = $P < 0.001$, vTN stimulation within fictive appetitive bite vs. fictive appetitive bite only = $P < 0.001$) (**Figure 5.1B**). Therefore the number of cycles triggered by vTN was not affected by the presence of a fictive appetitive bite. The number of cycles generated after the first fictive appetitive bite in vitro was compared with the number of cycles generated after the first appetitive bite in vivo from Section 3.2.1 (0.47 ±0.1). No significant difference was present between the two (unpaired t-test $df = 28$, $t = 1.9$, $P > 0.05$) (**Figure 5.1Ci**). This confirms that the use of CBI or N1M stimulation was a suitable analogue of appetitive bites seen in vivo. The number of cycles initiated by

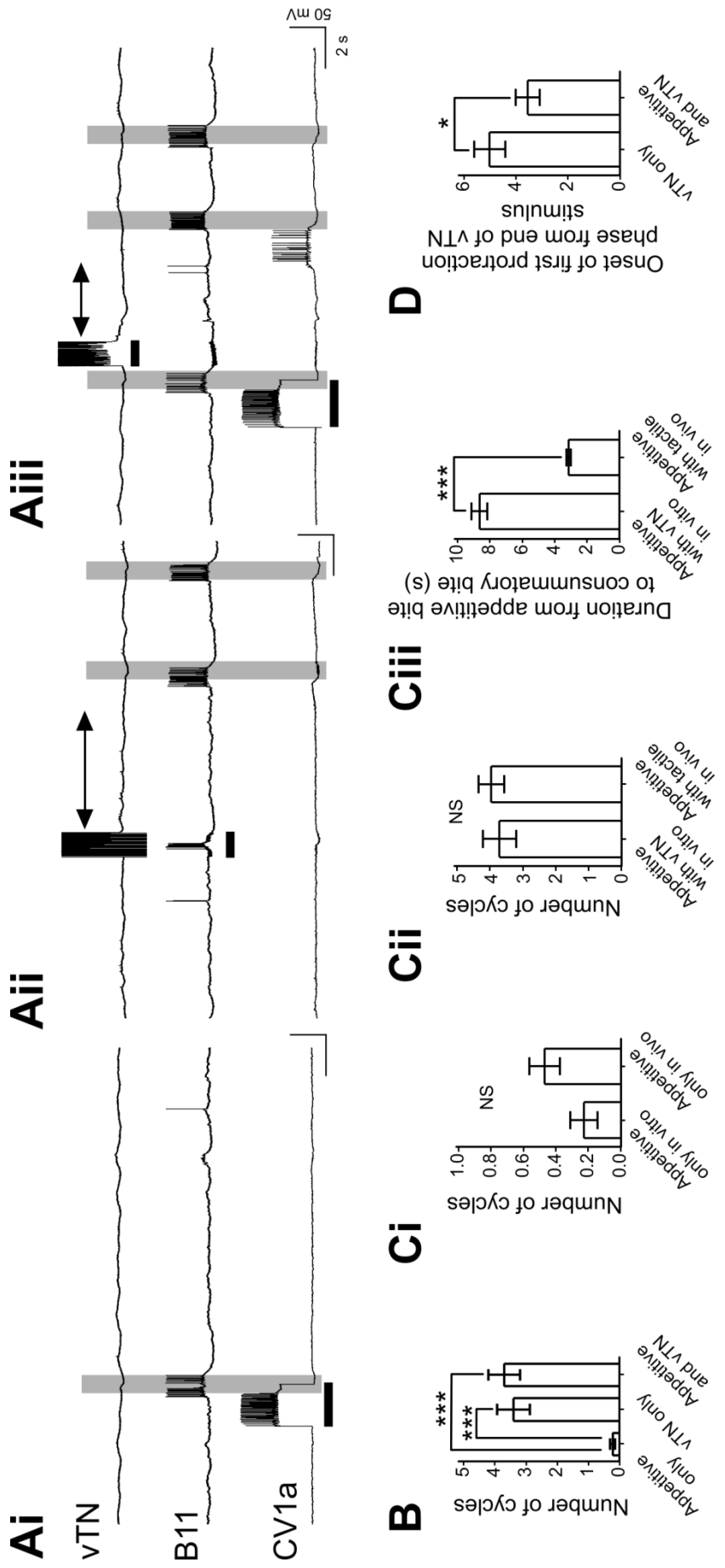
Ai
Aii
Aiii
vTN
B11
CV1a
50 mV
2 s
B
Number of cycles
***
***
Appetitive only
vTN only
Appetitive and vTN
Ci
Number of cycles
NS
Appetitive only in vitro
Appetitive only in vivo
Cii
Number of cycles
NS
Appetitive with vTN in vitro
Appetitive with tactile in vivo
Ciii
Duration from appetitive bite to consummatory bite (s)
***
Appetitive with vTN in vitro
Appetitive with tactile in vivo
D
Onset of first protraction phase from end of vTN stimulus
*
vTN only
Appetitive and vTN

Figure 5.1 In vitro analogue of decision making - vTN's role as a stimulus present decision neuron **Ai.** A CV1a was depolarised to fire until the onset of the rasp phase and then the stimulus was removed from the cell, resulting in a full fictive feeding cycle, as seen by the excitatory input to B11. No further cycles were generated once the stimulus was removed from the cell. Therefore this was referred to as a fictive appetitive bite since it resembled the single appetitive bites seen in vivo. **Aii.** Stimulating vTN to fire in quiescence triggered two fictive feeding cycles, as seen by the spiking activity of B11 in the rasp phase. The arrowed line is a measure of the time from the end of the stimulus to vTN to the onset of the first protraction phase. **Aiii.** CV1a was stimulated similarly to in Ai, driving a fictive appetitive bite. vTN was stimulated to fire similarly to in Aii, but within the swallow phase of the fictive appetitive bite. This triggered two further cycles, as seen by spiking activity in B11 in the rasp phase. The onset of the protraction phase from the end of the stimulus to vTN was reduced compared to Aii. **B.** Significantly more cycles were generated by vTN stimulation in quiescence and vTN stimulation within a fictive appetitive bite compared with a fictive appetitive bite alone. No significant difference was present between the number of cycles triggered by vTN when stimulated in quiescence and when stimulated within a fictive appetitive bite. **Ci.** No significant difference was present between the number of cycles initiated after the first fictive appetitive bite in vitro and the number of cycles initiated after the first appetitive bite in vivo in the absence of a sensory stimulus (Section 3.2.1). **Cii.** No significant difference was present between the number of cycles initiated after the first fictive appetitive bite when vTN was stimulated to fire within the cycle compared with the number of cycles initiated after the first appetitive bite in vivo when the tactile stimulus was presented to the animal in the stimulus present trial. **Ciii.** The duration from the start of the fictive appetitive bite until the onset of the next bite by vTN stimulation in vitro was significantly longer than the duration from the appetitive bite until the onset of the consummatory bite due to the presence of the tactile stimulus in vivo from Section 3.2.1. **D.** The duration from the end of the stimulus to vTN until the onset of the protraction phase was significantly reduced when vTN was stimulated within a fictive appetitive bite compared to vTN stimulation in quiescence. Black horizontal bars represent depolarising current. Grey vertical bars represent the rasp phase of a fictive feeding cycle. * $P < 0.05$, *** $P < 0.001$, NS not significant.

vTN in a fictive appetitive bite was compared with the number of cycles initiated by the tactile stimulus in the behavioural experiments in Section 3.2.1. No significant difference was present between number of cycles initiated after the first appetitive bite between the tactile stimulus in vivo (4.00 ±0.4) and vTN stimulation in vitro (unpaired t-test $df = 28$, $t = 0.4$, $P > 0.05$) (**Figure 5.1Cii**). This provides evidence that vTN is sufficient to elicit the switch from fictive appetitive to fictive consummatory bites in a similar manner as the tactile stimulus in vivo.

The duration from the start of the appetitive bite until the onset of the first consummatory bite in the behavioural experiments due to the presence of the tactile stimulus was 3.15 s (±0.1). However in the in vitro experiments the duration was 8.4 s (±0.4). This was significantly longer than the duration seen in vivo (unpaired t-test $df = 28$, $t = 13$, $P < 0.0001$) (**Figure 5.1Ciii**). However cycles generated in vitro are often much longer than those seen in vivo (Kemenes et al., 1986, Staras et al., 1998a, Kemenes et al., 2001, Vehovszky et al., 2004). Indeed, the duration of the protraction phase alone of the fictive appetitive bites in the in vitro experiments was 2.9 s (±0.5). In light of this, therefore, it is perhaps not surprising that the duration of the switch from appetitive to consummatory cycles in vitro was significantly longer. The onset time of the protraction phase from the end of the stimulus to vTN was reduced when vTN was stimulated within a fictive appetitive bite compared with when stimulated in quiescence (Onset of protraction phase from end of vTN stimulus - vTN stimulus within fictive appetitive bite = 3.5 s (±0.5), vTN in quiescence = 5.0 s (±0.6) – paired t-test $df = 14$, $t = 2.4$, $P < 0.05$) (**Figure 5.1D**). The presence of the fictive appetitive bite therefore shortens the onset of the subsequent cycle. These experiments suggest that vTN is sufficient to initiate the switch from appetitive to consummatory bites when presented at a physiologically-relevant time and rate.

5.2.2 Is vTN necessary for a stimulus present decision?

Having established that vTN could mediate the switch from appetitive to consummatory behaviours when presented at a physiologically-relevant time point, the next objective was to test whether vTN was necessary for the stimulus present decision. To determine this, the Radula-CNS semi-intact preparation was used (see Section 2.2.1.2). The fictive appetitive bite was induced by stimulating a single CBI as in Section 5.2.1 whilst recording from a single vTN. One other suitable cell-type was recorded to monitor the fictive feeding response. In **Figure 5.2Ai** a CV3 motor neuron was simultaneously recorded with a CV1b and vTN. On average 0.5 cycles (±0.2) were

generated after the first fictive appetitive bite in the absence of sensory input (n=5). In the next trial, a tactile stimulus was applied to the ipsilateral side of the radula to the vTN recorded in the late rasp/early swallow phase of the fictive appetitive bite. This elicited a high frequency burst of somatic spikes in vTN, and initiated, on average, 1.7 cycles (±0.5). **Figure 5.2Aii** shows an example of the generation of two further cycles from tactile stimulation of the radula. Therefore tactile stimulation of the radula, if presented within cycle, is sufficient to switch the single cycle into further cycles. To test whether vTN activity was necessary for this switching mechanism, experiments were next performed with vTN hyperpolarised prior to the fictive appetitive bite and tactile stimulation, to prevent its action potential generation. When the tactile stimulus was applied during the cycle, on average 0.6 cycles (±0.1) were generated. In **Figure 5.2Aiii**, the tactile stimulus caused a depolarization of vTN, and a number of EPSPs are evident (presumably arising from RM – see Section 3.2.3) but no spikes were elicited. The number of cycles generated by tactile stimulation of the radula when vTN was activated was significantly higher than the fictive appetitive bite in the absence of the stimulus and in trials where vTN was hyperpolarised to prevent somatic spiking, whereas no significant difference was present between the fictive appetitive bite in the absence of the stimulus and in trials where vTN was hyperpolarised (**Figure 5.2B**) (Repeated-measures ANOVA: $F[2,4] = 7.65$, $P < 0.05$, Tukey's Multiple Comparison Test fictive appetitive bite in the absence of the stimulus vs. fictive appetitive bite in the presence of the stimulus with vTN activated $P < 0.05$, fictive appetitive bite in the presence of the stimulus with vTN activated vs. fictive appetitive bite in the presence of the stimulus with vTN hyperpolarised $P < 0.05$, fictive appetitive bite in the absence of the stimulus vs. fictive appetitive bite in the presence of the stimulus with vTN hyperpolarised $P > 0.05$).

In these experiments the tactile stimulus was not automated. As such, there remains the possibility that the stimulus intensities were different in the two conditions. Automation of the stimulus proved difficult to implement because CBI stimulation caused substantial movement of the odontophore, presumably via activation of motor neurons projecting down the PBN. This movement meant that the tactile probe had to be re-aligned for each trial to ensure that the stimulus was applied to the radula, and specifically to the same region. However, tactile stimuli to the radula typically only triggered further cycles if vTN was sufficiently activated by it. When vTN was hyperpolarised, tactile stimulation of a relatively large magnitude remained unreliable to initiate further cycles. Only hyperpolarising one vTN was considered sufficient in this protocol due to the fact that only the ipsilateral side of the radula was stimulated, and

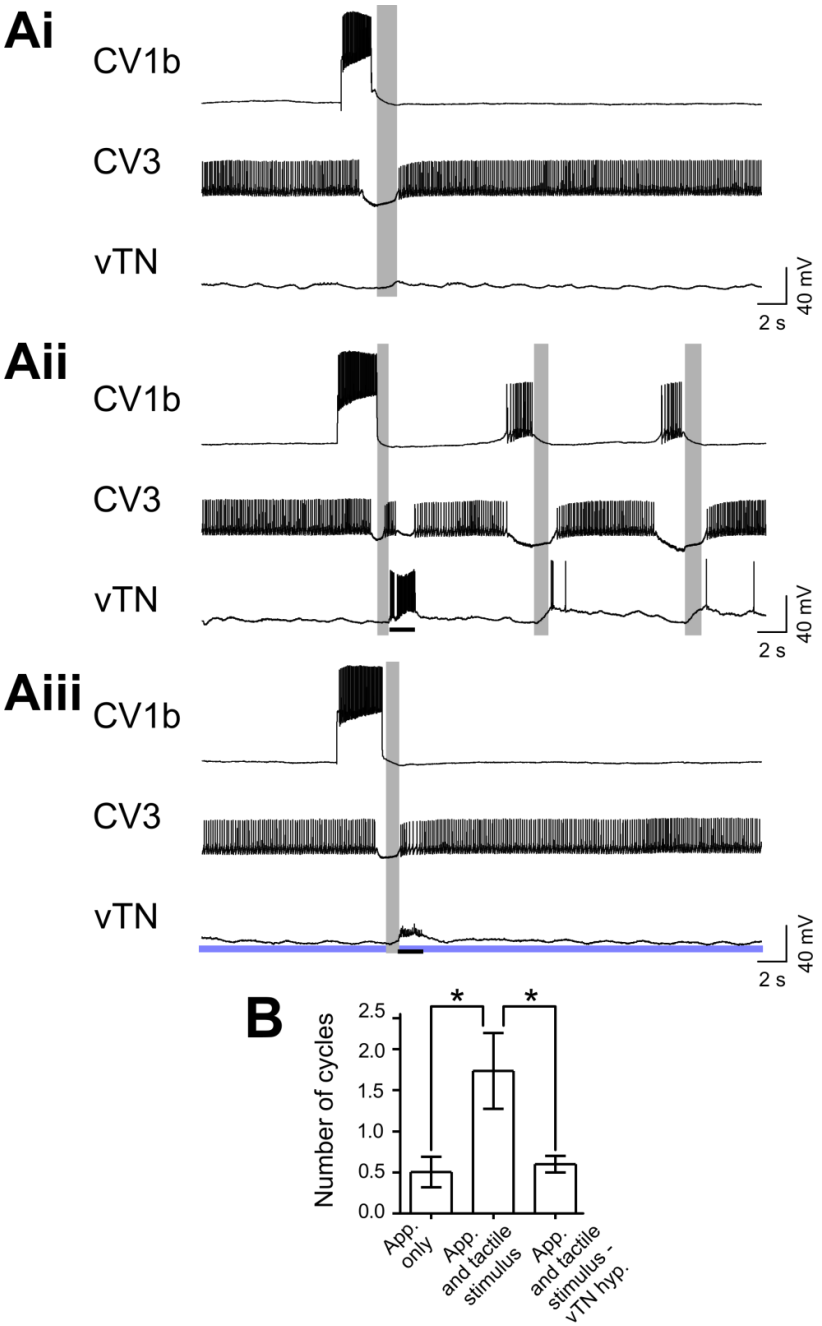

Figure 5.2 Evidence that vTN is important for a stimulus present decision using an in vitro radula-CNS semi-intact preparation **Ai.** A CV1b was depolarised to fire until the onset of the rasp phase and then the stimulus was removed from the cell, resulting in a fictive appetitive bite. No further cycles were generated once the stimulus was removed from the cell. **Aii.** Applying a tactile stimulus to the radula in the early swallow phase of a fictive appetitive bite caused a burst of spikes in the ipsilateral vTN. Two further cycles were initiated, as seen by the rhythmic activity of CV1b and CV3. **Aiii.** Applying a tactile stimulus to the radula during a fictive appetitive bite whilst vTN was hyperpolarised caused a depolarization of vTN, but no somatic spikes were triggered. No further cycles were generated. **B.** Significantly more cycles were generated when vTN was activated by the tactile stimulus than when no tactile stimulus was applied to the radula within the fictive appetitive bite or when vTN was hyperpolarised to prevent activation by the tactile stimulus. No significant difference was present between fictive appetitive bites alone and fictive appetitive bites with a tactile stimulus to the radula whilst vTN was hyperpolarised. Black horizontal lines represent time and duration of tactile stimulus to the radula. Blue horizontal lines represent hyperpolarising current. Grey vertical lines represent rasp phase of a cycle. * $P < 0.05$.

the contralateral vTN is only minimally activated by this stimulation (see Section 3.2.3 **Figure 3.5B** and **3.6Ai**). These experiments provide compelling evidence that vTN is a key stimulus present decision neuron.

5.2.3 The neural mechanisms of the stimulus absent decision

Having determined the neural correlates of the stimulus present decision, it was important to identify those of the stimulus absent decision. During the stimulus absent decision, the animal performs a single appetitive bite and enters back into quiescence. There are two mechanisms that might underlie this. The first is that the lack of sensory information prevents the expression of further feeding cycles, i.e. no vTN activity. The second is that a stimulus absent neuron actively inhibits the system and prevents further cycles. A strong candidate for the second mechanism was the N3t interneuron. N3t fires tonically during periods of quiescence preventing N1M from reaching threshold and initiating a fictive feeding cycle (Staras et al., 2003). During a feeding cycle it is inhibited in the protraction and rasp phases and then fires via PIR in the swallow phase (**Figure 5.3Ai**). Results in Section 4.2.5 provide evidence that vTN is able to trigger fictive feeding by reducing N3t's firing rate. In Section 4.2.5 it was also shown that artificially reducing N3t firing rates allowed for further cycles to be generated after CBI activation. This suggests that N3t actively prevents the generation of further cycles after fictive appetitive bites in the absence of a sensory stimulus. In 11 preparations where single cycles were generated spontaneously or by a protraction phase command-like interneuron, N3t firing rates were examined in detail. N3t firing rates were split into 0.5 s bins for 15 s prior to the initiation of the protraction phase (and onset of inhibition of N3t). This was referred to as baseline N3t firing rate. This data was averaged and compared against 0.5 s bins of N3t firing rates from the onset of the swallow phase (**Figure 5.3Aii**). The mean baseline firing rate of N3t was 4.6 Hz (±0.4). There was a significant increase in N3t firing rate from the onset of the swallow phase vs. baseline levels (Repeated-measures ANOVA: $F[19,10] = 19.82$, $P < 0.0001$). A Dunnetts' test revealed that there was a significant increase in N3t firing rates compared with baseline levels from the start of the swallow phase for 3.5 s (0-0.5 s $P < 0.001$, 0.5-1 s $P < 0.001$, 1-1.5 s $P < 0.001$, 1.5-2 s $P < 0.01$, 2-2.5 s $P < 0.01$, 2.5-3 s $P < 0.01$, 3-3.5 s $P < 0.01$, all other conditions $P > 0.05$) (0-0.5 s = 12.6 ±1, 0.5-1 s = 10.7 ±0.7, 1-1.5 s = 8.4 ±0.7, 1.5-2 s = 7.2 ±0.7, 2-2.5 s = 7.3 ±0.8, 2.5-3 s = 7.2 ±0.9, 3-3.5 s = 7.3 ±0.7, 3.5-4 s = 6.2 ±0.8, 4-4.5 s = 6.2 ±0.9, 4.5-5 s = 6.6 ±0.4, 5-5.5 s = 5.3 ±0.7, 5.5-6 s = 5.7 ±0.8, 6-6.5 s = 5.7 ±0.8, 6.5-7 s = 5.3 ±0.8, 7-7.5 s = 5.8 ±0.8, 7.5-8 s = 5.5 ±0.6, 8-8.5 s = 5.1 ±0.7, 8.5-9 s = 4.1 ±0.6, 9-9.5 s = 4.2

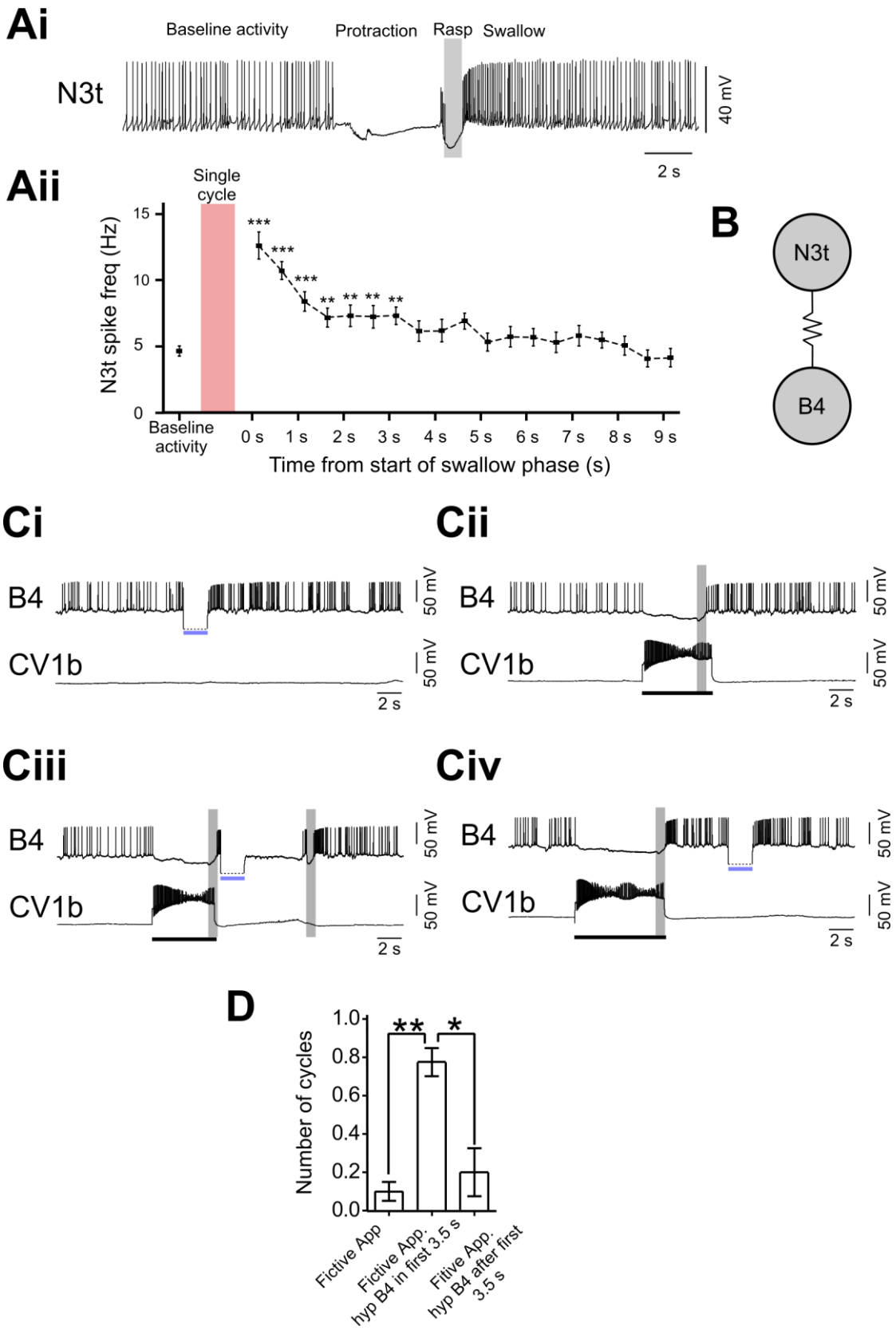
Ai
Baseline activity
Protraction
Rasp
Swallow
N3t
40 mV
2 s
Aii
Single cycle
N3t spike freq (Hz)
15
10
5
0
***
**
Baseline activity
0 s
1 s
2 s
3 s
4 s
5 s
6 s
7 s
8 s
9 s
Time from start of swallow phase (s)
B
N3t
B4
Ci
Cii
Ciii
Civ
B4
CV1b
50 mV
2 s
D
Number of cycles
1.0
0.8
0.6
0.4
0.2
0.0
**
*
Fictive App
Fictive App. hyp B4 in first 3.5 s
Fitive App. hyp B4 after first 3.5 s

Figure 5.3 Evidence that N3t is a stimulus absent decision neuron **Ai.** N3t activity in a single fictive appetitive bite. N3t shows baseline tonic activity during periods of quiescence. During both the protraction and rasp phase N3t is inhibited, it then fires a burst of spikes via PIR in the swallow phase. **Aii.** Averaged N3t data from 11 preparations showing a significant increase in N3t firing rate over baseline levels for up to 3.5 s from the start of the swallow phase. Data grouped into bins of 0.5 s. Baseline activity in 0.5 s bins and then averaged over a 15 s period prior to onset of the protraction phase. **B.** Circuit diagram showing electrical synapse between N3t and B4 motor neuron. **Ci.** Injecting B4 with negative current disrupts N3t activity due to the electrical synapse between the two. This level of disruption was not sufficient for the generation of a fictive feeding cycle (as seen in Staras et al., 2003). **Cii.** CV1b was stimulated until the generation of a fictive appetitive bite. B4 is inhibited in the protraction and rasp phases and fires by PIR in the swallow phase, similarly to N3t. No further cycles were generated. **Ciii.** Applying the same stimulus to B4 within the first 3.5 s of a fictive appetitive bite was sufficient to allow the generation of a subsequent cycle. **Civ.** Applying the same stimulus to B4 outside of the first 3.5 s of a fictive appetitive bite was insufficient to allow the generation of a subsequent cycle. **D.** The number of cycles initiated after a fictive appetitive bite was significantly higher when the B4 stimulus was presented within the first 3.5 s of the swallow phase than when it was presented outside of this time period or not presented at all. Black horizontal bars represent depolarising current. Blue horizontal bars represent hyperpolarising current. Grey vertical bars represent the rasp phase of a fictive feeding cycle. * $P < 0.05$, ** $P < 0.01$, *** $P < 0.001$.

±0.7). This could represent a critical period after a fictive appetitive bite has occurred in the absence of stimulus present activity, in which the high levels of N3t activity prevents the generation of further cycles by increasing levels of inhibition on the protraction phase interneurons.

To test whether there was a critical period of N3t inhibition after a fictive appetitive bite preliminary disruption experiments were performed. N3t is electrotonically coupled with the B4 motor neurons (**Figure 5.3B**) (see Section 4.2.6 and Staras et al., 1998b). By hyperpolarising B4 sufficiently, levels of N3t activity can be disrupted (Staras et al., 1998b, Staras et al., 2003). During a period of quiescence, a B4 was injected with negative current. A level was identified which was insufficient to initiate fictive feeding on its own (n=8) (**Figure 5.3Ci**) (0 cycles generated, average stimulus duration = 2.16 s (±0.1), average current injected into B4 = -6.25 nA (±1.1)). Fictive appetitive bites were initiated by stimulating a CBI (**Figure 5.3Cii**). These elicited on average 0.1 cycles (±0.1) after the first initiated cycle. This stimulus was then presented within the first 3.5 s of the swallow phase of a fictive appetitive bite (**Figure 5.3Ciii**). This generated on average 0.78 cycles (±0.1). This protocol was repeated but with the same stimulus to the B4 presented after the first 3.5 s from the start of the swallow phase (**Figure 5.3iv**). This generated on average 0.2 cycles (±0.1). There was a significant increase in the number of cycles generated when B4 was hyperpolarised within the first 3.5 s of the swallow phase compared with a fictive appetitive bite only and a fictive appetitive bite with B4 hyperpolarization after 3.5 s of the swallow phase, whereas there was no significant difference between any of the other conditions (Friedman test: df = 7, $\chi^2 = 12.96$, $P < 0.001$ – Dunn's test – B4 hyperpolarization within first 3.5 s of swallow phase vs. fictive appetitive bite only $P < 0.01$, B4 hyperpolarization within first 3.5 s of swallow phase vs. B4 hyperpolarization after first 3.5 s of swallow phase $P < 0.05$, fictive appetitive bite only vs. B4 hyperpolarization after first 3.5 s of swallow phase $P > 0.05$) (**Figure 5.3D**).

Taken together, these findings strongly suggest that there is a critical period of increased N3t activity after a fictive appetitive bite which prevents the generation of further cycles. As such, N3t prevents the generation of further cycles in the absence of a sensory stimulus and represents the stimulus absent decision.

5.2.4 Interactions of stimulus present and stimulus absent decision neurons during a stimulus present decision

Having identified both the neural correlates of the stimulus present decision (vTN) and the stimulus absent decision (N3t), it was now feasible to explore how the two interact at the decision point during a stimulus present decision.

The same in vitro paradigm was used as in Section 5.2.1. Stimulating a CBI in the absence of vTN stimulation represented the stimulus absent decision (**Figure 5.4Ai**). The results from Section 3.2.2 and Section 5.2.1 and 5.2.2 confirm that stimulating vTN alone can mimic the effects of the tactile stimulus to the radula, therefore vTN stimulation represented the stimulus present (**Figure 5.4Bi**), rather than using a semi-intact preparation. N3t activity was recorded indirectly via the unitary EPSPs on a B3 motor neuron (**Figure 5.4Aii**) (See Section 4.2.5 and Elliott and Benjamin, 1985a). B3 was impaled with two electrodes and current clamped to ~ -100 mV to increase the size of EPSP for unequivocal identification. N3t firing rates recorded on B3 were analysed as in Section 4.2.5. Only the tonic phase was recorded due to the fact that the high N3t firing rate in the PIR phase often caused a compound EPSP on B3 and unitary EPSPs could not easily be identified. However in Section 4.2.5 no change in the PIR phase was present in triggered vs. single cycles, indicating that a reduction in this phase is not necessary for the generation of further cycles. N3t frequencies were analysed at two points in the stimulus present trial. The first was in the tonic phase in which vTN was stimulated. This period represents the time at which the decision about the presence or absence of a sensory stimulus is made and was therefore referred to as the decision point (**Figure 5.4Bii**). The second was the tonic phase of the subsequently triggered cycles (with no further vTN activity) (**Figure 5.4Biii**). The average duration of the tonic phase of stimulus present trials was measured from within preparations and used to measure the duration of the tonic phase of the decision point in stimulus absent trials (as in Section 4.2.5). During stimulus absent trials, the average N3t firing rates at the decision point were found to be 7.8 Hz (±0.5) (n=8). This was similar to the rates seen in single cycles recorded on N3t in Section 4.2.5 (7.86 ±0.8 Hz). This confirms that recording N3t activity on B3 was applicable in this experiment. In the stimulus present trial at the decision point N3t firing rate in the tonic phase was 7.7 Hz (±0.6). The N3t firing rate in the tonic phase in the subsequently triggered cycles in stimulus present trials was 6.2 Hz (±0.5). No significant difference was present between N3t firing rates in the stimulus absent trial and in the decision point of the stimulus present trail, whereas there was a significant reduction in the tonic phase of the subsequently triggered cycles of the stimulus present trial compared with both the

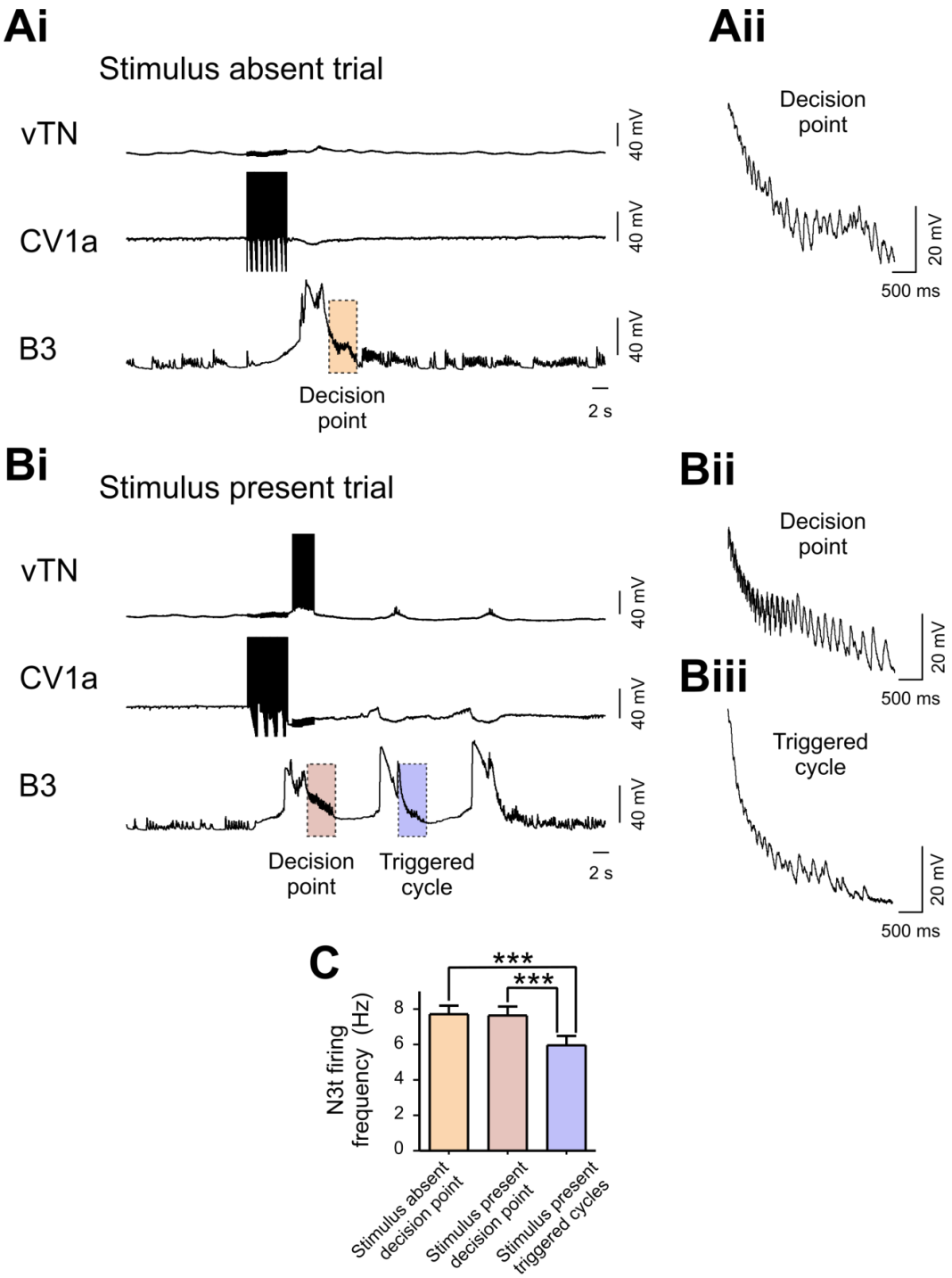

Figure 5.4 Interaction of the stimulus present and stimulus absent neurons at the decision point of the stimulus present decision **Ai.** A fictive appetitive bite was driven by stimulating CV1a. N3t activity was indirectly monitored by recording its EPSPs on a B3 motor neuron. B3 was current clamps to ~ -100 mV throughout. The absence of vTN stimulation represented a stimulus absent trial. N3t activity was analysed within the tonic phase, which was referred to as the decision point of the stimulus absent trial. **Aii.** Faster timebase of N3t input on B3 at decision point of stimulus absent trial. **Bi.** A fictive appetitive bite was initiated as in Ai. vTN stimulation was presented in the swallow phase to represent the presence of a tactile stimulus. This triggered two further cycles, as seen by rhythmic activity on CV1a and B3. N3t activity was monitored in the tonic phase at the decision point, and within the tonic phase of the triggered cycle. **Bi.** Faster timebase of N3t activity on B3 at the decision point of the stimulus present trial. **Biii.** Faster timebase of N3t activity on B3 in the triggered cycle. **C.** No significant difference was present between N3t firing rates within the decision points of both the stimulus absent and the stimulus present trials. There was a significant decrease in N3t firing rate within the triggered cycles compared with both decision points. *** $P < 0.001$.

stimulus absent trial and the decision point of the stimulus present trial (Repeated-measure ANOVA: $F[2,7] = 23.94$, $P < 0.0001$. Tukey's Multiple comparison test decision point in stimulus absent vs. decision point in stimulus present = $P > 0.05$, decision point in stimulus absent vs. triggered cycles in stimulus present = $P < 0.001$, decision point in stimulus present vs. triggered cycles in stimulus present = $P < 0.001$) (**Figure 5.4C**). Therefore at the decision point in the stimulus present trial, the increased levels of N3t activity present in stimulus absent trials, which prevent further cycles, remains present. However vTN activity, which represents the stimulus present, appears to be able to overcome this and trigger further cycles. Within the subsequently triggered cycles the reduction in N3t firing rate identified in Section 4.2.5 is evident. Therefore at the decision point, both the stimulus absent and stimulus present neurons are both active.

5.2.5 Goal-directed behaviours and decision making

Although the decision being considered here represents a simple decision about the presence or absence of a stimulus, it is being performed within a goal-directed behaviour, namely the search for a potential food. This offers the opportunity to study how goal-directed behaviours interact with, and affect, decision making processes. Previous work has shown that appetitive behaviours facilitate consummatory behaviours (Teyke et al., 1990, Teyke et al., 1997, Jing et al., 2008). It was therefore tested here whether appetitive bites facilitated the switch into the consummatory behaviour.

The same in vitro paradigm used in Section 5.2.1 was used to study this. A fictive appetitive bite was represented by CBI or N1M activation. A level of vTN activity was identified within each preparation which was below the threshold to trigger fictive feeding cycles in quiescence in the majority of trigger attempts (at least 5 trials per preparation. These must be below threshold to trigger cycles in at least 80% of trials) (**Figure 5.5Ai**). The average duration of vTN stimulation was 1.0 s (±0.1) (n=7). This triggered on average 0.05 cycles (±0.03). Stimulating a CBI or N1M only to generate a fictive appetitive cycle initiated 0.18 cycles (±0.1) after the first generated cycle (**Figure 5.5Aii**). Presenting the same vTN stimulus within a fictive appetitive cycle initiated 1.46 cycles (±0.29) after the first generated cycle (**Figure 5.5Aiii**). There was a significant increase in the number of cycles initiated by vTN after a fictive appetitive bite over both vTN in quiescence and fictive appetitive bite in the absence of vTN stimulation, whereas no difference was present between vTN in quiescence and fictive

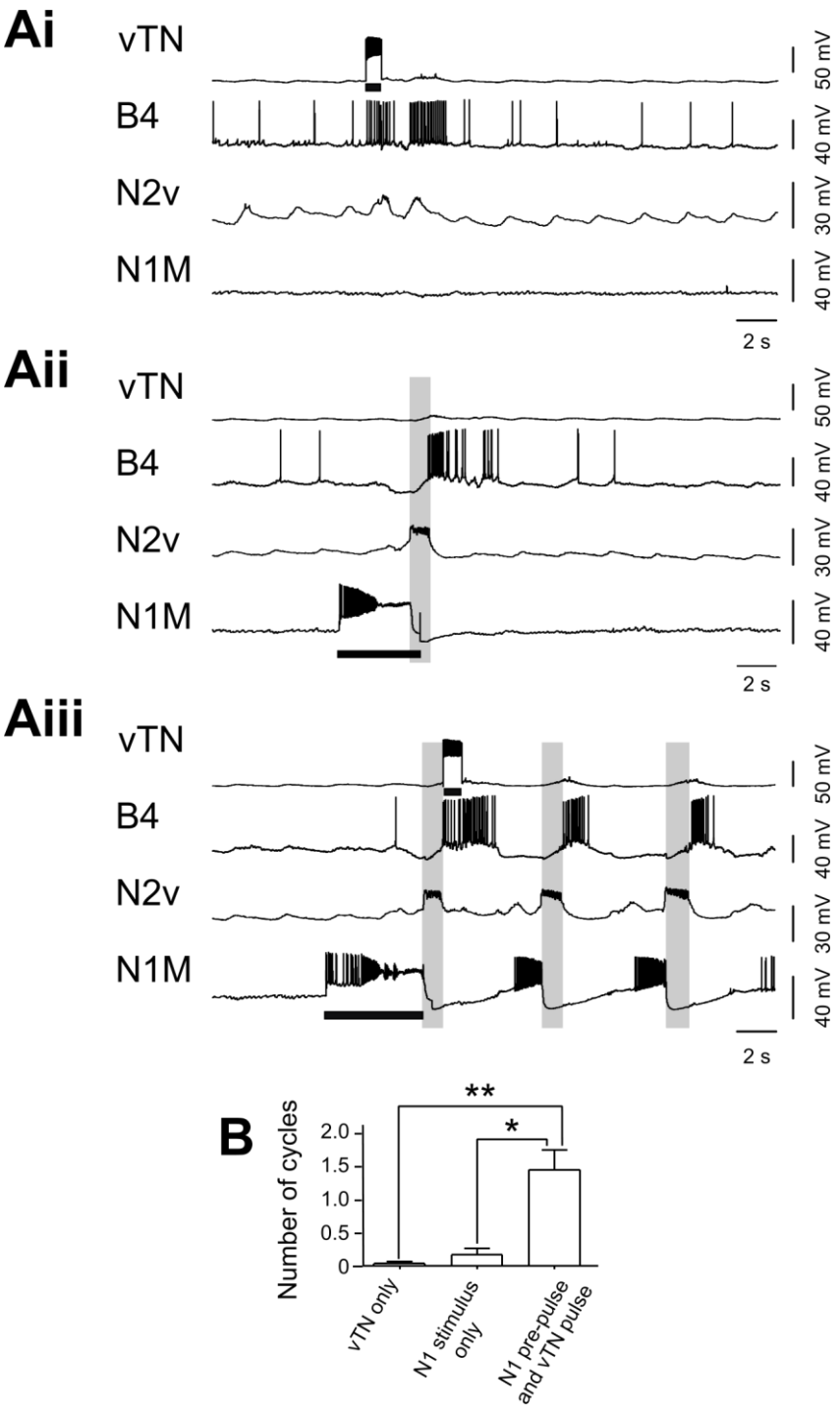

Figure 5.5 Fictive appetitive bites lower the threshold for vTN to trigger cycles **Ai.** A level of activity was identified which was below the threshold for vTN to trigger fictive feeding cycles during quiescence. This can be seen by the lack of rhythmic activity in the N1M and N2v CPG interneurons. **Aii.** A fictive appetitive bite was initiated by stimulating N1M to fire until the onset of the rasp phase, as seen by the activation of N2v. No further cycles were generated after this. **Aiii.** A fictive appetitive bite was initiated as in Aii. The same, previously subthreshold for triggering cycles, level of activity in vTN was presented within the swallow phase. Two further cycles were initiated following this, as seen by the rhythmic activity in N1M, N2v and B4. **B.** Significantly more cycles were generated when vTN was stimulated within a fictive appetitive bite than when it was stimulated in quiescence or when no stimulus was applied during a fictive appetitive bite. No significant difference was present between number of cycles initiated by stimulating vTN in quiescence and number of cycles initiated after the initiation of a fictive appetitive bite only. Black horizontal bars represent depolarising current. Grey vertical bars represent the rasp phase of a fictive feeding cycle. * $P < 0.05$, ** $P < 0.01$.

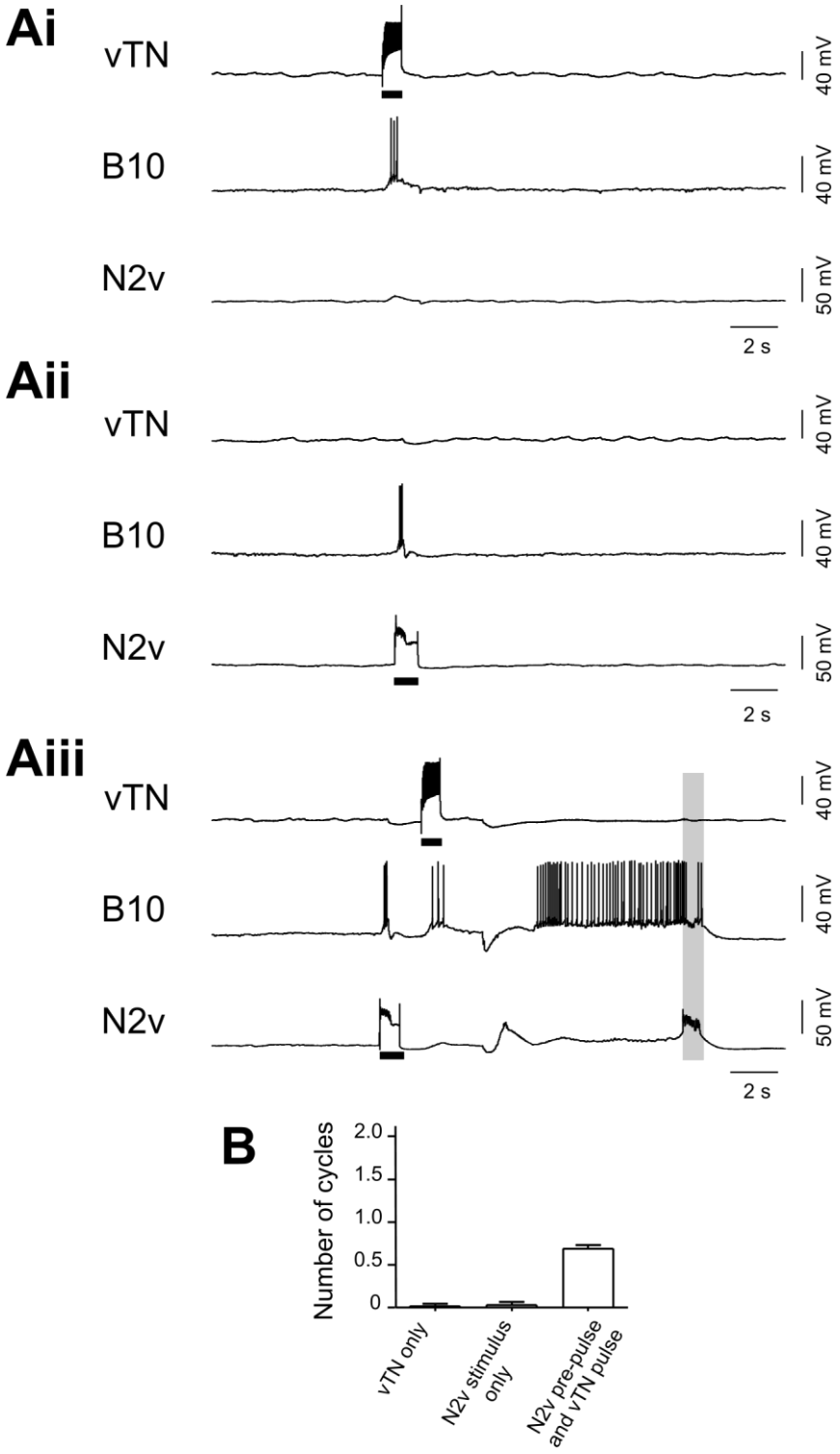

Figure 5.6 Prestimulation of N2v before vTN **Ai.** A level of activity was identified which was below the threshold for vTN to trigger fictive feeding cycles during quiescence as in Figure 5.5Ai. This can be seen by the lack of rhythmic activity in N2v and B10. **Aii.** The protraction phase of a fictive cycle was bypassed by stimulating an N2v interneuron alone. This caused an excitation of B10, but no further cycles were generated. **Aiii.** The same stimulus to N2v as in Aii. was accompanied by the same stimulus from Ai. to vTN afterwards. vTN was now able to initiate a single fictive feeding cycle, as seen by the activity of N2v and B10. **B.** No significance was revealed between conditions by a post hoc analysis (Dunn's test). . Black horizontal bars represent depolarising current. Grey vertical bars represent the rasp phase of a fictive feeding cycle.

appetitive bites in the absence of vTN stimulation (Friedman test: df = 6, χ^2] = 12.08, P < 0.001 - Dunn's test – vTN after fictive appetitive bite vs. vTN in quiescence P < 0.01, vTN after fictive appetitive bite vs. fictive appetitive bite in the absence of vTN stimulation P < 0.05, vTN in quiescence vs. fictive appetitive bite in the absence of vTN stimulation P > 0.05) (**Figure 5.5B**). Therefore the appetitive behaviour lowers the threshold for vTN to trigger fictive feeding cycles.

Using the knowledge of the system, it was possible to test whether a full fictive appetitive cycle was necessary to bring about the lowering of the threshold for vTN's trigger ability. Activating a CBI or N1M generates a full N1-N2-N3 (protraction-rasp-swallow) fictive appetitive bite. The N1 phase can be bypassed by stimulating an N2v interneuron only during quiescence. This generates a N2-N3 (rasp-swallow) cycle in the absence of any N1 activity. For this experiment, a level of vTN activity was identified which was below the threshold for triggering cycles similarly to the above experiment (**Figure 5.6Ai**). The average duration of the stimulus to vTN was 0.7 s (±0.1). The average number of cycles triggered by vTN stimulation was 0.02 (±0.02) (n=4). Stimulating an N2v alone initiated 0.04 cycles (±0.04) (**Figure 5.6Aii**). Presenting the same vTN stimulus after N2v stimulation initiated 0.69 cycles (±0.04) (**Figure 5.6Aiii**). A Friedman test revealed a significant difference (df = 3, χ^2 = 6.86, P < 0.01) however there was no significant difference in a post hoc analysis (Dunn's test P > 0.05 for all conditions) (**Figure 5.6B**). Further repeats would be needed to reveal the source of the significance.

5.3 Discussion

The objective of this chapter was to design an in vitro analogue of the decision making task from Section 3.2.1. The successful implementation of this analogue allows for the direct testing of vTN as a stimulus present decision neuron, permitting the further characterisation of the neural mechanisms of the decision.

Results in Section 4.2.3 provided an experimental design by which the single appetitive bites seen in vivo could be generated in vitro. Brief activation of any of the command-like neurons was able to initiate a single fictive feeding cycle only. This was similar to the single appetitive bites seen in vivo in the absence of a sensory stimulus, and therefore were referred to as 'fictive appetitive bites'. Results in Chapters 3 and 4 provided strong evidence for vTN being a stimulus present decision neuron for the behavioural task in Section 3.2.1. To test this in the in vitro analogue, the tactile

stimulus in vivo was replaced with stimulation of vTN to fire at a physiologically-relevant rate. When presented in this manner, vTN retained its ability to trigger fictive feeding cycles. Therefore vTN was able to switch the single fictive appetitive bite into an on-going consummatory rhythm similarly to in vivo. The number of cycles triggered was not different to the number triggered when vTN was activated during a period of quiescence. The number of cycles triggered in vitro was also within the range seen in vivo. There was a difference in the duration of the switch from appetitive to consummatory bites between in vitro and in vivo. In vitro experiments had a significantly longer latency until the onset of the consummatory bite in stimulus present trials. However, since the protraction phase alone in vitro (2.9 s) was at the upper limit of the duration from appetitive to consummatory bites in vivo (3.15 s) it was unsurprising that there was a difference between the two. Previous experiments have demonstrated that the feeding rate in vitro is greatly reduced (Staras et al., 1998a, Kemenes et al., 2001, Vehovszky et al., 2004). Therefore the larger latency seen in the in vitro experiments does not exclude vTN from its proposed role of a stimulus present decision neuron. Further evidence of vTN's role as a stimulus present decision neuron was found by combining the in vitro analogue of the behavioural task with the radula-CNS semi-intact preparation. By applying a tactile stimulus to the radula during a fictive appetitive bite, a switch into the consummatory behaviour could be elicited. These experiments provided evidence that activation of vTN is important for the switch. By hyperpolarising vTN prior to the experiment, the number of cycles initiated by the tactile stimulus was greatly reduced. This experiment was technically difficult due to the fact that the stimulus had to be presented at a certain time point in each trial (late rasp/early swallow) and to the same region of the radula. However, experiments from Section 3.2.4 support the conclusions from these experiments. Stimulating an RM was sufficient to trigger fictive feeding if it sufficiently activates the ipsilateral vTN. If vTN was hyperpolarised prior to RM stimulation, then RM was insufficient to trigger fictive feeding. Presumably in the in vitro experiment RM was active under both conditions (vTN active and vTN hyperpolarised), as can be seen by inputs on vTN in both conditions, yet it was only when vTN was active that the switch from fictive appetitive to consummatory behaviour was reliably initiated. These experiments provide strong evidence that vTN is involved in the stimulus present decision and can therefore be classified as a stimulus present decision neuron.

It was next necessary to identify the neural mechanisms of the stimulus absent decision. Results in Section 4.2.4 gave some insight into this. By artificially reducing N3t levels in fictive appetitive bites, it was possible to generate further cycles. This

suggested that N3t prevents the initiation of further cycles after fictive appetitive bites in the absence of a stimulus. Analysing N3t activity within fictive appetitive bites showed that there is a significant increase in N3t activity for up to 3.5 s from the start of the swallow phase. If N3t activity is disrupted within this time period, then another cycle is able to be generated. The same disruption presented either in quiescence, or outside of 3.5 s from the start of the swallow phase is unable to initiate another cycle. This suggests that after a fictive appetitive bite there is a critical period in which N3t activity is significantly higher than baseline levels, preventing the generation of further cycles in the absence of a sensory stimulus. Therefore N3t is a stimulus absent decision neuron. Neurons with the ability to terminate fictive behaviours have been identified in other species (Tr2 in Leech (O'Gara and Friesen, 1995, Taylor et al., 2003), MHRs in *Xenopus* (Perrins et al., 2002)). The *Xenopus* mechanism involves the inhibition of the swim network via direct sensory input to the head (Perrins et al., 2002). However, mechanisms by which the absence of a sensory stimulus is processed are less well known. Detection tasks in monkeys have provided strong evidence for neurons in the MPC whose activity strongly correlated with the decision about the presence of a stimulus (de Lafuente and Romo, 2005). de Lafuente and Romo (2005) stimulated the MPC in the absence of a stimulus, and found that this was sufficient for the monkey to report the presence of the stimulus. However, during stimulus absent decisions, neurons remained at baseline levels of activity. Stimulus absent neurons were identified in abstract decision making in a visual detection task in the monkey (Merten and Nieder, 2012). Neurons which exclusively responded during the stimulus present or stimulus absent decision were identified in the PFC. Their activity strongly correlated with the decision. However in their study, it was not possible to test whether the stimulus absent decision neurons could bias the decision in the same way as stimulating the MPC could in the study by de Lafuente and Romo (2005).

Having identified both the stimulus present and stimulus absent decision neurons, it was possible to use the in vitro preparation to test how the two interact at the decision point of a stimulus present decision. A simple mechanism by which vTN could cause the switch to the consummatory behaviour would be to provide inhibition to N3t within the critical period of the swallow phase of the fictive appetitive bite. A reduction in N3t activity is the proposed mechanism by which vTN activity is able to trigger on-going fictive feeding (Section 4.2.4). Interestingly at the decision point in stimulus present trials N3t activity remains at levels seen in stimulus absent trials. However, a stimulus is still judged to be present. The reduction in N3t firing rate in the tonic phase is then established in the subsequent triggered cycles. This is in agreement with the known

synaptic connections between vTN and N3t (Section 4.2.5). The weak electrotonic synapse between the two would not result in reduced N3t rates when vTN is activated by the tactile stimulus to the radula; in fact a slight increase would be expected. Therefore at the decision point, *Lymnaea* receive conflicting information during stimulus present trials. High N3t activity tries to prevent the generation of further cycles, signalling the stimulus absent decision. At the same time vTN becomes active and triggers further cycles, signalling the stimulus present decision. This level of activity is sufficient to overcome the high levels of N3t inhibition on the system, and the decision about the presence of the stimulus is made. Merten and Nieder (2012) found that in monkeys performing abstract decisions, stimulus absent neurons do not respond strongly in the stimulus present decision. This is in contrast with stimulus absent neurons in *Lymnaea* whose rate remains high at the decision point in both the stimulus absent and stimulus present decisions.

Previous work has found that appetitive behaviours facilitate consummatory behaviours. In *Aplysia* an appetitive behaviour interneuron excites several components of the consummatory network (Teyke et al., 1990, Teyke et al., 1997). Also neurons of the locomotor network respond to arousing stimuli by increasing the excitability of the Meta-cerebral cells (part of the consummatory network) (Jing et al., 2008), thereby increasing their response to food, and enhancing the consummatory behaviour. Here an enhancement of vTN's trigger ability was found when presented within a fictive appetitive bite. Activity levels which were below the threshold for triggering fictive feeding cycles in quiescence were sufficient to trigger cycles when preceded by a fictive appetitive bite. This would effectively lower the sensory threshold needed for a tactile stimulus to the radula to initiate the switch from appetitive to consummatory bites. At least a part of this effect remains in the absence of the protraction phase. Bypassing the protraction phase and initiating the rasp phase resulted in significantly more cycles being generated by vTN than when it was presented in quiescence. Interestingly it would be expected that it would be harder to trigger cycles after a fictive appetitive bite, since N3t levels are increased during this period over baseline levels in quiescence. One proposed mechanism for this is that pre-stimulation with a full fictive appetitive bite increases the vTN to N1M excitatory input via heterosynaptic facilitation. In *Tritonia,* activation of a swim interneuron enhances the transmitter release of a separate interneuron onto a follower neuron (Katz and Frost, 1995). This is technically difficult to test as the *Lymnaea* feeding system is highly dynamic such that it would be difficult to ascertain the strength of the vTN to N1M connection after a fictive appetitive bite.

These experiments suggest that a goal-directed behaviour is able to bias the decision towards a stimulus present decision in the presence of a sensory stimulus. Lowering the sensory threshold would also serve to increase the likelihood of locating food. Although activity levels which were sub-threshold for triggering cycles in quiescence were able to trigger cycles when preceded by a fictive appetitive bite, no enhancement was present when a level of activity which was sufficient to trigger cycles in quiescence was preceded by a fictive appetitive bite (**Figure 5.1Aii, 5.1Aiii** and **5.1B**). The number of cycles triggered under the two conditions was not significantly different. However the presence of the fictive appetitive bite did significantly reduce the onset time of the protraction phase from the end of vTN stimulation. Therefore the appetitive bite lowers the level of activity needed for vTN to initiate the switch to consummatory bites, and reduce the time to their onset.

In summary, an in vitro analogue of the decision made in Section 3.2.1 was developed. Single appetitive bites were generated by stimulating a CBI or N1M interneuron. These were able to generate single fictive appetitive bites in a similar manner as seen in vivo. Stimulating a vTN within the fictive appetitive bite was sufficient to initiate further cycles similarly to the tactile stimulus in vivo. vTN activity was found to be important for this switch. Using a semi-intact preparation showed that tactile stimuli to the radula only reliably initiated the switch to evoke further cycles if vTN was sufficiently active. Therefore vTN was a stimulus present decision neuron. N3t was identified as a stimulus absent decision neuron. High levels of N3t activity after a fictive appetitive bite prevented the generation of further cycles in the absence of a sensory stimulus. Disrupting this activity was sufficient to initiate further cycles. This facilitated a detailed investigation about how the stimulus present neuron and the stimulus absent neuron interact at the decision point of the stimulus present decision. N3t activity was found to remain high at both the stimulus absent and stimulus present decision points. vTN activity was sufficient to overcome this and initiate further cycles. Therefore at the decision point of a stimulus present decision, both the stimulus absent neuron and the stimulus present neuron are active. The act of performing the appetitive behaviour also lowered the threshold for vTN to trigger fictive feeding cycles. This provided evidence that goal-directed behaviours influence decision making.

6 Synaptic connections between vTN and feeding neurons

6.1 Introduction

Results in Section 4.2.2 showed that the N1M was the only protraction phase interneuron active in every vTN triggered cycle. A monosynaptic biphasic (i/e) connection was shown to be present from vTN to N1M which was sufficient to explain spiking activity in N1M in the first triggered protraction phase. The CBIs were active in a high percentage of cycles whereas the SO and N1Ls were only rarely active. In this Chapter, the synaptic connections from vTN to the other protraction phase interneurons recorded in Section 4.2.2 were tested (CV1a, CV1b, SO, N1L, BCI1) to determine whether monosynaptic connections from vTN could account for their relative activity within triggered cycles. vTN's synaptic outputs onto other feeding network interneurons and motor neurons were also tested. vTN showed diverse synaptic connectivity with all levels of the feeding network (CPG interneurons, sensory neurons, modulatory interneurons and motor neurons). vTN produced both short and long latency and duration responses of varying amplitudes on follower neurons.

Results in Sections 3.2.4 and 4.2.1 provide evidence that vTN received synaptic feedback from the feeding network during triggered cycles. This was often subthreshold, but was sometimes sufficient to elicit spiking in the swallow phase. The synaptic connections from feeding interneurons onto vTN were therefore tested to examine where the inputs on vTN originated from.

6.2 Results

6.2.1 vTN's synaptic connections to protraction phase interneurons

6.2.1.1 CBIs

The CBIs were active in a high percentage of vTN triggered cycles. It was therefore tested whether a monosynaptic connection existed from vTN to the CBIs which could account for this high level of activation. **Figure 6.1Ai** shows an example of vTN triggering three fictive feeding cycles. The CV1a and CV1b both show spiking activity within the protraction phase of all three cycles. Within the period of vTN spiking activity, both CV1a and CV1b receive a barrage of inputs (**Figure 6.1Aii**). CV1a is inhibited throughout the period that vTN is active. Once vTN activity has ceased, CV1a is depolarised. This continues until it reaches threshold in the first protraction phase.

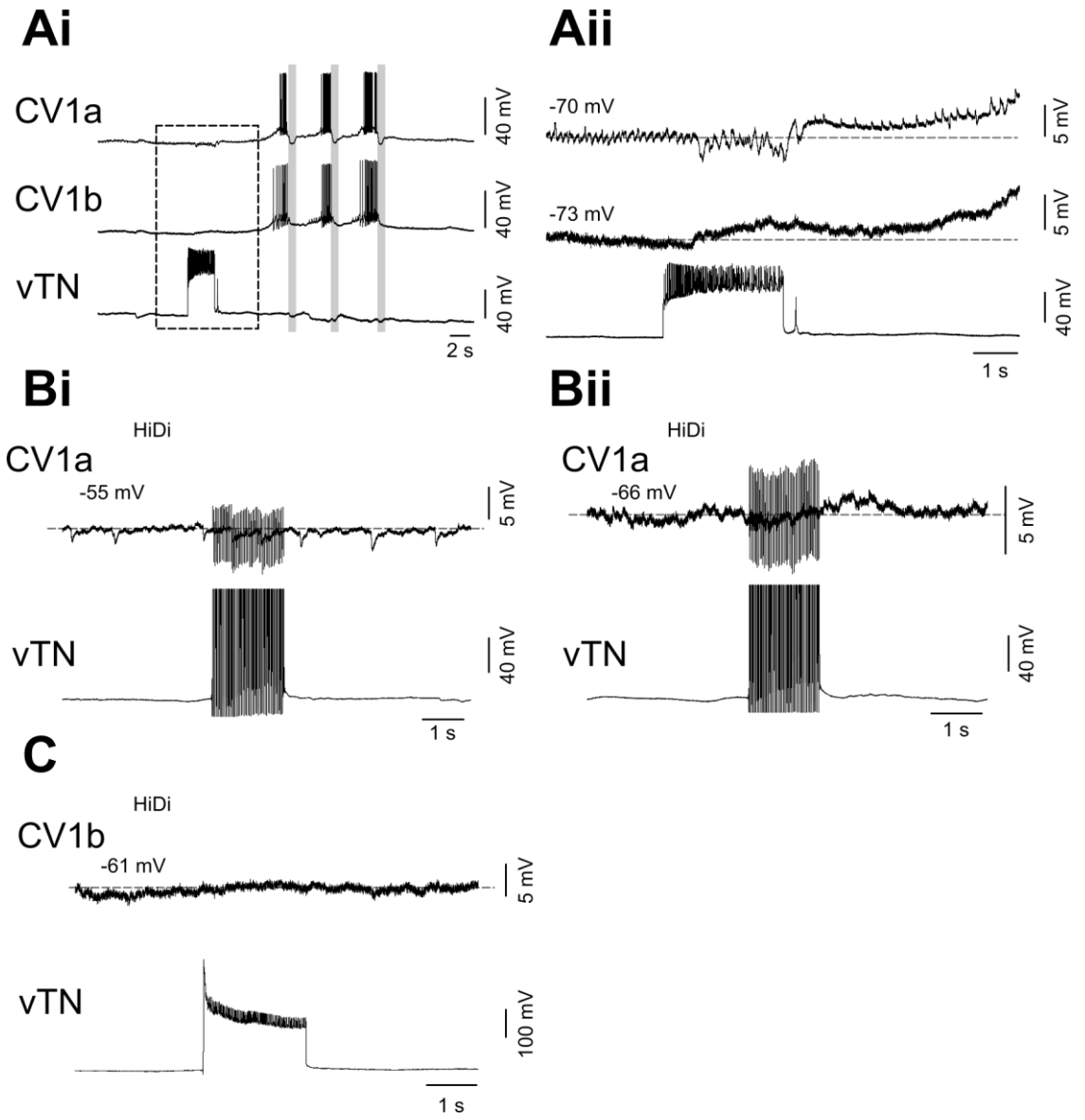

Figure 6.1 vTN's synaptic connections with CV1a and CV1b **Ai.** vTN activation in a period of quiescence triggers three fictive feeding cycles. Both CV1a and CV1b fire spikes in the protraction phase of each cycle. The dotted box represents the area expanded in Aii. **Aii.** Faster timebase of the boxed area in Ai. At the point of vTN activation CV1a receives a number of inhibitory inputs, whereas CV1b is depolarised. Once vTN activity has ceased, both CV1a and CV1b are depolarised. **Bi.** vTN activation causes no change in CV1a membrane potential in HiDi saline **Bii.** Example of another preparation showing no synaptic connection from vTN to CV1a at a lower membrane potential. **C.** vTN activation causes no change in CV1b membrane potential in HiDi saline. In all examples the values above each trace are the membrane potential of that neuron prior to vTN activation. Dotted grey lines show the neuron's membrane potential prior to vTN activation.

CV1b does not receive the same inhibitory inputs during the period of vTN activity, instead it is depolarised throughout. The depolarization continues until CV1b reaches threshold in the protraction phase. CV1b receives no strong inhibition in the rasp phase of fictive feeding cycles, unlike CV1a. CV1b remains depolarised throughout the rasp and swallow phase of the triggered cycles and then returns to RMP after the third cycle (**Figure 6.1Ai**). Therefore at the point of vTN activation, CV1a and CV1b receive different inputs; CV1a is hyperpolarised whereas CV1b is depolarised. However both are depolarised from the end of vTN activity. To test whether these inputs were due to monosynaptic connections from vTN, preparations were bathed in HiDi saline for more than 30 minutes. Both the inhibitory and excitatory inputs to CV1a were abolished in HiDi saline (**Figure 6.1Bi**), suggesting that these inputs seen in normal saline were not due to a monosynaptic connection from vTN (n=6). Altering CV1as membrane potential prior to vTN activation revealed no synaptic connections (**Figure 6.1Bi** and **6.1Bii**). The excitatory connection on CV1b seen in normal saline was also abolished when bathed in HiDi saline (**Figure 6.1C**), suggesting that there was no monosynaptic connection from vTN to CV1b (n=3). Therefore the inputs seen in normal saline on the CBIs during vTN activity arose via a polysynaptic connection. The high percentage of triggered cycles in which the CBIs are active in therefore cannot be accounted for by direct activation by vTN.

6.2.1.2 SO and N1L

Both the SO and N1L interneurons were found to show little activity during vTN triggered cycles (Section 4.2.2.3). **Figure 6.2Ai** provides an example of SO in a vTN triggered rhythm. SO only fires a single action potential during the second cycle. At the point of vTN activation (**Figure 6.2Aii**) SO was hyperpolarised. Once vTN activity had ceased, SO remained below RMP for over 1 s and was then depolarised during the protraction phase. The depolarization was not sufficient for SO to reach threshold in this cycle. To test whether the early inhibition and subsequent excitation of SO was due to a monosynaptic connection with vTN, the connection was tested in HiDi saline. vTN activation hyperpolarised SO in HiDi saline suggesting that a part of the inhibition seen in normal saline was due to a monosynaptic connection from vTN to SO (n=9) (**Figure 6.2Bi** and **6.2Bii**). Constant latency IPSPs were present following 1:1 from vTN spikes (**Figure 6.2Biii**), providing strong evidence that the connection was monosynaptic. vTN activation did not cause a delayed depolarising input to SO when SO was at either higher or lower membrane potentials (**Figure 6.2Bi** and **6.2Bii**). Therefore the connection from vTN to SO was purely inhibitory (**Figure 6.2C**).

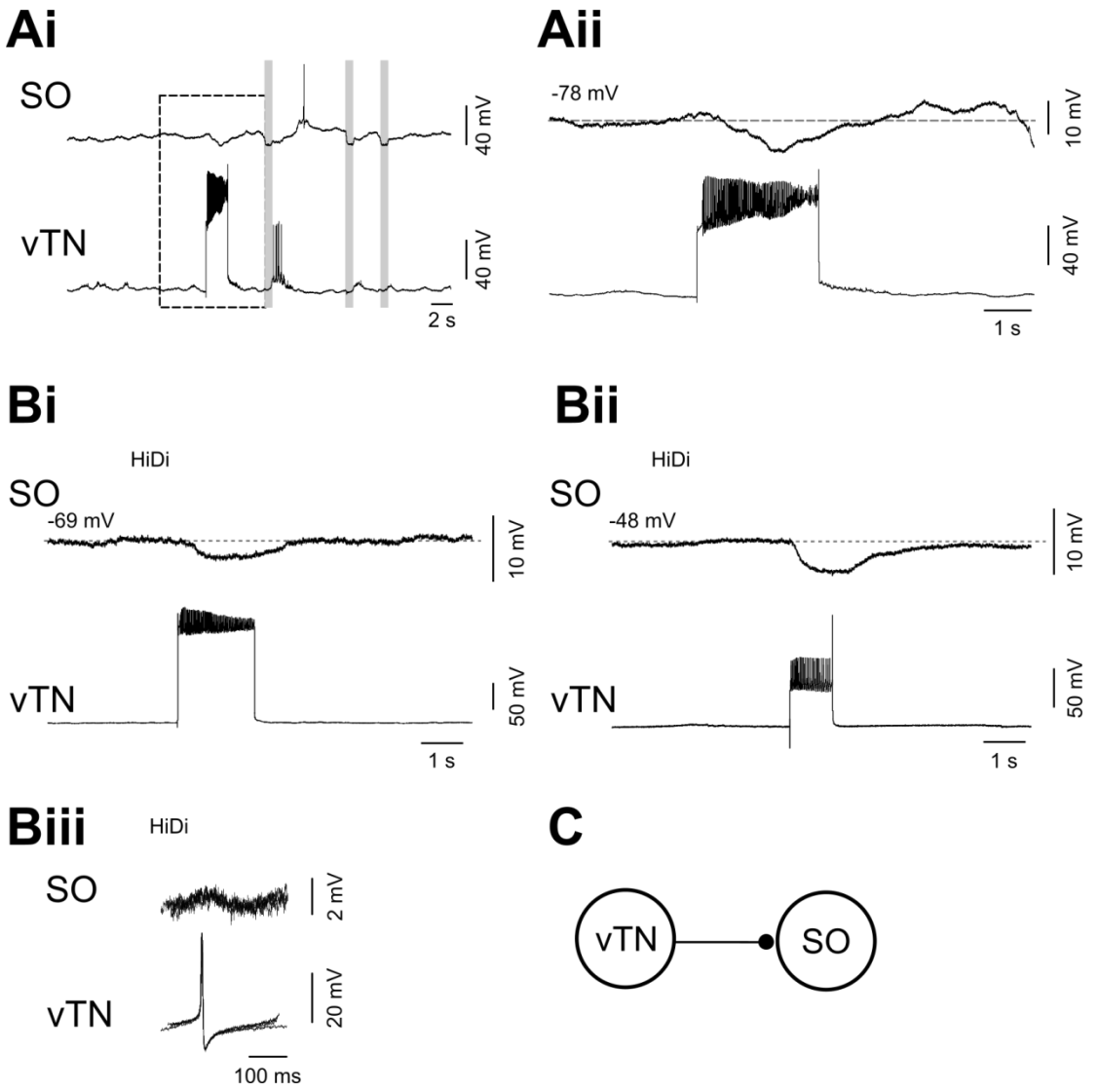

Figure 6.2 vTN's synaptic connections with SO **Ai.** vTN activation in a period of quiescence triggers three fictive feeding cycles. SO fires a single action potential at the start of the protraction phase of the second cycle. The box represents the area expanded in Aii. **Aii.** Faster timebase of the boxed area in Ai. At the point of vTN activation SO is hyperpolarised. Once vTN activity has ceased, SO becomes depolarised during the first protraction phase. **Bi.** vTN activation in HiDi saline hyperpolarised SO. **Bii.** vTN activation when SO was at a higher membrane potential also caused a hyperpolarisation of SO. No delayed excitatory input was present on SO at any membrane potential following vTN activation. **Biii.** Constant latency unitary IPSPs on SO we present following vTN spikes 1:1. Four spikes and the elicited IPSPs were superimposed. **C.** Summary circuit of purely inhibitory connection from vTN to SO. The solid black line represents the persistence of the connection in HiDi saline and evidence of unitary PSPs on the SO which follow vTN spikes 1:1. In all examples the values above each trace are the membrane potential of that neuron prior to vTN activation. Dotted grey lines show the neuron's membrane potential prior to vTN activation.

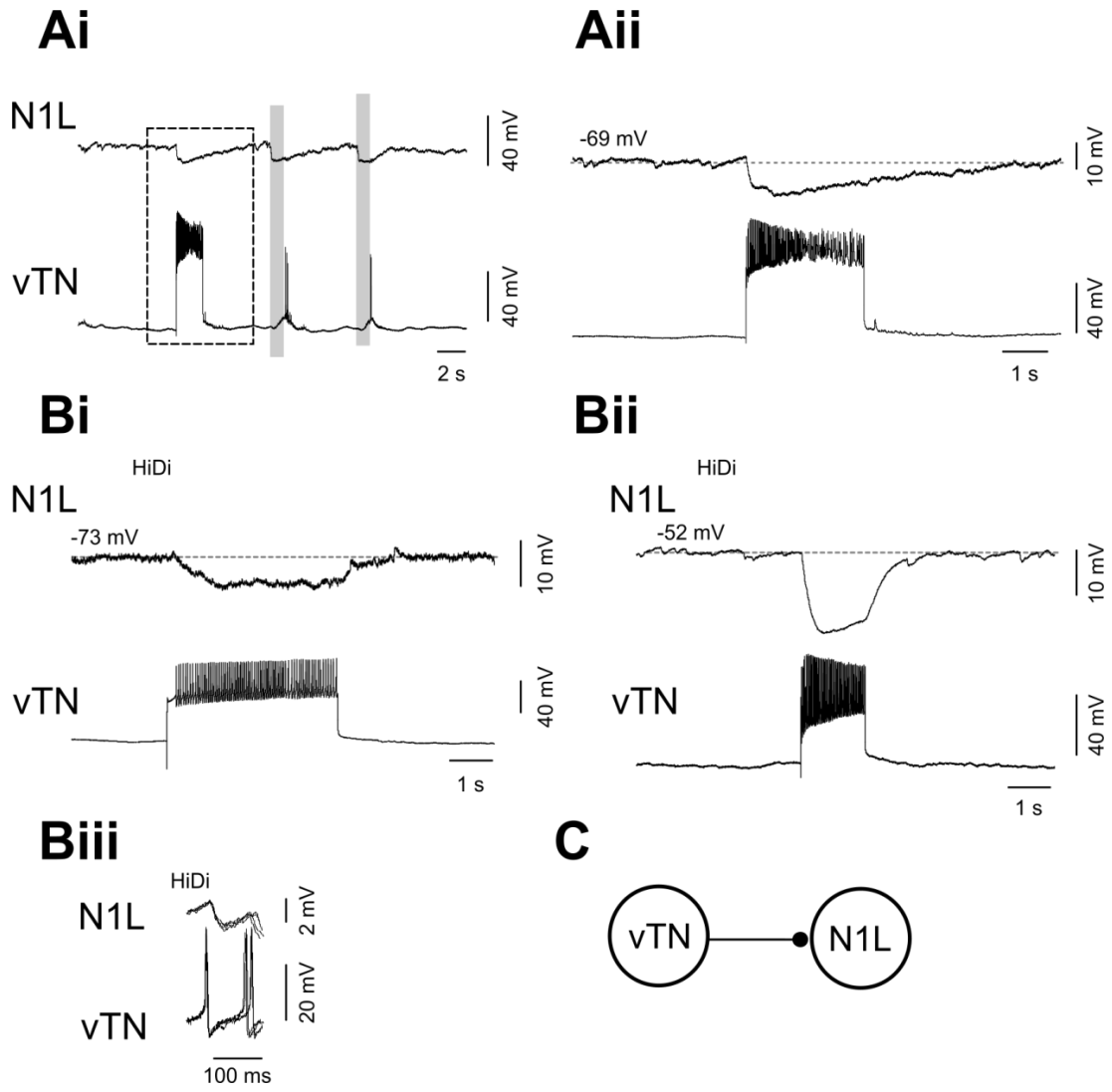

Figure 6.3 vTN's synaptic connections with N1L **Ai.** vTN activation in a period of quiescence triggers two fictive feeding cycles. N1L receives rhythmic inputs during the cycles but never reaches threshold. The box represents the area expanded in Aii. **Aii.** Faster timebase of the boxed area in Ai. At the point of vTN activation N1L is hyperpolarised. Once vTN activity has ceased, N1L returns to its pre-vTN activation membrane potential. N1L is depolarised briefly during the protraction phase, but not sufficiently to reach threshold to fire spikes. **Bi.** vTN activation in HiDi saline hyperpolarised N1L. **Bii.** vTN activation when N1L was at a higher membrane potential also caused a hyperpolarisation of N1L. No delayed excitatory input was present on N1L at any membrane potential following vTN activation. **Biii.** Constant latency unitary IPSPs on N1L we present following vTN spikes 1:1. Four spikes and the elicited IPSPs were superimposed. **C.** Summary circuit of purely inhibitory connection from vTN to N1L. The solid black line represents the persistence of the connection in HiDi saline and evidence of unitary PSPs on N1L which follow vTN spikes 1:1. In all examples the values above each trace are the membrane potential of that neuron prior to vTN activation. Dotted grey lines show the neuron's membrane potential prior to vTN activation.

Figure 6.3Ai shows an example of N1L in a triggered rhythm. N1L showed no spiking activity in either of the triggered cycles. At the point of vTN activation N1L was strongly hyperpolarised (**Figure 6.3Aii**). N1L only briefly rose above RMP within the protraction phase, but this was not sufficient to reach threshold. In HiDi saline, vTN activation strongly hyperpolarised N1L (n=6) (**Figure 6.3Bi** and **6.3Bii**). Constant latency 1:1 IPSPs were present on N1L following vTN spikes (**Figure 6.3Biii**). This strongly suggests that the connection from vTN to N1L was monosynaptic. No delayed depolarization was ever present on N1L after vTN activation. Therefore, like the vTN to SO connection, the vTN to N1L connection was purely inhibitory (**Figure 6.3C**).

6.2.1.3 BCI1

BCI1 showed activity in triggered cycles in less than half of the trials (Section 4.2.2.4). **Figure 6.4Ai** shows an example of BCI1 in a triggered rhythm. In this example, BCI1 shows no spiking activity within either of the triggered cycles. At the point of vTN activation (**Figure 6.4Aii**) BCI1 was hyperpolarised and then depolarised slightly above RMP. This depolarization did not persist until the onset of the protraction phase. In HiDi saline, vTN activation caused a small biphasic input (i/e) to BCI1 in 5 preparations (**Figure 6.4Bi**). However, in 6 preparations vTN activation caused no change in BCI1's membrane potential (**Figure 6.4Bii**). Therefore it is unlikely that the input seen on BCI1 was due to a monosynaptic connection from vTN.

Therefore the only protraction phase interneuron which vTN had any strong excitatory connection with was N1M.

6.2.2 Synaptic connections between protraction phase interneurons and vTN

Results in Sections 3.2.4 and 4.2.1 showed that vTN received synaptic inputs within its own triggered cycles. The largest was an excitatory input during the swallow phase which was sometimes sufficient to elicit spiking. **Figure 6.5A** shows an example of a single N1M driven cycle. vTN was hyperpolarised during the early protraction phase and in the early rasp phase. vTN depolarised in the late rasp and swallow phase. This is similar to the rhythmic inputs seen on vTN in vTN triggered cycles (Section 4.2.1). To determine the source of the inhibition in the protraction phase in both triggered and command-like neuron driven cycles, the synaptic connections from protraction phase interneurons to vTN were tested.

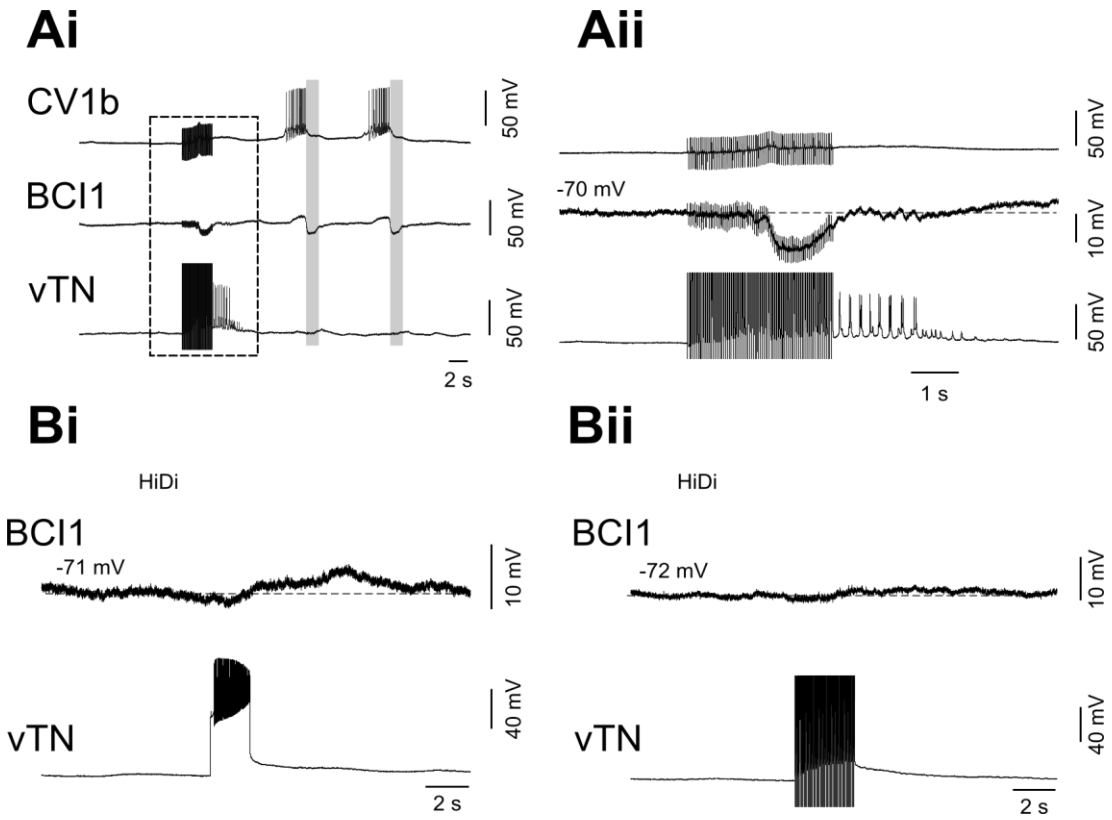

Figure 6.4 vTN's synaptic connections with BCI1 **Ai.** vTN activation in a period of quiescence triggers two fictive feeding cycles. BCI1 receives rhythmic inputs during the cycles but never reaches threshold. The box represents the area expanded in Aii. **Aii.** Faster timebase of the boxed area in Ai. At the point of vTN activation BCI1 is hyperpolarised. Once vTN activity has ceased, BCI1 becomes depolarised. **Bi.** vTN activation in HiDi saline caused a small inhibitory input followed by a small depolarisation. **Bii.** vTN activation caused no large change in BCI1's membrane potential in a separate preparation in HiDi saline. In all examples the values above each trace are the membrane potential of that neuron prior to vTN activation. Dotted grey lines show the neuron's membrane potential prior to vTN activation.

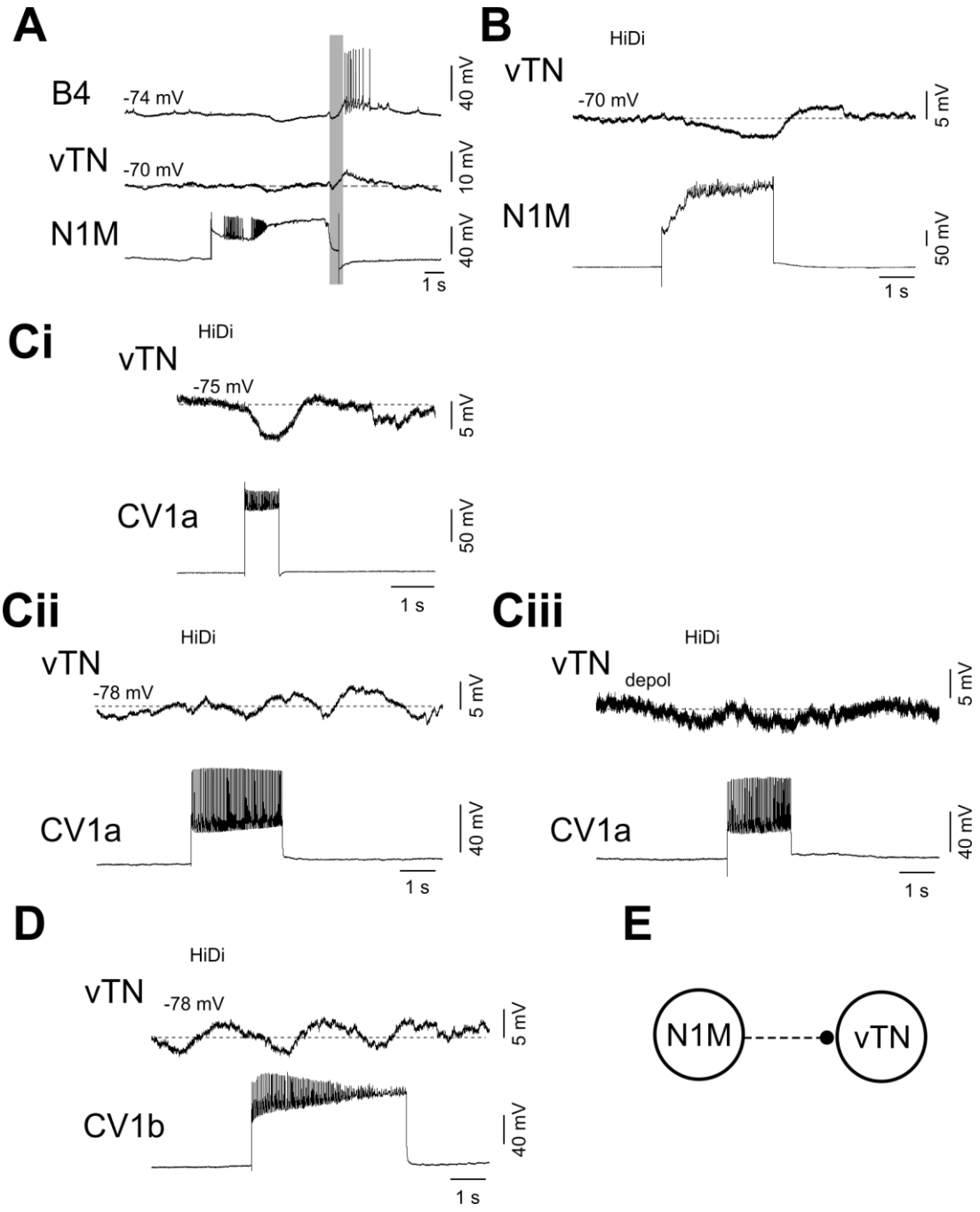

Figure 6.5 Connections to vTN from protraction phase interneurons N1M, CV1a and CV1b **A.** A single fictive feeding cycle was initiated by stimulating N1M. During the protraction phase vTN is hyperpolarised. vTN is hyperpolarised in the early rasp phase, and then depolarised in the late rasp phase. vTN is depolarised in the early swallow phase and then returns to RMP. **B.** N1M activation hyperpolarised vTN. No unitary PSPs were present on vTN following N1M spikes 1:1, however the persistence of the input on vTN in HiDi saline suggests that a component of the inhibitory connection is monosynaptic. **Ci.** CV1a activation hyperpolarises vTN in HiDi. **Cii.** In a different preparation, CV1a activation in HiDi saline causes no change in vTN membrane potential at RMP. **Ciii.** CV1a causes no change in vTN's membrane potential when vTN is depolarised prior to CV1a activation. **D.** CV1b activation in HiDi saline causes no change in vTN membrane potential. **E.** Summary circuit diagram of the inhibitory connection from N1M to vTN. The dotted black line indicates that the connection persists in HiDi saline but no unitary PSPs were evident on vTN following N1M spikes. In all examples the values above each trace are the membrane potential of vTN prior to activation of the protraction phase interneuron. Dotted grey lines show vTN's membrane potential prior to protraction phase interneuron activation.

The first cell type tested was N1M. In HiDi saline N1M activation hyperpolarised vTN (**Figure 6.5B**). No unitary 1:1 IPSPs were ever evident during the hyperpolarization, however the persistence in HiDi saline suggests that a component of the connection may be monosynaptic (n=9). Since N1M is active in the protraction phase of all triggered cycles and in other command-like neuron driven cycles, N1M inhibition of vTN alone would be sufficient to account for the inhibition seen on vTN in the protraction phase. It was next tested whether the CBIs provided any inputs on vTN. CV1a activation hyperpolarised vTN in 2 preparations in HiDi saline (**Figure 6.5Ci**). However this was not a reliable property. In 4 further preparations, CV1a activation caused no inhibitory input on vTN, even when vTN was depolarised prior to CV1a activation (**Figure 6.5Cii** and **6.5Ciii**). The unreliability of this connection suggests that it is not a monosynaptic connection. CV1b activation caused no change in vTN membrane potential (**Figure 6.5D**), suggesting that no monosynaptic connection was present (n=3). **Figure 6.5E** is a summary circuit of the connection from vTN to N1M.

It was next tested whether either SO or N1L provided any inputs to vTN in the protraction phase. SO activation in HiDi saline caused a large hyperpolarization on vTN (n=9) (**Figure 6.6Ai**). IPSPs on vTN followed SO spikes 1:1. There was evidence of facilitation of the IPSPs on vTN from SO (**Figure 6.6Aii**). N1L activation in HiDi also hyperpolarised vTN (n=6) (**Figure 6.6Bi**). Constant latency 1:1 IPSPs on vTN following N1L spikes were present (**Figure 6.6Bii**). There was no evidence of facilitation. BCI1 activity caused no change in vTN membrane potential in HiDi saline (**Figure 6.6C**) suggesting that there was no monosynaptic connection from BCI1 to vTN (n=11). **Figure 6.6D** is a summary circuit of the inhibitory connections from N1L and SO to vTN. Therefore during the protraction phase vTN receives inhibition from N1M, SO and N1L.

6.2.3 Synaptic connections between vTN and rasp phase interneurons

The next phase of the feeding cycle is the rasp phase. There are two identified rasp phase interneurons: N2v and N2d. The synaptic connections between vTN and the N2 interneurons were next tested. Activation of vTN in normal saline caused a large depolarization of N2v which was often sufficient to initiate N2v's plateau potential (**Figure 6.7Ai**). In HiDi saline, vTN activation was still able to depolarise N2v (**Figure 6.7Aii**). No unitary EPSPs were ever present; however the persistence in HiDi saline does not allow us to rule out that a component of the connection is monosynaptic (n=12). vTN activation also caused a depolarization of N2d in normal

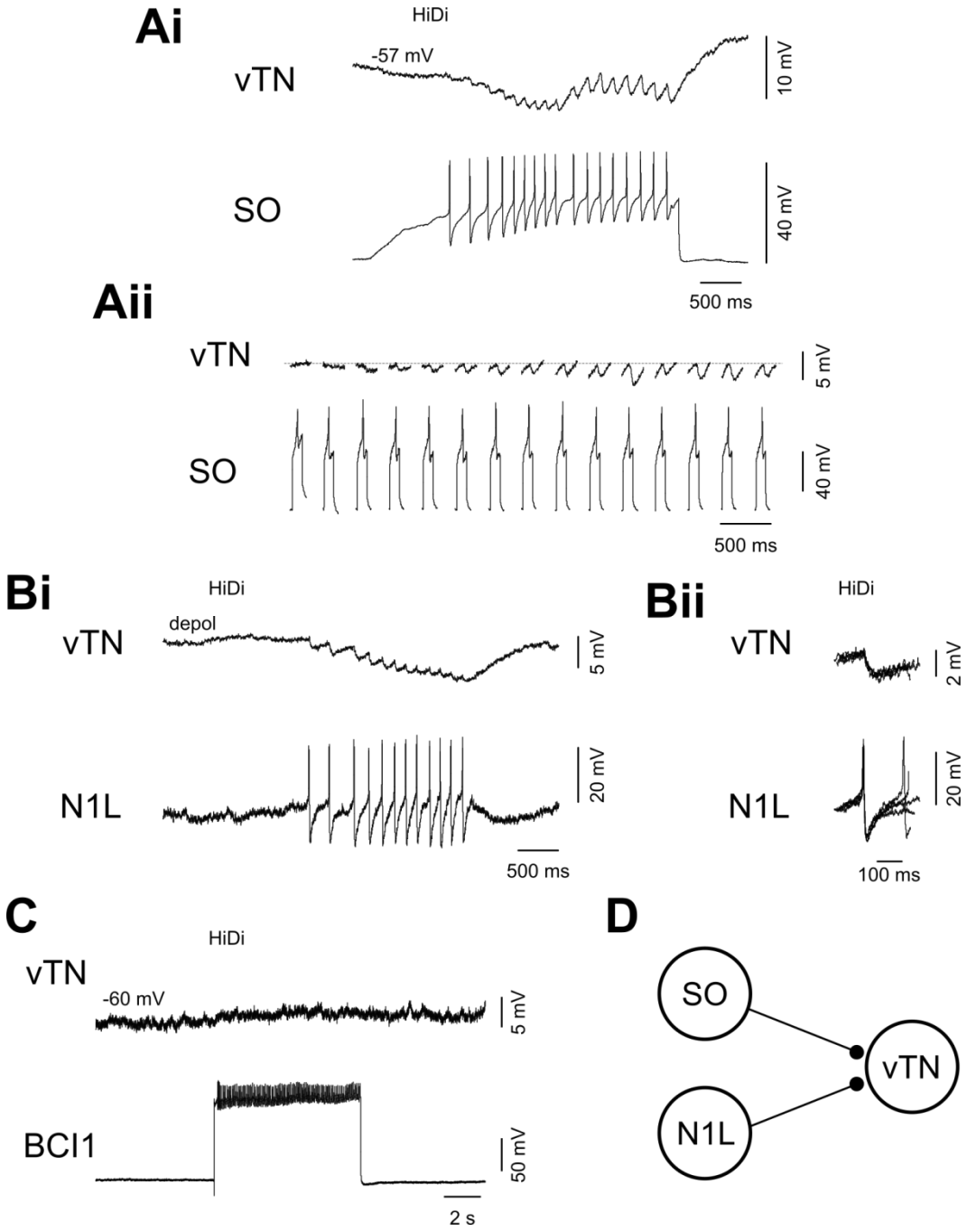

Figure 6.6 Connections to vTN from protraction phase interneurons SO, N1L and BCI1 **Ai.** SO activation in HiDi saline hyperpolarises vTN. **Aii.** SO spikes cause 1:1 IPSPs on vTN. IPSPs on vTN from SO facilitated with repetitive firing of SO. **Bi.** N1L activation in HiDi saline hyperpolarises vTN. **Bii.** N1L spikes cause 1:1 constant latency IPSPs on vTN. Four spikes and the elicited IPSPs were superimposed. **C.** BCI1 activation caused no change in vTN's membrane potential in HiDi saline **D.** Summary circuit diagram of inhibitory connections from SO and N1L to vTN. The solid black lines represents the persistence of the connections in HiDi saline and evidence of unitary PSPs on vTN which follow SO and N1L spikes 1:1. In all examples the values above each trace are the membrane potential of vTN prior to activation of the protraction phase interneuron. Dotted grey lines show vTN's membrane potential prior to protraction phase interneuron activation.

saline which was often sufficient to trigger spiking in the neuron (**Figure 6.7Bi**). In HiDi saline, vTN activation depolarised N2d (**Figure 6.7Bii**). Similarly to N2v, no EPSPs were evident (n=1). **Figure 6.7C** is a summary circuit of the connections from vTN to N2v and N2d. It was next tested whether either N2 interneuron had any synaptic inputs to vTN. N2v activation caused both a hyperpolarization and depolarization of vTN in normal saline which was sometimes sufficient to elicit spiking in vTN (**Figure 6.8Ai**). This was similar to the inputs seen on vTN in the rasp phase of both triggered and command-like neuron driven cycles (**Figure 6.5A**). Activation of N2v in HiDi saline caused a slow depolarisation of vTN which reached its peak after N2v activity had ceased (n=6) (**Figure 6.8Aii**). To test whether this was a reversed inhibitory input, vTN was depolarised to just below threshold prior to N2v activation. N2v activation depolarised vTN to fire spikes at this membrane potential (**Figure 6.8Aiii**). This confirms that the N2v to vTN connection was excitatory. The N2d to vTN connection was next tested. In HiDi saline when vTN was at RMP, N2d activation depolarised vTN (n=1) (**Figure 6.8Bi**). To ensure this was not a reversed inhibitory input, vTN was depolarised to just below threshold prior to N2d activation. N2d activation depolarised vTN at this membrane potential and initiated a number of spikes (**Figure 6.8Bii**). This confirms that the N2d to vTN connection was excitatory. **Figure 6.8C** is a summary circuit of the connections from N2v and N2d to vTN. Therefore neither N2v nor N2d can account for the inhibition of vTN in the rasp phase of both triggered and command-like neuron driven cycles.

Whilst searching for the source of the inhibitory input to vTN in the rasp phase, a novel rasp phase neuron was located on the ventral surface of the buccal ganglia. In a N1L driven fictive feeding rhythm the neuron was depolarised in the protraction and rasp phase but only fired spikes in the rasp phase (**Figure 6.9Ai**). It fired at a similar time as N2d, but at a lower rate. **Figure 6.9Aii** shows an example of a single N1M driven fictive feeding cycle. The neuron fired at a similar time as the N2v interneuron. The neuron fired large somatic spikes similar to N2d but was located on the ventral surface similar to N2v, thus was named N2dv. N2dv was located next to vTN close to the buccal commissure. There was one N2dv located in each buccal ganglion. **Figure 6.9Bi** shows the location of N2dv in relation to other neurons on the ventral surface of the buccal ganglion. Dye-injection of the soma revealed that it was a bipolar neuron (n=4). One branch left the neuron and projected into the contralateral buccal ganglion where it terminated (**Figure 6.9Bii**). The second branch projected across the ipsilateral buccal ganglion and left via the LBN. It was not however tested whether this reached the

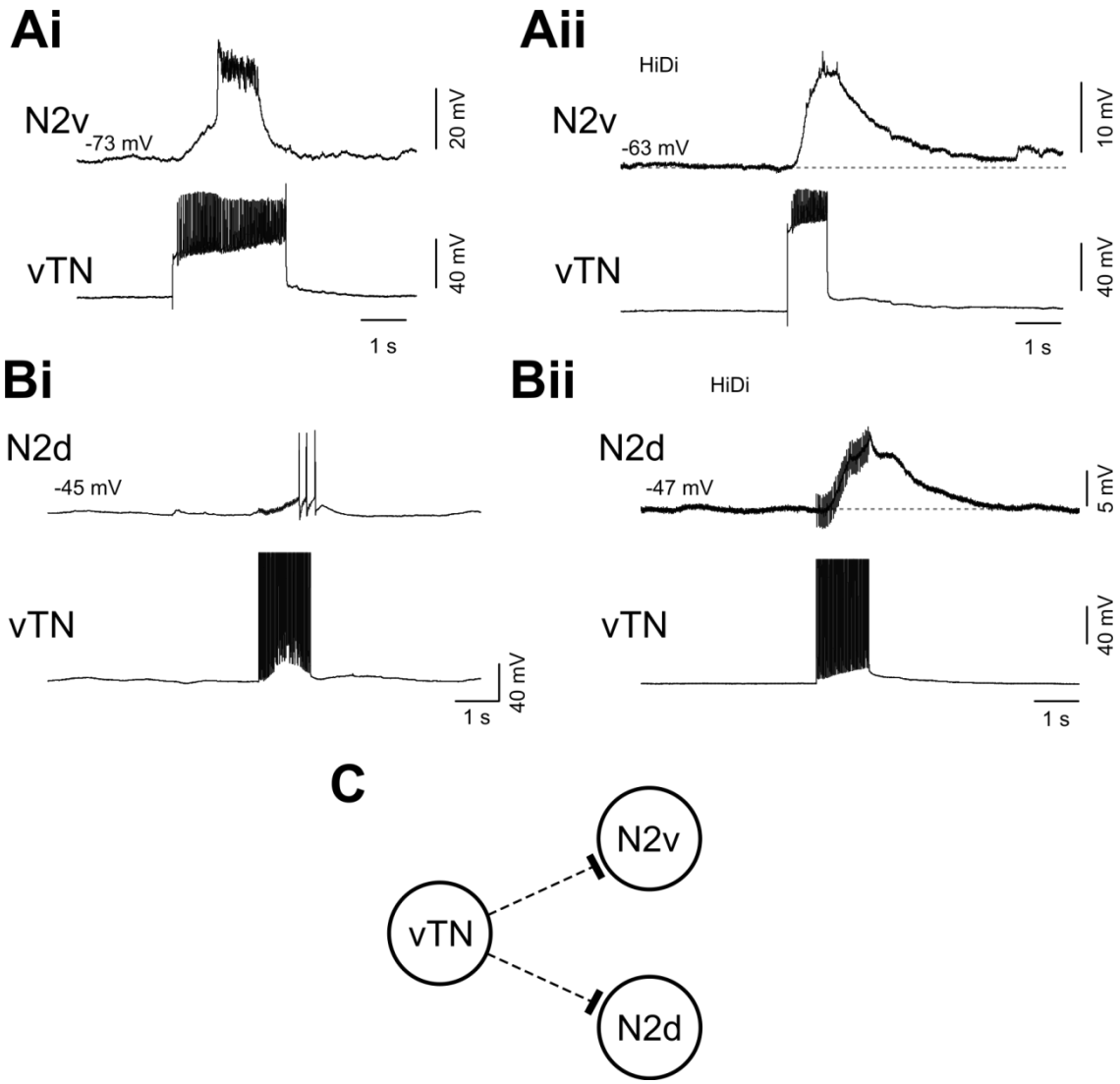

Figure 6.7 Connections from vTN to rasp phase interneurons N2v and N2d **Ai.** vTN activation in normal saline depolarises N2v sufficiently to trigger N2v's plateau potential. **Aii.** Excitation from vTN to N2v persists in HiDi saline suggesting the connection is monosynaptic. **Bi.** vTN activation in normal saline depolarises N2d sufficiently to elicit spiking activity. **Bii.** Excitation from vTN to N2d persists in HiDi saline suggesting the connection is monosynaptic. **C.** Summary circuit diagram of the excitatory connections from vTN to N2v and N2d. The dotted black lines represent that the connections persist in HiDi saline but no unitary PSPs were evident following vTN spikes. In all examples the values above each trace are the membrane potential of that neuron prior to vTN activation. Dotted grey lines show the neuron's membrane potential prior to vTN activation.

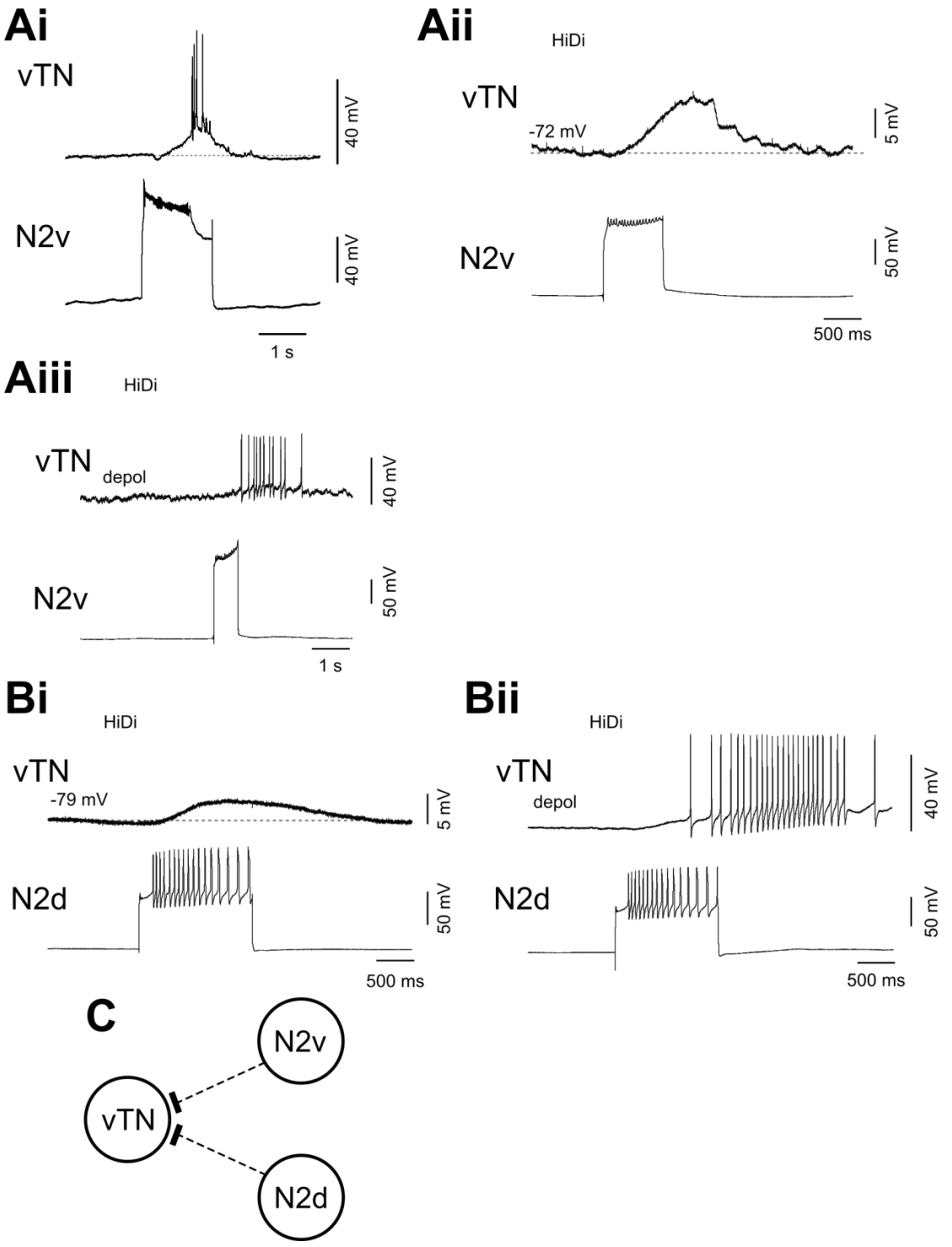

Figure 6.8 Connections from rasp phase interneurons N2v and N2d to vTN **Ai.** N2v activation in normal saline first hyperpolarises vTN and then depolarises it. This was sufficient to elicit spiking activity in vTN. **Aii.** N2v activation in HiDi saline depolarises vTN only. The hyperpolarising input seen in normal saline is abolished. **Aiii.** To test whether N2v provided any inhibitory inputs to N2v, vTN was depolarised prior to N2v activation. At this membrane potential, N2v activation depolarised vTN sufficiently to elicit spiking activity, confirming that the N2v to vTN connection is purely excitatory. **Bi.** N2d activation in HiDi saline depolarises vTN. **Bii.** When vTN is depolarised to a subthreshold level, N2d activation further depolarises vTN and elicits spiking activity. **C.** Summary circuit diagram of the excitatory connections from N2v and N2d to vTN The dotted black lines represent that the connections persist in HiDi saline but no unitary PSPs were evident on vTN following N2v or N2d spikes 1:1. In all examples the values above each trace are the membrane potential of vTN prior to N2v or N2d activation. Dotted grey lines show the neuron's membrane potential prior to N2v or N2d activation.

buccal mass. There were numerous arborisations within the ipsilateral buccal ganglion. Therefore N2dv differed in morphology from both N2v and N2d. Both of these neurons have a projection down the PBN but none in the LBN. The neuron was depolarised in the N2 phase as can be seen by its spiking activity whilst N2v is active (**Figure 6.9Ci**). Activating N2v in HiDi saline caused a large depolarization of N2dv (**Figure 6.9Cii**). Injecting either N2v or N2dv with a negative current pulse caused a similar yet attenuated hyperpolarization of the post-synaptic neuron (**Figure 6.9Di** and **6.9Dii**), suggesting that there was an electrotonic synapse between the two. Since N2dv was active in the rasp phase its synaptic connections with vTN were tested. Activation of N2dv hyperpolarised vTN in HiDi saline (n=5) (**Figure 6.10Ai**). There were constant latency IPSPs on vTN following N2dv spikes 1:1 (**Figure 6.10Aii**), providing strong evidence that the connection was monosynaptic. In one preparation a vTN was recorded with an N2v and an N2dv in HiDi saline. Activating N2v caused a depolarization of N2dv which was subthreshold and a depolarization of vTN (**Figure 6.10Bi**). N2dv was then depolarised prior to N2v activation. N2v activation now caused a depolarization of N2dv which was sufficient for N2dv to reach threshold and fire a single spike. vTN was depolarised as in **Figure 6.10Bi** but a large unitary IPSP was present following 1:1 from the N2dv spike (**Figure 6.10Bii**). This was similar to the mixed inhibitory/excitatory inputs seen on vTN in the rasp phase of triggered and command-like neuron driven cycles (**Figure 6.5A**). However, N2dv spiking was not necessary for the inhibitory input on vTN in the rasp phase. **Figure 6.11Ai** shows an example of N2dv activity in a vTN triggered rhythm. N2dv receives excitation in the rasp phases, but fires no spikes. vTN is hyperpolarised in both rasp phases even without N2dv activity (**Figure 6.11Aii**). It is possible that the contralateral N2dv was active, providing inhibition to vTN in this phase. Another possibility is that further as of yet unidentified N2 interneurons exist which provide inhibition to vTN in the rasp phase.

Similar to both N2v and N2d, N2dv was excited by vTN activation. In normal saline, vTN activation was often sufficient to elicit spiking in N2dv (**Figure 6.11Bi**). vTN's depolarization of N2dv was present in HiDi saline (n=10) (**Figure 6.11Bii**). Constant latency EPSPs were present on N2dv which followed from vTN spikes 1:1 (**Figure 6.11Biii**) providing strong evidence that the connection was monosynaptic. Therefore vTN has excitatory connections with N2v, N2d and the newly identified N2dv. **Figure 6.11C** is a summary circuit of the connections between vTN and N2dv.

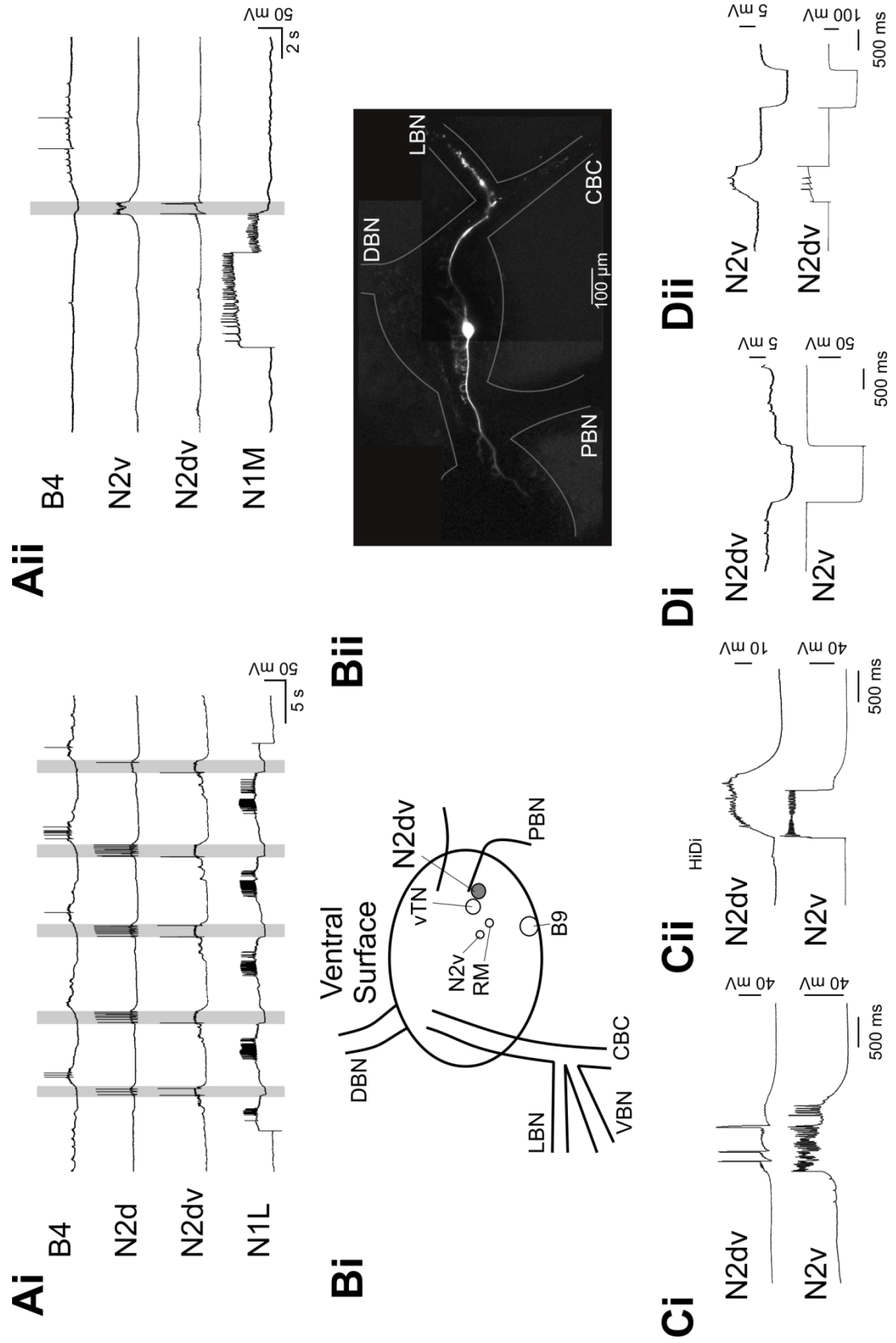
Ai
B4
N2d
N2dv
N1L
50 mV
5 s
Aii
B4
N2v
N2dv
N1M
50 mV
2 s
Bi
Ventral Surface
DBN
N2dv
vTN
N2v
RM
B9
PBN
CBC
LBN
VBN
Bii
DBN
LBN
CBC
PBN
100 µm
Ci
HiDi
N2dv
N2v
40 mV
500 ms
Cii
N2dv
N2v
10 mV
40 mV
500 ms
Di
N2dv
N2v
5 mV
50 mV
500 ms
Dii
N2v
N2dv
5 mV
100 mV
500 ms

Figure 6.9 Identification, morphology and connections of N2dv **Ai.** Continuous current injection into N1L drives fictive feeding cycles. N1L and B4 are inhibited in the rasp phase whereas N2d fires a burst of spikes in this phase. The newly identified N2dv is depolarised in the protraction phase and fires up to two spikes in the rasp phase. **Aii.** Current injection into N1M drives a series of spikes. The stimulus is then removed from N1M; however N1M remains depolarised and continues to spike due to the initiation of its plateau potential. N1M depolarises N2v, and N1M's plateau is terminated once N2v reaches threshold to trigger its own plateau, and the initiation of the rasp phase. N2dv fires two spikes in the rasp phase. **Bi.** A map of the ventral surface of a buccal ganglion with all identified neurons. A single N2dv is located in each buccal ganglion close to the buccal commissure, adjacent to vTN. **Bii.** A fill of a single N2dv with 5 (6)-carboxy fluorescein. N2dv is a bipolar neuron. One projection crosses the buccal commissure and enters the contralateral buccal ganglion where it terminates. The other projection leaves the buccal ganglia via the ipsilateral LBN. Fine neuritic branching occurs in both buccal ganglia. **Ci.** N2dv fires within the same phase as N2v. N2v shows its characteristic plateau potential with small spikes recorded at the soma. N2dv fires large somatic spikes. **Cii.** Activating N2v in HiDi causes a large depolarisation of N2dv suggesting N2v monosynaptically excites N2dv. **Di.** Injecting negative current into N2v causes a similar yet attenuated hyperpolarisation of N2dv suggesting that the two are connected by an electrical synapse. **Dii.** Injecting N2dv with positive or negative current causes a similar yet attenuated response in N2v. Grey vertical lines represent the rasp phase of a cycle.

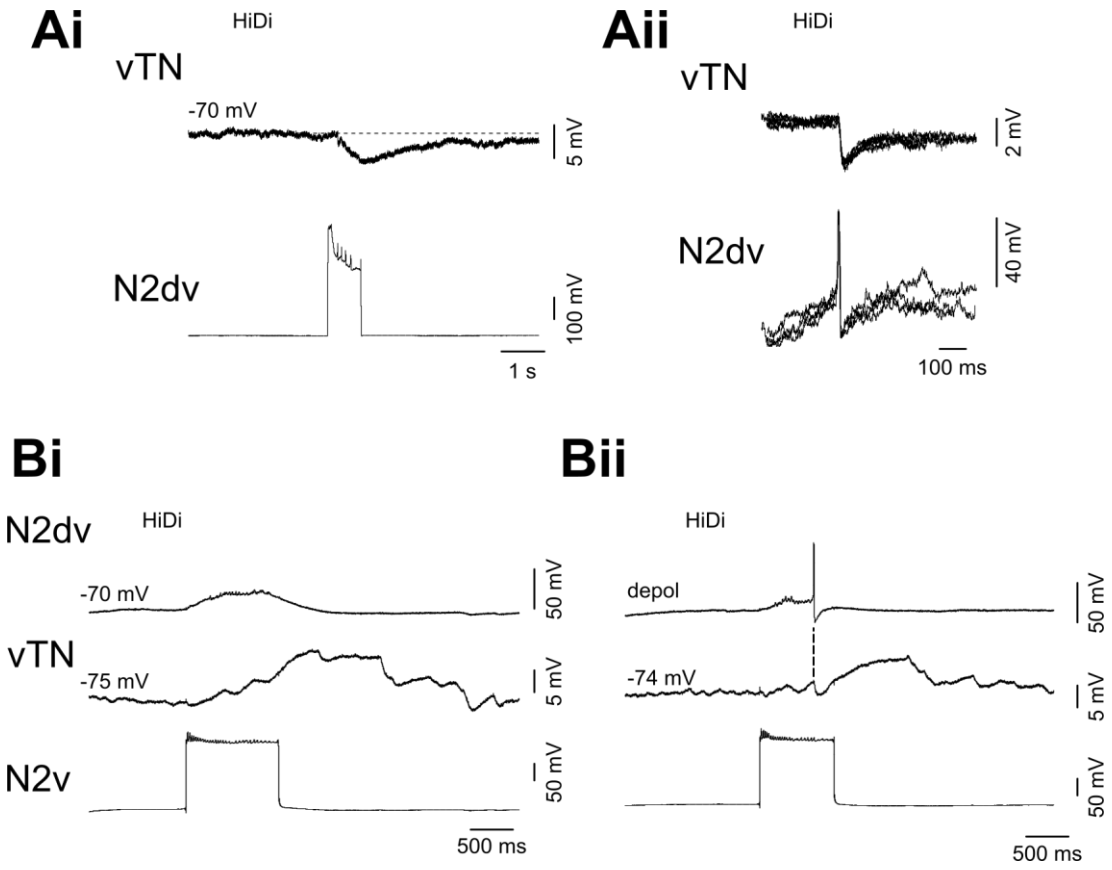

Figure 6.10 Connections from N2dv to vTN **Ai.** Activation of N2dv in HiDi saline hyperpolarises vTN. **Aii.** N2dv spikes cause 1:1 constant latency IPSPs on vTN. Four spikes and the elicited IPSPs were superimposed. **Bi.** Activating N2v depolarises both N2dv and vTN. **Bii.** N2dv was depolarised prior to N2v activation. N2v activation depolarises N2dv sufficiently to elicit a single spike. vTN receives a unitary IPSP from the N2dv spike and is then depolarises, similar to the response seen on vTN by N2v activation in normal saline. In all examples the values above each trace are the membrane potential of the neuron. Dotted grey lines show the neuron's membrane potential prior to N2dv activation.

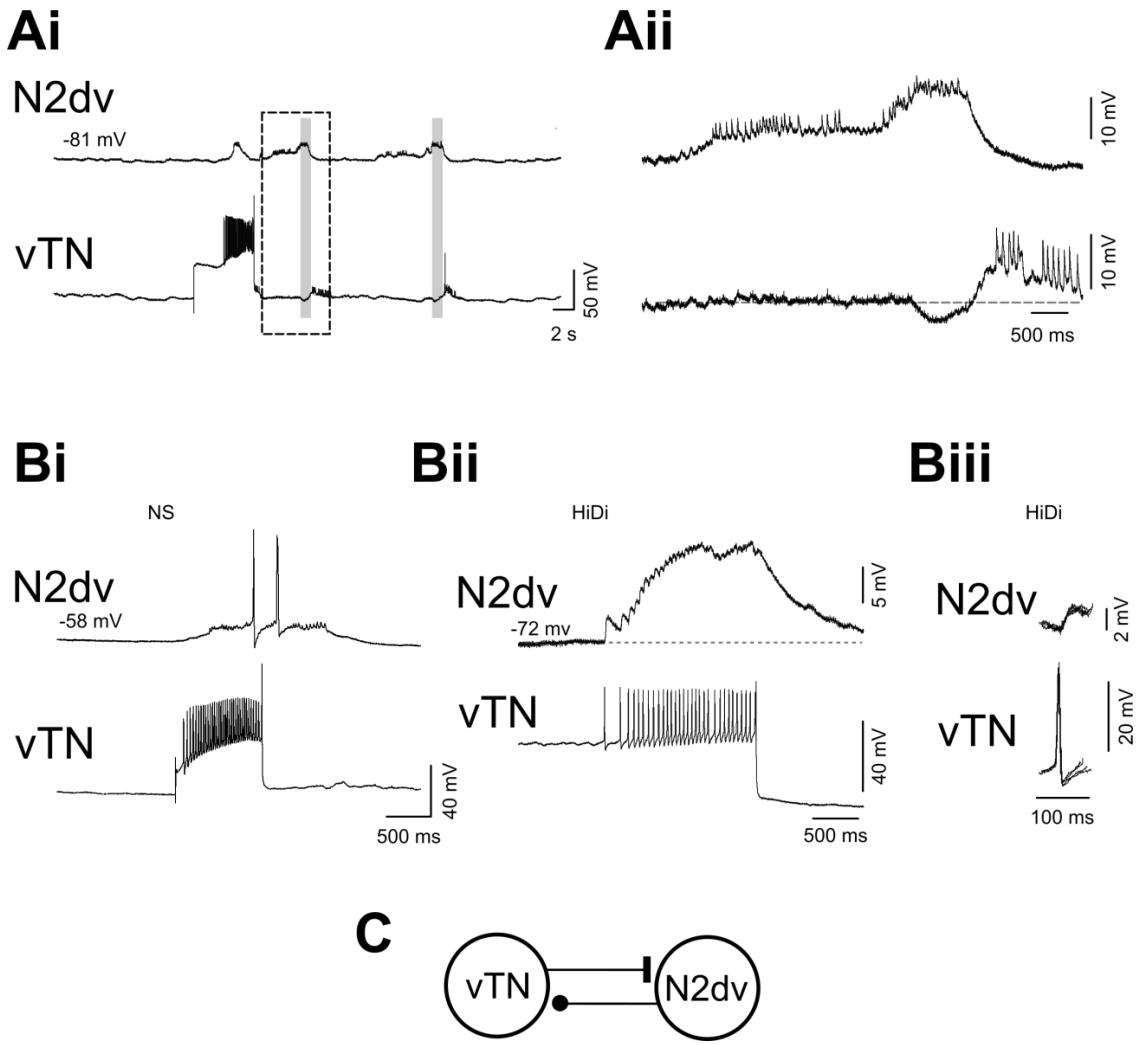

Figure 6.11 Connections from vTN to N2dv **Ai.** N2dv is depolarised in the protraction and rasp phase of a vTN triggered rhythm, but fires no spikes. **Aii.** vTN receives an inhibitory input in the rasp phase even though N2dv is not active. **Bi.** Activation of vTN in normal saline depolarises N2dv sufficiently to elicit spiking activity. **Bii.** The excitatory input to N2dv from vTN persists in HiDi saline. **Biii.** vTN spikes cause 1:1 constant latency EPSPs on N2dv. Four spikes and the elicited EPSPs were superimposed. **C.** Summary circuit diagram of inhibitory connection from N2dv to vTN and excitatory connection from vTN to N2dv. The solid black lines represent the persistence of the connection in HiDi saline and evidence of unitary PSPs following spikes 1:1. Dotted grey lines show N2dv and vTN's membrane potential prior to vTN activation or the onset of the rasp phase.

6.2.4 Synaptic connections between vTN and swallow phase interneurons

6.2.4.1 N3p

The third phase of the feeding cycle is the swallow phase. Three swallow phase interneurons have been identified in the buccal ganglia: N3t, N3p and OC. vTN's synaptic connections with N3t have already been identified in Section 4.2.5. **Figure 6.12A** shows an example of N3p activity within a vTN triggered rhythm. At the point of vTN activation N3p is depolarised which is sufficient to elicit a single somatic spike. An inhibitory input is seen on both N3p and B4 during vTN activation. Both N3p and vTN are simultaneously active in the first of the triggered cycles with both firing 7 spikes. Neither N3p nor vTN fire again during the next three cycles, but both show strong rhythmic inputs. In HiDi saline, vTN activation depolarised N3p (n=11) (**Figure 6.12Bi**). If N3p was depolarised prior to vTN activation, vTN activation was sufficient to elicit spiking in N3p (**Figure 6.12Bii**). Injecting vTN with negative current caused a similar yet attenuated hyperpolarization of N3p (n=11) (**Figure 6.12Ci**). This suggested that the two were connected by an electrotonic synapse. This was confirmed by bathing the preparation in HiLo saline. In HiLo saline the connection from vTN to N3p persisted (n=9). Interestingly, activation of vTN in HiLo saline reduced both the size and duration of excitation to N3p (**Figure 6.12Cii**). This suggests that vTN has both an electrotonic synapse and an excitatory chemical connection with N3p. The N3p to vTN connection was next tested. Injecting N3p with a negative current step caused a similar yet attenuated hyperpolarization of vTN (**Figure 6.12Di**). This response persisted in HiLo saline, suggesting that the synapse was electrotonic in nature (n=9). In HiDi saline, N3P activation caused a fast excitation of vTN followed by inhibition (**Figure 6.12Dii**). Constant latency IPSPs were present on vTN which followed 1:1 from N3p spikes (**Figure 6.12Diii**). In HiLo saline only the excitatory connection persisted (**Figure 6.12Ei**), even when vTN was depolarised prior to N3p activation (**Figure 6.12Eii**). This suggests that the fast excitatory component in HiDi is due to the electrotonic synapse and the inhibitory input due to a chemical inhibitory connection.

6.2.4.2 OC

Figure 6.13A shows an example of OC activity in a vTN triggered rhythm. At the point of vTN activation, OC is depolarised and fires a single spike before receiving an inhibitory input. OC is then further depolarised and fires a burst of spikes. OC then fires in the swallow phase of each of the triggered cycles. In HiDi saline, vTN activation

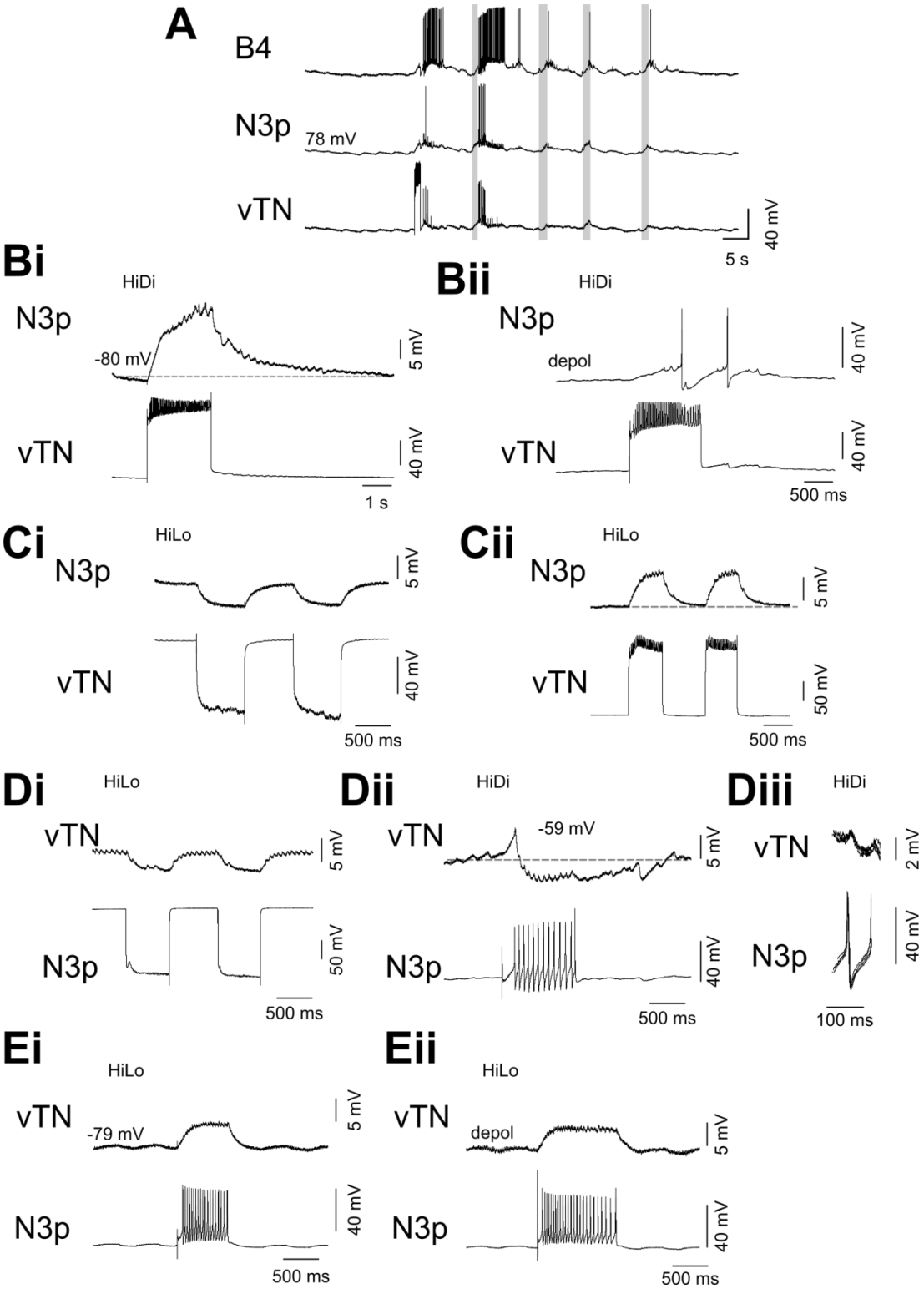
A
B4
N3p
78 mV
vTN
40 mV
5 s
Bi
HiDi
N3p
-80 mV
5 mV
vTN
40 mV
1 s
Bii
HiDi
N3p
depol
40 mV
vTN
40 mV
500 ms
Ci
HiLo
N3p
5 mV
vTN
40 mV
500 ms
Cii
HiLo
N3p
5 mV
vTN
50 mV
500 ms
Di
HiLo
vTN
5 mV
N3p
50 mV
500 ms
Dii
HiDi
vTN
-59 mV
5 mV
N3p
40 mV
500 ms
Diii
HiDi
vTN
2 mV
N3p
40 mV
100 ms
Ei
HiLo
vTN
-79 mV
5 mV
N3p
40 mV
500 ms
Eii
HiLo
vTN
depol
5 mV
N3p
40 mV
500 ms

Figure 6.12 Connections between vTN and swallow phase interneuron N3p **A.** vTN activation triggered four fictive feeding cycles. N3p was depolarised during the period of vTN activation and fired a single spike. N3p received rhythmic inputs during the four triggered cycles but only fired spikes in the first cycle in the early swallow phase. **Bi.** vTN activation depolarised N3p in HiDi saline. N3p depolarisation persisted after vTN activity had ceased. **Bii.** Depolarising N3p prior to vTN activation showed that the connection from vTN was purely excitatory. vTN activation depolarised N3p and triggered two spikes. **Ci.** Injecting vTN with negative current pulses elicited a similar yet attenuated hyperpolarisation of N3p which persisted in HiLo saline. **Cii.** Activating vTN in HiLo saline produce a greatly reduced, in size and duration, response on N3p, suggesting that an excitatory chemical connection is present from vTN to N3p which was blocked by the HiLo saline. **Di.** Injecting N3p with negative current caused a similar yet attenuated hyperpolarisation of vTN which persisted in HiLo saline. **Dii.** In HiDi saline, N3p activation caused a fast depolarisation of vTN, followed by hyperpolarisation. **Diii.** N3p spikes cause 1:1 constant latency IPSPs on vTN. Four spikes and the elicited IPSPs were superimposed. **Ei.** In HiLo saline, the inhibitory input from N3p to vTN is abolished. The fast excitatory component present in Dii. remains. **Eii.** vTN was depolarised prior to N3p activation. The inhibitory input from N3p to vTN remains absent, and only the excitatory component remains. This strongly suggests that the N3p to vTN connection consists of an electrical synapse and an inhibitory chemical synapse. In all examples the values above each trace are the membrane potential of the neuron prior to vTN or N3p activation. Dotted grey lines show the neuron's membrane potential prior to vTN or N3p activation.

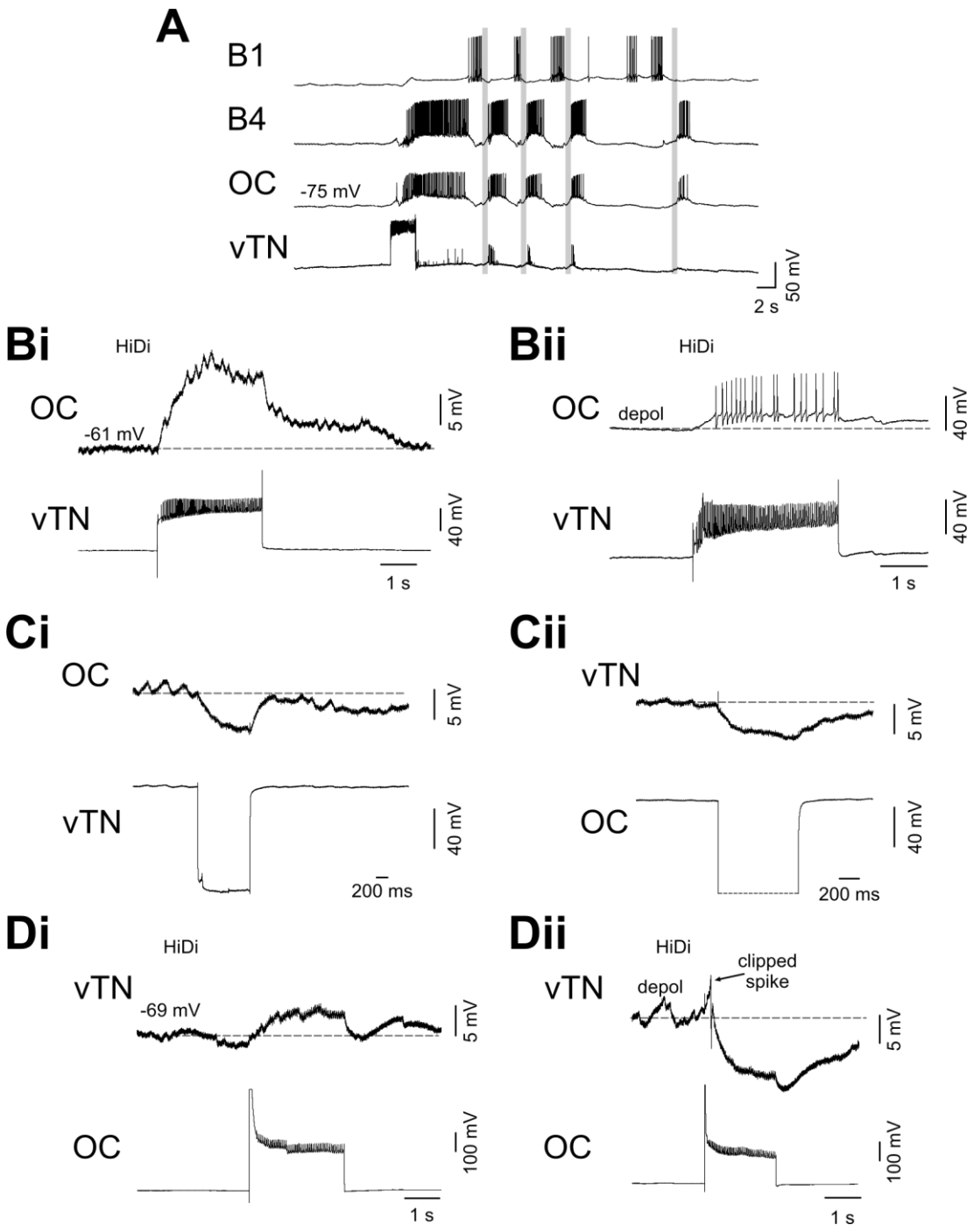
A
B1
B4
OC
-75 mV
vTN
50 mV
2 s
Bi
HiDi
OC
-61 mV
5 mV
vTN
40 mV
1 s
Bii
HiDi
OC
depol
40 mV
vTN
40 mV
1 s
Ci
OC
5 mV
vTN
40 mV
200 ms
Cii
vTN
5 mV
OC
40 mV
200 ms
Di
HiDi
vTN
-69 mV
5 mV
OC
100 mV
1 s
Dii
HiDi
vTN
depol
clipped
spike
5 mV
OC
100 mV
1 s

Figure 6.13 Connections between vTN and swallow phase interneuron OC **A.** vTN activation triggered four fictive feeding cycles. OC was depolarised during the period of vTN activation and fired a burst of spikes. OC received rhythmic inputs during the four triggered cycles and fired a burst or spikes in the swallow phase of each cycle. **Bi.** vTN activation depolarised OC in HiDi saline. OC depolarisation persisted after vTN activity had ceased. **Bii.** Depolarising OC prior to vTN activation showed that the connection from vTN was purely excitatory. vTN activation depolarised OC and triggered nineteen spikes **Ci.** Injecting vTN with negative current pulses elicited a similar yet attenuated hyperpolarisation of OC. **Cii.** Injecting OC with negative current caused a similar yet attenuated hyperpolarisation of vTN. **Di.** In HiDi saline, OC activation caused a small depolarisation of vTN which did not persist after OC activity had ceased. **Diii.** vTN was depolarised prior to OC activation. OC activity caused a fast excitation of vTN, which triggered a single spike. Then vTN was hyperpolarised by OC activity. This suggests that the early excitation is due to the electrical synapse and the inhibitory component due to an inhibitory chemical connection. In all examples the values above each trace are the membrane potential of the neuron prior to vTN or OC activation. Dotted grey lines show the neuron's membrane potential prior to vTN or OC activation.

causes a depolarisation of OC (n=2) (**Figure 6.13Bi**). **Figure 6.13Bii** shows that if OC is artificially depolarised prior to vTN activation then vTN activation is sufficient to elicit spiking in OC. OC depolarisation persists after vTN activity has ceased, similarly to the vTN-N3p connection (**Figure 6.12Bi**). Injecting negative current into vTN causes a similar yet attenuated hyperpolarising response on OC, suggesting that an electrotonic synapse is present between the two neurons (n=3) (**Figure 6.13Ci**). The persistent depolarisation of OC by vTN suggests that an excitatory chemical synapse is present from vTN to OC. Injecting negative current into OC causes a similar yet attenuated hyperpolarisation of vTN (**Figure 6.13Cii**). Activation of OC causes a depolarisation of vTN in HiDi saline when vTN is at RMP (n=2) (**Figure 6.13Di**). Notice that vTN returns to its RMP faster than OC does after vTN stimulation (compare **Figure 6.13Bi** with **Figure 6.13Di**). When vTN is depolarised prior to OC activation, OC activation causes a fast depolarisation of vTN (which elicits a single spike in this example) and then a delayed hyperpolarisation of vTN (n=2) (**Figure 6.13Dii**). This suggests that there is both an electrotonic synapse (providing the fast depolarisation to vTN) and an inhibitory chemical synapse (providing the delayed hyperpolarisation to vTN). This is only visible when vTN is at a high membrane potential. At lower membrane potentials, only the excitatory input from the electrotonic connection is visible.

6.2.5 Synaptic connections between vTN and the modulatory interneuron CGC

The CGC's are a pair of serotonergic CBIs. They show little rhythmic activity during fictive feeding cycles. **Figure 6.14A** is an example of a vTN triggered rhythm with a CGC and a B4. Both B4 and vTN show the standard rhythmic inputs whereas CGC continue to fire tonically, as prior to vTN activation. In HiDi saline, vTN activation caused no change in CGC spiking activity (**Figure 6.14Bi**). This was tested further by impaling a CGC with two electrodes and artificially reducing the membrane potential to prevent somatic action potentials (~-105 mV). In **Figure 6.14Bii** large depolarisations are still present on CGC but they fail to elicit somatic action potentials. These either arise due to spiking in the electrotonically coupled contralateral CGC or due to spikes generated further down the neurite which are propagated back to the soma but fail to reach threshold (McCrohan and Benjamin 1980). vTN activation when CGC is held at this level depolarises CGC. The previously subthreshold depolarisations on the CGC become suprathreshold and two action potentials are initiated (n=3). No 1:1 EPSPs were ever evident; however the persistence of the connection in HiDi suggests that a component of the connection may be monosynaptic. CGC's connection with vTN was

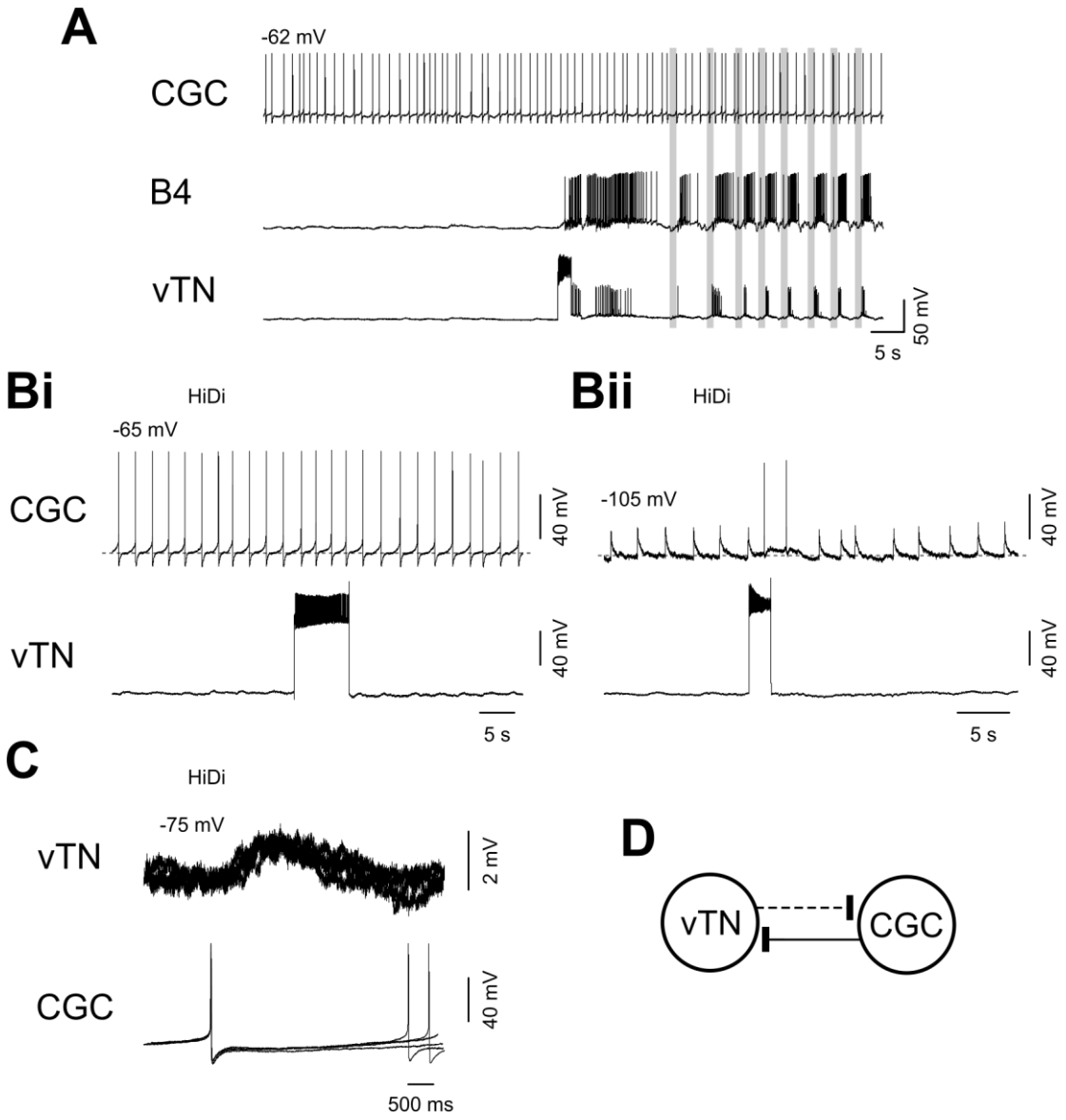

Figure 6.14 Connections between vTN and modulatory interneuron CGC **A.** vTN activation triggered eight fictive feeding cycles. CGC showed no change in firing rate during the triggered cycles. **Bi.** vTN activation in HiDi saline caused no change in CGC spike rate when CGC was at RMP. **Bii.** CGC was hyperpolarised to -105 mV prior to vTN activation. vTN activation depolarised CGC and triggered two somatic spikes. **C.** In HiDi saline, CGC spikes cause 1:1 constant latency EPSPs on vTN. Four spikes and the elicited EPSPs were superimposed. **D.** Summary circuit diagram of excitatory connections between vTN and CGC. The black dotted line represents the persistence of the connection from vTN to CGC in HiDi saline but the absence of unitary PSPs on CGC following vTN spikes 1:1. The solid black line represents the persistence of the connection from CGC to vTN in HiDi saline and the presence of unitary PSPs on vTN following CGC spikes 1:1. In all examples the values above each trace are the membrane potential of the neuron prior to vTN or CGC activity. Dotted grey lines show the neuron's membrane potential prior to vTN or CGC activity.

next tested. In HiDi saline, slow constant latency EPSPs were present on vTN following 1:1 from CGC spikes (n=3) (**Figure 6.14C**). Therefor vTN and CGC both have excitatory chemical connections with each other (**Figure 6.14D**).

6.2.6 vTN's synaptic connections with feeding motor neurons

vTN had diverse synaptic connections with many of the interneurons in the feeding network; therefore it was tested whether vTN also had connections with known motor neurons.

6.2.6.1 Protraction phase motor neurons

It was first tested whether vTN had any synaptic connections with protraction phase motor neurons. The first motor neuron tested was the B1 motor neuron, a putative salivary gland motor neuron (Benjamin et al., 1979). **Figure 6.15Ai** shows an example of B1 in a vTN triggered rhythm. vTN activation is followed by a delayed depolarisation of B1 which persists throughout the triggered cycles. In the protraction phase of each cycle B1 fires a burst of spikes. In HiDi saline, vTN activation caused a slow, long lasting depolarisation of B1 (**Figure 6.15Aii**). No unitary EPSPs were ever evident but the persistence of the connection in HiDi saline suggests that a component of the connection may be monosynaptic (n=9). The next motor neuron tested was the B5, a putative oesophageal motor neuron (Benjamin et al., 1979). **Figure 6.15Bi** shows an example of B5 activity within a vTN triggered rhythm. B5 was firing tonically prior to vTN activation. vTN activation caused a large hyperpolarization of B5 and prevented firing. B5 showed no spiking activity within the first cycle, but fired in the early protraction phase of the subsequent cycles. In HiDi saline, vTN activation caused an early hyperpolarization followed by a delayed depolarization, after vTN activity had ceased, which was often sufficient to elicit spiking activity (n=3) (**Figure 6.15Bii**). No unitary IPSPs were evident, however the persistence in HiDi saline suggests a component of the connection may be monosynaptic. The next protraction phase motor neuron tested was B7. B7 is a PJM motor neuron (Staras et al., 1998b). **Figure 6.15Ci** shows an example of a B7 in a vTN triggered rhythm. At the point of vTN activation, B7 is hyperpolarised. Within the rhythm, B7 fires a burst of spikes within each protraction phase and is inhibited in the rasp and swallow phases. In HiDi saline vTN activation strongly hyperpolarises B7 (**Figure 6.15Cii**). Once vTN activity has ceased, B7 repolarises and then depolarises (n=4). In this example, B7 remains above RMP for >7 s. Longer activation of vTN increases the depolarising component of the connection,

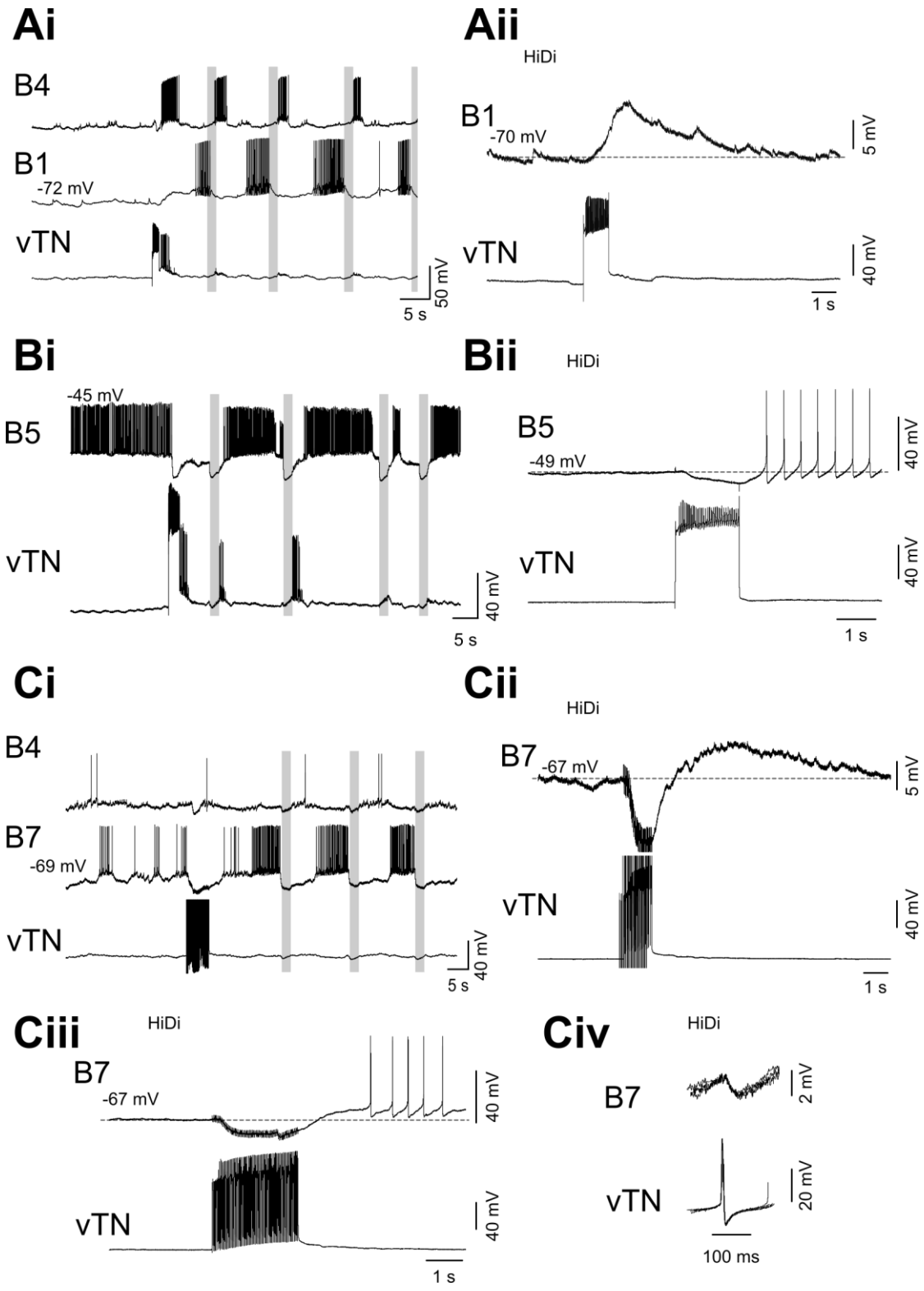
Ai
B4
B1
-72 mV
vTN
50 mV
5 s
Aii
HiDi
B1
-70 mV
5 mV
vTN
40 mV
1 s
Bi
-45 mV
B5
vTN
40 mV
5 s
Bii
HiDi
B5
-49 mV
40 mV
vTN
40 mV
1 s
Ci
B4
B7
-69 mV
vTN
40 mV
5 s
Cii
HiDi
B7
-67 mV
5 mV
vTN
40 mV
1 s
Ciii
HiDi
B7
-67 mV
40 mV
vTN
40 mV
1 s
Civ
HiDi
B7
2 mV
vTN
20 mV
100 ms

Figure 6.15 Connections from vTN to protraction phase motor neurons B1, B5 and B7 **Ai.** vTN activation triggered four fictive feeding cycles. B1 was depolarised and fired a burst of spikes in the protraction phase of each triggered cycle. **Aii.** In HiDi saline, vTN activation depolarised B1. This suggests that vTN has an excitatory connection with B1. **Bi.** vTN activation triggered four fictive feeding cycles. B5 was hyperpolarised during vTN activity and then fired in the early protraction phase of each triggered cycle. **Bii.** In HiDi saline, vTN activation caused an early hyperpolarisation of B5 followed by a depolarisation once vTN activity had ceased. This was sufficient to trigger spiking activity in B5. This suggests that vTN has a biphasic (i/e) connection with B5. **Ci.** vTN activation triggered three fictive feeding cycles. B7 was hyperpolarised during vTN activity. B7 fired spikes in the protraction phase of each triggered cycle. **Cii.** vTN activation in HiDi hyperpolarised B7. When vTN activity had ceased, B7 was depolarised. **Ciii.** If vTN activity was increased, the depolarising component of the input to B7 increased and was sufficient to trigger spiking activity. Therefore the connection from vTN to B7 was biphasic (i/e). **Civ.** vTN spikes cause 1:1 constant latency IPSPs on B7. Four spikes and the elicited IPSPs were superimposed. In all examples the values above each trace are the membrane potential of the motor neuron prior to vTN activation. Dotted grey lines show the motor neuron's membrane potential prior to vTN activation.

eliciting a number of action potentials (**Figure 6.15Ciii**). Constant latency IPSPs are present on B7 following 1:1 from vTN spikes (**Figure 6.15Civ**). This provides strong evidence that the connection is monosynaptic. Therefore vTN has a purely excitatory connection with B1 and a biphasic (i/e) connection with B5 and B7.

6.2.6.2 Rasp phase motor neurons

B10 is a rasp phase motor neuron. It innervates the radula tensor muscle in the buccal mass (Staras et al., 1998b). **Figure 6.16Ai** shows an example of B10 activity in a vTN triggered rhythm. Prior to vTN activation, B10 fires at a low rate. vTN activation causes an increase in firing rate which then decreases once vTN activity stops. B10 then fires in the protraction phase and then more strongly in the rasp phase of the triggered cycles. In HiDi saline, vTN activation causes a depolarisation of B10 (n=2). In **Figure 6.16Aii**, vTN activation was sufficient to elicit spiking in B10. No unitary EPSPs were present, but the persistence in HiDi suggests the a component of the connection is monosynaptic.

6.2.6.3 Swallow phase motor neurons

B4 is a swallow phase motor neuron which innervates the AJM (Rose and Benjamin, 1979, Staras et al., 1998b). **Figures 6.15Ai**, **6.15Ci** and **6.16Ai** show examples of B4 activity in vTN triggered rhythms. vTN activation depolarises B4. Often B4 receives a large inhibitory input during this period and then fires a burst of spikes (see **Figure 6.16Ai**). B4 then receives inhibition in both the protraction and rasp phase and is then depolarised in the swallow phase often sufficiently to fire a burst of spikes. In HiDi saline, vTN activation causes an early depolarisation followed by a longer depolarisation which persists after vTN activity has ceased (n=18) (**Figure 6.16Bi**). In HiLo saline, the long lasting depolarising component seen in HiDi from vTN to B4 is abolished, but the early depolarisation persists. This suggests that vTN has both an electrotonic and an excitatory chemical connection with B4.Injecting either vTN or B4 with negative current pulses elicited a similar but attenuated hyperpolarisation in the post-synaptic cell (**Figure 6.16Ci** and **6.16Cii**). This persisted in HiLo saline (n=12).

6.2.6.4 B2 and B3 motor neurons

The B2 motor neuron is a oesophageal motor neuron (Perry et al., 1998). **Figure 6.17Ai** shows an example of B2 in a vTN triggered rhythm. B2 fires in regular

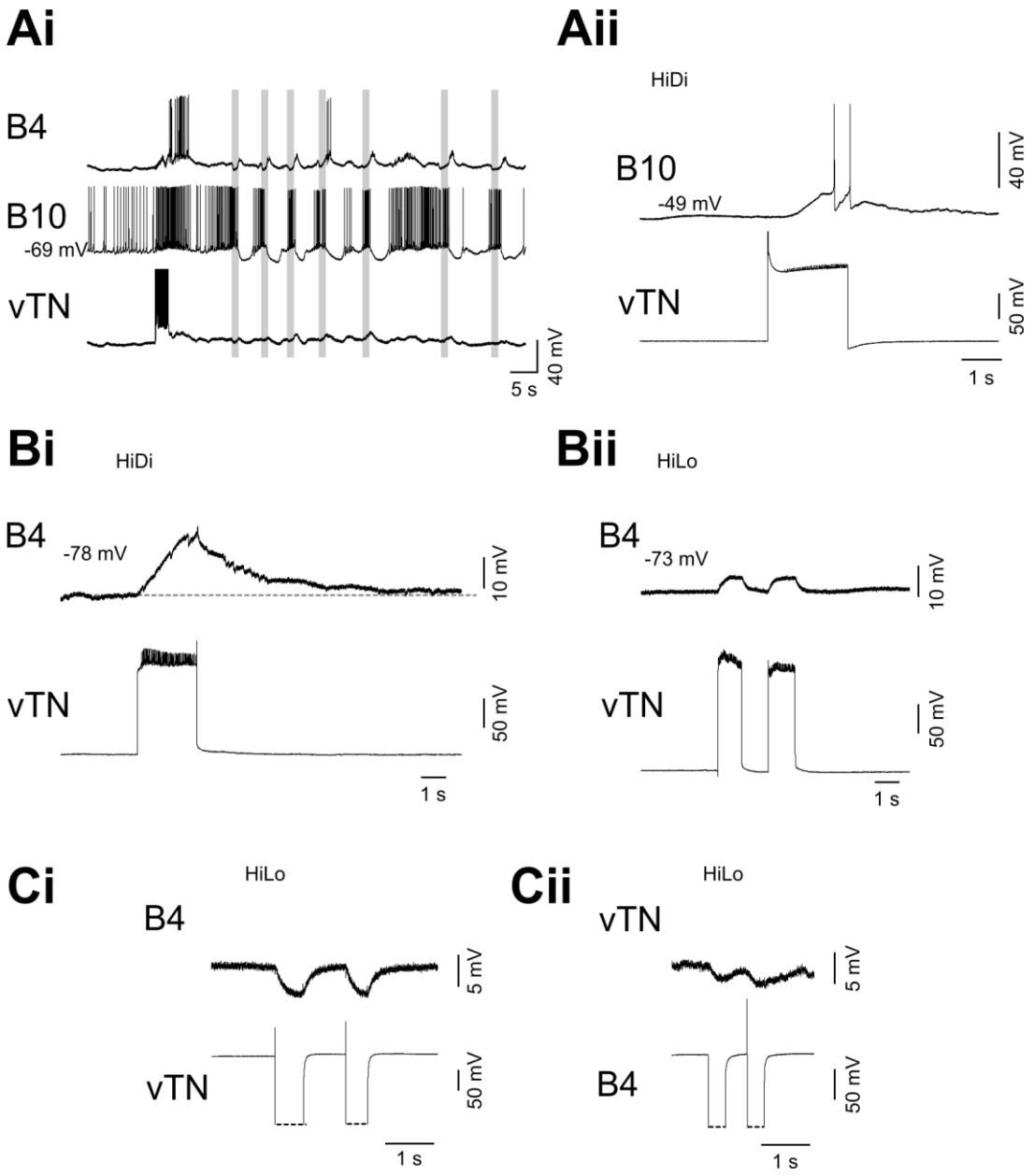

Figure 6.16 Connections from vTN to rasp phase motor neuron B10 and swallow phase motor neuron B4 **Ai.** vTN activation triggered eight fictive feeding cycles. B10 was depolarised and fired a burst of spikes during vTN activation. B10 then fired within the late protraction and in the rasp phase of each triggered cycle. **Aii.** In HiDi saline, vTN activation depolarised B10. This suggests that vTN has an excitatory connection with B10. **Bi.** vTN activation in HiDi saline depolarised B4. The depolarisation persisted after vTN activity had ceased. **Bii.** vTN activation in HiLo saline still depolarised B4, however the size and duration of the depolarisation was reduced. This suggests that part of the excitatory component seen in HiDi is due to an electrical synapse and a part due to an excitatory chemical connection. **Ci.** Injecting negative current into vTN causes a similar yet attenuated hyperpolarisation of B4 which persists in HiLo saline. **Cii.** Injecting negative current into B4 causes a similar yet attenuated hyperpolarisation of vTN which persists in HiLo saline. This suggests that the two are connected by an electrical synapse. In all examples the values above each trace are the membrane potential of the motor neuron prior to vTN activation. Dotted grey lines show the motor neuron's membrane potential prior to vTN activation.

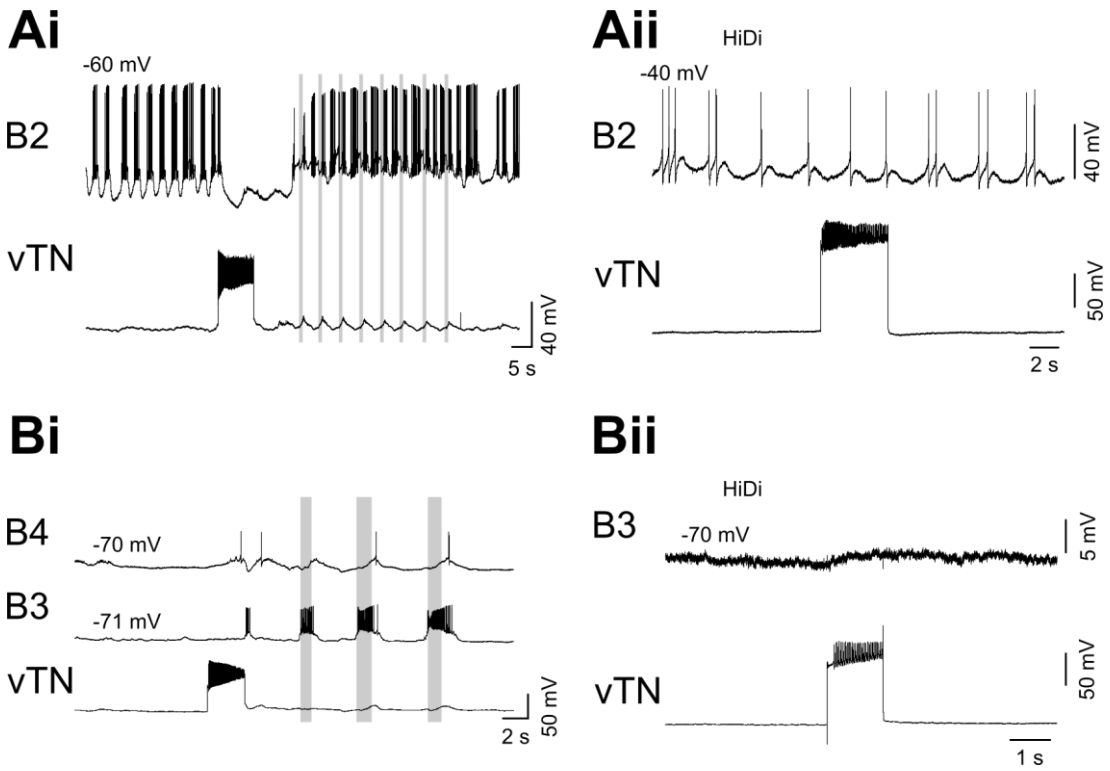

Figure 6.17 Connections from vTN to B2 and B3 motor neurons **Ai.** vTN activation triggered eight fictive feeding cycles. B2 fired in bursts prior to vTN activation. vTN activation strongly hyperpolarised B2. B2 fired in the protraction and swallow phase of the triggered cycles. **Aii.** In HiDi saline, vTN activation caused no change in B2's membrane potential or firing rate. **Bi.** vTN activation triggered three fictive feeding cycles. B3 fired a burst of spikes immediately after vTN activity had ceased and then fired in the rasp and early swallow phase of each triggered cycle. **Bii.** In HiDi saline, vTN activation caused no change in B3's membrane potential. In all examples the values above each trace are the membrane potential of the motor neuron prior to vTN activation.

bursts prior to vTN activation. vTN activation causes a strong hyperpolarization of B2 which prevents it from spiking for the duration that vTN is active. B2 remains hyperpolarised until the generation of the first cycle. B2 then fired a burst of spikes within the protraction and swallow phase of the triggered cycles. In HiDi saline, vTN activation did not cause any strong effect on B2 (**Figure 617Aii**) (n=5). The B3 motor neurons are a pair of large neurons in the buccal ganglia with no known function (Rose and Benjamin, 1979). **Figure 6.17Bi** shows an example of B3 activity in a triggered cycle. B3 fires a burst of spikes after vTN activation has ended, coinciding with the large inhibitory input to B4. B3 then fires a burst of spikes in the rasp and early swallow phase of the three triggered cycles. In HiDi saline, vTN activation caused no change in B3 membrane potential (n=15) (**Figure 6.17Bii**)

6.3 Discussion

6.3.1 vTN connections with feeding neurons

Results in this chapter demonstrate that vTN has diverse synaptic connections with all levels of the feeding network. Results in Section 3.2.3 and Sections 4.2.3 and 4.2.5 showed that vTN was connected to both sensory and CPG interneurons respectively. These connections accounted for vTN's activation by tactile stimulation of the radula (electrotonic synapse with RM) and vTN's ability to initiate the feeding network (biphasic connection with N1M). Section 4.2.2 provided evidence that N1M was the only protraction phase interneuron active in every vTN triggered cycle. It was also shown that vTN had a delayed excitatory connection with N1M which could account for N1M's activation in the first protraction phase (Section 4.2.3). vTN had no monosynaptic excitatory connection with any of the other protraction phase interneurons. Both SO and N1L showed little activity during vTN triggered cycles. Both neurons received monosynaptic inhibition from vTN. This could account for their lack of activation in the protraction phase of the first triggered cycle. CV1a, CV1b and BCI1 received no strong monosynaptic input from vTN. However all three neuron types had high levels of activation in triggered cycles (Section 4.2.2). The source of their activation therefore must arise via a polysynaptic connection. Indeed, in normal saline, all three neurons received strong inputs at the point of vTN activation which could not be accounted for by vTN activity. One possible source of input to CV1a and BCI1 was from N1M. As mentioned, N1M was active in all triggered cycles. N1M has an excitatory chemical connection with CV1a (McCrohan and Kyriakides, 1989) and an electrotonic connection with BCI1 (See Section 7.2.4.2), which could potentially

account for their activation. vTN excites N2v, N2d and the newly identified N2dv. This is often sufficient to elicit spiking in normal saline. Activation of the rasp/N2 network causes widespread inputs to feeding neurons (Elliott and Benjamin, 1985a, Brierley et al., 1997a, 1997b, 1997c). Therefore it is likely that some of the inputs seen on the protraction phase neurons and swallow phase neurons in normal saline arise from activity within the rasp/N2 network. vTN is electrotonically coupled with all three swallow phase interneurons, N3t, N3p and OC. There was evidence that vTN may have an additional excitatory chemical connection with both N3p and OC, which persists after vTN activity has ceased.

vTN also had synaptic connections with a number of feeding motor neurons. vTN excited B1 and had a biphasic (i/e) connection with B5 and B7. B10 received excitation from vTN. B4 was electrotonically coupled with vTN and received the same long lasting excitation that N3p and OC received from vTN. vTN therefore provided identical connections to neurons which are electrotonically coupled. SO and N1L are electrotonically coupled with each other and both receive inhibition from vTN. N1M is coupled with a type of B7 (Staras et al., 1998b) and a type of B5 (Elliott and Kemenes, 1992). All three neurons receive a biphasic (i/e) input from vTN activation. N2d, N2v and B10 are all electrotonically coupled (Staras et al., 1998b) and the newly identified N2dv is coupled to at least the N2v. vTN provides a similar excitatory input to all four neurons. N3p, OC and B4 are all electrotonically coupled (Staras et al., 1998b, Vehovszky and Elliott, 2001) and vTN has both an electrotonic connection and an excitatory chemical connection with all three neuron types.

Finally, vTN excites the modulatory interneuron CGC. vTN activation caused no noticeable change in CGC firing rate or membrane potential when CGC was at RMP. However when CGC was hyperpolarised, vTN activation caused a slow depolarization of CGC. The consequence of the depolarisation is not clear. Depolarising CGC increases its synaptic output (Kemenes et al., 2006); however at RMP vTN activation caused no noticeable depolarization. These results show that vTN is connected to all levels of the feeding network, and that the connections are in agreement with the relative recruitment and activation of neurons in triggered cycles.

Both fast and slow PSPs were present on followers of vTN. One possible explanation for this is that vTN releases different transmitters at different terminals – i.e. a classical neurotransmitter for fast PSPs and a neuropeptide for the slow PSPs. Another possibility is that vTN works on second-messenger pathways in some cases. A number of neurons in the feeding system of *Lymnaea* have been shown to use a classical

neurotransmitter and be immunopositive for a neuropeptide (SO uses ACh (Yeoman et al., 1993) and is immunopositive for myomodulin (Santama et al., 1994), B2 uses Ach and is immunopositive for myomodulin (Perry et al., 1998) and SCP (Perry et al., 1999), CGC is serotonergic (McCrohan and Audesirk, 1987, Yeoman et al., 1994b) and is immunopositive for myomodulin (Santama et al., 1994), N2v uses glutamate (Brierley et al., 1997b) and is immunopositive for myomodulin and SCP (Santama et al., 1994)). The transmitter used by vTN is not known. Numerous studies have been performed to identify the location of neurons immunoreactive for specific neurotransmitters. These maps show no neurons in the vicinity of vTN which are immunoreactive for dopamine (Elekes et al., 1991, Croll et al., 1999), glutamate (Hatakeyama et al., 2007), serotonin (Kemenes et al., 1989), GABA (Hatakeyama and Ito, 2000) or octopamine (Elekes et al., 1993). A cluster of SCP immunoreactive neurons are located on the ventral surface near the buccal commissure (Perry et al., 1999). RMs in both *Aplysia* (Miller et al., 1994) and *Helisoma* (Wentzell et al., 2009) are immunoreactive to SCPb. The RMs in *Lymnaea* appear to be homologous to those in *Aplysia* and *Helisoma*, suggesting they may be immunoreactive to SCPb. vTN is not homologous to the RM SCPb immunoreactive neurons in either *Aplysia* or *Helisoma*, however this does not discount the possibility that vTN is SCPb immunoreactive too.

6.3.2 Connections from feeding interneurons to vTN

During vTN triggered cycles and during command-like neuron driven cycles vTN receives feedback from the feeding network. In the protraction phase vTN receives inhibitory inputs. In the rasp phase, vTN receives both inhibitory and excitatory inputs. vTN reaches its largest depolarisation in the swallow phase. This is sometimes sufficient to elicit spiking in vTN. This suggests that vTN can be classified as a swallow phase interneuron. During the behavioural experiments in Section 3.2.1, close examination of the point at which the tactile probe comes into contact with the radula revealed that it was in the retraction phase. The most pressure was applied to the radula by the probe when the radula was being retracted into the mouth and came into apposition with either the dorsal mandible or the dorsal food channel. In the behaving animal, there is no clear distinction between the rasp and the swallow phases; therefore this was simply classified as the retraction phase. During an appetitive bite, vTN will be depolarised via synaptic inputs from the feeding network during the retraction phase (rasp/swallow phase). Therefore the activation of RM by the tactile stimulus will potentially result in a relatively large activation of vTN due to vTN being depolarised during the retraction phase.

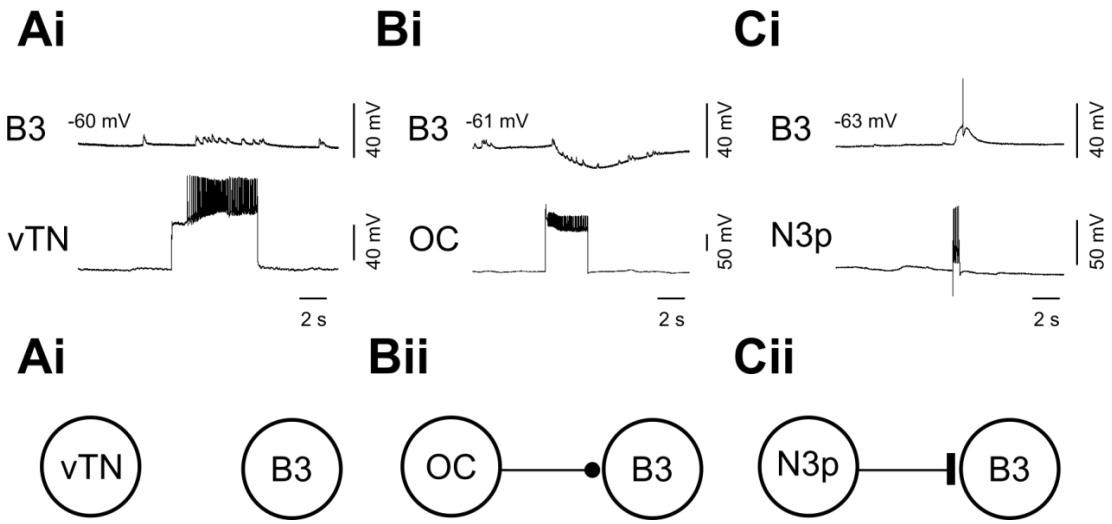

Figure 6.18 Different connection from three swallow phase interneurons to B3 motor neuron **Ai.** vTN activation causes no change in B3's membrane potential. EPSPs are present on B3 arising from N3t, which is excited by vTN activation. **Aii.** Circuit showing no connection from vTN to B3. **Bi.** OC activation hyperpolarises B3. **Bii.** Circuit showing inhibitory connection from OC to B3. **Ci.** N3p activation depolarises B3. **Cii.** Circuit showing excitatory connection from N3p to B3. In all examples the values above each trace are the membrane potential of B3 prior to activation of the swallow phase interneuron.

N1M, SO and N1L all inhibit vTN in the protraction phase. CV1a has an unreliable inhibitory input to vTN, whereas CV1b and BCI1 activation causes no change in vTN's membrane potential. Since N1M is active in all cycles, N1M inhibition to vTN can account for the protraction phase inhibition seen in vTN triggered cycles. Both the previously identified rasp phase interneurons, N2v and N2d, excite vTN. Neither was able to account for the inhibitory inputs seen on vTN in the rasp phase. The newly identified N2dv fires in the rasp phase and fires large action potentials similarly to N2d. N2dv spikes produce unitary 1:1 IPSPs on vTN. Therefore N2dv can account for a part of the inhibition of vTN in the rasp phase. However, N2dv somatic spiking is not necessary for vTN inhibition in the rasp phase, suggesting that further uncharacterised N2 interneurons exist.

vTN is electrotonically coupled with both N3p and OC, but unlike the excitatory connection from vTN to the two neuron types, N3p and OC provide chemical inhibitory inputs to vTN. The function of both N3p and OC and how they are activated in a feeding rhythm are unknown. Neither N3p nor OC is necessary for fictive feeding to occur and both are often silent or only weakly active in a rhythm (Vehovszky and Elliott, 2004). Both are electrotonically coupled and have mutually inhibitory connections with each other. One possibility is that each swallow phase interneuron is active within different variations of feeding, such as biting induced by a solid object versus a chemical food stimulus. Evidence for this comes from the fact that the three interneurons have varying connections with other feeding neurons. One example is the connections with B3. vTN has no connection with B3, whereas N3p strongly excites B3 (Rose and Benjamin, 1981b) and OC strongly inhibits B3 (Vehovszky and Elliott, 2001). **Figure 6.18A-C** show examples of the different connections of the three swallow phase interneurons with B3. The relative activation of each interneuron could reconfigure the network to produce a different motor output. For instance, OC activity within a rhythm has been shown to shorten both the swallow phase and the protraction phase and reduce B3 activity (Vehovszky and Elliott, 2001). One possibility is that vTN may serve the function of triggering feeding cycles due to the presence of an object based on its tactile properties whereas N3p and OC may serve to modulate the behaviour at a later stage. The OC may shorten cycle duration when food reaches the oesophagus, and switch vTN triggered bites into swallowing behaviours.

Reconfiguration of a network by modulatory neurons has been shown in the crustacean stomatogastric system (Meyrand et al., 1994) and the feeding system of *Aplysia* (Jing and Weiss, 2001, Morgan et al., 2002). In *Aplysia*, recruitment of specific buccal interneurons switches biting behaviours into swallowing behaviours (Jing et al., 2004,

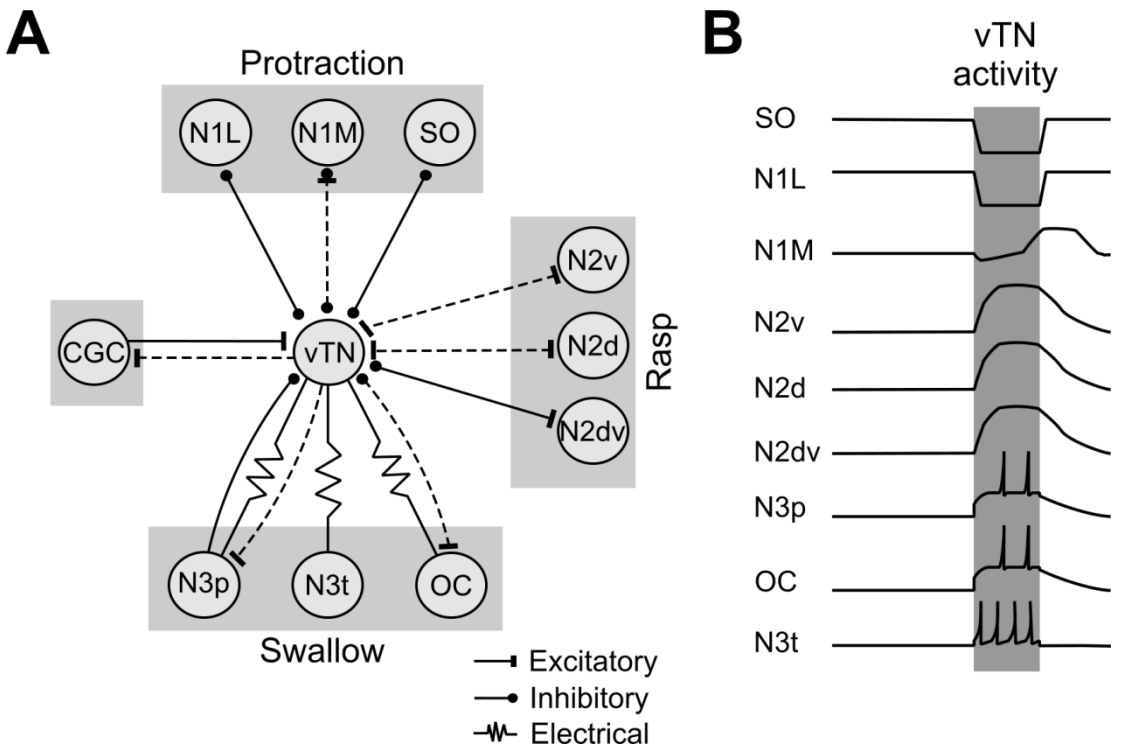

Figure 6.19 Synaptic connections between vTN and feeding network interneurons **A.** Summary circuit of synaptic connections identified in this Chapter between vTN and feeding network interneurons. Interneurons have been grouped into which phase they fire apart from the CGC. Black lines represent connections which persist in HiDi saline and there is evidence of unitary PSPs following presynaptic spikes. Dotted lines represent connections which persist in HiDi saline but where there is no evidence of unitary PSPs following presynaptic spikes. **B.** Summary cartoon showing response of buccal interneurons due to vTN activation.

Sasaki et al., 2013) and in *Helisoma* cycles of rasp/swallow phases have been observed in the absence of the protraction phase in vitro (Wentzell et al., 2009).

Finally, the CGCs, which provide extrinsic modulation to feeding network, monosynaptically excite vTN. This is similar to the connection from CGC to other swallow phase neurons (N3t, OC and B4 (McCrohan and Benjamin, 1980b, Yeoman et al., 1996, Vehovszky and Elliott, 2001). **Figure 6.19A** provides a summary of the synaptic connections between vTN and the feeding interneurons. **Figure 6.19B** is a cartoon of the inputs on feeding interneurons due to vTN activation.

In conclusion, vTN's synaptic connectivity with the protraction phase interneurons can partly account for the relative activation of each neuron type in triggered rhythms. The synaptic inputs to vTN in a fictive feeding cycle are inhibitory (N1M, SO and N1L) in the protraction phase, excitatory (N2v and N2d) and inhibitory (N2dv) in the rasp phase and a mix of excitatory electrotonic (N3t, N3p and OC) and inhibitory chemical (OC and N3P) in the swallow phase. Subsequently, vTN is depolarised in the late rasp/early swallow phase. Importantly this is the time point identified at which the most pressure is applied to the radula from a tactile stimulus. This would appear to increase the likelihood that vTN will reach threshold in response to spiking activity from RM, and thus trigger further feeding cycles.

7 Behavioural choice between ingestion and egestion

7.1 Introduction

In the previous chapters the neural mechanisms of a stimulus present and stimulus absent perceptual decision have been extensively characterised in *Lymnaea*. The aim of this chapter was to study decision making downstream from the stimulus present decision. Having identified the presence of a sensory stimulus, the animal must next make a judgement about whether the object giving rise to the stimulus is edible or not. Once the object has entered the buccal cavity the animal can perform one of two behaviours, ingest it if it is edible or egest it if it is inedible. These two behaviours are incompatible with each other and serve opposite purposes, therefore a choice must be made about which behaviour to elicit based on properties of the object. The neural mechanisms of behavioural choice have been studied extensively in invertebrate preparations with respect to how two stimuli can elicit competing behaviours (Kovac and Davis, 1980, Morton and Chiel, 1993a, Shaw and Kristan, 1997, Jing and Gillette, 2000, Shinkai et al., 2011). However of great interest is how the same stimulus can generate two different behaviours. This has been studied with respect to the behavioural state of the animal (Gillette et al., 2000, Hirayama and Gillette, 2012) and the context in which the stimulus is applied (Esch et al., 2002).

The ingestive behaviour and its underlying neural control are well characterised in *Lymnaea* (Carriker, 1946b, Rose and Benjamin, 1979, Rose and Benjamin, 1981b, Elliott and Benjamin, 1985a, Brierley et al., 1997c). The egestive behaviour has been observed in *Lymnaea* (Large et al., 2006) but has not been extensively studied and nothing is known about its neural control. This chapter aimed to further characterise the egestive behaviour and elucidate its underlying neural mechanisms.

7.2 Results

7.2.1 Behavioural choice in *Lymnaea*

7.2.1.1 Initiation of ingestion and egestion by a tactile stimulus

In order to study behavioural choice in *Lymnaea*, it was necessary to identify two incompatible behaviours and the stimuli which could initiate the switch between them. In the behavioural experiments in Section 3.2.1 the tactile probe was placed in the animal's mouth during an appetitive bite. The probe was then removed at the onset of

the subsequent bite program. An observation made during preliminary experiments was that if the probe was left in the animal's mouth then further bite programs were initiated. The early programs consisted of the standard ingestive buccal program as the animal tried to pull the probe further into the buccal cavity. During these cycles, the probe was maintained within the mouth so as that it could come into contact with feeding structures as the motor program was expressed, but could not be brought any further into the buccal cavity. After several ingestive bite programs a number of non-ingestive bite programs were generated (n=8) (data not shown). These were characterised by a reversal stroke of the odontophore. This often pushed the probe slightly out of the mouth, suggesting that the function of the reversal stroke was to egest the non-edible stimulus. This behaviour has previously been observed in *Lymnaea* (Large et al., 2006), but never studied in any detail. Interestingly, the preliminary experiments carried out with the tactile probe suggested that *Lymnaea* are able to make a judgement about the presence of a stimulus, and perform ingestive bite programs, and then make a subsequent judgement about the edibility of the stimulus based on the same tactile properties of the stimulus. Therefore the same stimulus can elicit two competing behaviours, ingestive behaviours which draw the stimulus into the mouth and egestive-like behaviours which push the stimulus out of the mouth. To study the neural mechanisms of these behaviours it was first necessary to further characterise the egestive-like behaviour.

7.2.1.2 Distinctions between ingestion and egestion in *Lymnaea*

To further characterise the egestive-like behaviour, a separate method was designed by which the ingestive and egestive-like behaviours could be reliably initiated and observed. The tactile stimulus protocol was not an ideal stimulus since it relied on the expression of an appetitive bite prior to the application of the tactile stimulus. Application of a sucrose solution to the lips was previously found to be a reliable stimulus for eliciting ingestive behaviours in *Lymnaea* (Kemenes et al., 1986, Kemenes et al., 2001, Kemenes et al., 2006). An emetic stimulus had not previously been described in *Lymnaea*; however aversive chemical stimuli have been identified. Previous work has shown that strong concentrations of amyl acetate (AA) can be used as an aversive stimulus in *Lymnaea* (Straub et al., 2006). It was therefore tested whether an aversive chemical stimulus could reliably initiate an egestive-like behaviour similar to those seen due to the maintained tactile stimulus. Sucrose was first applied to the lips to initiate ingestive bites (**Figure 7.1A**). Once an ingestive behaviour was in progress, 0.1% AA was applied to the lips (n=10) (**Figure 7.1B**). This caused a similar

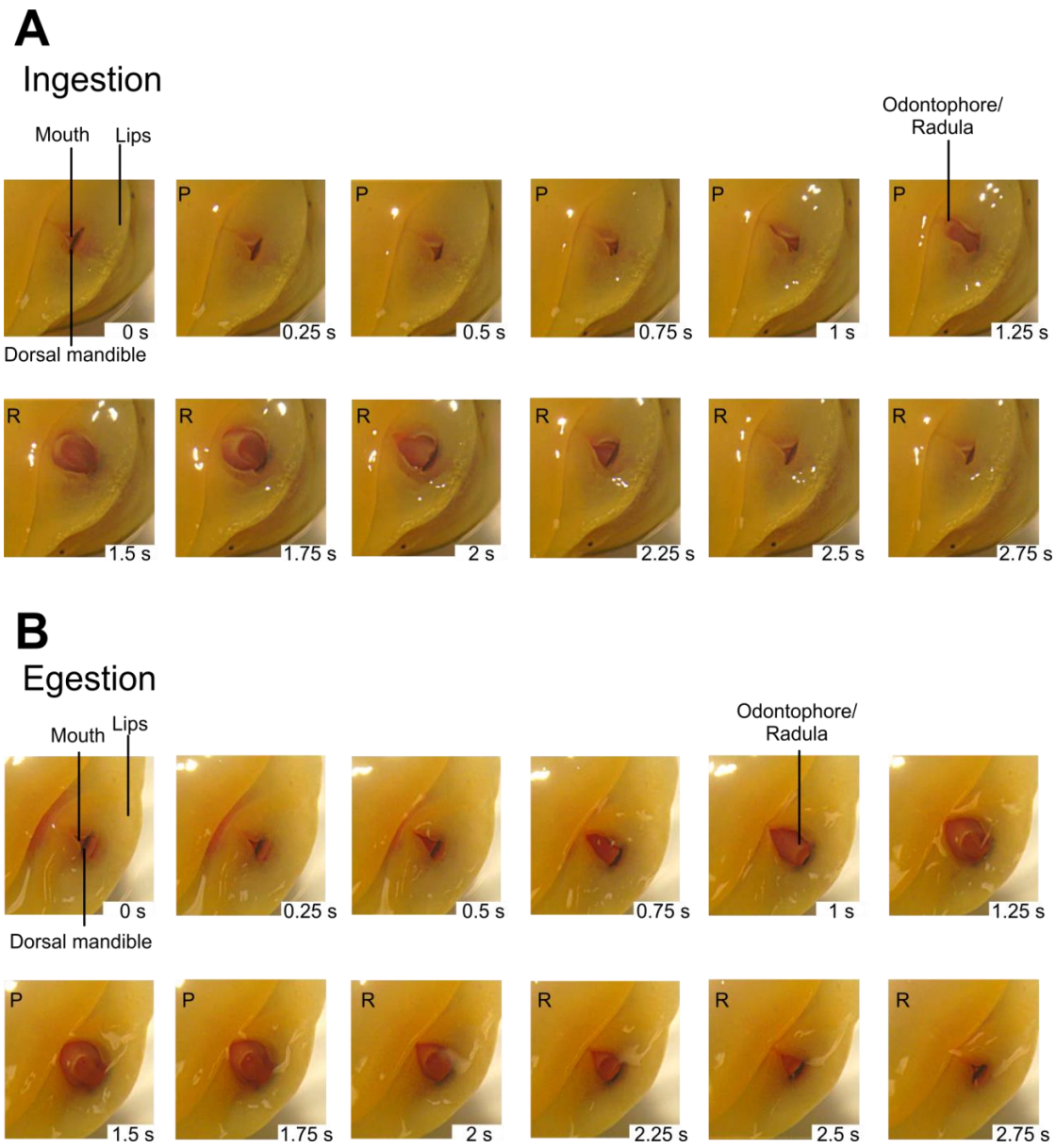

Figure 7.1 Still frames of ingestion and egestion **A.** Successive still frames of an ingestive behaviour elicited by the application of sucrose to the lips. The mouth is opened in the protraction phase and the odontophore/radula is positioned posteriorly in the mouth. During the retraction phase, the odontophore and radula is brought in a power stroke towards the dorsal mandible and retracted back into the mouth. The mouth is then closed. **B.** Successive still frames of an egestive behaviours elicited by the application of AA to the lips. The mouth is opened in the protraction phase as in ingestion. The odontophore/radula is positioned anteriorly in the mouth, against the dorsal mandible. The odontophore/radula is then further protracted out of the mouth and rotated towards the posterior region of the mouth away from the dorsal mandible. It is then retracted back into the mouth and the mouth closed. P - protraction, R - retraction

reversal stroke of the odontophore as the egestive-like behaviour seen due to the maintained tactile stimulus. This was a reliable response and was often accompanied by withdrawal away from the area of AA application. To test whether the behaviour observed was truly an egestive behaviour, in four animals solid lettuce was used to elicit ingestive behaviours instead of sucrose. The motor program expressed in the presence of solid lettuce resembled that seen due to the application of sucrose. The fact that the lettuce was moved into the mouth during each bite confirmed that this and the sucrose only generated motor programs were in fact ingestive. Application of AA whilst the animal was performing ingestive motor programs with the solid lettuce was reliable in eliciting the egestive-like behaviour. Importantly, the egestive-like behaviour resulted in the expulsion of lettuce from the buccal cavity, confirming that this was a true egestive motor program.

Both motor programs were observed in vivo and by using a semi-intact preparation (Buccal mass-CNS preparation). The two motor programs were initiated by using either sucrose (ingestion) or AA (egestion), as above, in order to identify features by which the two behaviours could be distinguished. Animals were filmed performing the two behaviours, and still frames were taken from the films every 0.25 s. **Figure 7.1A** shows a single episode of an ingestive behaviour and **Figure 7.1B** shows a single episode of an egestive behaviour. A schematic of the two behaviours is shown in **Figures 7.2A,B** to be referred to throughout this section. In the schematic a solid is shown moving into (ingestion **Figure 7.2A**) and out of (egestion **Figure 7.2B**) the buccal cavity. The ingestive motor program has been described in detail in Section 1.2.2 but will briefly be described again here. During the protraction phase the buccal mass was rotated ventrally. The odontophore within the buccal mass underwent further rotation so as that when the mouth was opened in the protraction phase the odontophore was located at the posterior opening of the mouth, at the opposite end of the mouth from the dorsal mandible (At 1.25 s in **Figure 7.1A** and **Figure 7.2Aii**). During the retraction phase, the odontophore was rotated dorso-anteriorly towards the dorsal mandible in the power stroke (At 1.75 s in **Figure 7.1A**). The odontophore was next retracted past the dorsal mandible (At 2 s in **Figure 7.1A**) and back into the buccal cavity against the dorsal food channel and the mouth closes (At 2.25 s in **Figure 7.1A** and **Figure 7.2Aiii,Aiv**). In egestive motor programs the mouth opened in the protraction phase. The odontophore was moved in a reverse stroke compared to the ingestive motor program. During protraction, the odontophore was positioned at the anterior region of the mouth, in apposition with the dorsal food channel as the mouth was opened (0.75-1 s in **Figure 7.1B** and **Figure 7.2Bii**). The odontophore was further protracted out of the

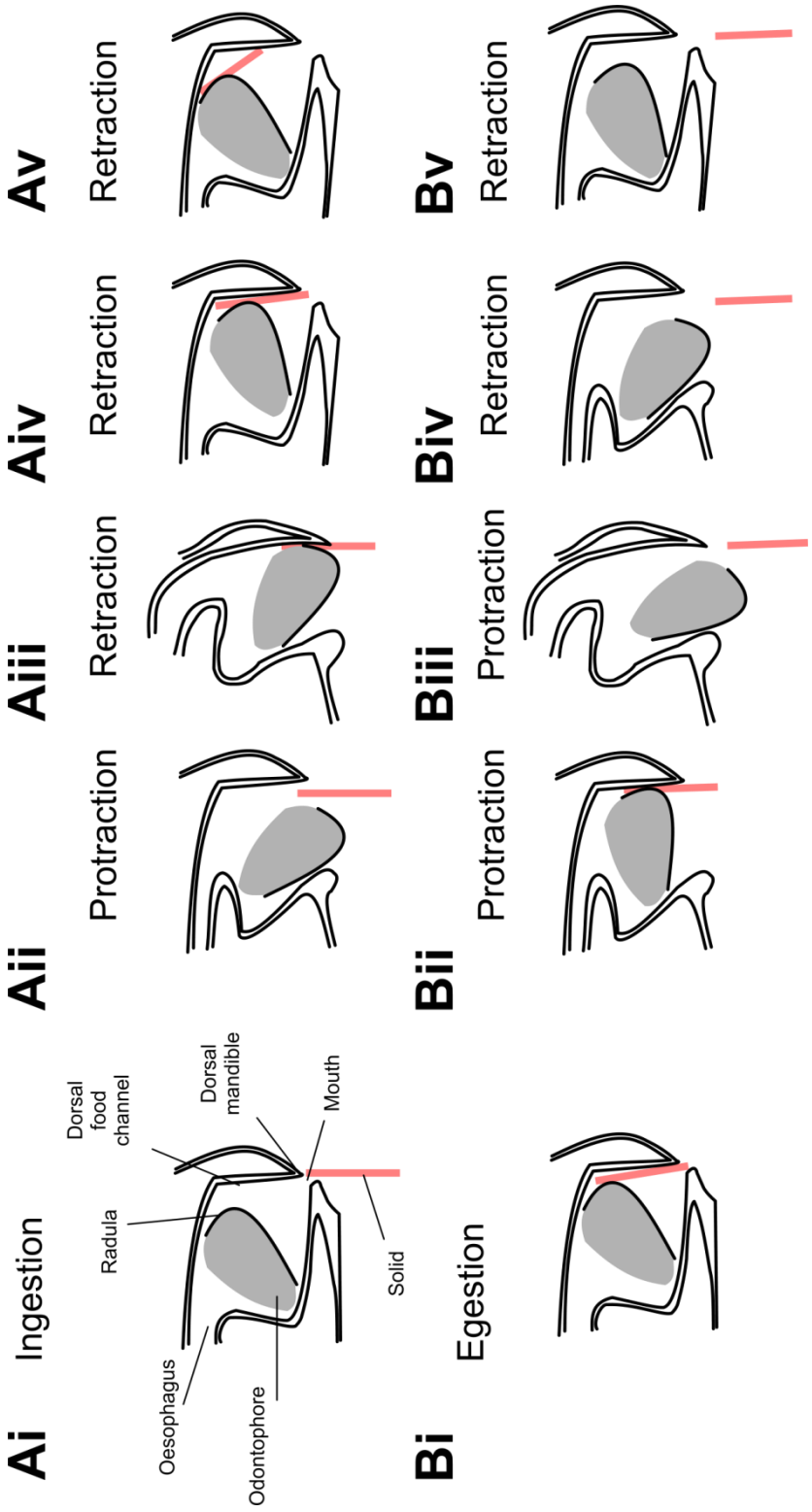
Ai
Ingestion
Dorsal food channel
Dorsal mandible
Mouth
Radula
Solid
Oesophagus
Odontophore
Aii
Protraction
Aiii
Retraction
Aiv
Retraction
Av
Retraction
Bi
Egestion
Bii
Protraction
Biii
Protraction
Biv
Retraction
Bv
Retraction

Figure 7.2 Schematic of ingestion and egestion behaviours **Ai.** At rest the odontophore is positioned in an almost dorsal/ventral position within the buccal cavity. **Aii.** During the protraction phase, the mouth is opened and the odontophore rotated to the posterior region of the mouth. **Aiii.** During retraction, the odontophore is brought towards the dorsal mandible in the power stroke. The solid in the schematic is shown coming into contact between the radula and the dorsal mandible in a bite motion. **Aiv.** The odontophore is retracted into the buccal cavity and the mouth begins to close. **Av.** The odontophore is further retracted into the buccal cavity, towards the oesophagus. The odontophore/radula is drawn against the dorsal food channel. **Bi.** Egestive motor programs were not observed occurring spontaneously, but only in the presence of a sensory stimulus, therefore, in the schematic a solid is shown in the buccal cavity at rest. **Bii.** During protraction the mouth is opened. The odontophore is positioned in the anterior region of the mouth, and drawn against the dorsal food channel and dorsal mandible. This serves to push the solid towards the mouth opening. **Biii.** The odontophore is further protracted towards the posterior region of the mouth and the solid is pushed out of the buccal cavity. **Biv.** The odontophore is retracted back into the mouth. **Bv.** The odontophore is returned to its resting position as the mouth closes.

mouth and moved ventro-posteriorly away from the dorsal mandible (1.25 s in **Figure 7.1B** and **Figure 7.2Biii**). The odontophore was then retracted back into the mouth (2 s in **Figure 1B** and **Figure 7.2Biv**). The power stroke seen in the retraction phase of ingestive motor programs was absent in egestive motor programs, instead the odontophore appeared to be rotated back into the mouth. The mouth was then closed as the odontophore was retracted.

There were several similarities and differences between the two behaviours. During both behaviours, the odontophore was protracted and retracted out of and subsequently into the mouth. Similarly the mouth was opened and closed in the protraction and retraction phases respectively in both behaviours. This suggests that the phase of certain buccal mass and mouth movements remained the same in both behaviours. The position of the odontophore in the early protraction phase provided a clear distinction between the two behaviours. In ingestion the odontophore was rotated to the posterior region of the mouth during the protraction phase (**Figure 7.2Aii**). In egestion the odontophore was at an anterior region of the mouth, next to the dorsal mandible during the early protraction phase (**Figure 7.2Bii**). The odontophore was further protracted from the mouth, moving from the dorsal mandible to the posterior region of the mouth. In the retraction phase of ingestion the odontophore was pulled towards the dorsal mandible in a power stroke. In egestion, the odontophore appeared to be retracted back into the mouth and the power stroke was absent. Several distinguishing features were most evident in the semi-intact preparation. During the ingestive behaviour, the odontophore's lateral edges were brought close together in the power stroke of the retraction phase (2-3 s in **Figure 7.3A**). During the protraction phase, the lateral edges were spread apart (1 s in **Figure 7.3A**). In egestion, the lateral edges of the odontophore were already close together in the early protraction phase (1-2 s in **Figure 7.3B**). As the odontophore was retracted, the lateral edges of the odontophore spread apart (3 s in **Figure 7.3B**). The odontophore was contracted dorsally in both behaviours. In ingestive motor programs, the odontophore contracted dorsally in the retraction phase (2-3 s in **Figure 7.3A**) whereas in egestive motor programs the odontophore contracted dorsally in the protraction phase (1-2 s in **Figure 7.3B**) This presumably contributed to the positioning of the odontophore during the two behaviours. The reversal stroke of the odontophore appeared to serve the purpose of pushing particles out of the mouth, in contrast to the standard ingestive motion which was used to pull particles into the mouth. Therefore the major phase of contraction of the odontophore and of its lateral edges provided a feature by which the two behaviours could be distinguished.

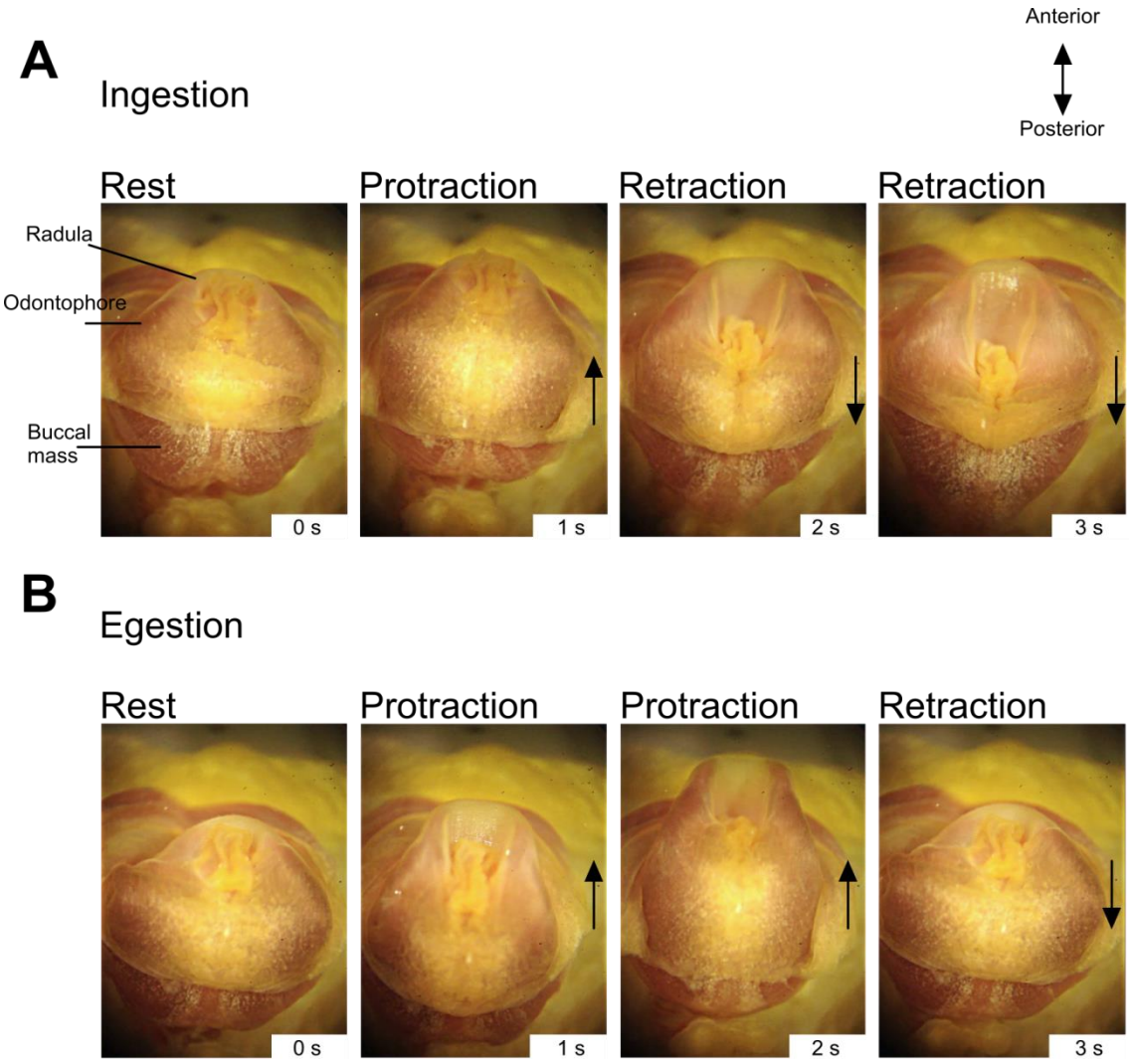

Figure 7.3 Successive still frames of odontophore movements in ingestion and egestion **A.** During protraction the odontophore is rotated anteriorly and ventrally and the lateral edges are spread apart. During retraction, the odontophore is rotated posteriorly and dorsally and the lateral edges are brought closer together. The odontophore also contracts dorsally during retraction. **B.** During protraction the odontophore is rotated anteriorly and ventrally. The odontophore is contracted dorsally and the lateral edges are brought close together. During retraction, the odontophore is rotated posteriorly and the lateral edges spread further apart. The black arrows show the direction of movement of the odontophore anteriorly or posteriorly.

7.2.2 Identification of an SLRT motor neuron

To further characterise the two behaviours, motor neurons involved in odontophore contraction were identified. Contraction of the odontophore and stretching of the radula over the odontophore are due in part to contraction of the paired supralateral radula tensor (SLRT) muscles (Carriker, 1946a, 1946b, Goldschmeding and De Vlieger, 1975, Rose and Benjamin, 1979, Smith, 1988). A novel pair of SLRT motor neurons was identified in the buccal ganglia. The pair of motor neurons, termed B11 to follow the conventional nomenclature for *Lymnaea* (Benjamin and Rose, 1979), was located on the ventral surface of the buccal ganglia, one per ganglion. **Figure 7.4A** shows the location of a B11 in the right buccal ganglion. Dye filling B11 (n=3) revealed that it had a single projection which exited the buccal ganglia via the VBN (**Figure 7.4B**). The VBN is known to innervate the SLRT muscle (Carriker, 1946a, Goldschmeding and De Vlieger, 1975, Wentzell et al., 2009). An SLRT-CNS preparation was developed (see Section 2.2.1.3) which permitted the recording of B11 whilst observing and/or recording the SLRT muscle via a suction electrode. Stimulating B11 caused the ipsilateral side of the odontophore to contract dorsally. This was similar to the movements seen in the Buccal-mass-CNS preparation in the retraction phase of ingestion and the protraction phase of egestion. Extracellular spikes were recorded on the SLRT muscle which followed B11 spikes in a 1:1 manner (n=3) (**Figure 7.4C**) providing strong confirmatory evidence that B11 was an SLRT motor neuron. A second novel putative motor neuron was identified next to B11 which was termed B12. Similar to B11, one B12 neuron was present in each buccal ganglion (**Figure 7.4A**) with a single projection out of the VBN (**Figure 7.4D**). However, stimulating B12 caused no response on the SLRT. Having identified B11 as an SLRT motor neuron, B11's firing activity in both ingestive and egestive motor programs was next examined using a Whole-lip semi-intact preparation.

7.2.3 In vitro distinctions between ingestion and egestion

Similar to the behavioural experiments in Section 7.2.1.2 sucrose application to the lips was used to elicit ingestive motor programs. 0.1% AA was used to elicit egestive motor programs during a sucrose driven fictive feeding rhythm. First it was determined how B11 fired during ingestive motor programs. **Figure 7.5Ai** shows an example of B11 recorded with an N2v interneuron and a B9 motor neuron. Application of sucrose caused rhythmic activity in all three neurons. B11 was active in the late protraction phase and throughout the rasp phase. **Figure 7.5Aii** shows an expanded time scale of the third motor program. B11 was active predominantly in the rasp phase, as seen by

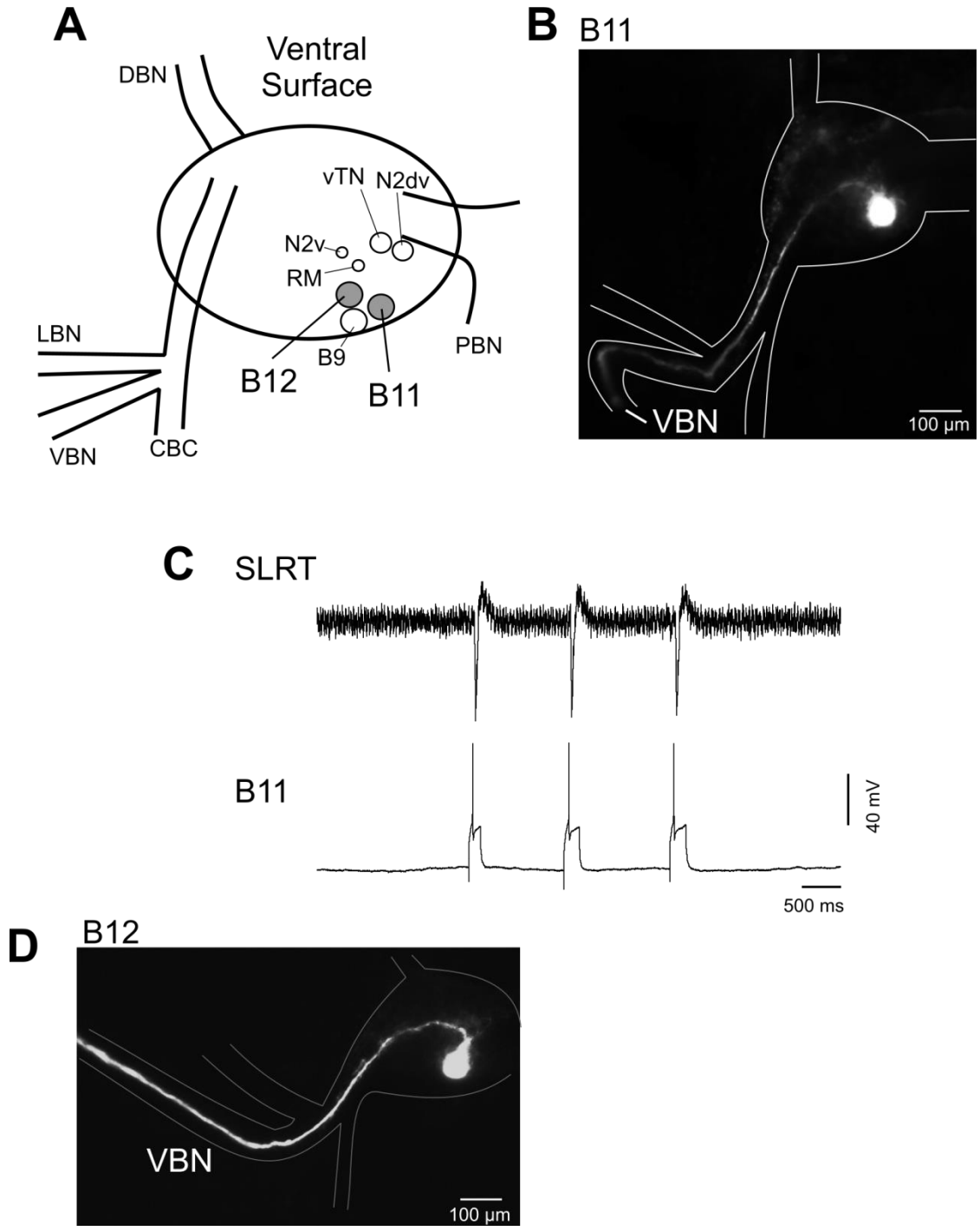

Figure 7.4 Identification and characterisation B11 and B12 **A.** B11 and B12 were located on the ventral surface of the buccal ganglia. There was one of each motor neuron per ganglion. B11 and B12 are marked grey in the schematic and shown in the right buccal ganglion only. **B.** B11 had a single projection which left the buccal ganglia via the ipsilateral VBN. **C.** Three positive current pulses were injected into a B11, eliciting a single spike per pulse. Extracellular spikes were recorded via a suction electrode on the SLRT muscle following the B11 spikes 1:1. **D.** B12 had a single process which left the buccal ganglia via the ipsilateral VBN.

its synchronous activity with the N2v interneuron. The frequency of B11 activity in the protraction and rasp phases was plotted for each cycle (**Figure 7.5B**), showing that B11 was indeed active predominantly in the rasp phase of the sucrose driven cycles. In vivo, the odontophore's major phase of contraction was during the retraction phase of sucrose driven rhythms, therefore activity of B11 (and subsequent contraction of the SLRT muscle) in the rasp phase is in agreement with these observations. Similar experiments were performed using a B12 motor neuron. **Figure 7.5Ci** shows an example of B12 activity in a sucrose driven rhythm. B12 was active in the rasp phase at the same time as N2dv depolarisation (**Figure 7.5Cii**). The frequency of B12 activity in the protraction and rasp phases was plotted per cycle similarly to B11 above. B12 activity occurred predominantly in the rasp phase similarly to B11.

B11 and B12 activity in egestive motor programs was next tested. Sucrose was applied to the lips until the onset of a fictive feeding rhythm. Once the rhythm had started, sucrose application was stopped and AA was applied to the lips. **Figure 7.6Ai** shows an example of B11, B12 and an N2dv's response to sucrose and AA. **Figure 7.6Aii** shows a faster timescale of a fictive feeding cycle in sucrose only. B11 was active in both the protraction and rasp phases, whereas B12 was active in the rasp phase only. N2dv was also active in the rasp phase only. **Figure 7.6Aiii** shows a faster timescale of a fictive feeding cycle in AA. B11 was active throughout the protraction phase and fired a single spike only in the rasp phase. Similarly B11 was active in the protraction phase only. N2dv activity remained in the rasp phase only. **Figure 7.6Bi** shows a plot of B11 activity. During the first four cycles, B11 activity occurred predominantly in the rasp phase. In the fifth to seventh cycles, B11 activity progressively occurred in the protraction phase rather than the rasp phase, culminating in the seventh cycle where B11 was only active in the protraction phase. In the eighth and ninth cycles B11 activity returned to occurring predominantly in the rasp phase. B12 activity was similar to that seen in B11 (**Figure 7.6Bii**). B12 activity occurred predominantly in the rasp phase of the first four cycles. In the fifth to seventh cycles, B11 activity occurred at increasing rates in the protraction phase only. B12 activity returned to occurring in the rasp phase only in the eighth and ninth cycles. B11 and B12's response to sucrose only was also tested in this preparation. It was apparent that both were active predominantly in the rasp phase. **Figures 7.6Ci** and **7.6Cii** show the plots of the sucrose only rhythm. These results suggest that in ingestive motor programs, B11 and B12 activity occurs mainly in the rasp phase. Therefore SLRT contraction due to B11 activity occurs predominantly in the rasp phase in ingestion. In egestive cycles, B11 and B12 activity shifts phase from the rasp phase to the protraction phase. Therefore SLRT contraction

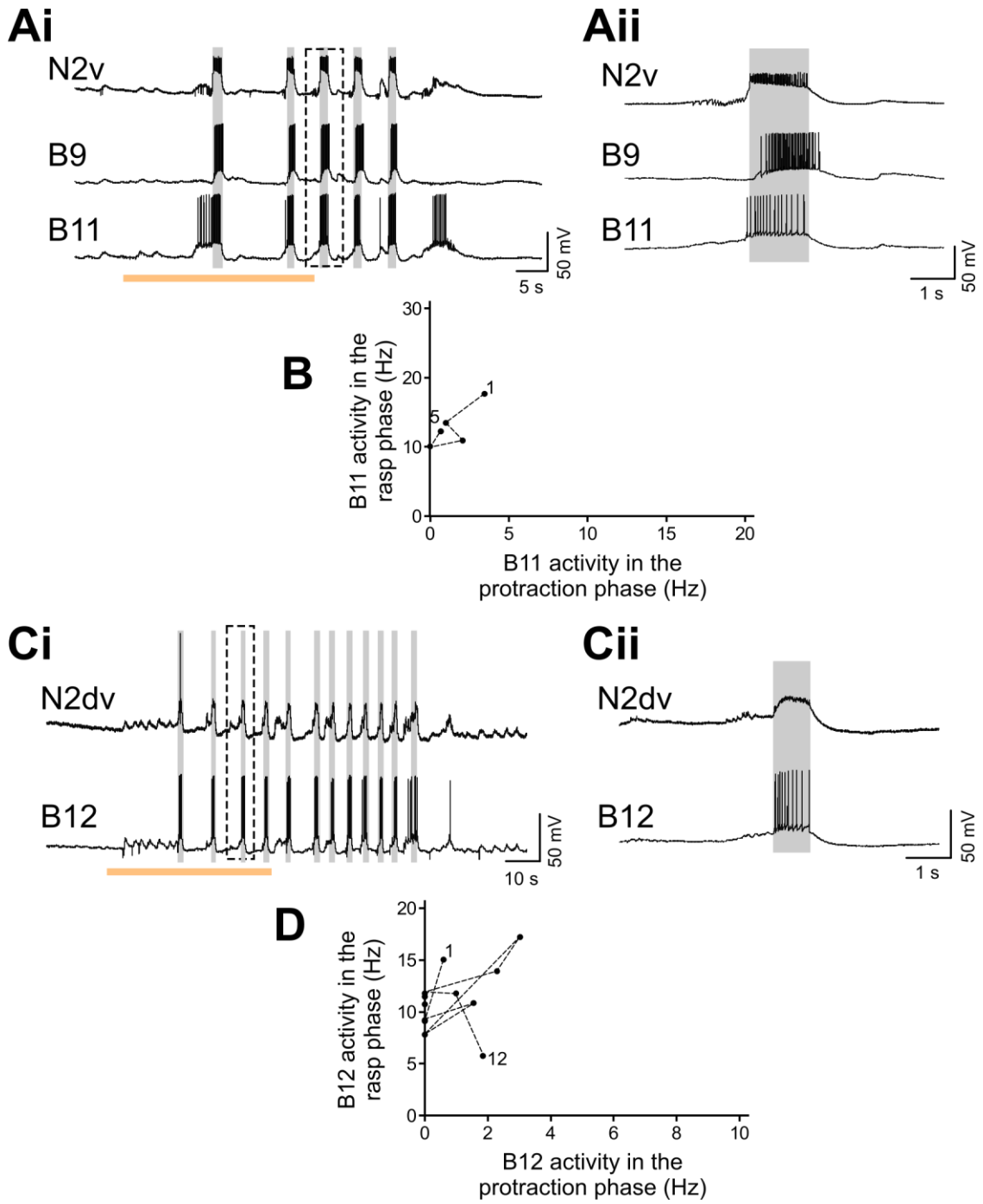

Figure 7.5 B11 and B12 activity in ingestive motor programs **Ai.** A B11 was recorded with a B9 and an N2v in a whole lip-CNS preparation. The orange bar under the trace represents the application of sucrose to the lips. This initiated five fictive feeding cycles as seen by the rhythmic activity in all three neurons. **Aii.** Faster timebase of the third cycle in Ai. B11 is active in the late protraction phase and throughout the rasp phase. N2v fires only in the rasp phase and B9 fires in the rasp and early swallow phases. **B.** B11's activity in the protraction and rasp phase was plotted for each of the five cycles. B11 was predominantly active in the rasp phase of all cycles. **Ci.** A B12 was recorded with an N2dv in a whole lip-CNS preparation. Application of sucrose to the lips initiated twelve fictive feeding cycles. **Cii.** Faster timebase of the third cycle in Bi. B12 is active in the rasp phase only. N2dv is depolarised in the rasp phase but not active in this cycle. **D.** B12's activity in the protraction and rasp phase was plotted for each of the twelve cycles. B12 was predominantly active in the rasp phase of all cycles. The numbers next to the points in B. and D. represent the cycle number. The dashed lines between points represent the order in which the cycles occurred. Grey vertical lines represent the rasp phase of a cycle.

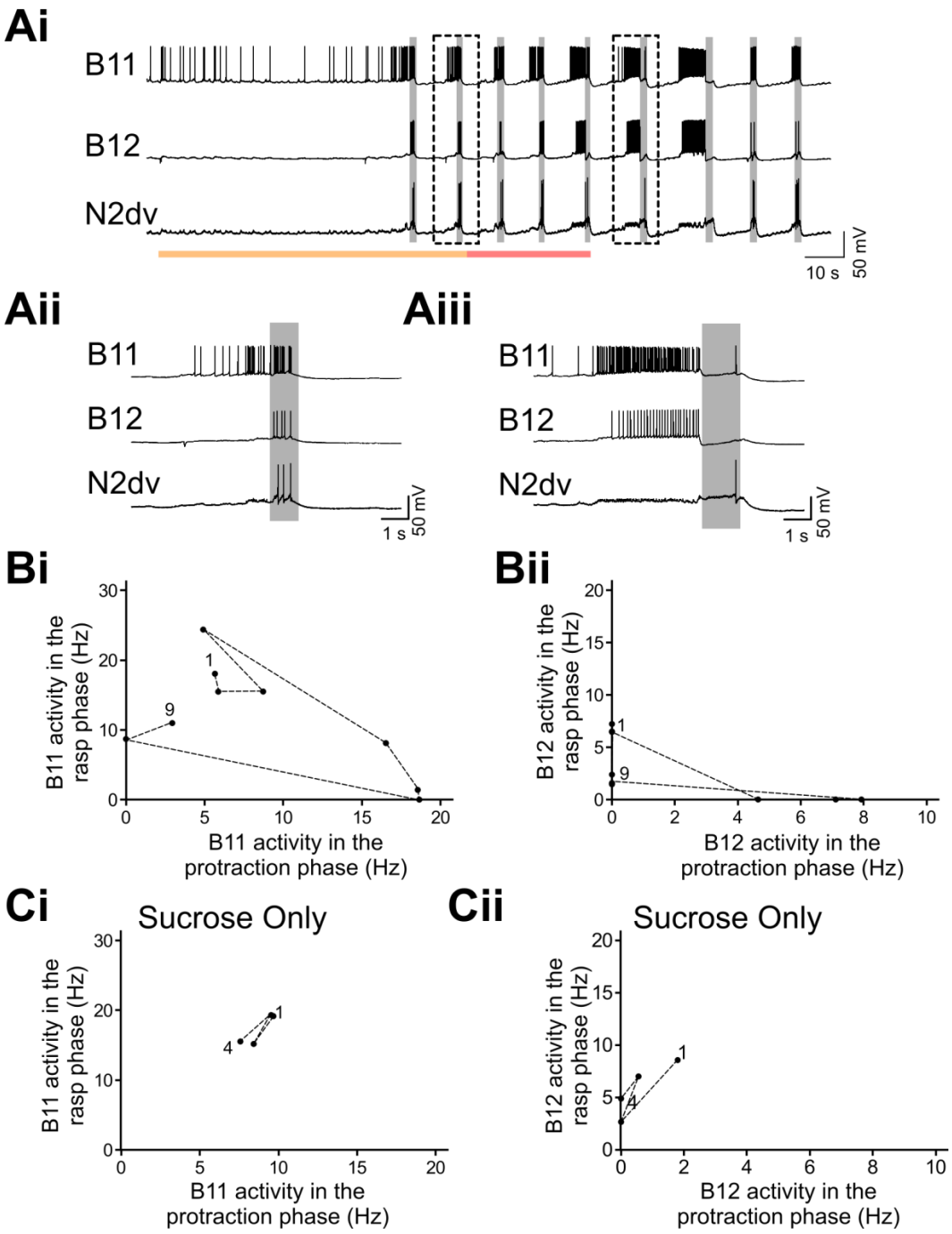

Figure 7.6 B11 and B12 activity in ingestive and egestive motor programs **Ai.** A B11 and a B12 were recorded with two N2dvs in a whole lip-CNS preparation. The orange bar under the trace represents the application of sucrose to the lips. This initiated fictive feeding cycles as seen by the rhythmic activity in all four neurons. AA was then applied to the lips, represented by the red bar under the trace, and sucrose was turned off. **Aii.** Faster timebase of the second cycle in Ai. This cycle is in the presence of sucrose. B11 is active in the protraction and rasp phase, whereas B12 is active in the rasp phase only. N2dv is active in the rasp phase only. **Aiii.** Faster timebase of the sixth cycle in Ai. This cycle is in the presence of AA. B11 and B12 are active throughout the protraction phase. B11 fires a single spike at the end of the rasp phase, whereas B12 is not active in the rasp phase. N2dv is active in the rasp phase only. **Bi.** B11's activity in the protraction and rasp phase was plotted for each of the nine cycles. **Bii.** B12's activity in the protraction and rasp phase was plotted for each of the nice cycles. **Ci.** In the same preparation, only sucrose was applied to the lips to determine the normal sucrose response. B11's activity in the protraction and rasp phase in response to sucrose only was plotted. **Cii.** B12's activity in the protraction and rasp phase of sucrose only was plotted. The numbers next to the points in Bi, Bii, Ci, and Cii. represent the cycle number. The dashed lines between points represent the order in which the cycles occurred. Grey vertical lines represent the rasp phase of a cycle.

due to B11 activity occurs predominantly in the protraction phase. This is in agreement with odontophore contraction seen in vivo from AA application, where the odontophore contraction occurs in the protraction phase. Thus B11 activity in ingestion and egestion switches from the rasp phase to the protraction phase respectively, altering the phase of SLRT innervation and contributing to switching between behaviours.

The phase switch seen in B11 and B12 activity from ingestion to egestion was not present on all neurons. This can be seen in **Figure 7.6Ai**. The N2dv interneuron was active in the rasp phase of both sucrose and AA cycles. Further evidence for this is shown in **Figure 7.7Ai**. A B11 was recorded with an N2dv and a B9 motor neuron. In sucrose B11 was active predominantly in the rasp phase, as were N2dv and B9 (**Figure 7.7Aii**). Application of AA caused B11 activity to switch from the rasp phase to the protraction phase, whereas both N2dv and B9 activity remained in the rasp phase (**Figure 7.7Aiii**). **Figure 7.7B** shows a plot of B11 activity in the cycles of **Figure 7.7Ai**. Therefore, not all feeding neurons phase of activity changed between ingestion and egestion. The lack of phase switching of all neurons is in agreement with the observations in vivo that the protraction and retraction of the buccal mass and of the odontophore into and out of the mouth both occur in the same order in ingestion and egestion.

B11 activity in the protraction and rasp phase of all preparations was plotted together in **Figure 7.8A**. B11's response to sucrose and then AA was tested in four preparations. 24 cycles were recorded on B11 in the presence of sucrose only and 31 cycles in the presence of AA. B11 showed significantly less activity in the protraction phase of sucrose cycles (3.9 ±0.7 Hz) than AA cycles (9.2 ±1 Hz) (unpaired t-test df =53, t = 4.2, < 0.0001). B11 showed a significantly higher level of activity in the rasp phase of sucrose cycles (15.3 ±1.1 Hz) than AA cycles (8.6 ±1.8 Hz) (unpaired t-test df =53, t = 3.0, P < 0.01). B11 activity in sucrose and AA was plotted using the cloudplot function in MatLab, which represents the dataset as a surface plot with colour-coding for signal density. In sucrose, B11 activity was of greatest intensity in the rasp phase of sucrose cycles (**Figure 7.8Ci**) and in the protraction phase of AA cycles (**Figure 7.8Cii**), confirming that B11 activity switched from firing predominantly in the rasp phase to the protraction phase in the switch from ingestion to egestion respectively.

B12's response in sucrose only was tested in 5 preparations. B12's response to sucrose and then AA was tested in 3 preparations. 53 cycles were recorded on B12 in the presence of sucrose and 14 cycles in the presence of AA. B12 showed significantly

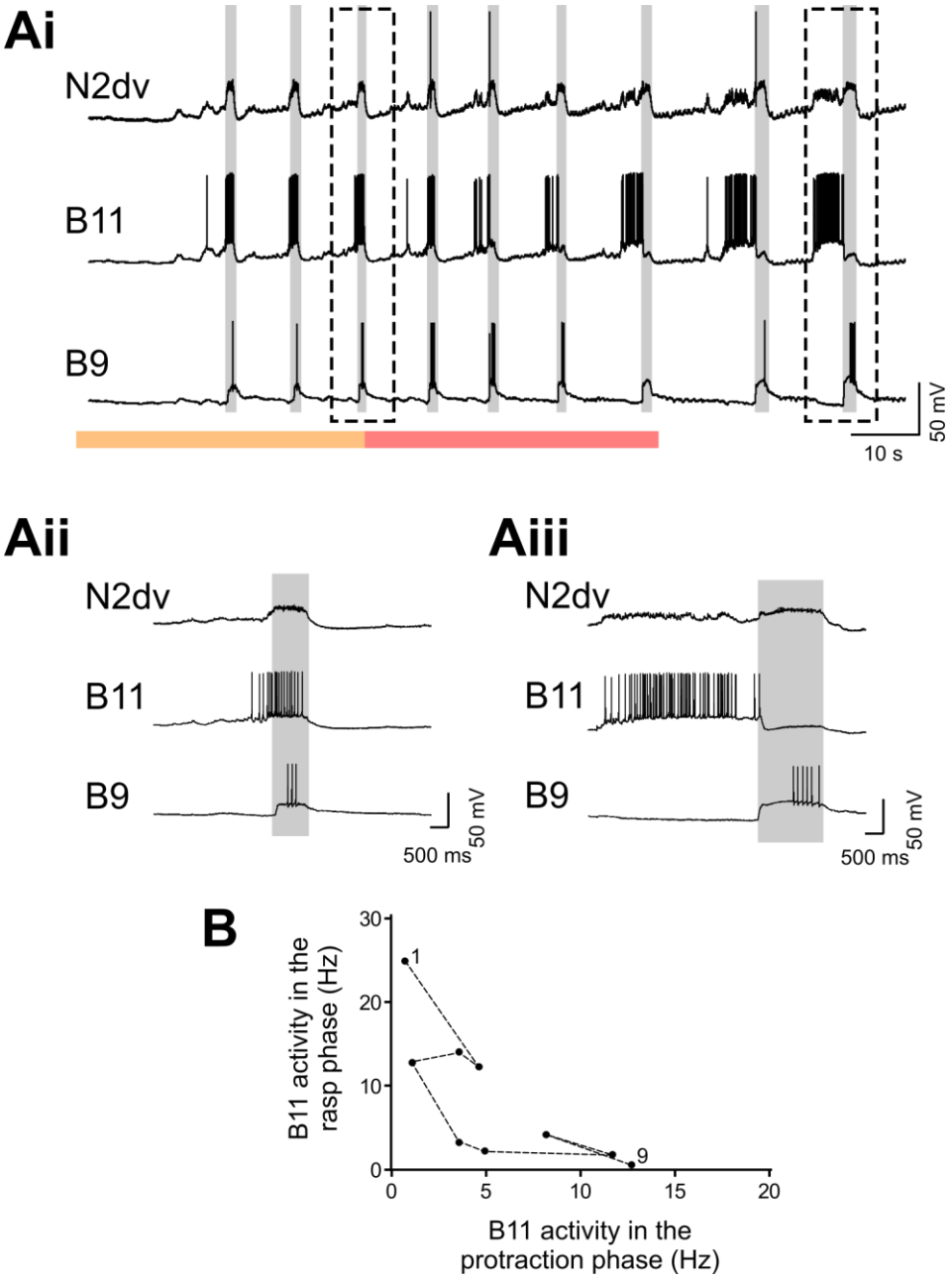

Figure 7.7 B11 and B9 activity in ingestive and egestive motor programs **Ai.** A B11 and a B9 were recorded with an N2dv in a whole lip-CNS preparation. The orange bar under the trace represents the application of sucrose to the lips. This initiated fictive feeding cycles as seen by the rhythmic activity in all four neurons. AA was then applied to the lips, represented by the red bar under the trace, and sucrose was turned off. **Aii.** Faster timebase of the third cycle in Ai. This cycle is in the presence of sucrose. B11 is active in the late protraction phase and throughout the rasp phase. B9 is active in the rasp phase. **Aiii.** Faster timebase of the ninth cycle in Ai. This cycle is after the application of AA. B11 is active throughout the protraction phase but not the rasp phase. B9 activity remains in the rasp phase only. **B.** B11's activity in the protraction and rasp phase was plotted for each of the nine cycles. The numbers next to the points in B represent the cycle number. The dashed lines between points represent the order in which the cycles occurred. Grey vertical lines represent the rasp phase of a cycle.

less activity in the protraction phase of sucrose cycles (1.2 ±0.2 Hz) than AA cycles (5 ±1.4 Hz) (unpaired t-test df = 65, t = 4.6 P < 0.0001). B12 showed a significantly higher level of activity in the rasp phase of sucrose cycles (11.4 ±1 Hz) than AA cycles (3.4 ±0.8 Hz) (unpaired t-test df = 65, t = 4.2 P < 0.0001). B12 activity in sucrose and AA was plotted using a cloudplot in MatLab. In sucrose, B12 activity was of greatest intensity in the rasp phase of sucrose cycles (**Figure 7.9Ci**). In AA cycles, B12 activity appeared to cluster at a similar point as in sucrose; however there was evidence of a second cluster forming in the protraction phase of AA cycles (**Figure 7.9Cii**). The lack of a strong cluster in the protraction phase was likely due to the low number of cycles recorded in AA combined with the fact that some of the cycles in AA are presumably still sucrose driven cycles, since the phase switch of B11 and B12 had a much slower onset in vitro than in vivo.

To ensure that the 0.1% AA had no direct effect on the CNS, 0.1% AA was applied to the lips similarly to the experiments above. However in this preparation the MLN, SLN and TN were cut to prevent any sensory inputs from the lips to the CNS. The inflow of normal saline to the CNS, and the two outflow tubes on either side of the lips however were kept the same. In these preparations, application of 0.1% AA caused no noticeable change in activity in buccal ganglia neurons (data not shown) confirming that the switch in B11 and B12 firing was not due to a direct effect of AA on the CNS but rather due to AA initiating egestive motor programs..

7.2.4 Interneuronal control of ingestive and egestive motor programs

7.2.4.1 Ingestion protraction phase interneurons

Having identified a method to distinguish between ingestive and egestive motor programs, the interneuronal control of the two behaviours was examined. Several command-like interneurons have been identified in *Lymnaea* with the ability to initiate fictive feeding cycles (McCrohan, 1984a, Elliott and Benjamin, 1985b, Yeoman et al., 1995, McCrohan and Croll, 1997). It was therefore tested whether these interneurons were involved in ingestive or egestive behaviours.

To identify the neural control of ingestive and egestive behaviours, each candidate interneuron was recorded with either a B11 or B12 motor neuron. The interneuron being tested was then stimulated to drive a cycle and the motor neuron's activity in the protraction and rasp phase plotted as in **Figures 7.8A** and **7.9A**. The data from each interneuron was plotted on the same graph as the results from the in vitro preparations

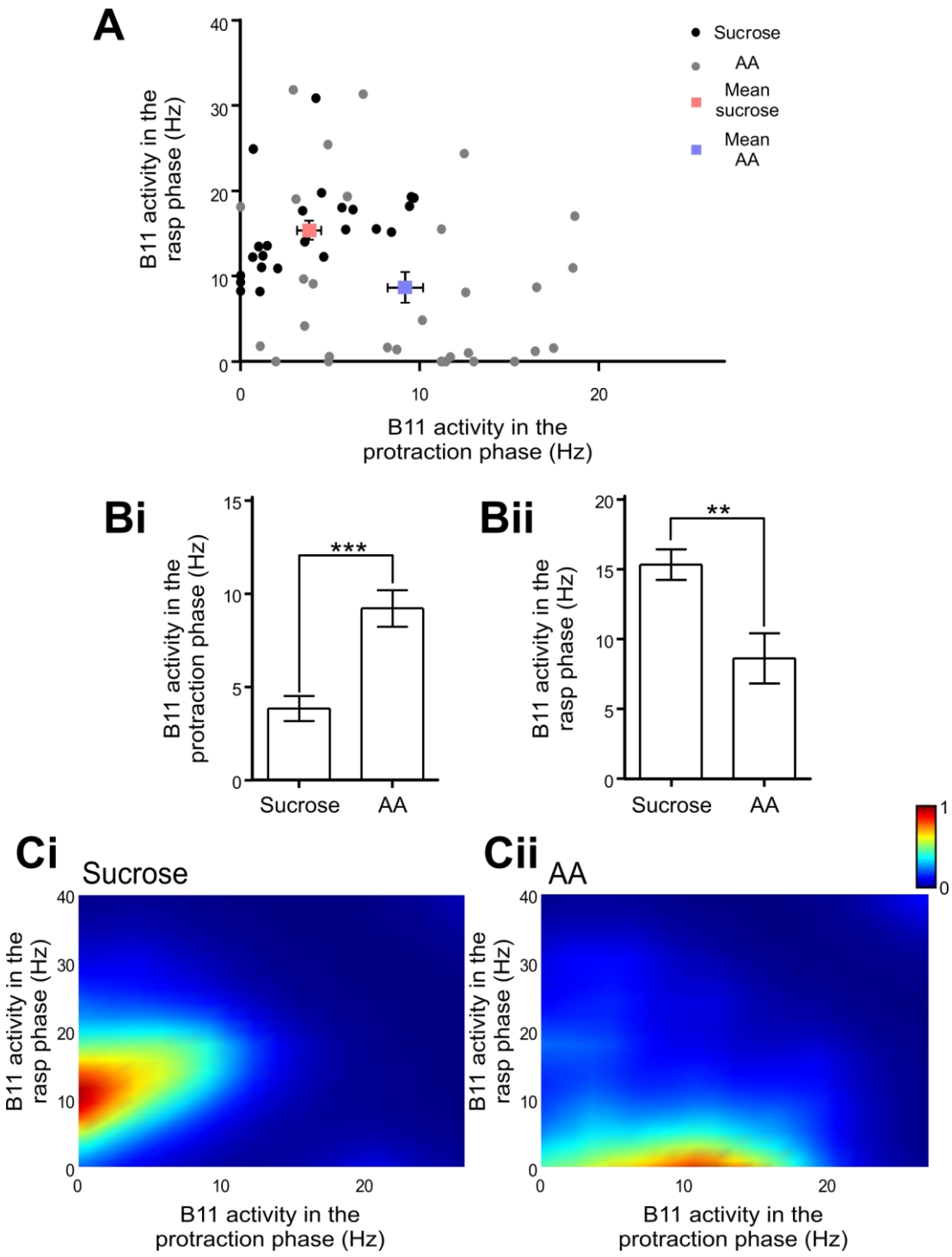

Figure 7.8 B11 activity in ingestion and egestion **A.** B11's activity in the protraction and rasp phase was plotted for all trials in sucrose and AA. **Bi.** There was significantly less B11 activity in the protraction phase of cycles in the presence of sucrose than cycles in the presence of AA. **Bii.** There was significantly more B11 activity in the rasp phase of cycles in the presence of sucrose than cycles in the presence of AA. **Ci.** B11's activity in the protraction and rasp phase of cycles in the presence of sucrose was plotted in a cloudplot to reveal clusters of activity. B11 activity clustered in the rasp phase. **Cii.** B11's activity in the protraction and rasp phase of cycles in the presence of AA was plotted in a cloudplot to reveal clusters of activity. B11 activity clustered in the protraction phase. Areas of high intensity clustering are shown in red and low intensity in blue. ** $P < 0.01$, *** $P < 0.001$.

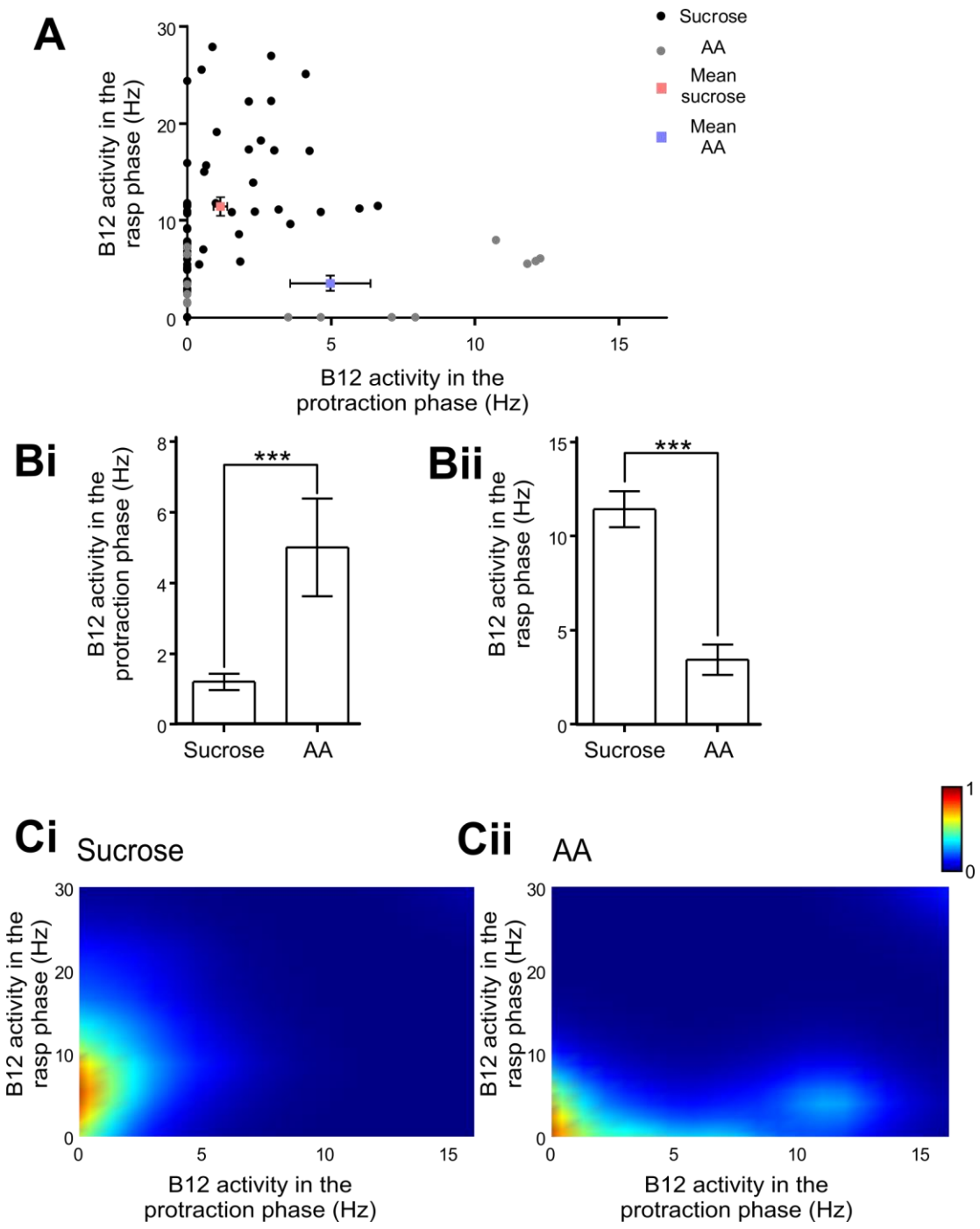

Figure 7.9 B12 activity in ingestion and egestion **A.** B12's activity in the protraction and rasp phase was plotted for all trials in sucrose and AA. **Bi.** There was significantly less B12 activity in the protraction phase of cycles in the presence of sucrose than cycles in the presence of AA. **Bii.** There was significantly more B12 activity in the rasp phase of cycles in the presence of sucrose than cycles in the presence of AA. **Ci.** B12's activity in the protraction and rasp phase of cycles in the presence of sucrose was plotted in a cloudplot to reveal clusters of activity. B12 activity clustered in the rasp phase. **Cii.** B12's activity in the protraction and rasp phase of cycles in the presence of AA was plotted in a cloudplot to reveal clusters of activity. B12's activity clustered around no activity, however the beginnings of a second cluster is evident in the protraction phase. Areas of high intensity clustering are shown in red and low intensity in blue. *** $P < 0.001$.

for either B11 or B12. This provided an approach for establishing whether a given interneuron drove motor programs that most resembled ingestive (sucrose) or egestive (AA) motor programs seen in vitro.

CV1a

The first cell type tested was CV1a. B11 was recorded in 32 CV1a driven cycles in 7 preparations. **Figure 7.10Ai** shows an example of B11 activity in a CV1a driven cycle. B11 was active in the late protraction phase and throughout the rasp phase. In CV1a driven cycles the average B11 activity in the protraction phase was 5.9 Hz (±0.6) and in the rasp phase was 23.2 Hz (±1.3). B12 was recorded in 14 CV1a driven cycles in 4 preparations. **Figure 7.10Bi** shows an example of B12 activity in a CV1a driven cycle. B12 was active in the late protraction phase and throughout the rasp phase. The average B12 activity in the protraction phase was 3.3 Hz (±0.5) and in the rasp phase was 19.6 Hz (±1.8). B11 (**Figure 7.10Aii**) and B12 (**Figure 7.10Bii**) activity was predominantly in the rasp phase of CV1a driven cycles, and the cycles clustered amongst the sucrose driven cycles in vitro. Therefore, CV1a drove motor programs which resembled ingestive motor programs. This is in agreement with previous studies that have shown that CV1a was active in sucrose driven rhythms (Kemenes et al., 2001).

CV1b

The next cell type tested was CV1b. B11 was recorded in 4 CV1b driven cycles in 3 preparations. **Figure 7.11Ai** shows an example of B11 activity in a CV1b driven cycle. B11 was active in both the protraction and rasp phase. In CV1b driven cycles the average B11 activity in the protraction phase was 10.8 Hz (±1.8) and in the rasp phase was 19.6 Hz (±1.8). B12 was recorded in 30 CV1b driven cycles in 9 preparations. **Figure 7.11Bi** shows an example of B12 activity in a CV1b driven cycle. B12 was active in the late protraction phase and in the rasp phase. The average B12 activity in the protraction phase was 2.2 Hz (±0.5) and in the rasp phase was 17.3 Hz (±5.4). B11 activity in two CV1b driven cycles was close to levels of activity seen in sucrose driven cycles (**Figure 7.11Aii**) however the other two showed a much higher level of activity in the protraction phase than seen in sucrose driven cycles. In these two cycles, B11 also showed a high level of activity in the rasp phase, suggesting that these were not similar to the egestive cycles seen in the presence of AA. B12 activity in CV1b driven cycles occurred mostly in the rasp phase and the cycles clustered tightly with the sucrose driven cycles (**Figure 7.11Bii**). B12's activity in CV1b driven cycles suggest that CV1b

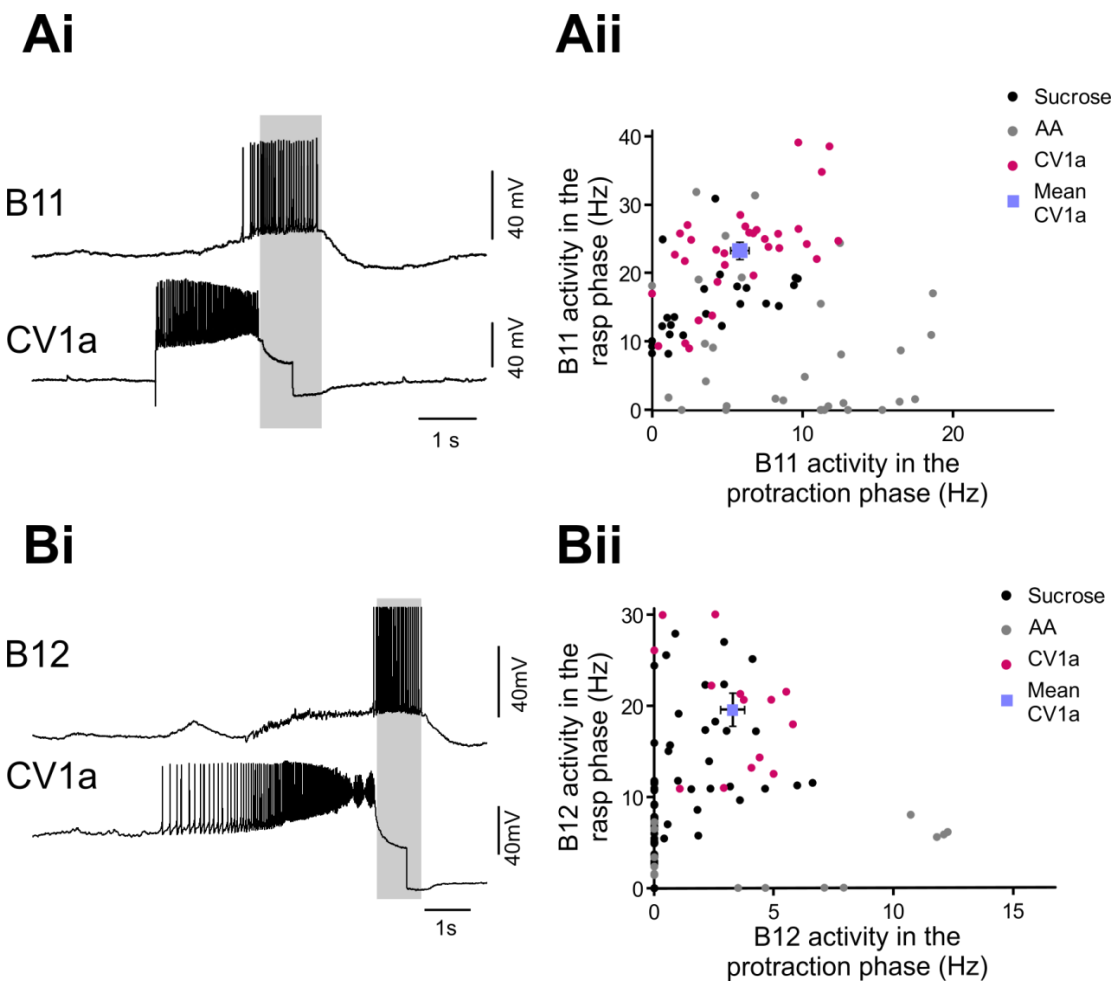

Figure 7.10 B11 and B12 activity in CV1a driven cycles **Ai.** A CV1a was activated to drive a fictive feeding cycle whilst recording a B11. B11 was active in the late protraction phase and throughout the rasp phase. **Aii.** B11's activity in the protraction and rasp phase in CV1a driven cycles plotted with B11's activity in the protraction and rasp phase of sucrose and AA cycles from Figure 7.8A. **Bi.** CV1a was activated to drive a fictive feeding cycle whilst recording a B12. B12 was active throughout the rasp phase of the cycle. **Bii.** B12's activity in the protraction and rasp phase in CV1a driven cycles plotted with B12's activity in the protraction and rasp phase of sucrose and AA cycles from Figure 7.9A. Grey vertical lines represent the rasp phase of a cycle.

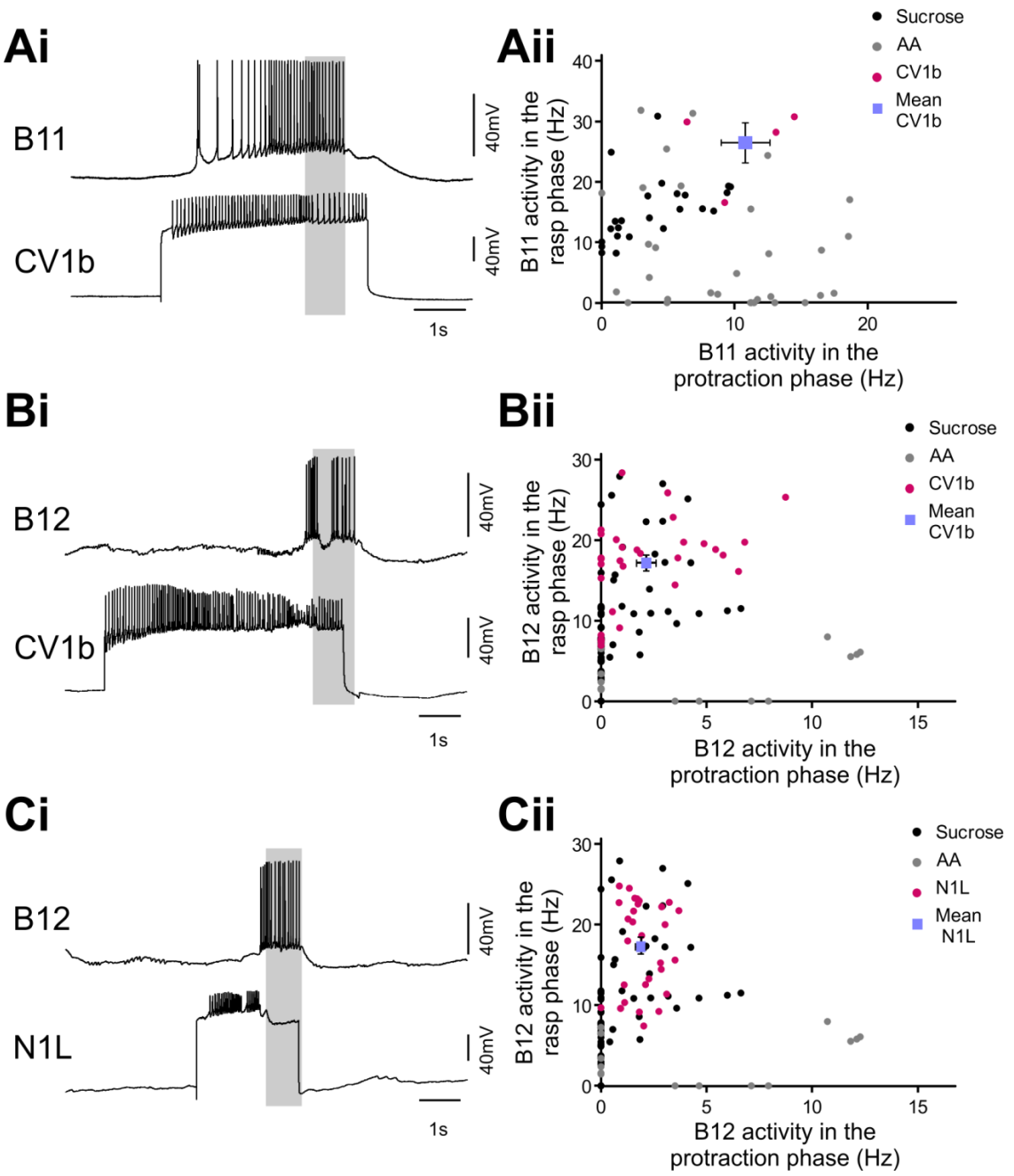

Figure 7.11 B11 and B12 activity in CV1b and N1L driven cycles **Ai.** A CV1b was activated to drive a fictive feeding cycle whilst recording a B11. B11 was active in the protraction and rasp phases. **Aii.** B11's activity in the protraction and rasp phase in CV1b driven cycles plotted with B11's activity in the protraction and rasp phase of sucrose and AA cycles from Figure 7.8A. **Bi.** CV1b was activated to drive a fictive feeding cycle whilst recording a B12. B12 was active in the rasp phase of the cycle. **Bii.** B12's activity in the protraction and rasp phase in CV1b driven cycles plotted with B12's activity in the protraction and rasp phase of sucrose and AA cycles from Figure 7.9A. **Ci.** N1L was activated to drive a fictive feeding cycle whilst recording a B12. B12 was active in the late protraction phase and throughout the rasp phase. **Cii.** B12's activity in the protraction and rasp phase in N1L driven cycles plotted with B12's activity in the protraction and rasp phase of sucrose and AA cycles from Figure 7.9A. Grey vertical lines represent the rasp phase of a cycle.

may be involved in ingestive motor programs, however B11's activity in CV1b driven cycles remains ambiguous.

N1L

The next cell type tested was N1L. B12 was recorded in 30 N1L driven cycles in 3 preparations. **Figure 7.11Ci** shows an example of B12 activity in a N1L driven cycle. B12 was active in the late protraction phase and in the rasp phase. The average B12 activity in the protraction phase was 2.0 Hz (±0.2) and in the rasp phase was 17.5 Hz (±1). B12 activity in N1L driven cycles occurred predominantly in the rasp phase and the cycles were tightly clustered amongst the sucrose driven cycles (**Figure 7.11Cii**), suggesting that N1L was involved in generating ingestive motor programs. N1L's role as an ingestive interneuron is in agreement with findings by Yeoman et al. (1995) who showed that N1L was active in sucrose driven rhythms. Therefore, CV1a and N1L both drive ingestive motor programs and were therefore classified as ingestive interneurons. CV1b drove ingestive looking motor programs on B12 but ambiguous cycles on B11; suggesting that CV1b was an ingestive interneuron. The SO was not tested, however since SO driven cycles strongly recruit N1L (Yeoman et al., 1995), it is likely that the SO is involved in ingestive motor programs too. Therefore none of the previously identified protraction phase command-like interneurons drive egestive motor programs.

7.2.4.2 Protraction phase egestion interneurons

BCI1

Two novel interneurons were identified as candidate egestion interneurons. The first interneuron type was a pair of bilaterally symmetrical interneurons located on the ventral surface of the buccal ganglia (**Figure 7.12A**). Dye injection of the cell (n=6) revealed that the neuron was a bipolar interneuron (**Figure 7.12Bi**). One branch left the cell body and crossed the buccal commissure and entered the contralateral buccal ganglion where it exited via the CBC (**Figure 7.12Bii**). This projection entered the cerebral ganglion where it terminated. The second projection exited the ipsilateral buccal ganglion via the ipsilateral CBC where it also terminated in the cerebral ganglion. It was therefore named Buccal-Cerebral Interneuron 1 (BCI1). In Section 4.2.3 it was shown that activation of BCI1 was able to drive fictive feeding cycles. It was therefore tested whether BCI1 drove ingestive or egestive motor programs. B11 was recorded in 56 BCI1 driven cycles in 11 preparations. **Figure 7.12Ci** shows an example of B11 activity in a BCI1 driven cycle. B11 was active

throughout the protraction phase only, and there was little activity in the rasp phase. In BCI1 driven cycles the average B11 activity in the protraction phase was 16.6 Hz (±0.5) and in the rasp phase was 4.6 Hz (±0.7).B12 was recorded in 44 BCI1 driven cycles in 11 preparations. **Figure 7.12Di** shows an example of B12 activity in a BCI1 driven cycle. B12 was active throughout the protraction phase. B12 fired two spikes in the early rasp phase only. The average B12 activity in the protraction phase was 7.5 Hz (±0.4) and in the rasp phase was 3.5 Hz (±0.6). B11 and B12 activity occurred predominantly in the protraction phase of BCI1 driven cycles. B11 activity clustered amongst the AA driven cycles rather than the sucrose driven cycles. (**Figure 7.12Cii**). B12 activity in BCI1 driven cycles clustered nearer the AA driven cycles than the sucrose driven cycles (**Figure 7.12Dii**). Therefore, BCI1 drove cycles which most resembled those in AA and were classified as egestive cycles.

BCI1's connections were further characterised. It was tested whether BCI1 had synaptic connections with N1M, since most other protraction phase command-like interneurons had an excitatory connection with N1M. BCI1 had an electrotonic synaptic connection with N1M. Injecting negative current into either BCI1 or N1M caused a similar yet attenuated hyperpolarisation on the postsynaptic neuron (n=3) (**Figure 7.13Ai,Aii**). This response persisted in HiLo saline (n=1) providing compelling evidence that the connection was electrotonic in nature. Similar to other protraction phase buccal interneurons, BCI1 was hyperpolarised by N2v activation. This connection persisted in HiDi saline (n=4). **Figure 7.13B** shows an example of N2v inhibition of BCI1 in HiDi saline. The first short duration activation of N2v caused a small hyperpolarisation of BCI1. The second longer activation of N2v caused a two stage hyperpolarisation, possibly via activation of other N2 interneurons.

BCI1 did not cause any change in the phase of activity in any of the previously identified buccal interneurons or motor neurons. **Figures 7.14Ai,Aii,Aiii** show examples of the protraction phase interneuron N1M and the protraction phase motor neurons B7 and B1's activity in BCI1 driven cycles. All three protraction phase neurons were active in the protraction phase only. **Figures 7.14Bi,Bii,Bii** show examples of rasp phase interneuron N2v and rasp phase motor neurons B3, B10 and B9's activity in BCI1 driven cycles. All rasp phase neurons were active predominantly in the rasp phase. **Figure 7.14C** shows an example of the swallow phase interneuron N3t and the swallow phase motor neuron B4 in a BCI1 driven cycle. N3t was active in the swallow phase. B4 did not fire in the swallow phase; however it received the greatest excitation in this phase. Therefore BCI1 selectively shifted the phase of activation of B11 and B12, but not other identified buccal neurons. These results support the hypothesis that

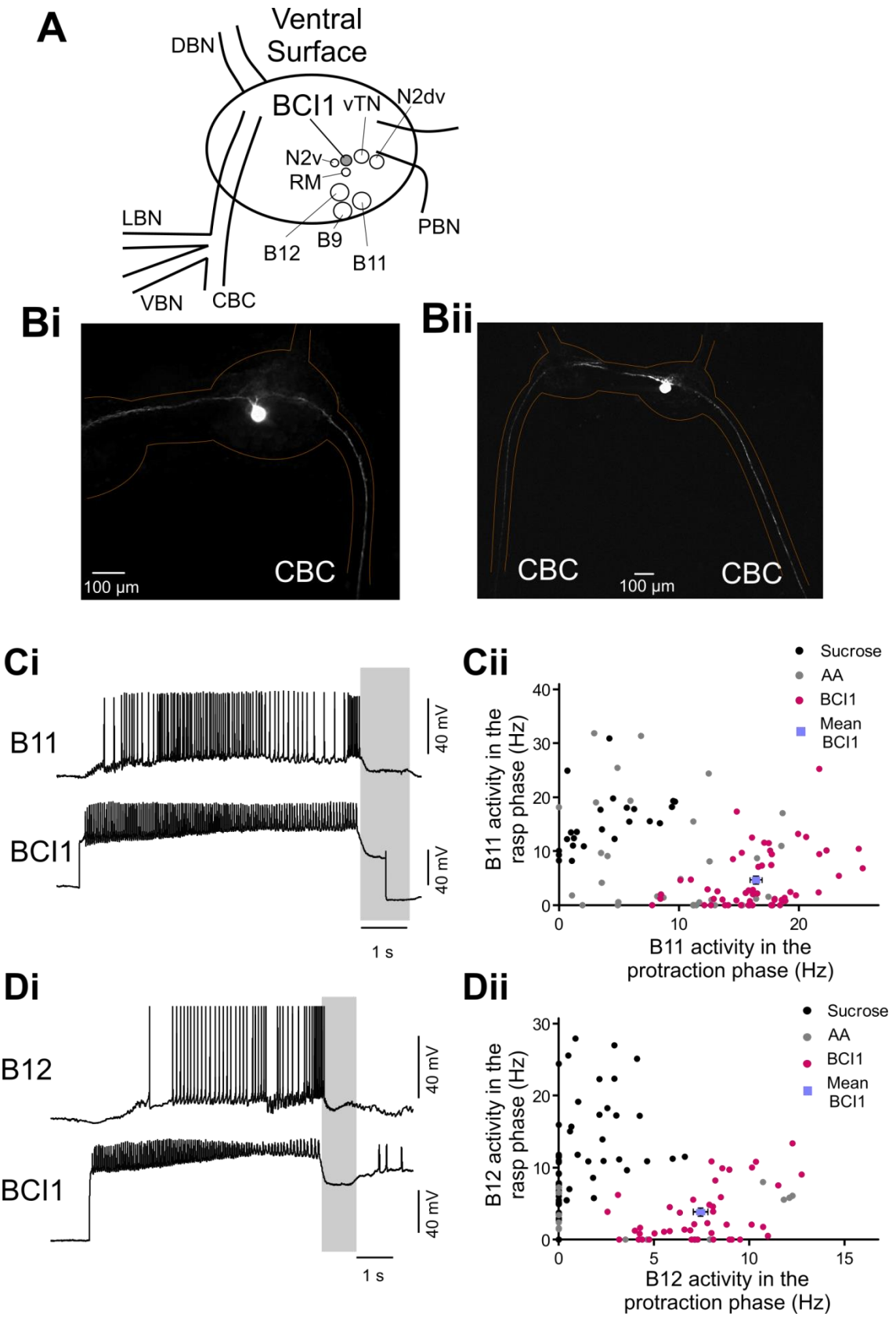
A
Ventral Surface
DBN
BCI1
vTN
N2dv
N2v
RM
LBN
PBN
B12
B9
B11
VBN
CBC
Bi
CBC
100 µm
Bii
CBC
100 µm
CBC
Ci
B11
BCI1
40 mV
40 mV
1 s
Cii
Sucrose
AA
BCI1
Mean BCI1
B11 activity in the rasp phase (Hz)
B11 activity in the protraction phase (Hz)
Di
B12
BCI1
40 mV
40 mV
1 s
Dii
Sucrose
AA
BCI1
Mean BCI1
B12 activity in the rasp phase (Hz)
B12 activity in the protraction phase (Hz)

Figure 7.12 Identification and Characterisation of BCI1 **A.** BCI1 was located on the ventral surface of the buccal ganglion, near vTN and N2v. There was one BCI1 per buccal ganglion. BCI1 is marked in grey and shown in the right buccal ganglion only. **Bi.** BCI1 had two projections leaving the cell body. One projected across the buccal commissure into the contralateral buccal ganglion and the other to the ipsilateral CBC. **Bii.** BCI1 had projections down both the ipsi- and contralateral CBCs. No projections to the periphery were ever present, confirming that BCI1 was an interneuron. **Ci.** BCI1 was activated to drive a fictive feeding cycle whilst recording a B11. B11 was active in the protraction phase only of the cycle. **Cii.** B11's activity in the protraction and rasp phase in BCI1 driven cycles plotted with B11's activity in the protraction and rasp phase of sucrose and AA cycles from Figure 7.8A. **Di.** BCI1 was activated to drive a fictive feeding cycle whilst recording a B12. B12 was active in the protraction and early rasp phase of the cycle. **Dii.** B12's activity in the protraction and rasp phase in BCI1 driven cycles plotted with B12's activity in the protraction and rasp phase of sucrose and AA cycles from Figure 7.9A. Grey vertical lines represent the rasp phase of a cycle.

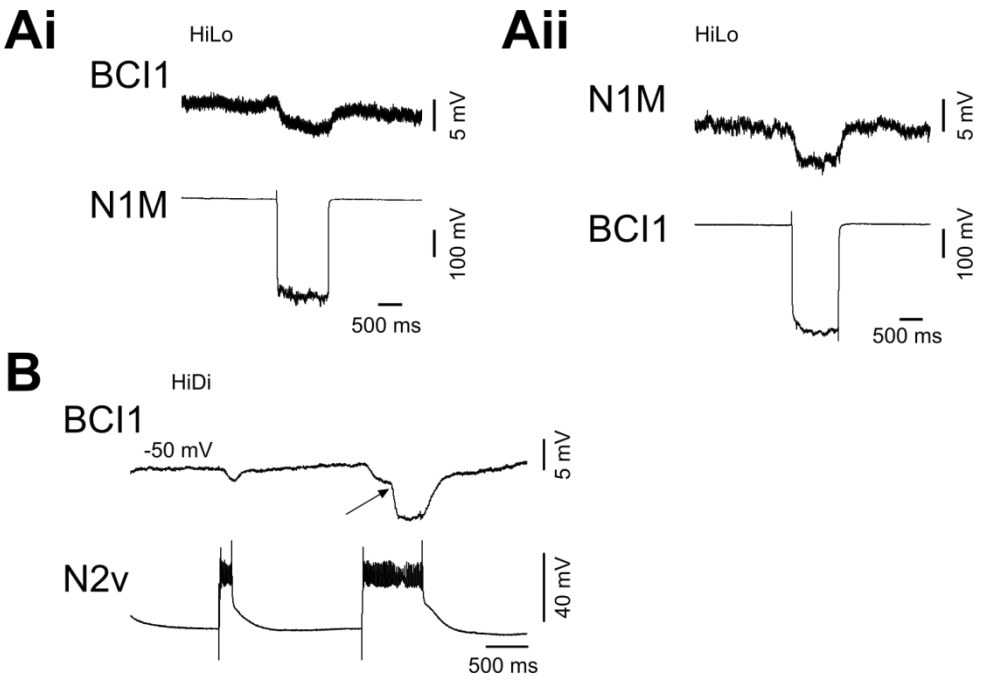

Figure 7.13 BCI1 connections with N1M and N2v **Ai.** Injecting negative current into N1M caused a similar yet attenuated hyperpolarisation of BCI1 in HiLo saline. **Aii.** Injecting negative current into BCI1 caused a similar yet attenuated hyperpolarisation of N1M in HiLo saline. **B.** Short duration activation of N2v caused a small hyperpolarisation of BCI1 in HiDi saline. Long activation of N2v caused a large hyperpolarisation of BCI1 in HiDi saline. The large hyperpolarisation of BCI1 appeared to have two components, one which resembled the small hyperpolarisation seen due to a short duration activation of N2v, and a second later onset hyperpolarisation. Values above the trace of BCI1 represent BCI1's membrane potential prior to N2v activation.

the phase of many buccal mass movements remains the same in both ingestion and egestion.

BCI2

The second candidate egestion interneuron was a novel pair of bilaterally symmetrical interneurons located on the dorsal surface of the buccal ganglia. **Figure 7.15A** shows the location of the interneuron. It was located laterally from the B1 motor neuron, often near the N3t and N1L interneurons. Dye filling the neuron revealed that it had a projection which crossed to the contralateral buccal ganglion via the buccal commissure. A second projection extended down the ipsilateral CBC where it was seen to enter the cerebral ganglion (n=3) (**Figure 7.15Bi**). The neuron was therefore named Buccal-Cerebral Interneuron 2 (BCI2). Large varicosities were present along the length of BCI2's neurite projecting down the CBC (**Figure 7.15Bii**).

BCI2 was able to drive fictive feeding cycles. **Figure 7.15C** shows an example of BCI2 driving three fictive feeding cycles recorded on a B3 motor neuron. The standard triphasic inputs were present on B3 in BCI2 driven cycles. It was therefore a question as to whether BCI2 drove ingestive or egestive motor programs. B12 was recorded in 13 BCI2 drive cycles in 3 preparations. **Figure 7.15Di** shows an example of B12 activity in a BCI2 driven cycle. B12 was active throughout the protraction phase only. The average B12 activity in the protraction phase was 9.2 Hz (±0.9) and in the rasp phase was 3.2 Hz (±1.5). B12 activity occurred predominantly in the protraction phase of BCI2 driven cycles. B12 activity in BCI2 driven cycles clustered near the AA driven cycles, and none clustered amongst the sucrose driven cycles (**Figure 7.15Dii**). Therefore BCI2 drove cycles which most resembled those in AA and were classified as egestive cycles. The two BCIs were therefore classified as egestive interneurons.

7.2.5 Synaptic inputs to B11 and B12 in the protraction phase of ingestive and egestive motor programs

7.2.5.1 Inhibitory inputs

It was next tested how the ingestive and egestive interneurons changed the phase of firing in B11 and B12. During ingestive motor programs, B12 received a barrage of IPSPs during the protraction phase. The IPSPs were present in every CV1a (**Figure 7.16A**) and CV1b (**Figure 7.16C**) driven cycle. The IPSPs were present in some N1L driven cycles (**Figure 7.16B**) but not all (**Figure 7.11Ci**). Interestingly they were also present in BCI1 driven cycles (**Figure 7.16D**). None of these interneurons

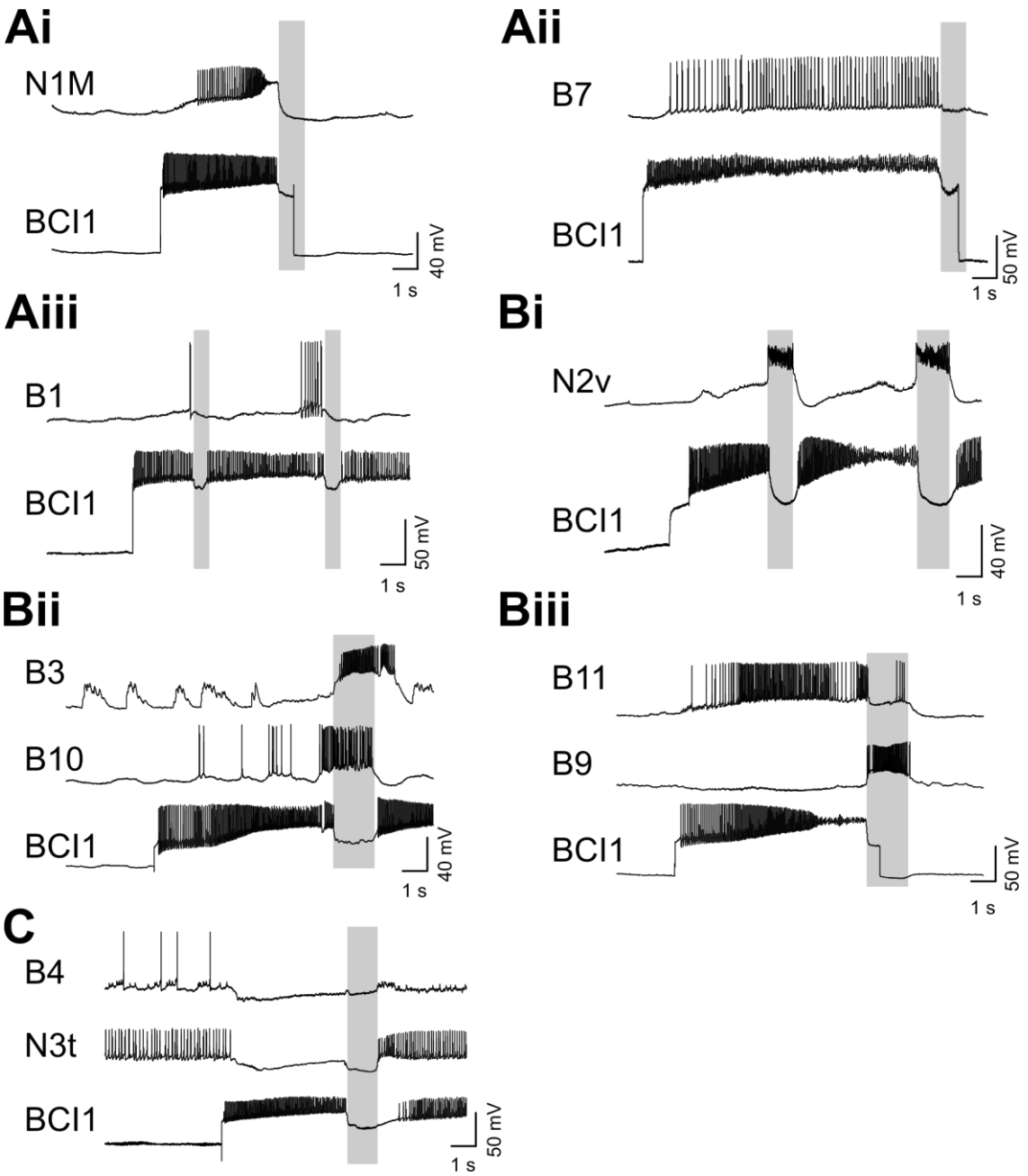

Figure 7.14 Activity of buccal neurons in BCI1 driven cycles **Ai.** N1M was active in the protraction phase of a BCI1 driven cycle **Aii.** B7 was active throughout the protraction phase of a BCI1 driven cycle **Aiii.** B1 was active in the protraction phase of both BCI1 driven cycles. **Bi.** N2v was active in the rasp phase of both BCI1 driven cycles. **Bii.** B3 was active in the rasp and early swallow phases and B10 the late protraction and rasp phases of a BCI1 driven cycle. **Biii.** B9 was active in the rasp phase of a BCI1 driven cycle, whilst B11 was active throughout the protraction phase. **C.** N3t was active in the quiescent period prior to and after the BCI1 cycle and fired a burst of PIR spikes in the swallow phase. B4 was not active in the cycle, but received the greatest excitation in the swallow phase. Grey vertical lines represent the rasp phase of a cycle.

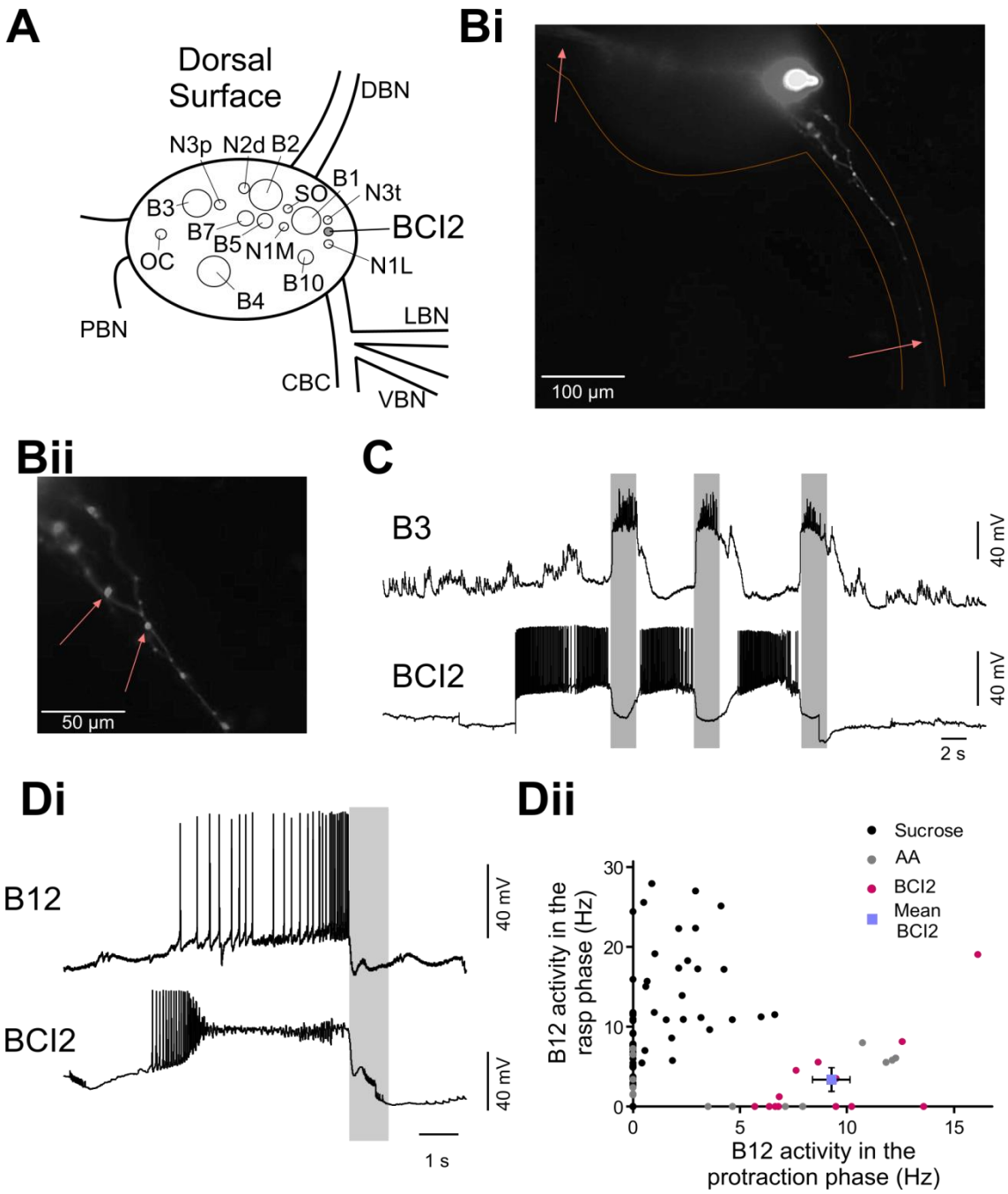

Figure 7.15 Identification and characterisation of BCI2 **A.** BCI2 was locater on the dorsal surface of the buccal ganglia, near the N1L and N3t interneurons. **Bi.** BCI2 projected down the ipsilateral CBC to the cerebral ganglion and to the contralateral buccal ganglion via the buccal commissure. The red arrows mark where BCI2 projects across the buccal commissure and the CBC **Bii.** Varicosities were present on BCI2's CBC neuritic projection. Two of these are marked by red arrows **C.** Activation of BCI2 during a period of quiescence was sufficient to drive fictive feeding cycles. B3 fired in the rasp phase of each of the three cycles. BCI2 was inhibited in the rasp phase of all three cycles. **Di.** BCI2 was activated to drive a fictive feeding cycle whilst recording a B12. B12 was active in the protraction phase only of the cycle. **Dii.** B12's activity in the protraction and rasp phase in BCI2 driven cycles plotted with B12's activity in the protraction and rasp phase of sucrose and AA cycles from Figure 7.9A. Grey vertical lines represent the rasp phase of a cycle.

(CV1a, CV1b, N1L or BCI1) were the source of the inhibitory inputs seen in the protraction phase on B12, as the IPSPs did not follow 1:1 from their spikes. The source of the IPSPs to B12 in the protraction phase was identified as a novel interneuron in the cerebral ganglion. The neuron was located in the CV region under the CV3 motor neuron, near the CV1 interneurons. Dye filling the neuron revealed that it projected to the buccal ganglia via the ipsilateral CBC (n=1). **Figure 7.17A** shows its projection up the CBC to the buccal ganglia. It entered the ipsilateral buccal ganglion and crossed the buccal commissure to enter the contralateral buccal ganglion. This morphological feature meant that the neuron was a CBI. Due to its location and morphology it was named CV1d. Activation of CV1d hyperpolarised B12 in HiDi saline (n=3) (**Figure 7.17Bi**). Unitary IPSPs on B12 followed CV1d spikes 1:1 providing strong evidence that the connection was monosynaptic (**Figure 7.17Bii**). Strong activation of CV1d was sufficient to drive fictive feeding cycles. B12 was recorded in 16 CV1d driven cycles in 3 preparations. **Figure 7.17Ci** shows an example of a CV1d driven cycle. B12 was inhibited throughout the duration of CV1d activity and fired in the rasp phase, when CV1d, similar to CV1a, received strong inhibition. In CV1d driven cycles the average B12 activity in the protraction phase was 1.3 Hz (±1.4) and in the rasp phase was 17.1 Hz (±1.4). A plot of B12 activity in CV1d driven cycles revealed that B12 activity occurred predominantly in the rasp phase (**Figure 7.17Cii**). B12 activity in CV1d driven cycles clustered amongst the sucrose driven cycles, rather than the AA cycles. Therefore CV1d was also categorised as an ingestive interneuron. CV1d was strongly active in CV1a driven cycles (**Figure 7.17Di**), suggesting that CV1d activity could account for the inhibitory inputs seen on B12 in the protraction phase of CV1a driven cycles, however this was not directly tested. Interestingly a CV1d was recorded during a BCI1 driven cycle with a B12 motor neuron (**Figure 7.17Dii**). B12 fired throughout the protraction phase, but similar periods of inhibition occurred, as in **Figure 7.16D**. CV1d was active during these periods of inhibition on B12 in the protraction phase, and unitary IPSPs were present on B12 following 1:1 from CV1d spikes. These results suggest that the inhibition on B12 throughout the protraction phase of ingestive cycles and in bursts in BCI1 driven egestive cycles arise from CV1d activity.

During ingestive motor programs, B11 received no obvious unitary EPSPs or IPSPs during the protraction phase. There was a slight depolarisation which culminated in spiking activity in the late protraction phase. However, it was not tested whether CV1a, CV1b or N1L was directly responsible for this.

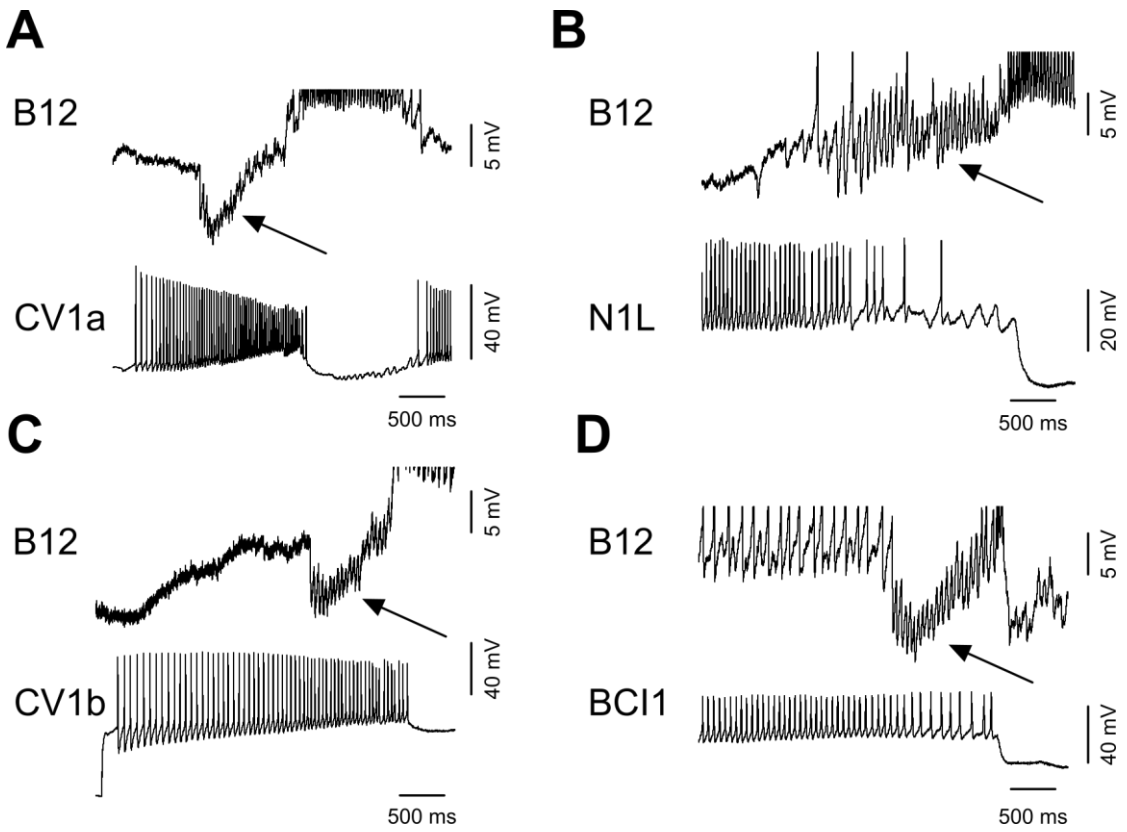

Figure 7.16 Protraction phase inputs on B12 **A.** B12 receives large unitary IPSPs in the protraction phase of a CV1a driven cycle. These do not follow 1:1 from CV1a spikes. **B.** B12 receives large unitary IPSPs in the protraction phase of a N1L driven cycle. These do not follow 1:1 from N1L spikes. **C.** B12 receives large unitary IPSPs in the protraction phase of a CV1b driven cycle. These do not follow 1:1 from CV1b spikes. **D.** B12 receives excitation in the protraction phase of a BCI1 driven cycle and fires spikes. B12 also receives some inhibitory inputs in the protraction phase. B12 spikes in these traces are clipped.

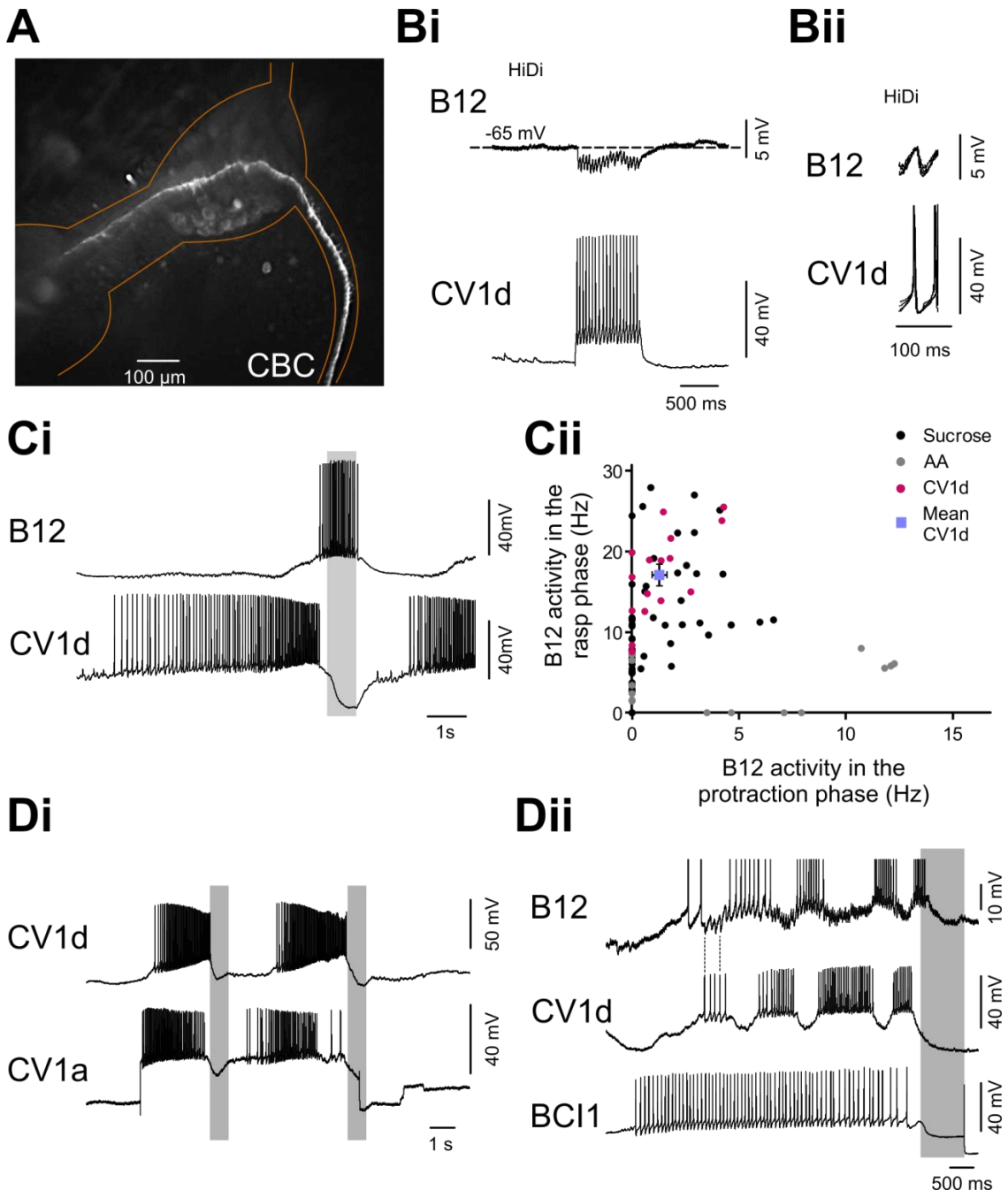

Figure 7.17 Identification and characterisation of CV1d **A.** The projection of CV1d up the ipsilateral CBC entering the ipsilateral buccal ganglion. It then crossed the buccal commissure and entered the contralateral buccal ganglion. **Bi.** CV1d activation hyperpolarised B12 in HiDi saline **Bii.** Unitary IPSPs on B12 followed CV1d spikes 1:1. **Ci.** CV1d was activated to drive a fictive feeding cycle whilst recording a B12. B12 was active in the late protraction and in the rasp phase of the cycle. **Bii.** B12's activity in the protraction and rasp phase in CV1d driven cycles plotted with B12's activity in the protraction and rasp phase of sucrose and AA cycles from Figure 7.9A. **Di.** CV1d was active in the protraction phase of CV1a driven cycles and inhibited in the rasp phase. **Dii.** CV1d was active in bursts in the protraction phase of a BCI1 driven cycle. Each burst of CV1d activity inhibited B12, preventing it from spiking. Once CV1d activity stopped after each burst, B12 fired spikes again in the protraction phase. Grey vertical lines represent the rasp phase of a cycle.

7.2.5.2 Excitatory inputs

Both B11 and B12 received strong excitation throughout the protraction phase of both AA driven cycles in semi-intact preparations and in BCI1 and BCI2 driven cycles. It was therefore tested from where the excitation to B11 and B12 in the protraction phase of egestive cycles arose from. BCI1 had a strong excitatory connection with B11 which persisted in HiDi saline (n=6) (**Figure 7.18Ai**). Unitary EPSPs on B11 followed 1:1 from BCI1 spikes (**Figure 7.18Ai**), providing strong evidence that the connection was monosynaptic. BCI1 activation also depolarised B12 (**Figure 7.18B**). This was often sufficient to elicit spiking and persisted in HiDi saline (n=4), however no unitary EPSPs were ever present on B12. The persistence in HiDi saline suggests that a component of the connection may be monosynaptic in nature. Therefore during the protraction phase of egestive cycles, BCI1 provides monosynaptic excitation to B11 and B12 shifting their activity to the protraction phase.

Results in this section suggested that during ingestive motor programs, the recruitment of CV1d by CV1a, and possibly CV1b and N1L, inhibited B12 during the protraction phase. In egestive motor programs, BCI1's excitation to both B11 and B12 activated the motor neurons in the protraction phase. The relative recruitment of different protraction phase interneurons therefore could account for the excitation or inhibition of the motor neurons during the protraction phase of either ingestion or egestion. However these connections cannot account for the inputs to B11 and B12 in the rasp phase of ingestion or egestion cycles since none of the protraction phase interneurons were active in the rasp phase.

7.2.6 Synaptic connections from N2v to B11 and B12

During ingestive motor programs, both B11 and B12 were active throughout the rasp phase. Next, experiments were carried out to establish the source of excitation to the two motor neurons. The N2v interneuron is active throughout the rasp phase and has excitatory connections with all rasp phase motor neurons (Brierley et al., 1997a). **Figure 7.19A** shows an example of activating N2v whilst recording a B11 and the ipsi- and contralateral B12. B11 and the two B12s were depolarised and fired a burst of spikes throughout N2v activation. In HiDi saline, the excitatory connection from N2v to B11 persisted (n=3) (**Figure 7.19B**). Injecting N2v or B11 with hyperpolarising current pulses caused a similar yet attenuated response on the post-synaptic neuron (**Figure 7.19Ci,Cii**). The connection was present in normal saline (n=6) and persisted in HiLo saline (n=2) strongly suggesting that the connection was electrotonic in nature.

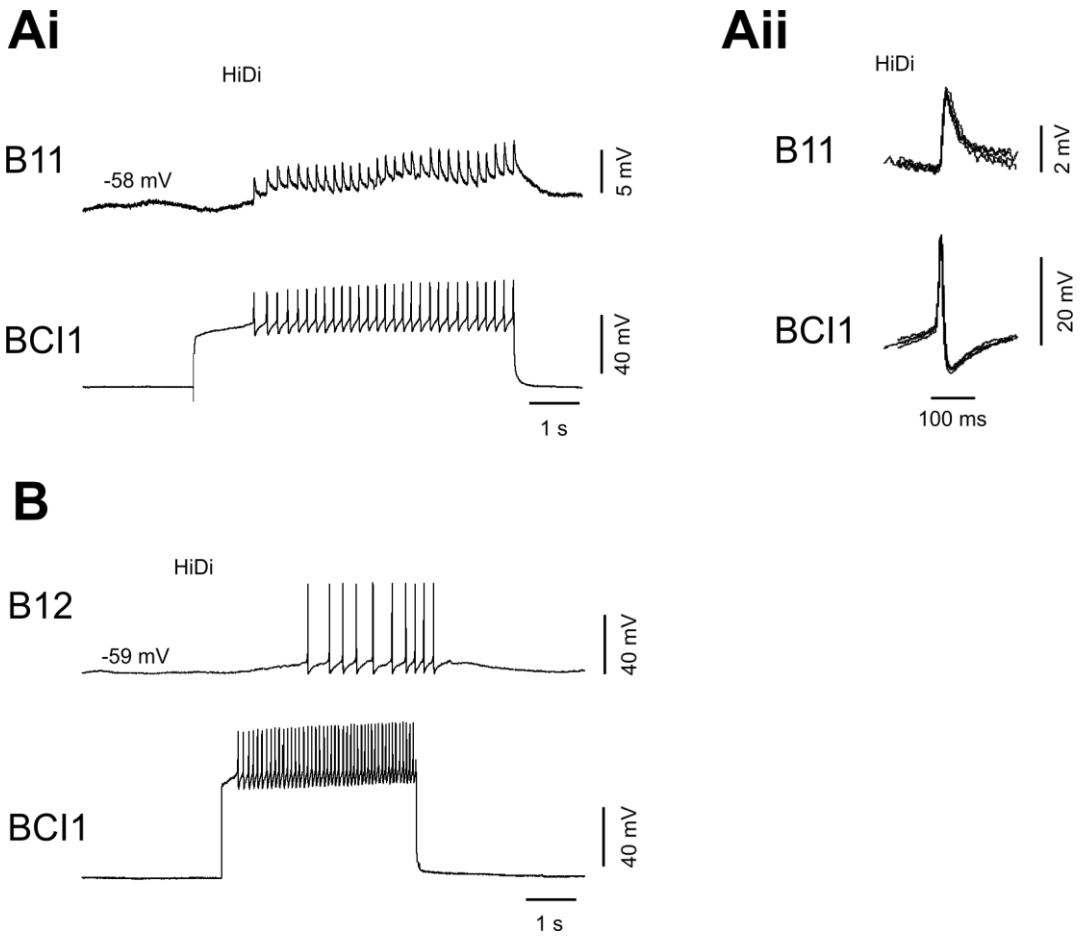

Figure 7.18 Synaptic connections from BCI1 to B11 and B12 **A.** Activation of BCI1 depolarised B11 in HiDi saline. **Ai.** Unitary EPSPs on B11 followed BCI1 spikes 1:1. **B.** Activation of BCI1 depolarised B12 in HiDi saline. The depolarisation was sufficient to elicit spiking activity in B12.

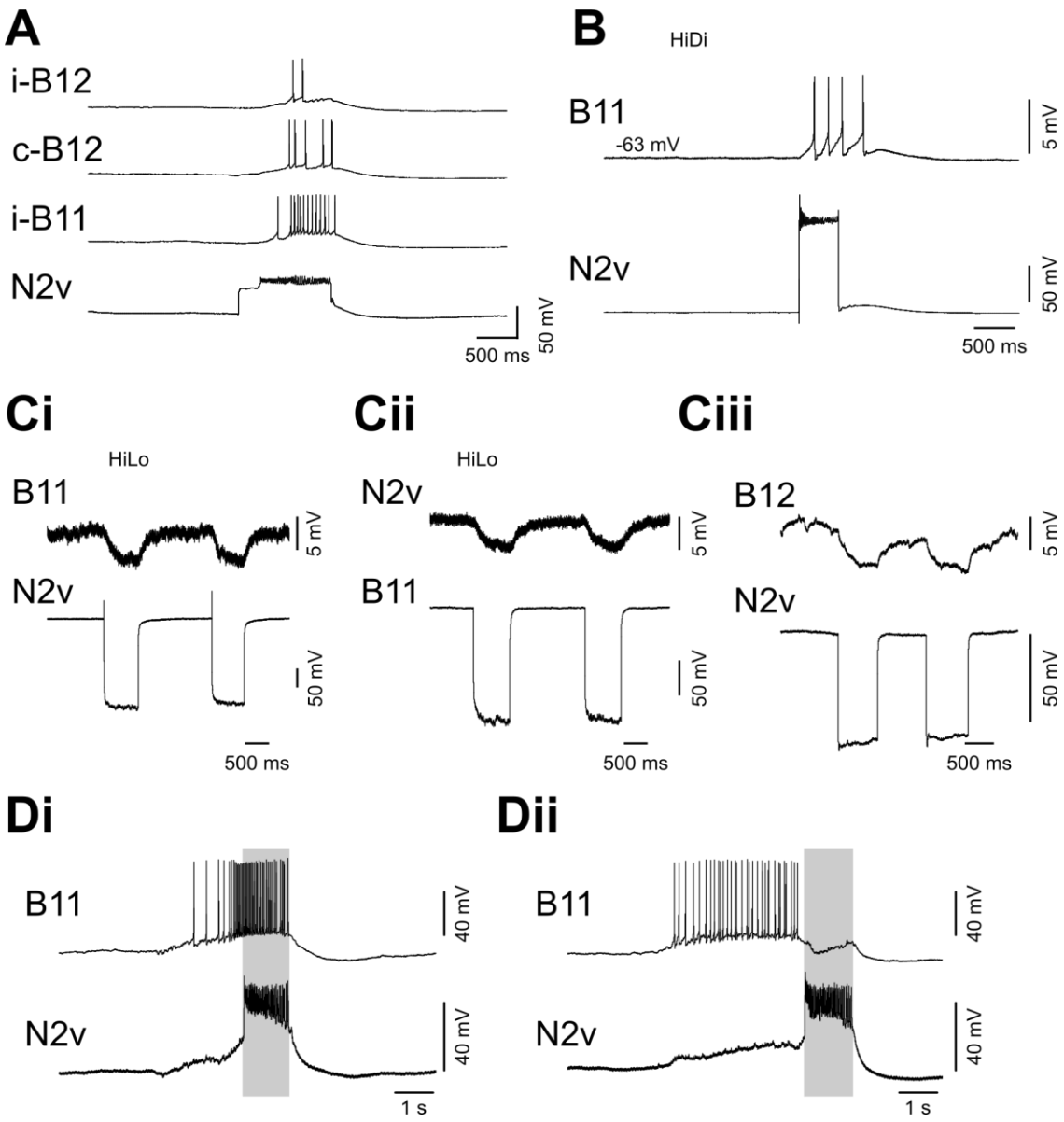

Figure 7.19 Synaptic connections between N2v and B11 and B12 **A.** Activation of N2v depolarised B11 and both the ipsi- and contralateral B12. All three motor neurons were sufficiently depolarised to elicit spiking activity. **B.** N2v depolarisation of B11 persisted in HiDi saline. **Ci.** Injecting negative current into N2v caused a similar yet attenuated hyperpolarisation of B11 in HiLo saline. **Cii.** Injecting negative current into B11 caused a similar yet attenuated hyperpolarisation of N2v in HiLo saline. **Ciii.** Injecting negative current into N2v caused a similar yet attenuated hyperpolarisation of B12 in normal saline. **Di.** N2v was active in the rasp phase of ingestive motor programs. B11 was active throughout the rasp phase. **Dii.** N2v was active in the rasp phase of egestive motor programs. B11 was active in the protraction phase only. Grey vertical lines represent the rasp phase of a cycle.

A similar electrotonic synapse was present between N2v and B12 (**Figure 7.19Ciii**) in normal saline (n=2). Since N2v was active in sucrose driven ingestive cycles (**Figure 7.5Ai**) and CV1a cycles (**Figure 4.9C**), the N2v to B11 and B12 connection was sufficient to account for the excitation to the motor neurons during ingestive motor programs. However, N2v was not only active in ingestive motor programs (**Figure 7.19Di**), but also egestive motor programs (**Figure 7.19Dii**). In **Figure 7.19Dii** B11 was active in the protraction phase but not in the rasp phase of a spontaneous cycle. N2v activity, however, persisted in the rasp phase. This was also in agreement with that fact that N2v is active in BCI1 driven cycles (**Figure 7.14Bi**). Therefore, during egestive motor programs, the absence of activity of B11 and B12 during the rasp phase was not due to lack of N2v activity.

7.2.7 Synaptic inputs to B11 and B12 in the rasp phase of egestive motor programs

7.2.7.1 B45 identification and connections with B11 and B12

A novel neuron was identified as a candidate for providing inhibition to B11 and B12 during the rasp phase of egestive motor programs. The neuron was located on the ventral surface of the buccal ganglia. There were at least two per ganglion, located near the buccal commissure (**Figure 7.20A**). Dye filling the neuron (n=3) revealed that it had extensive arborisation within the ipsilateral buccal ganglion, but no projections into the contralateral ganglion (**Figure 7.20B**). The neuron projected out of the buccal ganglia via the VBN. Whether this reached the buccal mass was not examined. The neuron was named B45 (see Section 7.3.3 for the rationale for this). B45 showed evidence of endogenous PIR which persisted in HiDi saline (n=8) and HiLo saline (n=1) (**Figure 7.20C**). B45 was also depolarised to spike by N2v activation in normal saline (n=3) and in HiDi saline (n=2) (**Figure 7.20D**). Activation of B45 caused a large hyperpolarisation of B11 in normal saline (n=3). This connection persisted in HiDi saline (n=1) (**Figure 7.20Ei**). Unitary 1:1 IPSPs were present on B11 following B45 spikes (**Figure 7.20Eii**) strongly suggesting that the inhibitory connection from B45 to B11 was monosynaptic. B45 activation also hyperpolarised B12 in HiDi saline (n=7) (**Figure 7.20Fi**). Unitary 1:1 IPSPs were present on B12 following B45 spikes (**Figure 7.20Fii**), strongly suggesting that the connection was monosynaptic.

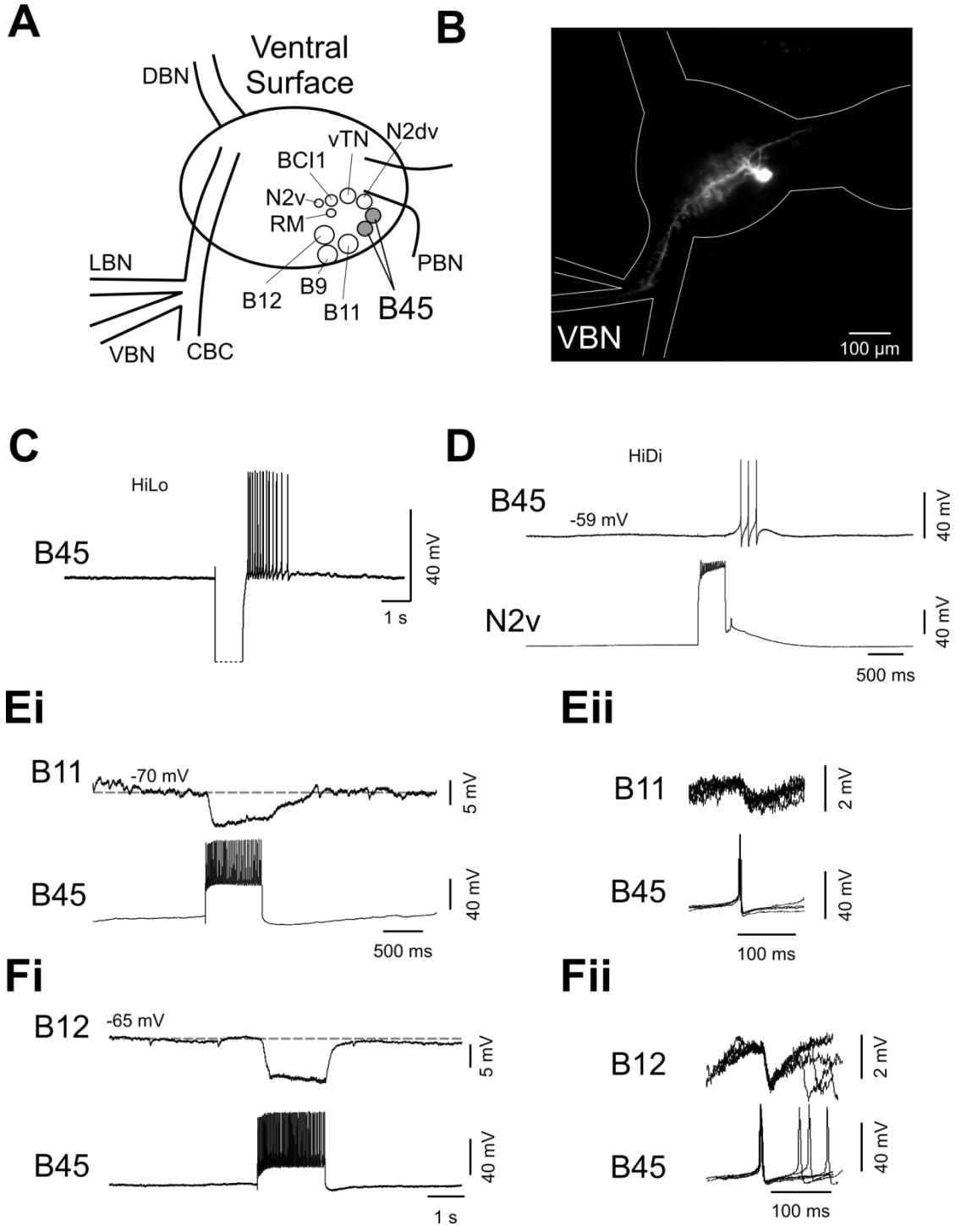

Figure 7.20 Identification and characterisation of B45 **A.** B45 was located on the ventral surface of the buccal ganglion. There were at least two per ganglion, located near the buccal commissure. **B.** B45 had numerous arborisations within the ipsilateral buccal ganglion and a single projection down the VBN. No projections entered the contralateral buccal ganglion. **C.** B45 showed evidence of PIR. B45 was injected with negative current. Once the current had been removed from the neuron, B45 fired a burst of spikes. This persisted in HiLo saline strongly suggesting that it was an endogenous property of the neuron. **D.** Activation of N2v depolarised B45. This was sufficient to elicit spiking activity in B45. **Ei.** Activation of B45 hyperpolarised B11. **Eii.** Unitary IPSPs on B11 followed B45 spikes 1:1. **Fi.** Activation of B45 hyperpolarised B12. **Fii.** Unitary IPSPS on B12 followed B45 spikes 1:1.

7.2.7.2 B45 activity in ingestion and egestion

Next, experiments were performed to examine B45's firing activity during CBI and BCI driven cycles. **Figure 7.21Ai** shows an example of B45 activity in a BCI1 and CV1a driven cycle. B45 fired tonically prior to activation of either interneuron. BCI1 activation hyperpolarised B45 and reduced its spiking activity in the protraction phase. B45 fired a burst of spikes in the rasp phase and then returned to firing tonically. CV1a activation also hyperpolarised B45 in the protraction phase, however more so than in the BCI1 driven cycle. B45 fired a burst of spikes in the rasp phase similar to the BCI1 driven cycle. To quantify B45 activity, spike frequency was plotted in 0.3 s bins which revealed that B45 activity was higher in the rasp phase of the BCI1 driven cycle than the CV1a driven cycle (**Figure 7.21Ai**). **Figure 7.21Aii** shows a separate preparation in which the same experiment was performed. Similarly, B45 was hyperpolarised sufficiently to prevent spiking activity throughout the protraction phase of the CV1a driven cycle. However in this preparation, B45 was only depolarised in the rasp phase, but fired no spikes. In contrast, in the BCI1 driven cycle, B45 was hyperpolarised only at the end of the protraction phase and then fired a burst of spikes in the rasp phase. B45 activity was plotted into 0.3 s bins which showed the difference between B45 activity in the rasp phase of the CV1a and BCI1 driven cycles (**Figure 7.21Aii**). Therefore, B45 monosynaptically inhibited both B11 and B12 and was active at a higher frequency in the rasp phase of BCI1 driven cycles than in CV1a driven cycles. This made B45 a good candidate for the source of the inhibition of B11 and B12 during the rasp phase of egestive motor programs.

To test whether B45 was the source of inhibition to B11 and B12 in egestive motor programs, B45 activity was artificially manipulated in BCI1 driven cycles whilst recording a B11 or B12. **Figure 7.21Bi** shows an example of a BCI1 driven cycle. B11 was active throughout the protraction phase and was then inhibited in the early rasp phase and fired spikes in the late rasp phase. B45 fired a burst of spikes throughout the rasp phase. In **Figure 7.21Bii** B45 was injected with negative current to prevent spiking activity throughout the experiments. BCI1 was activated to drive a cycle. B11 was active throughout the protraction phase, as previously, but also throughout the entire rasp phase. **Figure 7.21Ci** shows an example of B12 activity in a similar experiment. In the BCI1 driven cycle, B12 was active throughout the protraction phase and inhibited in the rasp phase. B45 fired a burst of spikes throughout the rasp phase of the cycle. In **Figure 7.21Cii** B45 was injected with negative current to prevent spiking activity. B12 was active throughout the protraction phases of the two BCI1 driven cycles as previously. However without any B45 activity in the rasp phase, B12

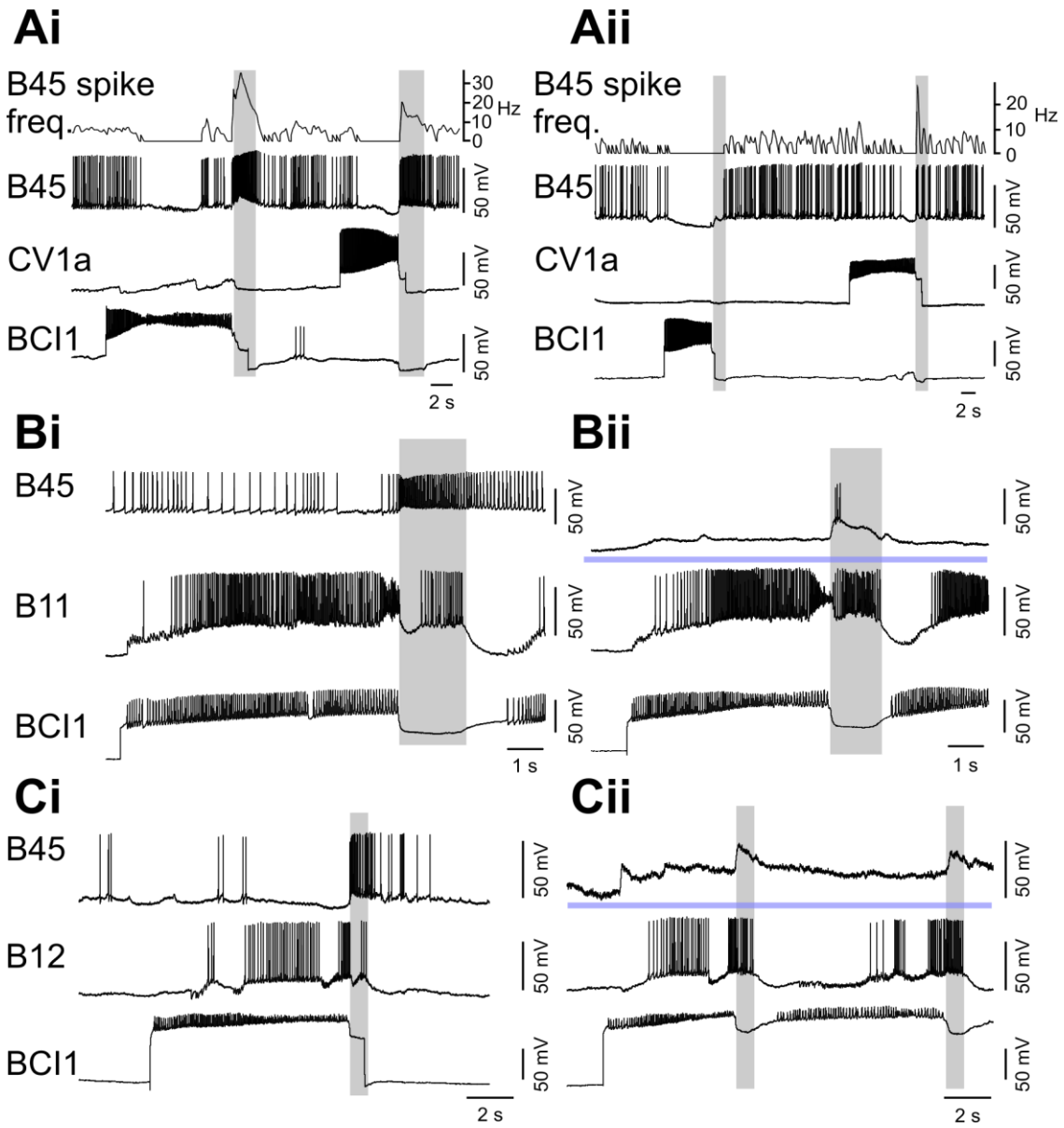

Figure 7.21 B45 activity in CV1a and BCI1 driven cycles **Ai.** B45 was tonically active prior to CV1a or BCI1 activation. BCI1 activation hyperpolarised B45 in the protraction phase. B45 fired a burst of spikes in the rasp phase and then returned to firing tonically. CV1a activation hyperpolarised B45 and prevented spiking activity in the protraction phase. B45 fired a burst of spikes in the rasp phase and then returned to firing tonically. B45 spikes were plotted in 0.3s bins to show its firing frequency in the two cycles. B45 activity was higher in the rasp phase of the BCI1 driven cycle. **Aii.** B45 was hyperpolarised in the protraction phase of the CV1a driven cycle. B45 depolarised in the rasp phase, but not sufficiently to elicit spiking activity. B45 activity was reduced in the protraction phase of the BCI1 driven cycle and then fired a burst of spikes in the rasp phase. B45 spikes were plotted in 0.3s bins, revealing that B45 fired at a much higher rate in the BCI1 driven cycle than the CV1a driven cycle. **Bi.** Activation of BCI1 drove a single cycle recorded on a B11 and B45. B11 fired throughout the protraction phase and the end of the rasp phase. B45 fired a burst of spikes in the rasp phase. **Bii.** BCI1 activation drove a cycle. B45 was injected with negative current prior to BCI1 activation to prevent spiking activity. B11 fired throughout the protraction phase as in Bi. but also fired throughout the entire rasp phase in the absence of B45 inhibition. **Ci.** BCI1 activation drove a single cycle recorded on a B12 and B45. B12 fired in the protraction phase of the cycle and the late rasp phase. B45 fired a burst of spikes in the rasp phase. **Cii.** BCI1 activation drove two cycles. B45 was injected with negative current prior to BCI1 activation to prevent spiking activity. B12 fired in the protraction and rasp phase of both cycles in the absence of B45 inhibition in the rasp phase. Blue horizontal lines represent hyperpolarising current. Grey vertical lines represent the rasp phase of a cycle.

was also active throughout the rasp phase of both cycles. These experiments provide strong evidence that during BCI driven egestive motor programs B45 fires in the rasp phase and consequently prevents B11 and B12 activity in the same phase.

7.2.7.3 Connections from BCI1 to B45

It was next tested how BCI1 increased B45 firing rate in the rasp phase whereas CV1a decreased B45 activity. In HiDi saline, BCI1 activation caused a delayed excitation of B45 (n=10). **Figure 7.22A** shows an example of BCI1 activation causing the depolarisation of B45 above spike threshold. B45 spiking occurred after BCI1 activity had stopped. B45 was only sufficiently depolarised to spike by BCI1 if B45 was artificially depolarised prior to BCI1 activity, as in **Figure 7.22A**. B45 fired in the opposite phase (rasp) to BCI1 (protraction) therefore the delayed onset of the depolarisation could allow for increased B45 activity within the rasp phase. This was further tested by examining B45's excitability after BCI1 activity. B45 was injected with a 1 s square pulse in the absence of BCI1 activity. This triggered a single action potential in B45 (**Figure 7.22Bi**). BCI1 was then activated prior to the same stimulus to B45. B45 fired 7 action potentials after BCI1 pre-stimulation (**Figure 7.22Bii**). The same stimulus was then applied to B45 in the absence of BCI1 pre-stimulation, and B45 fired a single action potential again (**Figure 7.22Biii**). There was a significant increase in B45 excitability in the BCI1 pre-stimulation trial compared with both the before and after trials, whereas there was no significant difference between the before and after trials (n=7) (Number of B45 spikes Before = 5.5 ±1, BCI1 pre stimulation = 10 ±1.6, After = 5.6 ±1.4, Friedman test: df = 6, $\chi^2 = 10.57$, $P < 0.01$. Dunn's test Before vs. BCI1 pre stimulation $P < 0.01$, After vs. BCI1 pre stimulation $P < 0.05$, Before vs. After $P > 0.05$) (**Figure 7.22Biv**). B45 was found to show evidence of PIR in Section 7.2.7.1. It was therefore tested whether BCI1 activity enhanced PIR in B45. B45 was injected with a square negative current pulse for 1 s (n=5). B45 depolarised after the negative stimulus was removed from the neuron, but not sufficiently to reach threshold (**Figure 7.2Ci**). In the next trial, BCI1 was stimulated prior to the negative stimulus to B45. B45 fired two PIR spikes once the negative stimulus was removed from the neuron (**Figure 7.22Cii**). The same stimulus was applied to B45 in the absence of BCI1 activation again and B45 fired no PIR spikes (**Figure 7.22Ciii**). A Friedman test revealed a significant difference (df = 4, $\chi^2 = 8.8$, $P < 0.001$) however post hoc analysis revealed no significant difference between conditions (Dunn's test $P > 0.05$ for all conditions). (**Figure 7.22Civ**) (Number of B45 PIR spikes Before = 1.8 ±0.9, BCI1 pre stimulation = 6 ±1.5, After = 1.8 ±0.9). Therefore BCI1 increased

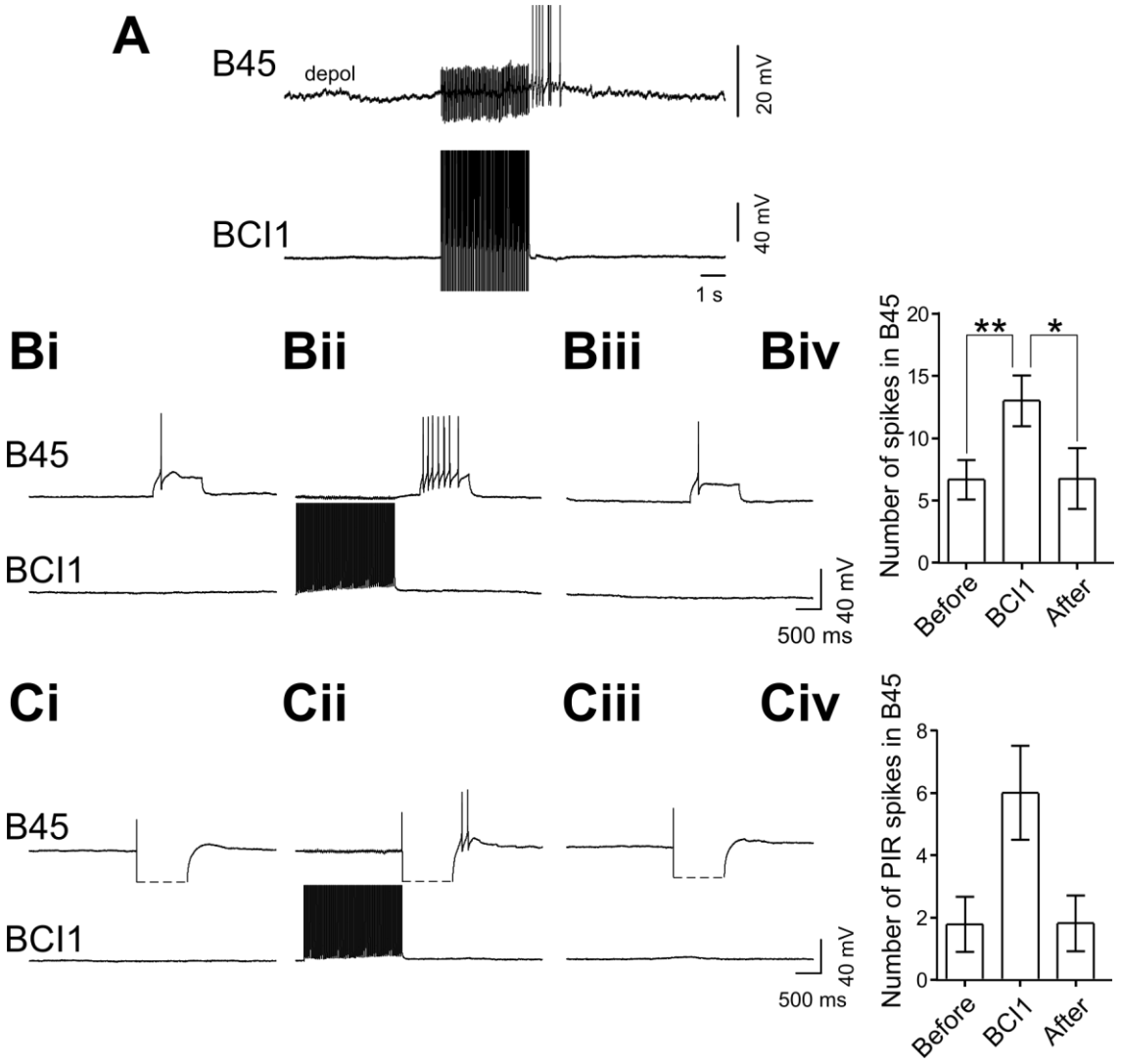

Figure 7.22 BCI1 connections with B45 **A.** Activation of BCI1 depolarised B45. This was sufficient to elicit spiking if B45 was depolarised prior to BCI1 activation. **Bi.** B45 was injected with a positive current square pulse. This elicited a single spike. **Bii.** B45 was injected with the same stimulus as in Bi. but after BCI1 activation. The stimulus elicited 7 spikes in B45. **Biii.** B45 was injected with the same stimulus as in Bi. and Bii. in the absence of BCI1 activation, eliciting a single spike only. **Biv.** There was a significant increase in B45's excitability in the BCI1 pre-activation trial compared with both the before and after trials. **Ci.** B45 was injected with a negative current square pulse. Upon release, B45 depolarised, however this was subthreshold. **Cii.** BCI1 was activated prior to B45 hyperpolarisation. After the stimulus, B45 fired two spikes. **Ciii.** B45 was injected with the same stimulus as in Bi. and Bii. but in the absence of BCI1 activation. B45 fired no spikes. **Civ.** Dunn's test revealed no significant difference between conditions. All experiments in HiDi saline. * $P < 0.05$, ** $P < 0.01$.

B45 activity in the rasp phase via a delayed depolarisation which increased B45's excitability. This was likely to increase B45 activity due to N2v excitation in the rasp phase, providing more inhibition to B11 and B12 in the rasp phase of egestive motor programs.

7.2.7.4 Connections from CBIs to B45

It was next tested how CV1a reduced B45 activity in the rasp phase. CV1a activity hyperpolarised B45 activity in HiDi saline (n=8) (**Figure 7.23A**). This can therefore account for some of the hyperpolarisation of B45 seen in the protraction phase of CV1a driven cycles. Since CV1a and B45 fire out of phase with each other, it was tested whether CV1a reduced B45 firing activity after CV1a activity had stopped. B45 was injected with positive current to fire a burst of action potentials, in the absence of CV1a activation (**Figure 7.23Bi**). In the next trial CV1a was stimulated prior to the stimulus to B45 (**Figure 7.23Bii**). The same stimulus to B45 was then presented again in the absence of CV1a activation (**Figure 7.23Biii**). There was a significant decrease in B45's excitability in the CV1a pre-stimulation trial compared with both the before and after trials, whereas there was no significant difference between the before and after trial (n=6) (Number of B45 spikes Before = 10.3 ±2.1, CV1a pre stimulation = 4.9 ±2.2, After = 10.7 ±2.1, Friedman test: df = 5, χ^2 = 9.48, $P < 0.01$. Dunn's test Before vs. CV1a pre stimulation $P < 0.05$, After vs. CV1a pre stimulation $P < 0.05$, Before vs. After $P > 0.05$) (**Figure 7.23Biv**). Preliminary experiments were performed to determine whether CV1a activity reduced B45's PIR. A similar protocol as in the BCI pre-stimulation was used. However a larger negative current was used to increase the size of the PIR on B45, to elicit spiking activity (**Figure 7.23Ci**). CV1a pre-stimulation prevented any PIR spikes in B45 (**Figure 7.23Cii**). B45's PIR was again tested in the absence of CV1a activity, and B45 elicited PIR spikes again (**Figure 7.23Ciii**). This was only performed in two preparations with mean values as follows: Before = 4 ±1, CV1a pre stimulation = 0.8 ±02, After = 6.5 ±0.5 (**Figure 7.23Civ**). Therefore CV1a produces an opposite effect on B45 from BCI1. CV1a inhibits B45 in the protraction phase, but also reduces B45 excitability once CV1a activity has stopped, reducing B45 activity in the rasp phase. Preliminary data also suggests that CV1a reduces B45 PIR activity. In two preparation it was found that CV1d inhibited B45 in HiDi saline (**Figure 7.23Di**). Unitary IPSPs on B45 followed CV1d spikes 1:1 (**Figure 7.23Dii**). The synaptic connections from BCI1 and CV1a to B45 were sufficient to explain the relative activation of B45 in ingestive and egestive motor programs, and in turn the relative activity of B11 and B12 in the rasp phase of each motor program.

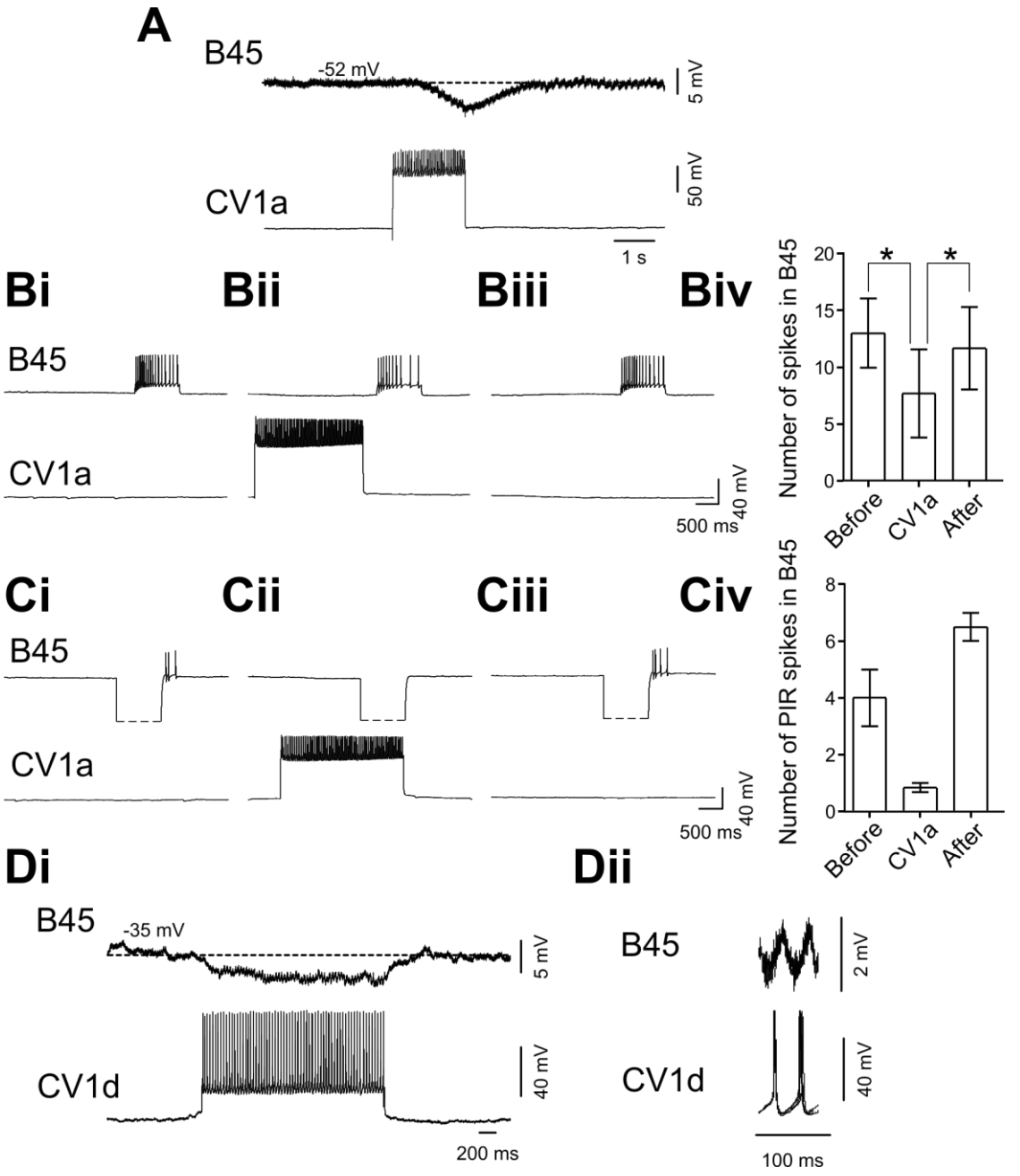

Figure 7.23 CV1a and CV1d connections with B45 **A.** Activation of CV1a hyperpolarised B45. **Bi.** B45 was injected with a positive current square pulse. This elicited 17 spikes. **Bii.** B45 was injected with the same stimulus as in Bi. but after CV1a activation. The stimulus elicited 10 spikes in B45. **Biii.** B45 was injected with the same stimulus as in Bi. and Bii. in the absence of CV1a activation, eliciting 15 spikes. **Biv.** There was a significant decrease in B45's excitability in the CV1a pre-activation trial compared with both the before and after trials. **Ci.** B45 was injected with a negative current square pulse. Upon release, B45 depolarised and fired 3 PIR spikes **Cii.** CV1a was activated prior to B45 hyperpolarisation. After the stimulus, B45 fired no spikes. **Ciii.** B45 was injected with the same stimulus as in Bi. and Bii. but in the absence of CV1a activation. B45 fired 4 spikes. **Civ.** This was only performed in 2 preparations, so the data could not be statistically analysed, however there appears to be a reduction in B45's PIR in the CV1a pre stimulation trial. **Di.** CV1d activation hyperpolarised B45. **Dii.** Unitary IPSPs on B45 followed CV1d spikes 1:1. All experiments in HiDi saline. * $P < 0.05$

7.2.8 Activity of protraction phase ingestion and egestion interneurons in different motor programs

Results in the above section provide evidence that activation of different command-like interneurons can drive B11 and B12 activity in different phases. It was next tested how the ingestive protraction phase interneurons and egestive protraction phase interneurons interacted with each other. During an ingestive motor program, the activation of BCI1 during the protraction phase would provide excitation to B11 and SLRT contraction in the protraction phase, which would produce a non-ingestive motor program. Similarly, in an egestive motor program, activation of CV1a would reduce the activity of B45 in the rasp phase, therefore increasing B11 activity and SLRT contraction in the rasp phase, producing a non-egestive motor program. Pair-wise recordings were made of ingestive protraction phase interneurons with egestive protraction phase interneurons. **Figure 7.24A** shows an example of BCI1 activity in a CV1a driven cycle. BCI1 showed no activity during the protraction phase, and was strongly hyperpolarised in the rasp phase. CV1a therefore does not activate BCI1 during CV1a ingestive motor programs. **Figure 7.24B** shows an example of BCI2 activity in a CV1a driven cycle. BCI2 was strongly hyperpolarised from the onset of CV1a activity throughout the protraction phase. BCI2 then showed the typical hyperpolarisation in the rasp phase. Therefore BCI2 was not active in CV1a ingestive motor programs either. This ensures that during CV1a driven ingestive motor programs, B11 and B12 receive no excitation from either BCI1 or BCI2 in the protraction phase, ensuring that the majority of their activity occurs in the rasp phase. **Figure 7.24C** shows an example of BCI1 activity in a CV1d driven cycle. BCI1 was depolarised in the protraction phase, however not sufficiently to reach threshold. **Figure 7.24D** shows an example of BCI1 activity in N1L driven cycles. BCI1 was not active in the protraction phase of the cycles. Therefore the ingestive protraction phase interneurons do not activate the egestive protraction phase interneurons.

Both the BCIs drive egestive motor programs. It was therefore tested whether each interneuron was active in the others driven cycle. **Figure 7.25Ai** shows an example of BCI2 activity in a BCI1 driven cycle. BCI2 was active throughout the protraction phase and hyperpolarised in the rasp phase. **Figure 7.25Aii** shows an example of BCI1 activity in a BCI2 driven cycle. BCI1 was active throughout the protraction phase and hyperpolarised in the rasp phase. Therefore the two egestive protraction phase interneurons recruit each other into their driven rhythms. It was next tested whether the BCIs activated the ingestive protraction phase interneurons. **Figure 7.25B** shows an example of CV1a activity in a BCI1 driven cycle. CV1a was hyperpolarised in the

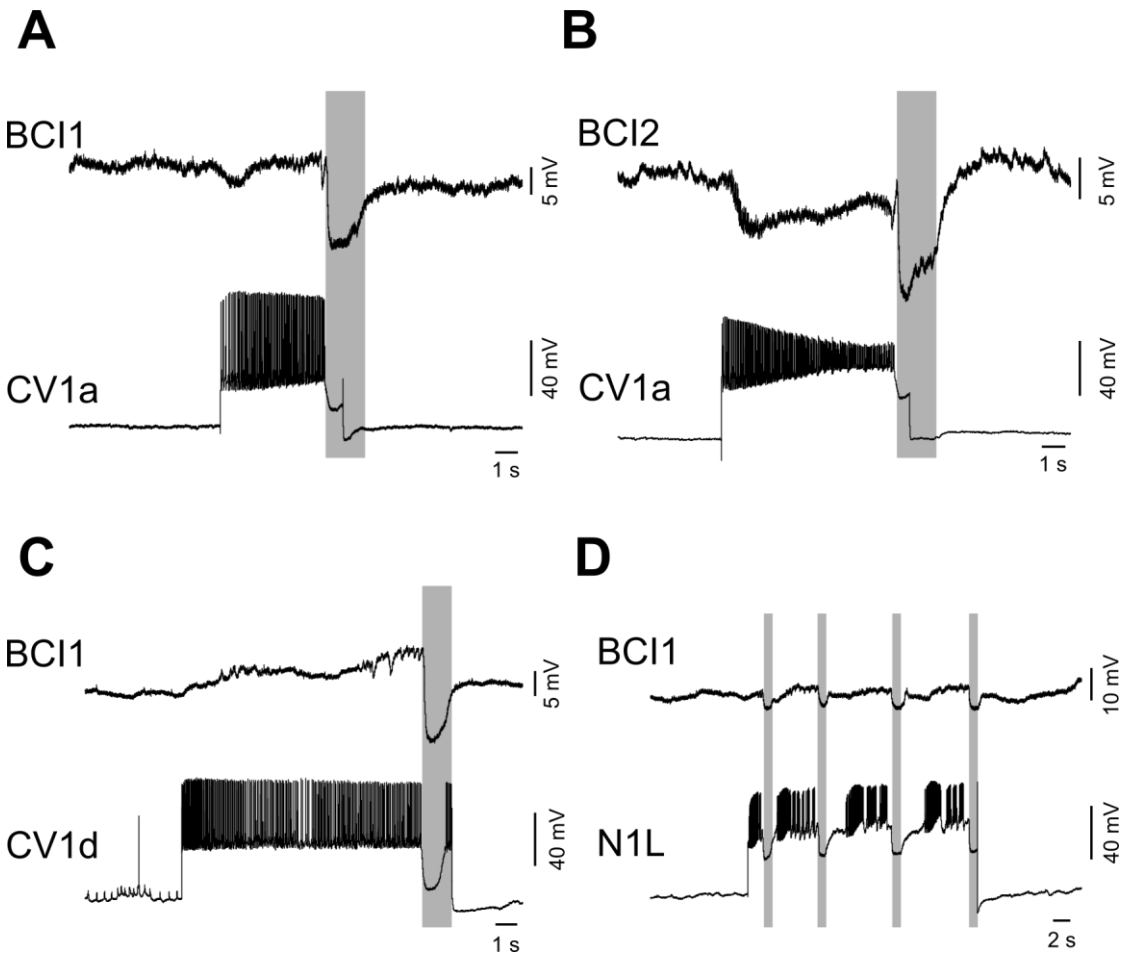

Figure 7.24 BCI activity in CBI and N1L cycles **A.** Activation of CV1a drives a single cycle. BCI1 fires no spikes in the protraction phase, and shows the usual hyperpolarisation in the rasp phase. **B.** Activation of CV1a drives a single cycle. BCI2 is hyperpolarised from the onset of CV1a activity and throughout the protraction and rasp phases. **C.** Activation of CV1d drives a single cycle. BCI1 is depolarised in the protraction phase, but not sufficiently to reach threshold. BCI1 and CV1d are hyperpolarised in the rasp phase. **D.** N1L activation drives four cycles. BCI1 is weakly depolarised in the protraction phases and hyperpolarised in the rasp phase, but is not active in any of the cycles. Grey vertical lines represent the rasp phase of a cycle.

protraction and rasp phase of the cycle. Interestingly, CV1a was not hyperpolarised throughout the entire protraction phase; rather the hyperpolarisations occurred in bursts at four points in the protraction phase. **Figure 7.25C** shows an example of CV1a activity in BCI2 driven cycles. CV1a was hyperpolarised in both the protraction and rasp phase of both BCI2 cycles. CV1a received similar inputs in the protraction phase in the BCI2 driven cycles as it did in BCI1 driven cycles. Therefore CV1a showed no activity in BCI driven cycles, ensuring that CV1a provides no inhibition to B45 in egestive motor programs. **Figure 7.25D** shows an example of CV1d and CV1a activity in BCI1 driven cycles. CV1d showed activity in the protraction phase of both cycles, whereas CV1a was not active. CV1d received the same hyperpolarising inputs as CV1a in the protraction and rasp phase. This confirms findings in Section 7.2.5.1 showing that CV1d can be active in BCI1 driven cycles **Figure 7.25E** shows an example of N1L activity in a BCI1 driven rhythm. N1L was excited in the protraction phase of each cycle, and fired two spikes in the second cycle. Therefore the BCIs do not strongly activate the ingestive protraction phase interneurons.

7.2.9 N1M activity in ingestive and egestive motor programs

The N1M interneuron is a CPG interneuron and has been shown to be necessary for fictive feeding to occur (Kemenes and Elliott, 1994, Kemenes et al., 2001). N1M was also found to be active in both CBI (Kemenes et al., 2001) and BCI (Section 4.2.3) driven cycles. **Figure 7.26A** shows an example of a CV1d and a BCI1 driven cycle. N1M was active in the protraction phase of both cycles. N1M was recorded firing in both a spontaneous ingestive (**Figure 7.26Bi**) and egestive motor programs (**Figure 7.26Bii**) recorded on a B12. In one preparation, activating N1M was able to generate both ingestive (**Figure 7.26Ci**) and egestive (**Figure 7.26Cii**) motor programs.

7.2.10 Connections between ingestive and egestive protraction phase interneurons

The connections between the ingestive protraction phase interneurons and egestive protraction phase interneurons was tested to see whether they could explain the relative activity of each of the interneurons in each motor program. Activation of CV1a in HiDi saline caused a small depolarisation of BCI1 (n=3) (**Figure 7.27A**). No 1:1 EPSPs were ever present; however the persistence in HiDi saline suggests that a component of the excitatory connection may be monosynaptic. In normal saline,

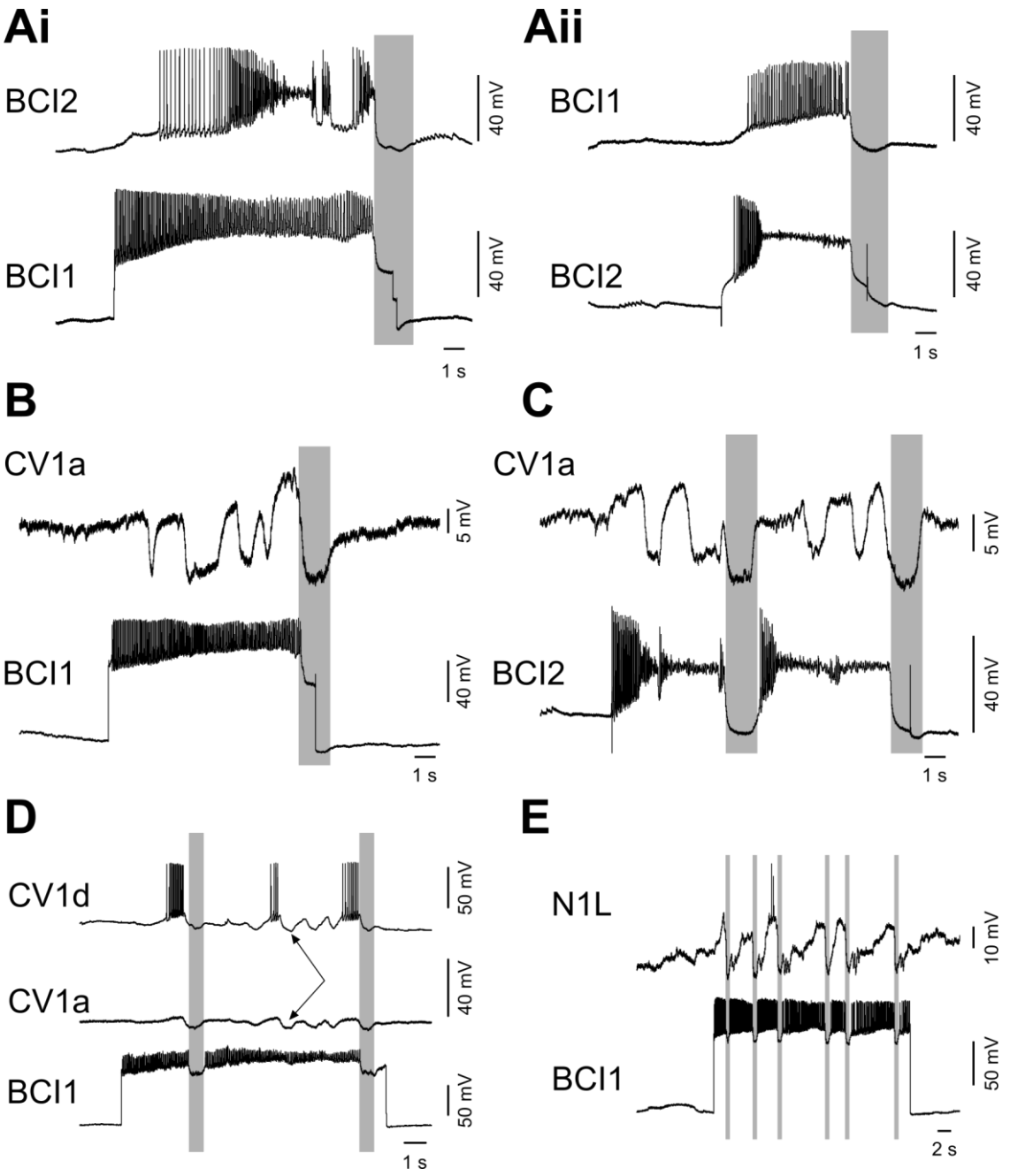

Figure 7.25 CBI and N1L activity in BCI driven cycles **Ai.** Activation of BCI1 drives a single cycle. BCI2 is active throughout the protraction phase and is hyperpolarised in the rasp phase. **Aii.** Activation of BCI2 drives a single cycle. BCI1 is active throughout the protraction phase of the cycle and is hyperpolarised in the rasp phase. **B.** Activation of BCI1 drives a single cycle. CV1a receives hyperpolarising inputs in the protraction and rasp phases. **C.** Activation of BCI2 drives a single cycle. CV1a receives hyperpolarising inputs in the protraction and rasp phases. **D.** BCI1 activation drives two cycles. CV1d fires in the protraction phase of both cycles, but receives similar hyperpolarising inputs in the protraction and rasp phases as CV1a. The black arrows indicate the similar inputs on CV1a and CV1d. **E.** BCI1 drives six cycles. N1L is depolarised in the protraction phase of each cycle but only fires two spikes in the third cycle. Grey vertical lines represent the rasp phase of a cycle.

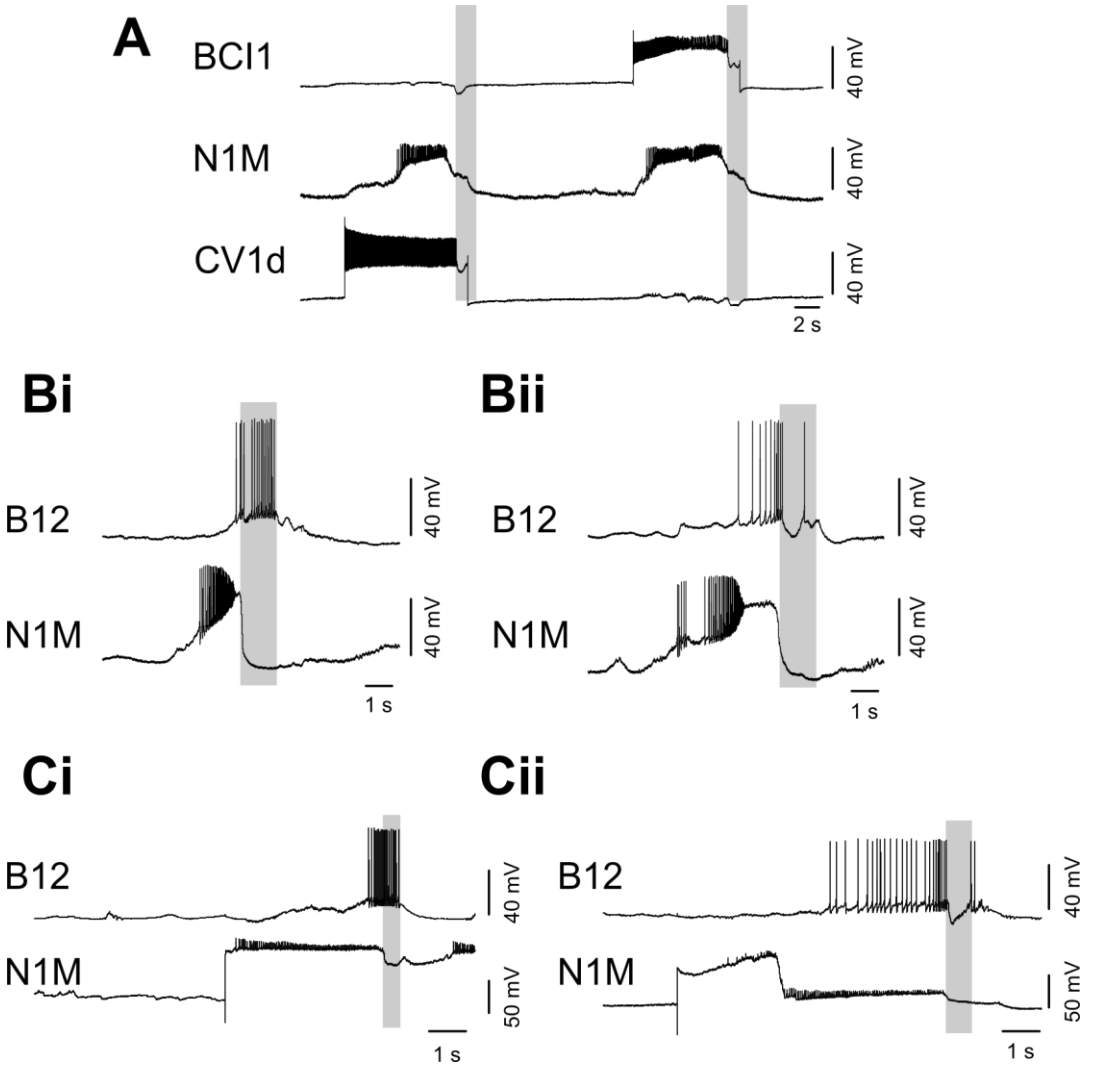

Figure 7.26 N1M activity in ingestive and egestive motor programs **A.** N1M was active in both a CV1d and a BCI1 driven cycle. Neither CV1d nor BCI1 was active in the other's driven cycle. N1M was active throughout the protraction phase of both cycles. **Bi.** N1M was active in a spontaneous ingestive motor program. B12 fired predominantly in the rasp phase and N1M the protraction phase. **Bii.** N1M was active in a spontaneous egestive motor program from the same preparation. B12 fired predominantly in the protraction phase, as did N1M. B12 received a large inhibitory input in the rasp phase. **Ci.** Activation of N1M drives B12 to fire predominantly in the rasp phase. **Cii.** Activation of N1M in the same preparation drives a single cycle. B12 fires predominantly in the protraction phase. Grey vertical lines represent the rasp phase of a cycle.

activation of CV1a inhibited the contralateral BCI2 (**Figure 7.27Bi**). Unitary IPSPs on BCI2 were present following CV1a spikes 1:1 (**Figure 7.27Bii**) suggesting that the connection was monosynaptic (n=3), however this was not tested in HiDi saline. No IPSPs were present on the ipsilateral BCI2 when CV1a was activated in normal saline (n=1) (**Figure 7.27C**). The inhibitory connection from CV1a to BCI2 can account for the lack of BCI2 activity in CV1a driven cycles, however the excitatory connection from CV1a to BCI1 is not sufficient to explain the lack of activity in BCI1 in CV1a driven cycles.

An electrotonic synapse was present between the two BCIs. Injecting negative current into the presynaptic neuron caused a similar yet attenuated hyperpolarisation of the postsynaptic neuron in normal saline (n=2) (**Figure 7.28Ai,Aii**). The electrotonic coupling between the two BCIs could account for the fact that each interneuron fires in driven cycles of the other. Activation of BCI1 in HiDi when CV1a was at RMP caused no change in CV1a's membrane potential (n=3) (**Figure 7.28Bi**). When CV1a was depolarised prior to BCI1 activation, BCI1 caused no hyperpolarisation of CV1a (**Figure 7.28Bii**). Therefore BCI1 was not the source of the inhibitory inputs seen on CV1a in the protraction phase of BCI1 driven cycles. BCI1 activation depolarised CV1d in HiDi saline in one preparation. In **Figure 7.28C** the depolarisation was sufficient to elicit spiking activity in CV1d. Therefore BCI1 did not monosynaptically inhibit the CBIs in the protraction phase of egestive motor programs. The BCI2 to CV1a connection was not tested in HiDi saline, however in normal saline, the hyperpolarising inputs to CV1a did not follow 1:1 from BCI2 spikes (see **Figure 7.25C**).

7.2.11 Identification and function of BCI3 in motor programs

A candidate for the source of the inhibition on CV1a in the protraction phase of egestive cycles was identified in the buccal ganglia. A pair of bilaterally symmetrical neurons was identified on the ventral surface of the buccal ganglia (**Figure 7.29A**). Dye injection revealed that the neuron had a single projection down the ipsilateral CBC which entered the cerebral ganglion (n=3) (**Figure 7.29B**). It was therefore named Buccal-Cerebral interneuron 3 (BCI3). BCI3 showed evidence of an endogenous plateau potential. When BCI3 was injected with a short duration positive current pulse, activity in BCI3 persisted after the stimulus had been removed (**Figure 7.29Ci**). Injecting BCI3 with a short duration negative current pulse during the plateau terminated the plateau potential (**Figure 7.29Cii**). BCI3's plateau potential persisted in HiLo saline (n=5) (**Figure 7.29D**), strongly suggesting that this was an endogenous

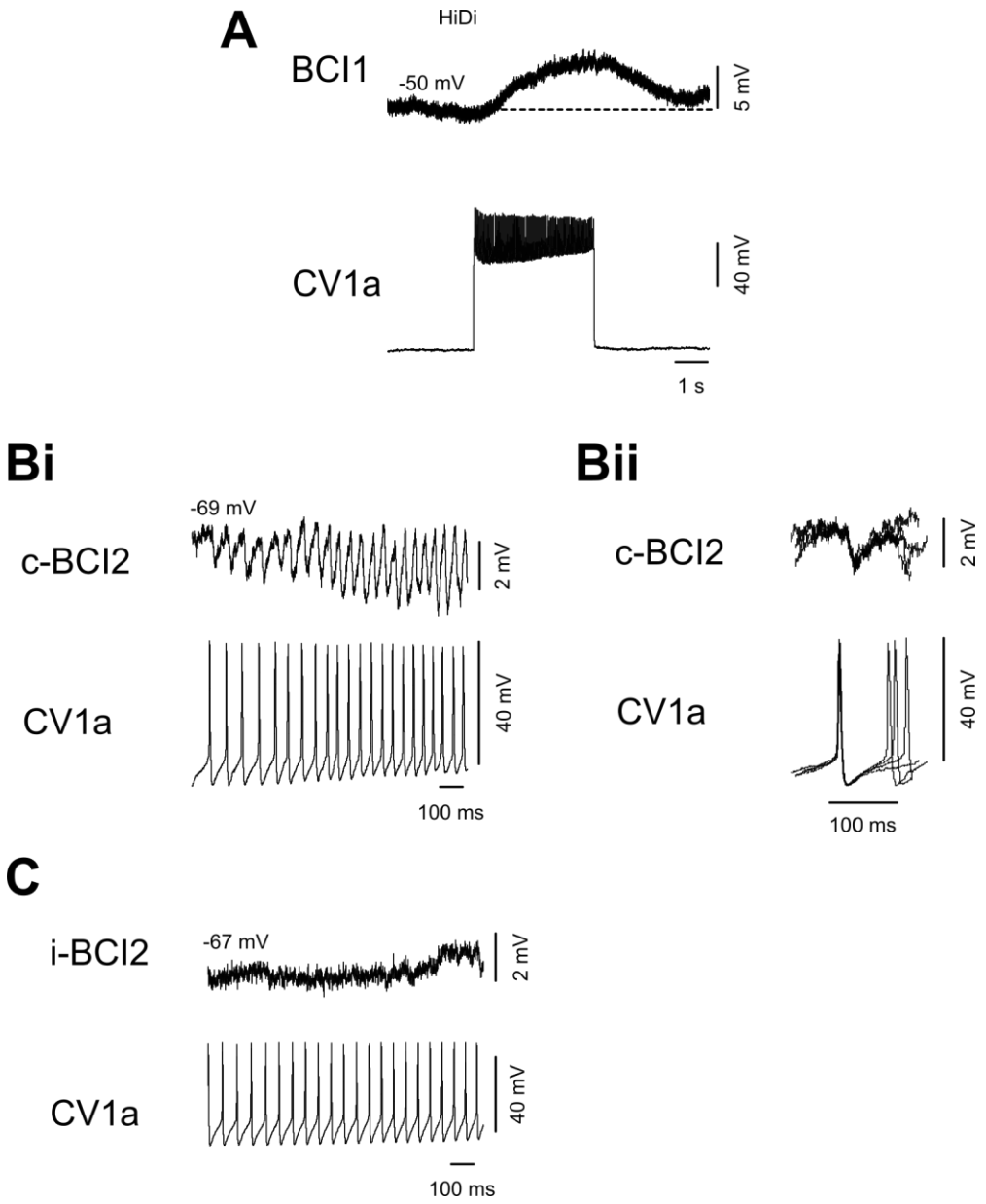

Figure 7.27 Connections from CV1a to BCI1 and BCI2 **A.** Activation of CV1a in HiDi saline caused a depolarisation of BCI1. **Bi.** Activation of CV1a in normal saline hyperpolarised the contralateral BCI2. **Bii.** Unitary IPSPs on the contralateral BCI2 followed CV1a spikes 1:1 **C.** Activation of CV1a caused no change in the membrane potential of the ipsilateral BCI2 in normal saline and there was no evidence of 1:1 IPSPS on BCI2. Values above each trace indicate membrane potential prior to CV1a activation.

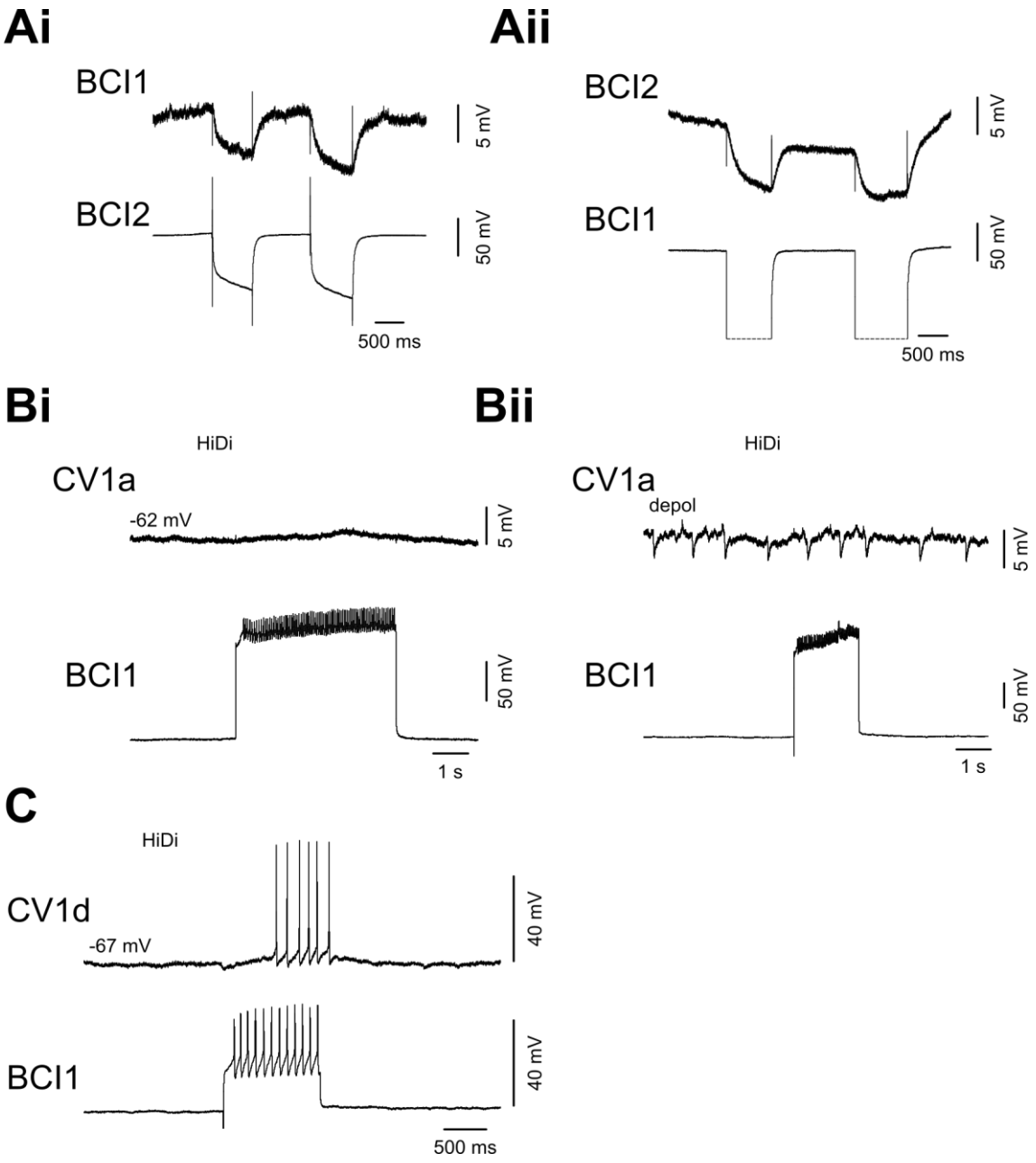

Figure 7.28 Connections between BCIs and CBIs **A.** Injecting negative current into BCI1 caused a similar yet attenuated hyperpolarisation of BCI2. **Ai.** Injecting negative current into BCI2 caused a similar yet attenuated hyperpolarisation of BCI1. **Bi.** Activation of BCI1 caused no change in CV1a membrane potential in HiDi saline. **Bii.** Depolarising CV1a prior to BCI1 activation revealed that there was no inhibitory connection from BCI1 to CV1a. **C.** Activation of BCI1 depolarised CV1d in HiDi saline. This was sufficient to elicit spiking activity in CV1d. Values above traces indicate the neurons membrane potential before BCI1 activation.

property of the interneuron. BCI3 activation in HiDi saline caused a large hyperpolarisation of CV1a (**Figure 7.29E**). No unitary IPSPs were ever present, however the persistence in HiDi saline does not allow us to rule out that a component of the connection was monosynaptic (n=3). The inhibitory connection from BCI3 to CV1a made BCI3 a good candidate for the inhibitory inputs seen on CV1a in BCI1 and BCI2 driven cycles.

During a CV1a driven cycle, BCI3 was active in the late protraction phase and throughout the rasp phase (**Figure 7.30Ai**). In a BCI1 driven cycle, BCI3 was active in the protraction phase and then throughout the rasp phase (**Figure 7.30Aii**). CV1a hyperpolarisation in BCI1 driven cycles occurred at the onset of BCI3 activity. This was most evident when BCI3 activity stopped in the protraction phase, allowing CV1a to return to RMP before BCI3 became active again, hyperpolarising CV1a again. The percentage of the protraction phase at which BCI3 became active was analysed in CV1a and BCI1 driven cycles. BCI3 become active at 75.2% (±3.3) of the protraction phase in CV1a driven cycles (30 CV1a driven cycles in 8 preparations), whereas BCI3 was active at 3.3% (±1.8) of the protraction phase in BCI1 driven cycles (22 BCI1 driven cycles in 7 preparations). There was a significant difference between BCI3's onset in the protraction phase of CV1a and BCI1 driven cycles (unpaired t-test $df = 50$, $t = 17.5$, $P < 0.0001$) (**Figure 7.30Bi**). The percentage of the rasp phase at which BCI3 stopped firing was analysed in CV1a and BCI1 driven cycles. BCI3 stopped firing at 99.27% (±0.3) of the rasp phase in CV1a driven cycles, whereas BCI3 stopped firing at 94.8% (±1.5) of the rasp phase in BCI1 driven cycles. There was a significant difference between the cessation of firing of BCI3 in the rasp phase in CV1a and BCI1 driven cycles (unpaired t-test $df = 50$, $t = 3.4$, $P < 0.01$) (**Figure 7.30Bii**). Therefore, BCI3 fired predominantly in the rasp phase of CV1a driven cycles, whereas BCI3 fired in both the protraction and rasp phase in BCI1 driven cycles.

To test whether BCI3 was the source of the inhibitory inputs to CV1a in the protraction phase, suppression experiments were performed. BCI1 was activated to drive three cycles (**Figure 7.30Ci**). BCI3 fired in the protraction phase of all three cycles. CV1a received hyperpolarising inputs in the protraction phase of all three cycles and only fired at the end of the second protraction phase. BCI3 was then injected with negative current prior to BCI1 activation (**Figure 7.30Cii**). BCI1 was then activated to drive three cycles. CV1a fired in the protraction phase of all three cycles with BCI3 activity absent. Therefore, BCI3 was the source of inhibition on CV1a in the protraction phase of BCI1 driven cycles.

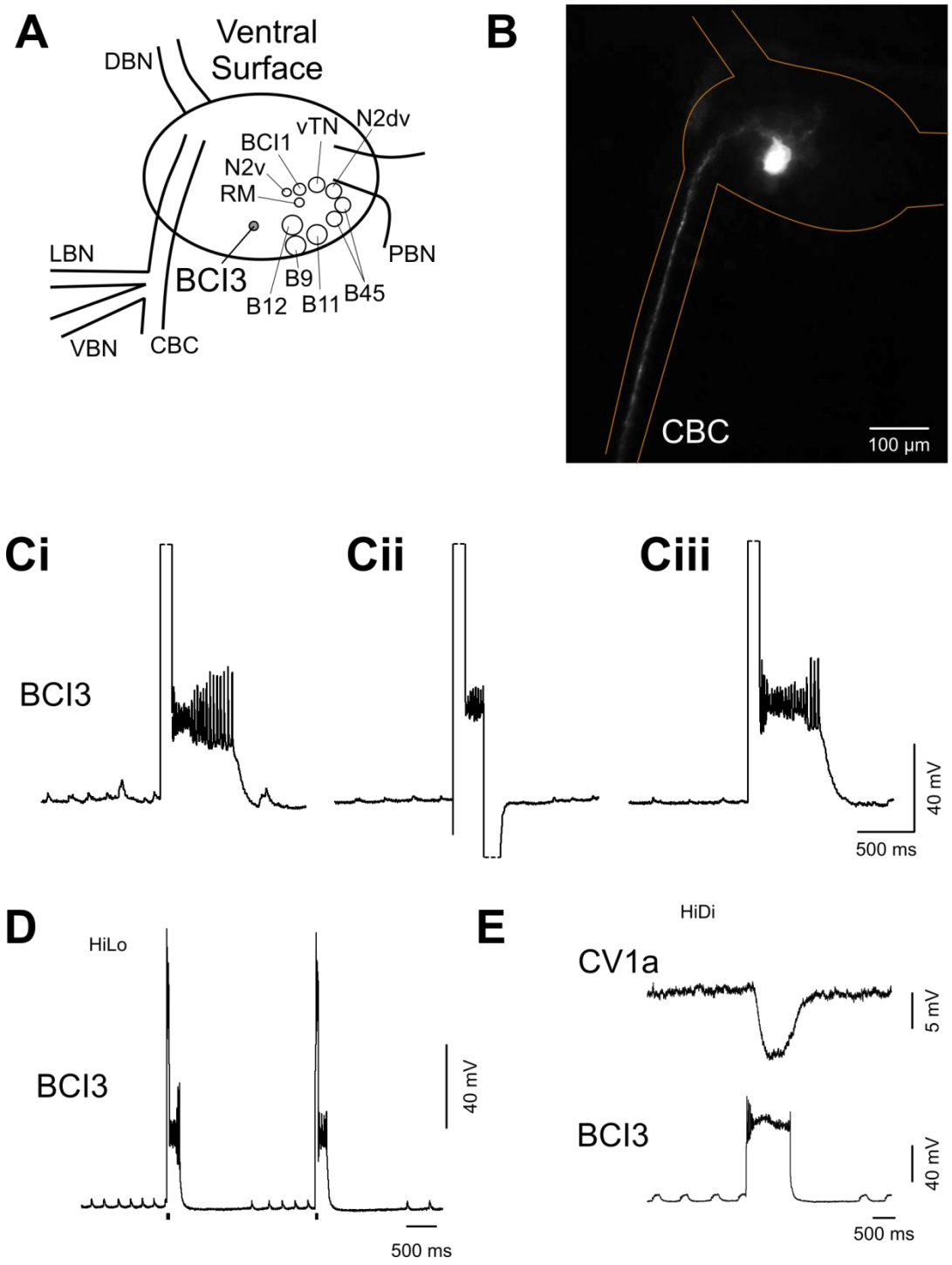

Figure 7.29 Identification and characterisation of BCI3 **A.** BCI3 was located on the ventral surface of the buccal ganglion. There was a single BCI3 per buccal ganglia. **B.** BCI3 had a single projection which left the buccal ganglion via the ipsilateral CBC. **Ci.** BCI3 showed evidence of an endogenous plateau potential. BCI3 was injected with a short duration positive current pulse. BCI3 remained depolarised after the stimulus had been removed from the neuron. **Cii.** BCI3s plateau potential could be prematurely terminated by injecting a negative current pulse into BCI3 during the plateau. **Ciii.** BCI3s plateau was present in the absence of the negative current pulse. **D.** BCI3s plateau potential was present in HiLo saline. Black bars under the trace indicate duration of the pulse to BCI3. **E.** Activation of BCI3 hyperpolarised CV1a in HiDi saline.

BCI1's connection with BCI3 was tested to determine how BCI3 was recruited into BCI1 cycles. In HiDi saline BCI1 depolarised BCI3 (n=5). Unitary EPSPs were present on BCI3 following BCI1 spikes 1:1 (**Figure 7.31A**), providing strong evidence that the connection was monosynaptic. Injecting either neuron with negative current caused a similar yet attenuated hyperpolarisation of the postsynaptic neuron in normal saline (n=6). This persisted in HiLo saline (n=2) (**Figure 7.31Bi,Bii**) strongly suggesting that the connection was electrotonic in nature. A BCI3 was injected with identical positive current pulses at regular intervals which did not initiate plateau potentials (**Figure 7.31C**). BCI1 activation depolarised BCI3 and the pulses to BCI3 initiated plateau potentials. This was then studied with respect to CV1a. Subthreshold regular interval pulses were applied to BCI3. BCI1 activation converted these into suprathreshold and plateau potentials were initiated in BCI3. The BCI3 plateau potentials hyperpolarised CV1a (**Figure 7.31D**). This provides strong evidence that BCI1 inhibits CV1a via activation of BCI3. In normal saline, BCI2 activated BCI3 in the protraction and rasp phases (**Figure 7.31Ei**). When BCI3 was injected with negative current prior to BCI2 activation, unitary EPSPs were present on BCI3 following BCI2 spikes 1:1 (**Figure 7.31Eii**) in normal saline, suggesting that BCI2 monosynaptically excites BCI3.

7.2.12 BCI3 connections with N2v and B11/12

Similar to B11 and B12, BCI3 could fire in both the protraction and rasp phase. The excitatory inputs from BCI1 and BCI2 to BCI3 could account for the excitation in the protraction phase, but not the activity in the rasp phase. It was therefore tested whether BCI3 was excited by N2v. In HiDi saline, activation of N2v depolarised BCI3 sufficiently to elicit spiking activity (n=4) (**Figure 7.32Ai**). Injecting negative current into N2v caused a similar yet attenuated hyperpolarisation of BCI3 (**Figure 7.32Aii**), this connection persisted in HiLo saline (n=3). Artificial activation of BCI3's plateau potential revealed that BCI3's plateau depolarised N2v sufficiently to initiate N2v spiking activity (**Figure 7.32Bi**). Importantly, BCI3's plateau occurred before the onset of N2v's plateau and could occur in the absence of any N2v activity (**Figure 7.32Bii**). BCI3 activation elicited spiking activity in both B11 (**Figure 7.32Ci**) and B12 (**Figure 7.32Di**).

BCI3 was electrotonically coupled with both B11 and B12. Injecting negative current into BCI3 caused a similar yet attenuated hyperpolarisation of B11 (**Figure 7.32Cii**) and B12 (**Figure 732Dii**) and injecting negative current into either B11 (**Figure 7.32Cii**) or B12 (**Figure 7.32Diii**) caused a similar yet attenuated hyperpolarisation of BCI3

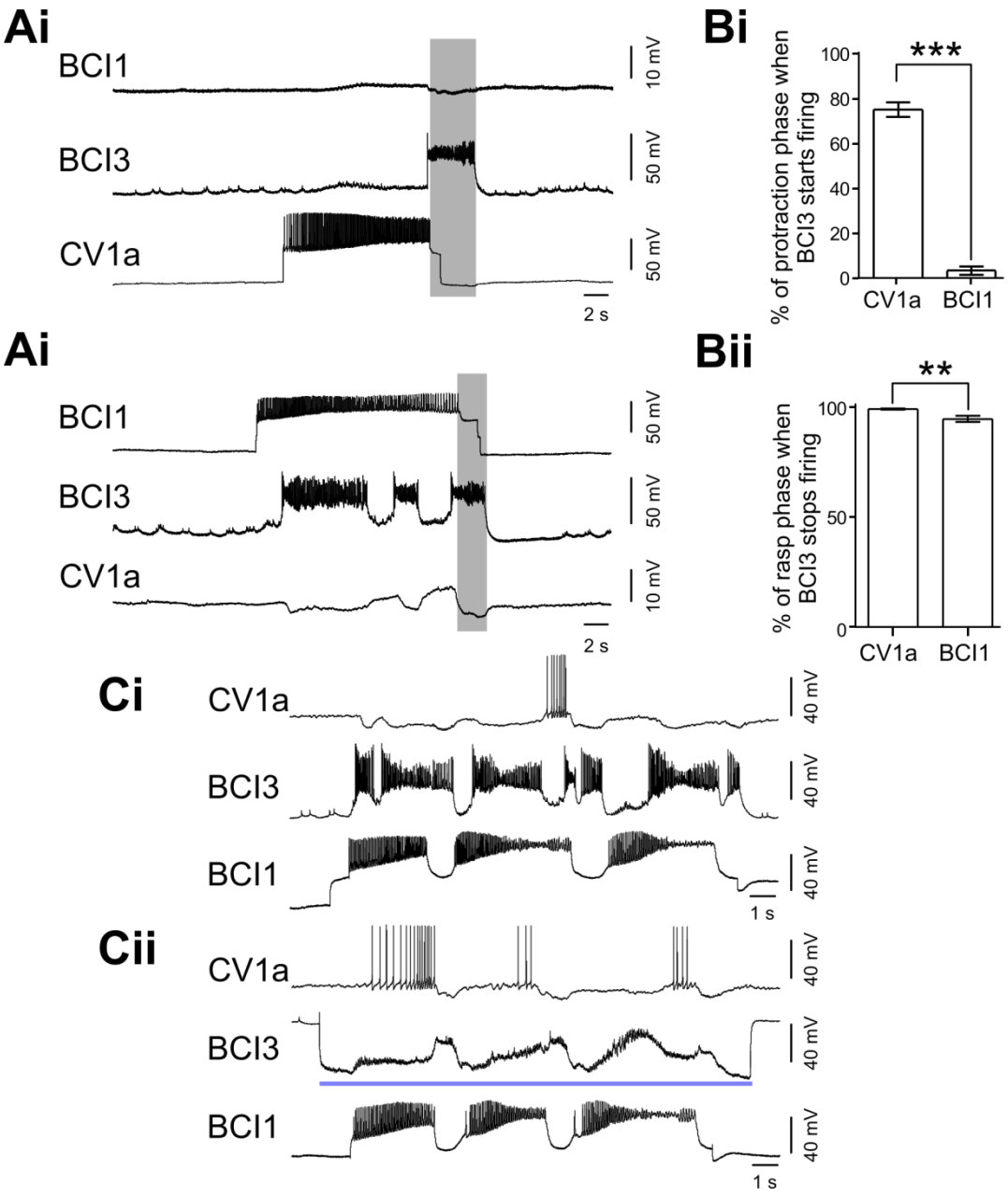

Figure 7.30 BCI3 activity in CV1a and BCI1 cycles **Ai.** Activation of CV1a drove a single cycle. BCI3 was active in the late protraction phase and throughout the rasp phase of the cycle only. **Aii.** Activation of BCI1 drove a single cycle. BCI3 was active in the protraction and rasp phases. Each burst of BCI3 activity was accompanied by hyperpolarising inputs on CV1a in the protraction phase. **Bi.** The onset of BCI3 activity in the protraction phase was earlier in BCI1 driven cycles than CV1a driven cycles **Bii.** BCI3 activity persisted later into the rasp phase in CV1a cycles than BCI1 cycles. **Ci.** Activation of BCI1 drove three cycles. BCI3 was active in the protraction and rasp phase of all cycles. CV1a was only active in the protraction phase of the second cycle. **Cii.** BCI3 was injected with negative current to prevent spiking activity prior to BCI1 activation. BCI1 activation drove three cycles. CV1a was active in the protraction phase of all three cycles, in the absence of BCI3 inhibition. The blue rectangle represents the injection of hyperpolarising current into BCI3. Grey vertical lines represent the rasp phase of a cycle. ** $P < 0.01$, *** $P < 0.001$.

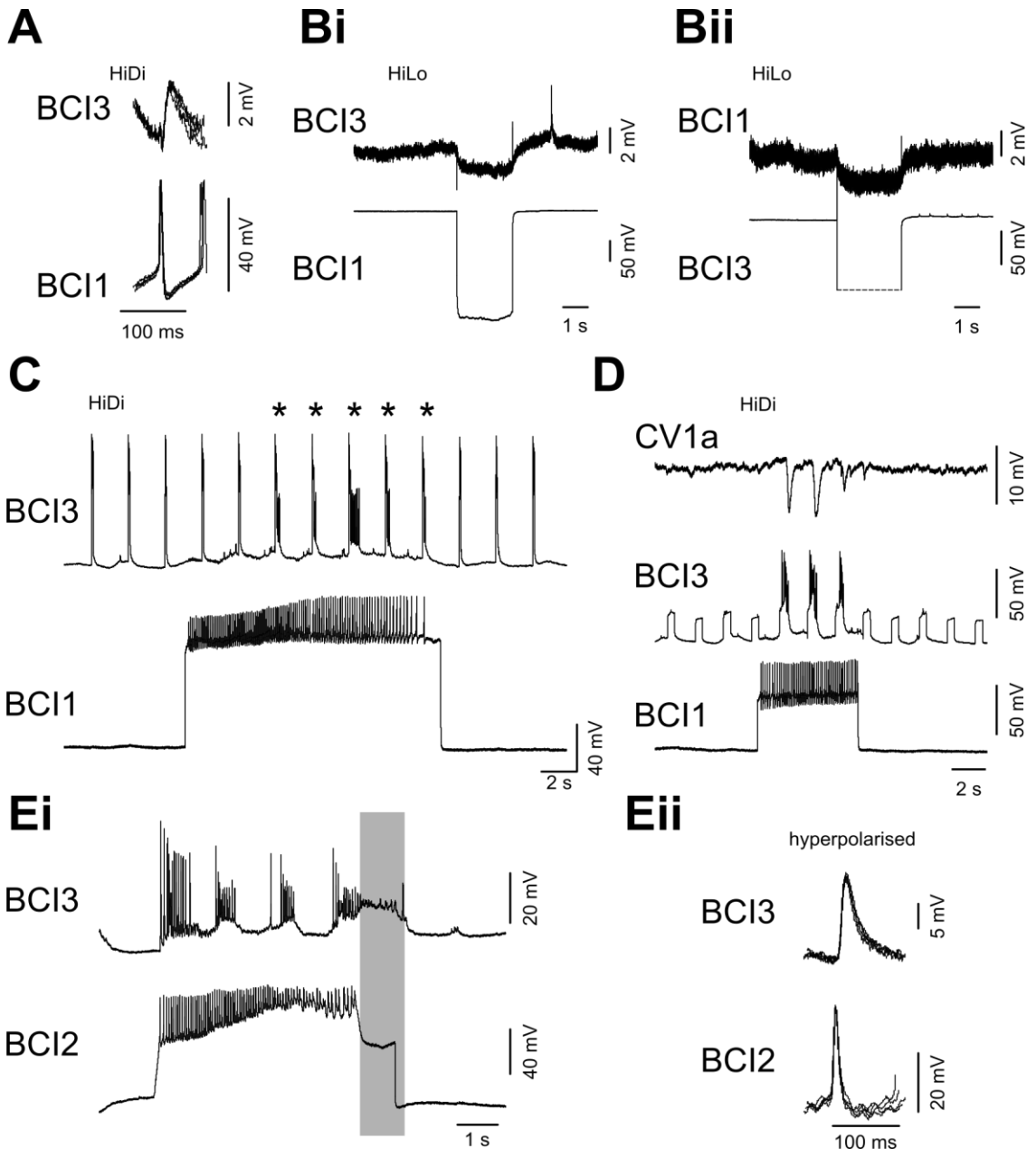

Figure 7.31 BCI1 and BCI2 connections with BCI3 **Ai.** Unitary EPSPs on BCI3 followed BCI1 spikes 1:1 in HiDi saline. **Bi.** Injecting negative current into BCI1 caused a similar yet attenuated hyperpolarisation of BCI3 in HiLo saline. **Bii.** Injecting negative current into BCI3 caused a similar yet attenuated hyperpolarisation of BCI1 in HiLo saline. **C.** BCI3 was injected with short duration positive current pulses which were insufficient to trigger BCI3's plateau potential. BCI1 was then activated. The same pulses to BCI3 elicited plateau potentials in BCI3 for the duration of BCI1 activation. The asterisk symbols above each pulse marks each BCI3 plateau potential. **D.** BCI3 was injected with short duration sub-threshold positive current pulses whilst a CV1a was recorded. BCI1 activation depolarised BCI3 and the pulses became suprathreshold and generated plateau potentials. BCI3 activation hyperpolarised CV1a. **Ei.** BCI2 activation drove a single cycle. BCI3 was active in the protraction and rasp phases of the cycle. **Eii.** Unitary EPSPs on BCI3 followed BCI2 spikes 1:1 in normal saline. BCI3 was hyperpolarised prior to BCI2 activation.

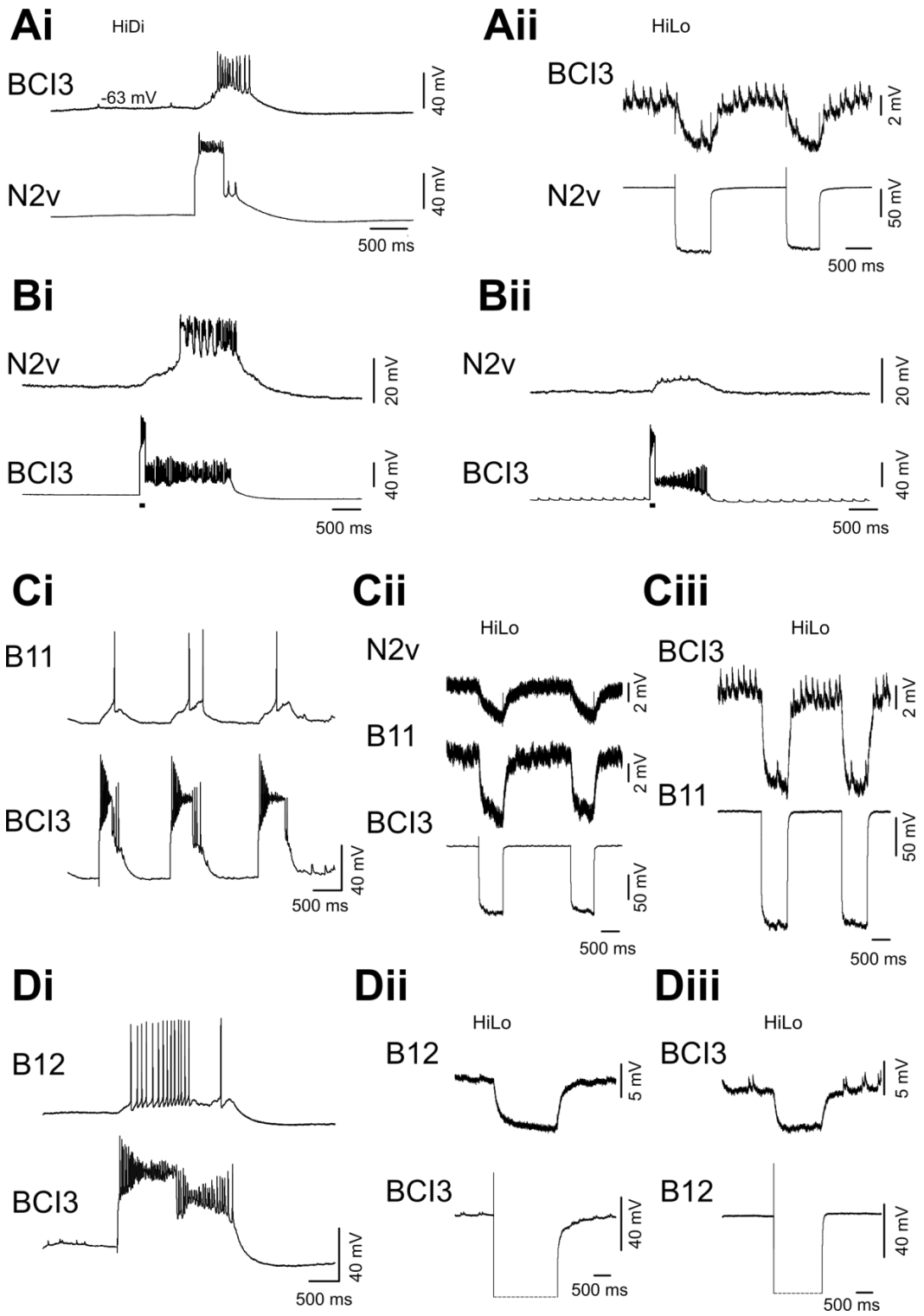

Figure 7.32 BCI3 connections with N2v, B11 and B12 **Ai.** Activation of N2v depolarised BCI3 in HiDi saline. This was sufficient to elicit spiking activity in BCI3. **Aii.** Injecting negative current into N2v caused a similar yet attenuated hyperpolarisation of BCI3 in HiLo saline. **Bi.** BCI3's plateau potential could activate a plateau potential in N2v. BCI3's plateau potential occurs before the onset of N2v's plateau. **Bii.** BCI3's plateau potential could be initiated in the absence of an N2v plateau. **Ci.** Activation of BCI3 depolarised B11 in normal saline. **Cii.** Injecting negative current into BCI3 caused a similar yet attenuated hyperpolarisation of N2v and B11 in HiLo saline. **Ciii.** Injecting negative current into B11 caused a similar yet attenuated hyperpolarisation of BCI3 in HiLo saline. **Di.** Activation of BCI3 depolarised B12 in normal saline. **Dii.** Injecting negative current into BCI3 caused a similar yet attenuated hyperpolarisation of B12 in HiLo saline. **Diii.** Injecting negative current into B12 caused a similar yet attenuated hyperpolarisation of BCI3 in HiLo saline.

(BCI3-B11 in normal saline n=4, BCI3-B12 in normal saline n=3). This persisted in HiLo saline (BCI3-B11 n=2 and BCI3-B12 n=1) strongly suggesting that the connection was electrotonic in nature. **Figure 7.32Cii** also shows an example of coupling from BCI3 to N2v in HiLo saline. Therefore, BCI3 may play a role in B11 and B12 activation in ingestion and egestion as well as inhibiting CV1a in the protraction phase of egestive cycles.

7.2.13 Characterisation of vTN triggered motor programs

vTN was shown to be able to reliably trigger fictive feeding cycles in Chapters 3, 4, 5 and 6. The type of motor program which vTN initiated was tested by recording a B11 or B12 motor neuron during triggered cycles. vTN was found to be able to trigger both ingestive and egestive motor programs. B11 was recorded in 56 triggered cycles by vTN in 12 preparations. The average B11 activity in the protraction phase was 7.7 Hz (±0.8) and in the rasp phase was 12.8 Hz (±1.4). B12 was recorded in 86 cycles triggered by vTN in 13 preparations. The average B12 activity in the protraction phase was 2.1 Hz (±0.3) and in the rasp phase was 13.0 Hz (±0.8). **Figure 7.33A** shows an example of B11 activity in a vTN triggered rhythm. vTN triggered three cycles. B11 was active predominantly in the rasp phase of all three cycles, similar to ingestive motor programs. **Figure 7.33B** shows an example of B11 activity in a vTN triggered rhythm from a separate preparation. B11 activity occurred predominantly in the protraction phase of all cycles, similar to egestive motor programs. B11 (**Figure 7.33C**) and B12 (**Figure 7.33D**) activity in the protraction and rasp phases of vTN triggered cycles was plotted on the same axis as B11 and B12 activity in sucrose and AA cycles. Interestingly, B11 and B12 activity in vTN triggered cycles did not cluster around either the sucrose or the AA cycles only. vTN triggered cycles clustered amongst both the sucrose and the AA cycles, suggesting that vTN was able to trigger both ingestive and egestive motor programs. Interestingly, within the same preparation, vTN could trigger either ingestive or egestive motor programs.

Figure 7.34Ai shows an example of a single cycle ingestive motor program triggered by vTN. B11 was active predominantly in the rasp phase of the cycle. A CV1a and a BCI1 were also recorded in this preparation. CV1a was active throughout the protraction phase of the triggered cycle, whereas BCI1 was not active in the cycle. **Figure 7.34Aii** shows an example from the same preparation of a single egestive motor program triggered by vTN. B11 was active throughout the protraction phase and in the early rasp phase only of the cycle. In this cycle, CV1a was not active in the protraction phase, whereas BCI1 was active throughout the protraction phase. It remains unknown how vTN was able to drive the two different behaviours. There was

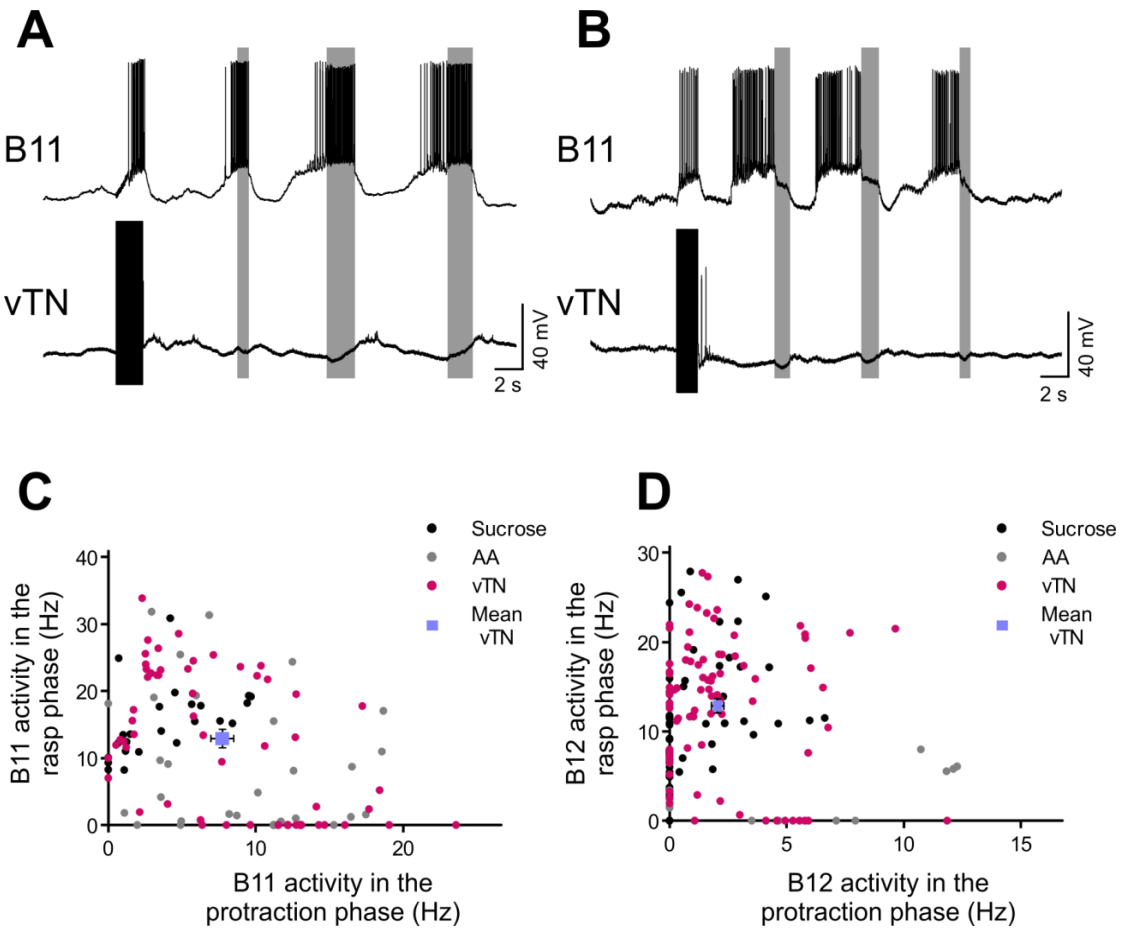

Figure 7.33 B11 and B12 activity in vTN triggered cycles **A.** vTN triggered three cycles recorded on a B11. B11 fired in the late protraction and throughout the rasp phase of all three cycles. **B.** vTN triggered three cycles recorded on a B11. B11 fired predominantly in the protraction phase and in the early rasp phase of all three cycles. **C.** B11's activity in the protraction and rasp phase of vTN triggered cycles plotted with B11's activity in the protraction and rasp phase of sucrose and AA cycles from Figure 7.8A. **D.** B12's activity in the protraction and rasp phase of vTN triggered cycles plotted with B12's activity in the protraction and rasp phase of sucrose and AA cycles from Figure 7.9A. Grey vertical lines represent the rasp phase of a cycle.

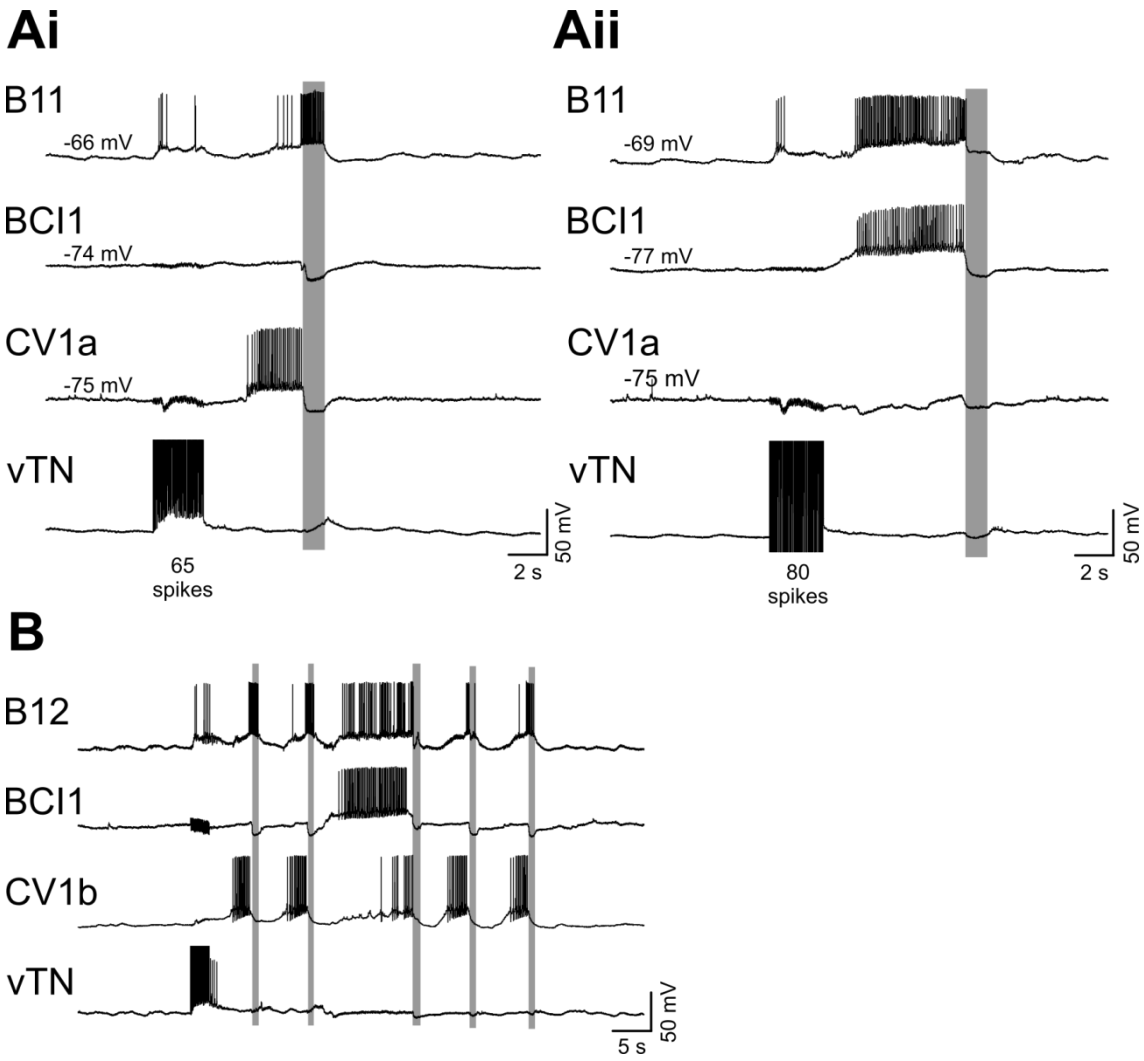

Figure 7.34 vTN triggers both ingestive and egestive motor programs **Ai.** vTN triggered a single cycle. B11 was active predominantly in the rasp phase. CV1a was active in the protraction phase of the cycle. BCI1 showed no activity in the cycle. **Aii.** vTN triggered a single cycle in the same preparation. B11 was active in the protraction phase only. CV1a was hyperpolarised in the protraction and rasp phases of the cycle. BCI1 was active throughout the protraction phase of the cycle. **B.** vTN triggered five cycles recorded on a B12.In the first, second, fourth and fifth cycles, B12 was active predominantly in the rasp phase. CV1b was active in the protraction phase of all of the cycles, whereas BCI1 was not in any of the cycles. In the third triggered cycle, B12 was active predominantly in the protraction phase and in the early rasp phase only. CV1b was weakly active in the cycle, whereas BCI1 was active throughout the protraction phase. The values above the traces indicate the neuron's membrane potential prior to vTN activation. Grey vertical lines represent the rasp phase of a cycle.

no large difference between the membrane potential of the two protraction phase interneurons at the time of vTN activation which would bias their activity. One difference was the number of vTN spikes elicited to trigger the two cycles. In the ingestive motor program, only 65 vTN spikes were elicited, whereas in the egestive motor program 80 vTN spikes were elicited. One interesting feature of vTN triggered motor programs was that they were not always either ingestive or egestive only. **Figure 7.34B** shows an example of vTN triggering five cycles. B12's activity occurred predominantly in the rasp phase of the first, second, fourth and fifth cycles, suggesting that these were ingestive motor programs. In the third cycle, B12 activity occurred predominantly in the protraction phase, suggesting that this was an egestive motor program. This experiment showed that the type of motor program could change within triggered cycles

7.3 Discussion

7.3.1 Ingestion and egestion in *Lymnaea* and *Aplysia*

In this chapter the egestion behaviour and its neural control in *Lymnaea* was studied. The choice to switch from an ingestive motor program to an egestive motor program could be initiated by the application of an aversive stimulus (AA) or by maintaining the same stimulus which generated the ingestive motor programs (maintained tactile stimulus). In order to characterise the mechanisms of behavioural choice under these two conditions it was first necessary to characterise the egestion behaviour. The egestion behaviour differed from the ingestion behaviour in two ways: the major phase of odontophore contraction switched from the rasp phase in ingestion to the protraction phase in egestion and the lateral edges of the odontophore were spread apart in protraction of ingestion and drawn close together in protraction of egestion. The consequence of this was that food was brought into the mouth in ingestion and pushed out of the mouth in egestion. The characterisation of both the ingestive and egestive motor programs has been most extensively been studied in *Aplysia*; therefore it proved informative to directly compare this behaviour in *Aplysia* versus *Lymnaea*. During ingestion in *Aplysia*, the radula is opened during protraction and closed during retraction, bringing food into the mouth. During egestion the radula is closed during protraction and opened during retraction, removing food from the mouth (Morton and Chiel, 1993a). The radula of *Lymnaea* differs from *Aplysia* in that the two halves cannot be brought fully together. However, the movements of the radula, via odontophore contraction, are similar. During the protraction phase of ingestion in *Lymnaea*, the

odontophore's lateral edges (and radula), are spread apart from each other, whereas during retraction the odontophore contracts and the two lateral edges are brought close together. During egestion the lateral edges of the odontophore are brought close together during the protraction phase and the odontophore flattens in the retraction phase. Therefore the actions appear similar to *Aplysia*; however since *Lymnaea* do not 'grasp' food between the two halves of the radula, the reversal stroke of the odontophore is used to remove food from the buccal cavity in *Lymnaea*. Interestingly, traces of ingestive behaviours in *Aplysia* in Morton and Chiel (1993a) reveal that the odontophore exits the mouth during the protraction phase from the posterior region of the mouth, whereas in egestion, the odontophore is protracted out of the mouth from the anterior region of the mouth, similar to *Lymnaea*. Therefore the two behaviours serve the same purpose in the two molluscs and are achieved in a similar manner.

The SLRT was the muscle identified as involved in odontophore contraction in *Lymnaea*. The homologous muscle in *Aplysia* is thought to be the I_4 muscle (Wentzell et al., 2009) which is involved in radula closing in ingestion and egestion (Morton and Chiel, 1993b) and involved in the switch between ingestion and egestion. Therefore the two molluscs use similar muscles to perform the same task but achieve it differently owing to the different capabilities of their odontophores.

B11 was identified as a SLRT motor neuron. Activation of B11 contracted the SLRT muscle, causing the movement of the odontophore dorsally, similar to the movements seen in the rasp phase of ingestion and the protraction phase of egestion. B11 fired predominantly in the rasp phase of sucrose driven cycles. These were considered ingestive since sucrose reliably initiated ingestive motor programs in vivo. Therefore during ingestive motor programs B11 activity causes SLRT contraction during retraction. This is in confirmation of the observations made in vivo and in the buccal mass preparation. Application of AA to the whole lip-CNS preparation caused a delayed phase shift of B11 activity from the rasp phase to the protraction phase. This did not occur immediately after the application of AA in vitro as it did in vivo. However, sucrose application often has a similar delayed onset in vitro which is not seen in vivo. The cycles whose phase shifted in the presence of AA in vitro were considered egestive because the application of AA during ingestive sucrose or solid lettuce driven cycles in vivo caused egestive motor programs. The phase shift of B11 from the rasp phase to the protraction phase would serve to shift the phase of the SLRT contraction from retraction to protraction, similar to the phase shift of odontophore contraction in egestive cycles. Therefore the switch of B11's activity from the rasp phase to the protraction phase represents a method to distinguish between ingestive and egestive

motor programs. This was an important distinction to make, since many aspects of the two behaviours appear the same. This can most clearly be seen by the fact that N2dv and B9's activity does not shift phases between the two behaviours. This is likely to be true of other feeding neurons, considering that the protraction and retraction of the odontophore remain within the same phases in both ingestion and egestion. The B12 motor neurons were also found to undergo a similar phase shift as B11 during ingestive and egestive motor programs. The function of B12 remains unknown.

7.3.2 Interneuronal control of ingestion and egestion in *Lymnaea*

The interneuronal control of ingestive and egestive motor programs was characterised by testing the phase of B11 and B12 activity in the protraction and rasp phases of protraction phase interneuron driven cycles. The CBIs (including the novel CV1d) and the local buccal interneuron N1L all generated ingestive motor programs, whereas the novel BCIs generated egestive motor programs. Therefore the CBIs and N1L were part of the ingestive network whereas the BCIs part of the egestive network. The motor neurons phase of firing was achieved via monosynaptic connections from the protraction phase interneurons with the motor neurons themselves (inhibition of B12 by CV1d, excitation of B11 and B12 by BCI1) and through preventing activity or activating a rasp phase neuron (B45) which was inhibitory to the motor neurons. Therefore there was a subset of ingestion interneurons and egestion interneurons. The two egestion interneurons were found to be either not active (BCI1) or strongly inhibited (BCI2) in CV1a driven cycles. This presumably prevented contradictor inputs to the motor neurons by preventing BCI excitation of them during the protraction phase. The ingestion neurons were inhibited (CV1a), not active (N1L) or active (CV1d) in BCI driven cycles. CV1a and CV1d received similar periods of inhibition in the protraction phase. Interestingly CV1d was occasionally active in BCI1 driven cycles, providing inhibitory inputs to B12 in the protraction phase. The function of this is unknown, since B12 still fired predominantly in the protraction phase of these cycles.

The egestive network prevented the activation of the ingestive network via activation of the multifunctional interneuron BCI3. BCI3 activity was similar to that of B11 and B12. It fired in the rasp phase of CV1a driven cycles and in the protraction phase of BCI1 driven cycles. BCI3 was coupled with both a protraction phase interneuron (BCI1) and a rasp phase interneuron (N2v). Coupling between neurons which fire in different phase has not been observed before in the feeding network of *Lymnaea* (Staras et al.,

1998b). However, BCI3 is able to fire in both phases; therefore its coupling with both the protraction and rasp phase is functionally relevant.

The recruitment of BCI3 was interesting, since it served the function of exciting B11 and B12 in the rasp phase of ingestive cycles and exciting B11 and B12 in the protraction phase of egestive cycles whilst also preventing CV1a activity. The neural circuitry involved in the two behaviours therefore showed examples of dedicated interneurons (CV1a, BCI1, and BCI2) and multifunctional interneurons (BCI3 and CV1d). The distinction between dedicated and multifunctional neurons has been studied in depth in the medicinal Leech. Many of the command-like interneurons for swimming were found to be active in a separate behaviour, shortening (Shaw and Kristan, 1997). They were therefore classified as multifunctional interneurons. Neuron 204 was found to be a dedicated swim interneuron since it was only active in swimming. Similarly, Briggman and Kristan (2006) found that a large proportion of cells active in swimming were also active in a separate behaviour, crawling. Within the two networks, both dedicated and multifunctional interneurons were also identified. Therefore the use of both dedicated and multifunctional neurons for the generation of similar behaviours is a common mechanism.

N1M and N2v were shown to be active in both ingestive and egestive motor programs. The two are CPG interneurons, suggesting that the same CPG is used for both ingestion and egestion. N1M has been shown to be important for driving activity in protraction phase buccal mass motor neurons (Elliott and Kemenes, 1992, Staras et al., 1998b), whereas N2v excites many of the rasp phase motor neurons (Brierley et al., 1997a). The two are also important for generating the protraction-rasp order of firing (Rose and Benjamin, 1981b, Brierley et al., 1997c). This is in agreement with observations in vivo and in vitro which show that the odontophore is protracted and retracted in the same order in both ingestive and egestive motor programs. Therefore the use of the same CPG for the two behaviours allows for the generation of similar movements, whereas the recruitment of different interneuron elements allows for the modification of specific motor neurons' phase of firing, altering the motor output.

A summary of the firing activity of key interneurons and motor neurons involved in ingestion and egestion is given in **Figure 7.35A**. Two ingestive motor programs are shown followed by two egestive motor programs. A summary of the neural circuits for ingestion and egestion are shown in **Figure 7.35Bi,Bii**.

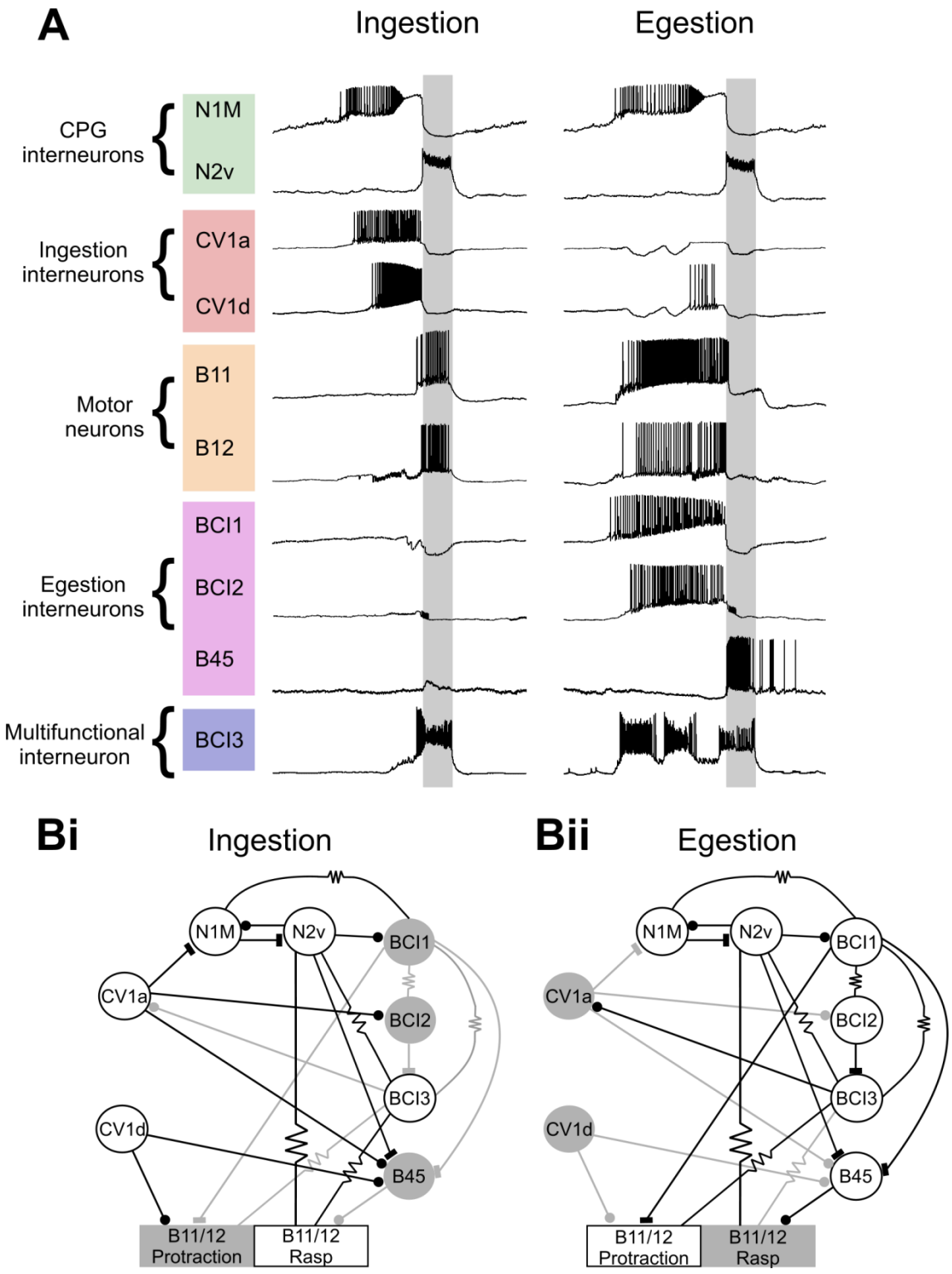

Figure 7.35 Schematic diagram of sequence of firing and circuit diagrams of ingestion and egestion **A.** A summary schematic of the firing activity of key interneurons and motor neurons involved in ingestion and egestion. The first cycle is ingestive whereas the second cycle is egestive. Grey vertical lines represent the rasp phase of a cycle. **Bi.** Summary circuit of the interneuronal control of ingestive motor programs. **Bii.** Summary circuit of the interneuronal control of egestive motor programs. Black lines represent neurons and connections which are active, grey lines represent neurons and connections which are not active. B11/B12 activity has been split to indicate the phase in which the motor neuron is active. Only known connections are included in the circuit. For simplicity CV1d is shown as not active in egestion in Bii.

7.3.3 Comparison of interneuronal control of ingestion and egestion in *Lymnaea* with *Aplysia*

The neural networks involved in generating ingestive and egestive motor programs have been most extensively studied in *Aplysia*. It is therefore necessary to make comparisons between the two networks. The B8 motor neuron is most often used as a read out of whether a cycle is ingestive or egestive (Morton and Chiel, 1993b, Morgan et al., 2002, Jing and Weiss, 2001, 2002). B8 innervates the I_4 muscle (Morton and Chiel, 1993b) and is often referred to as a radula closer motor neuron. B8 firing, resulting in the closing of the radula, occurs in the retraction phase of ingestive motor programs and in the protraction phase of egestive motor programs (Morton and Chiel, 1993b). This is similar to the activity of B11 and B12 in *Lymnaea*. However the motor neurons are not homologous as their morphology differs (B8 projects down the radula nerve which is the PBN in *Lymnaea*). Motor programs are often initiated in *Aplysia* by activation of the command-like interneuron CBI-2. CBI-2 appears homologous to CV1a in *Lymnaea*, since the two are in a similar location, have comparable morphologies, can both reliably drive fictive motor programs and achieve this via a facilitating excitatory connection with the protraction phase CPG interneurons (Rosen et al., 1991, Hurwitz et al., 2003, McCrohan, 1984a, McCrohan and Kyriakides, 1989). However, unlike CV1a, CBI-2 can generate either ingestive or egestive motor programs (Morton and Chiel, 1993b, Jing and Weiss, 2001, 2002). CBI-2 cycles are biased towards ingestion via co-activation of CBI-3 (Morgan et al., 2002, Jing and Weiss, 2001).

CBI-3 is an APGWamide immunoreactive CBI, similar to CV1b (Morgan et al., 2002, McCrohan and Croll, 1997). Unlike CV1b though, CBI-3 cannot drive motor programs. However the two, CV1b and CBI-3, appear to be involved in generating ingestive motor programs. In *Aplysia*, the BCI B40 is important for the expression of CBI-2 ingestive motor programs (Jing and Weiss, 2002). No neuron has been identified in *Lymnaea* which is homologous to B40. B40 provides inhibition to the radula closer motor neuron B8 in the protraction phase. This most closely resembles the inhibition that CV1d provides to B12 during the protraction phase in *Lymnaea*. Therefore the same effect is achieved via a CBI in *Lymnaea*. The N1L interneuron is most similar to the B65 interneuron in *Aplysia*. Both are located in a similar region of the buccal ganglia and have similar morphologies (Kabotyanski et al., 1998, Yeoman et al., 1995). However, B65 generates egestive motor programs (Proekt et al., 2007). Therefore the two are involved in different behaviours in the two systems.

In the egestive network, The BCI1 interneuron most closely resembles the B20 interneuron in *Aplysia*. BCI1 and B20 are both located on the ventral surface, have

similar morphologies and are electrotonically coupled with protraction phase CPG interneurons (Teyke et al., 1993, Jing and Weiss, 2001, Diaz-Rios and Miller, 2005). B20 drives egestive motor programs providing excitation to B8 in the protraction phase. In *Aplysia* there is no identified homologous neuron to BCI2. The protraction phase CPG interneurons B63 and B34 in *Aplysia* are active in both ingestion and egestion in *Aplysia* (Jing and Weiss, 2001), similarly to N1M in *Lymnaea*.

During the retraction phase, B8 activity is increased via a delayed excitation from B40 (Jing and Weiss, 2002) and via excitation from the CPG interneuron B64 (Jing and Weiss, 2001). B64 shows many similar characteristics to N2v in *Lymnaea* (Hurwitz and Susswein, 1996, Brierley et al., 1997a). During egestion, B8 is inhibited by the multi-action B4/5 interneuron (Jing and Weiss, 2001). B4/5 are a pair of rasp phase neurons which project down buccal nerve 3 (BN3) (Warman and Chiel, 1995) which is homologous to the VBN in *Lymnaea*. B4/5 activity is reduced by CBI-3 and increased by B20 (Jing and Weiss, 2001). B4/5 resembles B45 in *Lymnaea* due to its morphology and connection with motor neurons; therefore B45 in *Lymnaea* was named after B4/5 in *Aplysia*. B45 activity was similarly modulated in the rasp phase by CBIs and BCIs in *Lymnaea*. Therefore there were many similarities between the two networks involved in generating the same two behaviours. The differences between the two may represent lack of full characterisation of the networks in both molluscs.

7.3.4 Choice variability in *Lymnaea*

An important finding of this chapter was that the same tactile stimulus was able to generate both ingestive and egestive behaviours when it was maintained in the mouth. The animal received no new information about the stimulus, but was able to make a decision that the stimulus was not edible and switch to an egestive behaviour. Application of an identical stimulus which is able to elicit two competing behaviours on separate trials is known as choice variability (Briggman et al., 2005).

The interneuron vTN was shown in Chapter 5 to be important in the decision about the presence of a stimulus. Maintaining the probe in the mouth presumably provided further excitation to the radula, exciting vTN with each bite. Therefore vTN may be involved in switching from ingestion to egestion. vTN was found to be able to generate both ingestive and egestive motor programs. The majority of cycles generated by vTN were gathered amongst sucrose driven cycles (**Figure 7.33C,D)**, suggesting that vTN was biased towards generating ingestive behaviours. Interestingly, within the same preparation vTN was able to trigger both ingestive and egestive cycles in separate

trials. The switch between ingestive and egestive was also seen to occur within a vTN triggered rhythm. It remains unknown how vTN was able to generate both ingestive and egestive cycles. vTN had no strong connection with CV1a, CV1b or BCI1 and strongly inhibits N1L (Section 6.2.1). The only protraction phase interneuron vTN has a reliable connection with was N1M. N1M was found to be active in both ingestion and egestion and preliminary experiments showed that activating N1M could activate both motor programs. Therefore vTN activated a rhythm but did not specify the type of motor program that was initiated. This potentially allowed for the modification of vTN triggered rhythms due the behavioural state of the animal or due to previous experience.

Another possibility is that the motor program generated depended on the level or the frequency of vTN activity. This, however, was not investigated. A study by Large et al. (2006) showed that by increasing the mechanical properties of the food, egestive, as well as ingestive, motor programs were generated in *Lymnaea*. In *Aplysia*, egestion could be initiated via constant stimulation of the radula (Morton and Chiel, 1993a). In *Tritonia* it was hypothesised that the animal makes a decision about the edibility of a stimulus based on both its chemical and tactile properties (Audesirk and Audesirk, 1979). If the stimulus provided only tactile cues, and no chemical cues, then the substance was egested. This is a possible mechanism used by *Lymnaea*. A judgement about the tactile probe's edibility may be made, and in the absence of any chemical cues it is deemed inedible.

These results provided a basis for discriminating between the ingestive and the egestive feeding behaviours in *Lymnaea*. Importantly, activity in two motor neurons, B11 and B12, was found to correspond to the expression of each behaviour. The neural circuitry involved in the two behaviours involved the use of the same CPG interneurons (N1M and N2v) and activation of dedicated (CV1a, BCI1, BCI2) and multifunctional (BCI3, CV1d) interneurons. The decision neuron vTN was found to be able to generate both ingestive and egestive motor programs. Therefore vTN is a potential site for decision making about which behaviour to generate.

8 General discussion

The experiments in this thesis utilize the feeding behaviour of *Lymnaea* to study the neural mechanisms of decision making. Two separate decisions faced by the animal were studied. The first was a simple decision about the presence or absence of a sensory stimulus encountered during an appetitive behaviour. The second was the decision between two incompatible behaviours which share the same muscles: ingestion and egestion. Two separate mechanisms were identified for the two decisions. In the first, stimulus absent and stimulus present decision neurons were identified. During stimulus absent decisions, the stimulus absent neuron's activity increased, preventing any further behaviour. During stimulus present decisions, the stimulus present decision neuron became active and switched the network into the consummatory mode. Importantly, at the decision point of the stimulus present decision, both the stimulus present and stimulus absent decision neurons were active but the stimulus absent neuron's activity was overcome, resulting in a decision about the presence of a sensory stimulus. The decision between ingestion and egestion, however, involved active inhibition amongst ingestive and egestive interneurons as well as reconfiguration of a multifunctional interneuron's activity. Therefore, the relatively simple feeding network of *Lymnaea* shows evidence of two different mechanisms for decision making.

8.1 Stimulus absent and stimulus present decision making in *Lymnaea*

Experiments in Chapter 3 show *Lymnaea* can perform simple stimulus present and stimulus absent decisions. The appetitive food searching behaviour and the switch into the consummatory behaviour in the presence of a sensory stimulus was used as a read out of the animal's decision about whether a stimulus was judged to be present or absent. At the level of satiety used, *Lymnaea* typically produced unitary appetitive bites in the absence of a sensory stimulus. This suggested that the animal was correctly able to judge the absence of a potential food during the bite. This was therefore referred to as a stimulus absent trial. Presenting the animal with a piece of solid lettuce during an appetitive bite program was sufficient to elicit consummatory bite programs. Therefore, the animal was able to make a correct judgement about the presence of a sensory stimulus and perform an appropriate action in response, i.e. consummatory bite

programs. Thus, *Lymnaea* were able to perform a simple stimulus absent/stimulus present decision making task. *Lymnaea* report its decision either by producing no behaviour or switching into the consummatory behaviour. Decision making studies in invertebrate preparations have typically focused on choice between two action-based behaviours based on sensory stimuli, like swimming vs. crawling (Esch et al., 2002), ingestion vs. egestion (Morton and Chiel, 1993a) or aerial respiration vs. whole-body withdrawal (Inoue et al., 1996). The decision studied in Chapter 3 is a decision between action and inaction based on a sensory stimulus or no sensory stimulus respectively. Therefore, only one of the decisions can be based on sensory information. Such a decision making process has clear similarities with a mechanism studied in monkeys (de Lafuente and Romo, 2005, 2006, Carnevale et al., 2012, Merten and Nieder, 2012). In the behavioural task in monkeys, the animal is either presented with a near perceptual threshold stimulus or no stimulus. The animal must then make a perceptual judgement about the absence or presence of the sensory stimulus. The use of a near perceptual threshold stimulus can result in 'miss' trials where the animal makes a judgement about the absence of a stimulus which was in fact present. This allows for the activity in decision neurons to be dissociated from neurons which encode the sensory stimulus. The behavioural decision made by *Lymnaea* is based purely on the stimulus being present or the stimulus being absent, rather than using a near perceptual threshold stimulus.

Monkeys made the report of their decision by performing an action in both the stimulus present and stimulus absent trials. In *Lymnaea* a stimulus absent trial was reported by entering into a period of quiescence, whereas the stimulus present trial was reported by switching into the consummatory behaviour. The use of *Lymnaea's* food searching behaviour allowed for the study of decision making in a behaviourally relevant task. The monkeys received a reward for making a correct decision about the presence or absence of a sensory stimulus. In the tactile stimulus trials in Chapter 3 and 5, there was no reward for either the stimulus absent or stimulus present trials.

Even though there were clear differences between the two behavioural paradigms, the basic decision being studied is a simple stimulus absent or stimulus present decision. This therefore allows for the comparison of the neural mechanisms of decision making in an invertebrate and a vertebrate preparation. This will be discussed further in Section 8.3.

The behavioural experiments in Chapter 3 also suggested that *Lymnaea* use two mechanisms for locating food. The first relies on encountering a tactile stimulus during

an appetitive bite programs. The second mechanism involves short distance chemoreception in the absence of appetitive bite programs. Evidence to support this comes from the finding that during an appetitive bite program, the tactile probe alone elicited the switch to consummatory bite programs which most resembled the solid lettuce. The lettuce juice was sufficient to elicit the switch to consummatory bites, but this appeared to be independent of the appetitive bite. The latency of the onset of the consummatory bite was much longer than in the solid lettuce or the tactile stimulus trials. Application of the lettuce juice in the absence of an appetitive bite was sufficient to elicit consummatory bites and the latency of the onset of consummatory bites was similar to that seen by lettuce juice application in an appetitive bite. These results suggest that the chemical stimulus was sufficient to elicit consummatory bites, and that the appetitive bite did not affect this. Therefore, the appetitive bite appears to be for the purpose of locating a solid, since it relies on tactile cues to initiate consummatory bites, whereas chemical cues can elicit bites in the absence of an appetitive bite. The two cues are likely both used to locate food; however these experiments demonstrate that the two can be used independently.

8.2 Stimulus present and stimulus absent decision neurons

For neurons to be considered as being involved in the decision about the presence of a tactile stimulus they had to 1) be excited by tactile stimuli to the radula, and 2) be able to initiate the switch from appetitive to consummatory bites. The novel interneuron, vTN, fulfilled both of these criteria. In Chapter 5 an in vitro analogue of the stimulus absent and stimulus present decision made in vivo was developed to test vTN's role as a stimulus present decision neuron. Activation of a CBI or N1M interneuron was sufficient to drive single fictive appetitive bites similar to those seen in vivo in the absence of a sensory stimulus. Therefore, these were referred to as a stimulus absent decision. Activation of vTN within a fictive appetitive bite was reliable at initiating further cycles, similar to the tactile stimulus in vivo and was therefore referred to as a stimulus present decision. The in vitro analogue was shown to be applicable since both the stimulus absent and stimulus present decisions in vitro were comparable to results seen in vivo. Further evidence for vTN's role as the stimulus present decision neuron was shown in Chapter 5. By using the radula-CNS preparation, it was possible to apply a tactile stimulus to the radula during a fictive appetitive bite. This was sufficient to elicit the switch into fictive consummatory behaviours, as in vivo. Importantly, vTN was strongly activated by the tactile stimulus. Hyperpolarising vTN prior to the tactile

stimulus was sufficient to block the switch from the fictive appetitive to fictive consummatory behaviours. This confirmed that vTN was important for the decision about the presence of the stimulus. Further evidence for this was shown in Chapter 3 whereby activation of an RM was sufficient to elicit fictive feeding cycles only if vTN was sufficiently activated.

During stimulus absent decisions, vTN showed no spiking activity. de Lafuente and Romo (2005) showed that during a stimulus absent decision, stimulus present neurons also showed no change in their firing rates. An interesting finding of theirs was that no neurons were found whose activity co-varied with the stimulus absent decision. They hypothesised that the default response was a stimulus absent decision based on baseline levels of stimulus present decision neurons. Results in Chapter 4 and 5 indicated that in *Lymnaea* there was an active stimulus absent decision neuron, N3t. After a single fictive appetitive bite, N3t activity significantly increased over pre-cycle levels for 3.5 s. Disrupting N3t activity within this time was sufficient to initiate further cycles, suggesting that this was a critical period in which N3t actively prevented the generation of further cycles in the absence of sensory stimuli. Therefore, in *Lymnaea* a neuron was identified whose activity increased during stimulus absent decisions. Stimulus absent decision neurons were identified in monkeys only during an abstract decision making task (Merten and Nieder, 2012). These neurons, similar to N3t, co-varied their activity with stimulus absent decisions. Having identified both a stimulus absent and a stimulus present decision neuron it was possible to test how the two interact at the decision point. As mentioned, vTN showed no activity during stimulus absent decisions, whereas N3t's activity increased. However, during a stimulus present decision, vTN became active, but N3t activity also increased as in the stimulus absent decision. Therefore at the decision point of the stimulus present decision, both the stimulus present and stimulus absent decision neurons were active. This presumably provided conflicting information to the system about the presence or absence of the sensory stimulus. However, vTN activity was reliably sufficient to overcome N3t's inhibition on the system, and switch the network into the fictive consummatory behaviour. Similar experiments looking at the interaction of stimulus absent and stimulus present neurons were not performed in the studies by de Lafuente and Romo (2005, 2006) as no stimulus absent decision neurons were found. Merten and Nieder (2012) also did not directly record from the two classes of neuron at once. However, by comparing results of stimulus present and stimulus absent decision neurons in the study by Merten and Nieder (2012), the stimulus absent decision neurons activity

remains at baseline levels during stimulus present decisions, unlike in *Lymnaea* where it was active at both decision points.

The decision about the absence of a sensory stimulus has not been studied in invertebrate preparations. There are examples of neurons with the capability to terminate behaviours in response to a sensory stimulus (O'Gara and Friesen, 1995, Perrins et al., 2002, Taylor et al., 2003) but, uniquely, N3t is able to terminate a behaviour in the absence of a sensory stimulus. Inhibitory neuron B52 in the feeding system of *Aplysia* is active after the retraction phase, similar to N3t; however it functions to terminate the retraction phase only and has no inhibitory connections with protraction phase interneurons (Nargeot et al., 2002), suggesting that it terminates the cycle, but does not prevent the expression of further cycles.

The use of a separate stimulus absent and stimulus present neuron seems redundant. Both the stimulus absent and stimulus present decision could be achieved by having only a stimulus present decision neuron. In the absence of a sensory stimulus the stimulus present neuron is not active therefore it provides no drive to the system, resulting in a stimulus absent decision. This is similar to that seen in the study by de Lafuente and Romo (2005), who found no stimulus absent decision neurons. In fact, it could be argued that since N3t's activity increases in both the stimulus absent and stimulus present trials that this represents N3t's baseline response and therefore not the stimulus absent decision. However, since N3t plays such a pivotal role in preventing the generation of further cycles after a fictive appetitive bite, it appears that this increase in activity is functional to the system, actively inhibiting the system in the absence of a sensory stimulus. Therefore, in *Lymnaea* there appears to be two mechanisms for reporting the absence of a sensory stimulus: the lack of activity in vTN and the increased activity in N3t. One possible advantage of having two mechanisms is shown in experiments in Chapter 5. There is a 3.5s period after a fictive appetitive bite in which N3t activity is significantly higher than baseline levels. Within this time period, disruption of N3t activity can initiate further fictive feeding cycles, suggesting that this is a critical period in which N3t actively prevents the generation of further cycles. The level of vTN activity needed to trigger fictive feeding cycles is reduced within this time period. vTN was always stimulated within this time period and it has not been tested whether this effect on vTN was absent after 3.5s. Therefore these two experiments combined suggest that there is a critical period after a fictive appetitive bite in which the system is poised to switch into the consummatory behaviour. Having separate stimulus absent and stimulus present decision neurons may be beneficial for this. The system appears to be in a preparatory state after a fictive appetitive bite, on the brink of

producing further fictive feeding cycles. However, in the absence of a sensory stimulus N3t will prevent this via providing inhibition to the system. In the presence of a sensory stimulus, N3t activity remains high, as if there was no sensory stimulus; however vTN activity provides excitation to the system, which overcomes the N3t inhibition. Therefore, this mechanism may allow the system to be poised to switch into the consummatory behaviour after every appetitive bite, in preparation for a sensory stimulus, but still biased towards a stimulus absent decision in the absence of a stimulus. This appears to be a mechanism by which a state of arousal can be present in the system which can affect the decision in the presence of a sensory stimulus but which does not affect the decision in the absence of a stimulus.

Experiments in *Aplysia* show that appetitive behaviours facilitate consummatory behaviours by creating a state of arousal. Appetitive neurons excite numerous elements of the consummatory feeding network, but do not drive full consummatory behaviours suggesting that they served the role of preparing the animal for consummatory behaviours (Teyke et al., 1990, Teyke et al., 1997, Jing et al., 2008). It was possible that the fictive appetitive behaviour in *Lymnaea* increased the excitatory component of the connection from vTN to N1M, thus reducing the amount of vTN activity needed to initiate fictive feeding. This would be present in every fictive appetitive bite, but only during a stimulus present decision would it be relevant since vTN shows no activity during stimulus absent decisions This would also serve to create a state of arousal in the system which would mean that it was poised to switch to a consummatory behaviour in the presence of a sensory stimulus. However, this does not explain the fact that disruption of N3t activity within this period is also sufficient to elicit further cycles, in the absence of vTN activity. These results taken together suggest that there is a network wide anticipatory state, rather than just facilitation of a specific synaptic connection. It is possible that the fictive appetitive bite affects endogenous properties of N1M itself, potentially via increasing N1M's excitability within the 3.5s period after a cycle. This would serve to reduce the amount of vTN activity needed to trigger cycles but also necessitate high N3t levels during this period. Work by Carnevale et al. (2012) found that during stimulus present decisions in monkeys, activity of stimulus present decision neurons prior to onset of the stimulus was higher than in stimulus absent decisions. Therefore, the animal was biased towards a stimulus present decision prior to the stimulus. These results suggest that the internal state of the animal affected the decision made by the animal. Therefore, although the behavioural state of the animal was kept constant in the experiments in Chapters 3, 4 and 5 it appears that it is still able to affect the decision making process.

Internal signals are proposed to affect decision making in other studies too (de Lafuente and Romo, 2005, Gillette et al., 2000, Hirayama and Gillette, 2012).

8.3 Distinctions between ingestion and egestion in *Lymnaea*

The ingestive behaviour in *Lymnaea* has been extensively studied, however very little was known about the egestive behaviour. The two are incompatible behaviours which serve opposite purposes. Each behaviour can be elicited by either one of two separate chemical cues or by maintaining the same tactile cue. This provided an ideal system to study the neural mechanisms involved in the choice between the two behaviours and the role of sensory information in the process.

Observations made in vivo and by using semi-intact preparations in Chapter 7 provided a method to distinguish between the two behaviours. During ingestion the major phase of odontophore contraction was during the retraction phase whereas during egestion it was during the protraction phase. The newly identified B11 was shown to be an SLRT motor neuron whose activity underwent a shift in phase between ingestion and egestion. During ingestion, B11 was active predominantly in the rasp phase whereas during egestion B11 was active predominantly in the protraction phase. Therefore B11 was a critical determinant of the motor program generated. A second novel putative motor neuron, B12, was also identified which had a similar morphology and firing pattern as B11. It too showed the same phase shift of firing activity between the two motor programs. Therefore, *Lymnaea* reconfigure the phase of activity of the same muscles and motor neurons for two similar yet incompatible behaviours. Reconfiguration of a network is a mechanism identified in numerous studies in both invertebrates (Blitz and Nusbaum, 1997, Vehovszky and Elliott, 2001, Morgan et al., 2002, Briggman and Kristan, 2006) and vertebrates (Li et al., 2007, Berkowitz, 2010, Berkowitz et al., 2010).

There were several similarities between the mechanisms employed by *Lymnaea* in switching between ingestion and egestion and those described in *Aplysia*. The basic movements of the odontophore and radula complex appear to be conserved between the two molluscs. *Aplysia* are able to bring the two halves of their odontophore and radula complex fully together, grasping food between the two halves. During ingestion, the two halves are open during protraction and closed during retraction. During egestion, the two halves are closed during protraction and open during retraction (Morton and Chiel, 1993a). The lateral edges of the odontophore and radula complex in

Lymnaea are never brought fully together as they are in *Aplysia*. However, the lateral edges are brought close together and spread apart in the same phases in ingestion and egestion in *Lymnaea* as the movements of the two halves of the odontophore and radula complex in *Aplysia*. Homologous muscles appear to be involved in the contraction of the odontophore/radula complex in the two molluscs; the I4 in *Aplysia* (Morton and Chiel, 1993b) and the SLRT in *Lymnaea* (Wentzell et al., 2009). I4 in *Aplysia* is innervated by the radula closer motor neuron B8. The SLRT in *Lymnaea* is innervated by the newly identified B11 motor neurons. The two motor neurons are not homologous, as they differ in morphology. However, the two motor neurons undergo the same phase shift of activity between ingestion and egestion.

8.4 Interneuronal mechanisms of the choice between ingestion and egestion

The interneuronal mechanisms involved in ingestion and egestion were investigated by studying the control of B11 and B12 activity in the protraction and rasp phases of driven cycles. Previously identified command-like interneurons (CV1a, CV1b and N1L) were found to drive fictive motor programs which most resembled ingestive motor programs generated by sucrose application to the lips. These interneurons were therefore classified as ingestive interneurons. Two newly identified command-like interneurons, BCI1 and BCI2, were able to drive fictive motor programs which most resembled egestive motor programs generated by the emetic stimulus amyl acetate. These interneurons were therefore classified as egestive interneurons

The CPG interneurons N1M and N2v were shown to be active in both ingestive and egestive motor programs. *Aplysia* were shown to also use the same CPG in both ingestion and egestion (Jing and Weiss, 2001), and it has been hypothesised that turtles use the same CPG for scratching and locomotion (Berkowitz, 2010). The underlying movements of the buccal mass and phase of protraction and retraction of the odontophore remain the same in *Lymnaea*, therefore utilising the same CPG (and presumably many of the same muscles and motor neurons) provides a conservative method for eliciting two competing behaviours which utilise many of the same movements.

Having identified the interneuronal control of the two behaviours it was possible to study how behavioural choices were made between the two behaviours at the interneuronal level. Simultaneous activity in the ingestive and egestive interneurons

would provide conflicting inputs to the motor neurons and muscles and elicit non-functional behaviours which neither brought food into the mouth nor pushed it out. CV1a, an ingestive interneuron, monosynaptically inhibited BCI2 but excited BCI1, two egestive interneurons. The excitation to BCI1 was never sufficient to elicit spiking activity. Inhibition of BCI2 by CV1a could potentially reduce the likelihood of BCI1 firing via the electrotonic coupling between BCI1 and BCI2. However, BCI1 was also coupled with N1M, which CV1a strongly excites. This would therefore provide further excitation to BCI1. Sasaki et al. (2013) discuss the function of electrotonic synapses within a network. They show that asymmetric electrotonic synapses between two neurons can account for the biased activation of one neuron by the other but not in the reverse direction. It is therefore possible that the coupling is stronger from BCI1 to N1M than in the reverse direction, accounting for N1Ms activation by BCI1 but not BCI1 by N1M in CV1a driven cycles. However, the strength of the coupling between the two neurons has not been tested. The lack of BCI1 activity in CV1a driven cycles prevents any excitation to B11 and B12 in the protraction phase. CV1a and CV1d monosynaptically inhibited a novel rasp phase neuron, B45. B45 provided strong inhibition to B11 and B12 if active in the rasp phase, therefore during ingestive motor programs, it is necessary to reduce B45 activity to allow B11 and B12 activity in the rasp phase. This was achieved via a delayed inhibitory connection from CV1a to B45 which reduced B45 excitability and PIR. The reduction in B45 excitability would serve to reduce B45 activity due to excitation from N2v in the rasp phase.

During BCI1 and BCI2 egestive cycles, CV1a activity was prevented in the protraction phase due to large hyperpolarising inputs. These did not arise monosynaptically from either BCI1 or BCI2. A novel interneuron, BCI3, was shown to cause the inhibitory inputs on CV1a in BCI1 and BCI2 driven cycles. It is not clear why a third interneuron is employed to inhibit CV1a, when both BCI1 and BCI2 project to the cerebral ganglia where the CV1as are located. BCI3 was an interesting interneuron since it, like B11 and B12, was active in the rasp phase of ingestion and in the protraction phase of egestion. BCI3 was electrotonically coupled with both B11 and B12, therefore providing further excitation to the motor neurons in either the rasp or protraction phase. Therefore, the choice between ingestion and egestion involved both dedicated and multifunctional interneurons. The clearest examples of dedicated interneurons were CV1a, BCI1 and BCI2. These interneurons were not active in the behaviour that they themselves could not activate. The CV1a to BCI2 inhibitory connection is in agreement with the hypothesis put forward by Davis and Mpitsos (1971) that neurons from each network inhibited each other. Blitz and Nusbaum (1997) found a similar mechanism in

the stomatogastric nervous system of the crab *Cancer borealis*. The modulatory proctolin neuron, a pyloric rhythm command-like interneuron, monosynaptically inhibited two projection interneurons which controlled the gastric mill rhythm. The BCI3 was a clear example of a multifunctional interneuron. It was active in both ingestion and egestion but in different phases. In egestion, BCI3 prevented CV1a activity in the protraction phase and also provided excitation to B11 and B12. In ingestion, BCI3 was active in the rasp phase, and possibly provided excitation to B11 and B12. Therefore the dedicated ingestion and egestion interneurons altered BCI3's firing activity to promote their behavioural outcome.

A population of interneurons were identified in the turtle which were active in both scratching and swimming, suggesting that they were multifunctional interneurons (Berkowitz, 2010), however whether these were CPG interneurons or not remains unknown. In *Xenopus* tadpoles and zebrafish both dedicated and specialised interneurons have been identified for swimming and struggling behaviours (Berkowitz et al., 2010). A multifunctional interneuron has been described in *Pleurobranchaea*. During feeding, the interneuron fired phasically producing inhibitory inputs to feeding command-like interneurons and generating the alternating protraction-retraction movements of the odontophore. During swimming, the interneuron fired tonically providing constant inhibition to the feeding command-like interneurons (Jing and Gillette, 2000, Kristan and Gillette, 2007), thus preventing their activation. Therefore, in *Pleurobranchaea*, the switch between the two behaviours is partially achieved via a switch in the firing patterns (phasic vs. tonic firing) of an interneuron. This is not the case with BCI3. BCI3 appears to produce plateau potentials in both ingestion and egestion, but the onset of activity is significantly reduced in egestion.

It is unknown how the two chemical cues activate the two networks. Studies on the effect of sucrose on the feeding system of *Lymnaea* have shown that sucrose has diverse effects on the feeding network. Kemenes et al. (2001) showed that N1M was active before either the SO or CV1a interneurons. CV1a was active in a high proportion of sucrose driven cycles, but not all. N1L was also found to be active in sucrose driven cycles (Yeoman et al., 1995). The CBIs were found to receive excitatory inputs from sucrose application to the lips in HiDi saline (Styles, 2004). Chemosensory neurons are located in the periphery in *Lymnaea* (Straub et al., 2004) suggesting that they monosynaptically excite the CBIs and possibly N1M. Staras et al. (2003) showed that N3t received inhibition prior to N1M onset. These results taken together suggest that the effect of sucrose is distributed amongst command-like interneurons and CPG interneurons. The mechanism by which the high concentration of AA is able to elicit

egestive behaviours remains unknown. Varying concentrations of AA have been shown to be able to elicit fictive feeding, have no effect or terminate fictive feeding (Straub et al., 2006). It is unknown whether BCI1, BCI2 or BCI3 are monosynaptically excited by neurons in the periphery which respond to high concentrations of AA, but not lower concentrations. Activation of any one of these interneurons could initiate the others due to the electrotonic coupling between them.

Experiments whereby the same tactile stimulus was maintained within the buccal cavity provided a possible method for bypassing the issue of how two sensory cues elicit competing behaviours. The same tactile probe was able to elicit first ingestive then egestive motor programs. The tactile stimulus made the most contact with the radula in the behavioural experiments (see Section 3.2.2). Results in Chapter 3 and 5 show that vTN was activated by tactile stimulation of the radula. Therefore, vTN may play a role in a stimulus present decision and in behavioural switching. Presumably with each bite of the tactile stimulus, vTN is activated as the tactile stimulus comes into contact with the radula. vTN was shown to be able to trigger both ingestive and egestive like motor programs in Chapter 5. vTN was shown to have no excitatory synaptic connections with either the ingestive or egestive protraction phase interneurons in Chapter 6, but only with the CPG interneuron N1M. Therefore it remains unclear how vTN can activate either motor program. One possible mechanism for vTN's ability to trigger either ingestive or egestive motor programs is that vTN initiates fictive feeding cycles, but does not specify which type of motor program to produce. Instead it activates N1M, which is necessary and active in both motor programs. The decision about which motor program to perform is then made downstream from vTN. Different activity levels in a single neuron have been shown to elicit two competing behaviours in the *Xenopus* tadpole. Brief activation of a Rohon-Beard sensory neuron is sufficient to trigger fictive swimming (Soffe, 1997), whereas prolonged activation of the same neuron elicits fictive struggling. Longer activation of vTN or activation within each cycle may therefore alter the motor program from ingestion to egestion; however this has not been tested. Neurons with the ability to initiate two competing behaviours have also been identified in *Aplysia*. CBI-2 activation is sufficient to drive both ingestion and egestion (Morgan et al., 2002), via its synaptic connections with both ingestive and egestive interneurons (Jing and Weiss, 2001, 2002). CBI-2 is excited by stimuli which elicit both behaviours (Morgan et al., 2002), therefore it appears that CBI-2 initiates a behaviour but does not specify the type of behaviour.

These experiments imply that there are two separate mechanisms by which ingestion and egestion can be elicited. The first is via activation of chemosensory neurons in the

lips, the second via activation of mechanosensory neurons in the radula. Having both allows the animal to make judgements about the edibility of food based on both its chemical and tactile properties. If the food has the correct chemical properties but is too large or too mechanically robust then it may be deemed inedible and egested. Similarly if the food has the correct tactile properties but no chemical cues it may be deemed unacceptable. Similar decision making steps are made in *Aplysia* (Morton and Chiel, 1993a) and *Tritonia* (Audesirk and Audesirk, 1979). In *Aplysia* there are two mechanisms to elicit egestive motor programs; activation of a CBI or stimulation of the oesophageal nerve (Horn and Kupfermann, 2002, Cropper et al., 2004). The CBIs receive activation via inputs from the lips and the oesophageal nerve via inputs to the oesophagus; therefore there are two different sensory driven mechanisms to drive the same behaviour, as in *Lymnaea*.

8.5 vTN's trigger ability

vTN had synaptic connections with all elements of the feeding network. The vTN to N1M connection is the only one with any clear function ascribed to it. vTN's lack of connections with CV1a, CV1b, BCI1 and its inhibitory connections with SO and N1L may be related to its role in initiating a motor program but not the type of program to be generated, as discussed in Section 8.4. vTN's excitatory input to N1M is thought to be the mechanism by which vTN triggers the first fictive feeding cycle However, this was not sufficient to explain the on-going nature of vTN triggered cycles. The excitation from vTN to N1M did not persist for longer than the duration of a single cycle therefore it was not sufficient to account for the subsequently generated cycles. Injecting N1M with sufficient depolarising current to initiate a full fictive feeding cycle was shown, on average, to initiate only a single cycle. This suggests that activation of N1M alone is not sufficient to trigger on-going cycles. The modulatory interneurons, OC, were also able to trigger fictive feeding cycles (Vehovszky and Elliott, 2001). The proposed mechanism for this was via a biphasic (i/e) connection from OC to N1M, SO and N1L. However, this too is presumably only sufficient to explain the first of the triggered cycles, since the depolarising input to all three neurons was short lived. Trigger neurons in the leech monosynaptically excite command-like interneurons (Brodfuehrer et al., 1995), as do those in *Tritonia* (Frost et al., 2001). In the leech, levels of inhibition on the system have to be overcome in order for trigger neurons to initiate swimming (Brodfuehrer and Friesen, 1986b). The source of the inhibition was found to be an interneuron which was tonically active during periods of quiescence (Brodfuehrer and

Burns, 1995). Stimuli which elicited swimming inhibited the neuron. It was shown that inhibition of the neuron was necessary for swimming to be generated. N3t provides similar inhibition to the feeding network during periods of quiescence. vTN, similar to the trigger neurons in the leech, reduced levels of inhibition on the network by reducing N3t firing rates. Therefore, the two appear to use similar mechanisms for vastly different behaviours, suggesting that this is a common feature in motor networks.

Future experiments

The mechanism by which vTN was able to trigger fictive feeding appears reliant on the reduction of N3t firing rate within triggered cycles. It would be of considerable interest to determine the mechanism by which vTN reduced N3t firing rate. One possibility is that it occurs via activation of a third party neuron which provides direct inhibition to N3t during vTN triggered cycles. It would also be important to test whether OC was able to trigger fictive feeding cycles via a reduction in N3t firing rates or whether OC and vTN activate the feeding network via separate mechanisms.

After a fictive appetitive bite there was a critical period in which N3t activity increased and prevented the activation of further feeding cycles. Within this time period the level of vTN activity necessary to trigger fictive feeding was reduced. An interesting question is whether the level of vTN activity needed to trigger fictive feeding is only lowered during the critical period after a cycle.

Further characterisation of the egestive behaviour is also a future goal. The muscle innervated by the B12 neuron would be important to identify since B12 was also a critical determinant of the motor program generated. Presumably there are also other motor neurons involved in the two behaviours. To test difference in network wide activity between the two behaviours, voltage sensitive dyes or a multi electrode array could be used to record from a large number of neurons within the feeding network. Both of these techniques have successfully been utilised in invertebrate preparations (Briggman et al., 2005, Harris et al., 2010, 2012).

The necessity of specific interneurons could be tested via transiently removing them from the network during sensory driven cycles. This could be achieved via injection of hyperpolarising current into the neuron of interest or via a novel Photoswitchable Affinity Label which binds to voltage gated K^+ channels, conferring light sensitivity to

them without requiring genetic engineering and exogenous gene expression (Fortin et al., 2008).

Having identified a method for distinguishing the two behaviours, it would be of interest to test how vTN is able to trigger both ingestive and egestive motor programs. First it would be important to test whether there is a correlation between the generation of each behaviour within preparations and the level of vTN activity. An in vitro analogue of the maintained tactile stimulus behavioural experiments could be developed by modifying the one used in Chapter 5. A fictive appetitive bite could be initiated via CBI activation, initiating an ingestive motor program recorded on B11 or B12. vTN could be activated within the cycle, to represent the tactile stimulus to the radula, as in Chapter 5, triggering further feeding cycles. vTN could then be activated within each of the triggered cycles to represent the maintained tactile stimulus in the behavioural experiments. It would then be possible to see whether the motor programs underwent a switch from ingestive to egestive, as seen in vivo. This would facilitate the study of multiple stages of decision making (a stimulus present decision followed by a decision about the edibility of the stimulus) within the same in vitro preparation.

References

Alania, M., Sakharov, D. A. & Elliott, C. J. 2004. Multilevel inhibition of feeding by a peptidergic pleural interneuron in the mollusc *Lymnaea stagnalis*. *J Comp Physiol A,* 190**,** 379-90.

Audesirk, T. E. & Audesirk, G. J. 1979. Oral mechanoreceptors in *Tritonia diomedea*. II. Role in feeding. *J Comp Physiol,* 130**,** 79-86.

Benjamin, P. R. 2012. Distributed network organization underlying feeding behavior in the mollusk *Lymnaea*. *Neural Syst Circuits,* 2**,** 4.

Benjamin, P. R. & Rose, R. M. 1979. Central generation of bursting in the feeding system of the snail, *Lymnaea stagnalis*. *J Exp Biol,* 80**,** 93-118.

Benjamin, P. R., Rose, R. M., Slade, C. T. & Lacy, M. G. 1979. Morphology of identified neurones in the buccal ganglia of *Lymnaea stagnalis*. *J Exp Biol,* 80**,** 119-135.

Berkowitz, A. 2010. Multifunctional and specialized spinal interneurons for turtle limb movements. *Ann N Y Acad Sci,* 1198**,** 119-32.

Berkowitz, A., Roberts, A. & Soffe, S. R. 2010. Roles for multifunctional and specialized spinal interneurons during motor pattern generation in tadpoles, zebrafish larvae, and turtles. *Front Behav Neurosci,* 4**,** 36.

Blitz, D. M. & Nusbaum, M. P. 1997. Motor pattern selection via inhibition of parallel pathways. *J Neurosci,* 17**,** 4965-75.

Brembs, B., Lorenzetti, F. D., Reyes, F. D., Baxter, D. A. & Byrne, J. H. 2002. Operant reward learning in *Aplysia*: neuronal correlates and mechanisms. *Science,* 296**,** 1706-9.

Brierley, M. J., Staras, K. & Benjamin, P. R. 1997a. Behavioral function of glutamatergic interneurons in the feeding system of *Lymnaea*: plateauing properties and synaptic connections with motor neurons. *J Neurophysiol,* 78**,** 3386-95.

Brierley, M. J., Yeoman, M. S. & Benjamin, P. R. 1997b. Glutamate is the transmitter for N2v retraction phase interneurons of the *Lymnaea* feeding system. *J Neurophysiol,* 78**,** 3408-14.

Brierley, M. J., Yeoman, M. S. & Benjamin, P. R. 1997c. Glutamatergic N2v cells are central pattern generator interneurons of the *Lymnaea* feeding system: new model for rhythm generation. *J Neurophysiol,* 78**,** 3396-407.

Briggman, K. L., Abarbanel, H. D. & Kristan, W. B., JR. 2005. Optical imaging of neuronal populations during decision-making. *Science,* 307**,** 896-901.

Briggman, K. L. & Kristan, W. B., JR. 2006. Imaging dedicated and multifunctional neural circuits generating distinct behaviors. *J Neurosci,* 26**,** 10925-33.

Brodfuehrer, P. D. & Burns, A. 1995. Neuronal factors influencing the decision to swim in the medicinal leech. *Neurobiol Learn Mem,* 63**,** 192-9.

Brodfuehrer, P. D., Debski, E. A., O'gara, B. A. & Friesen, W. O. 1995. Neuronal control of leech swimming. *J Neurobiol,* 27**,** 403-18.

Brodfuehrer, P. D. & Friesen, W. O. 1986a. Initiation of swimming activity by trigger neurons in the leech subesophageal ganglion. I. Output connections of Tr1 and Tr2. *J Comp Physiol A,* 159**,** 489-502.

Brodfuehrer, P. D. & Friesen, W. O. 1986b. Initiation of swimming activity by trigger neurons in the leech subesophageal ganglion. II. Role of segmental swim-initiating interneurons. *J Comp Physiol A,* 159**,** 503-10.

Buhl, E., Roberts, A. & Soffe, S. R. 2012. The role of a trigeminal sensory nucleus in the initiation of locomotion. *J Physiol,* 590**,** 2453-69.

Carnevale, F., de Lafuente, V., Romo, R. & PARGA, N. 2012. Internal signal correlates neural populations and biases perceptual decision reports. *Proc Natl Acad Sci U S A,* 109**,** 18938-43.

Carriker, M. R. 1946a. Morphology of the alimentary system of the snail *Lymnaea stagnalis appressa Say*. *Trans. Wis. Acad. Sci. Arts Lett.,* 38**,** 1-88.

Carriker, M. R. 1946b. Observations on the functioning of the alimentary system of the snail *Lymnaea stagnalis* appressa Say. *Biol Bull,* 91**,** 88-111.

Croll, R. P., Voronezhskaya, E. E., Hiripi, L. & Elekes, K. 1999. Development of catecholaminergic neurons in the pond snail, *Lymnaea stagnalis*: II. Postembryonic development of central and peripheral cells. *J Comp Neurol,* 404**,** 297-309.

Cropper, E. C., Evans, C. G., Hurwitz, I., Jing, J., Proekt, A., Romero, A. & Rosen, S. C. 2004. Feeding neural networks in the mollusc *Aplysia*. *Neurosignals,* 13**,** 70-86.

Davis, W. J. 1979. Behavioural hierarchies. *Trends in neurosciences,* 2**,** 5-7.

Davis, W. J. & Mpitsos, G. J. 1971. Behavioral choice and habituation in the marine mollusk *Pleurobranchaea californica*. *J Comp Physiol,* 75**,** 207-232.

Davis, W. J., Mpitsos, G. J. & Pinneo, M. 1974. The behavioral hierarchy of the Mollusk *Pleurobranchaea* II: Hormonal suppression of feeding associated with egg-laying. *J. Comp. Physiol.,* 90**,** 225-243.

Dawkins, M. 1974. Behavioural analysis of co-ordinated feeding movements in the gastropod *Lymnaea stagnalis*. *J Comp Physiol,* 92**,** 255-271.

de Lafuente, V. & Romo, R. 2005. Neuronal correlates of subjective sensory experience. *Nat Neurosci,* 8**,** 1698-703.

de Lafuente, V. & Romo, R. 2006. Neural correlate of subjective sensory experience gradually builds up across cortical areas. *Proc Natl Acad Sci U S A,* 103**,** 14266-71.

Diaz-Rios, M. & Miller, M. W. 2005. Rapid dopaminergic signaling by interneurons that contain markers for catecholamines and GABA in the feeding circuitry of *Aplysia*. *J Neurophysiol,* 93**,** 2142-56.

Edwards, D. H., Heitler, W. J. & Krasne, F. B. 1999. Fifty years of a command neuron: the neurobiology of escape behavior in the crayfish. *Trends Neurosci,* 22**,** 153-61.

Elekes, K., Eckert, M. & Rapus, J. 1993. Small sets of putative interneurons are octopamine-immunoreactive in the central nervous system of the pond snail, *Lymnaea stagnalis*. *Brain Res,* 608**,** 191-7.

Elekes, K., Kemenes, G., Hiripi, L., Geffard, M. & Benjamin, P. R. 1991. Dopamine-immunoreactive neurones in the central nervous system of the pond snail *Lymnaea stagnalis*. *J Comp Neurol,* 307**,** 214-24.

Elliott, C. J. & Benjamin, P. R. 1985a. Interactions of pattern-generating interneurons controlling feeding in *Lymnaea stagnalis*. *J Neurophysiol,* 54**,** 1396-411.

Elliott, C. J. & Benjamin, P. R. 1985b. Interactions of the slow oscillator interneuron with feeding pattern-generating interneurons in *Lymnaea stagnalis*. *J Neurophysiol,* 54**,** 1412-21.

Elliott, C. J. & Kemenes, G. 1992. Cholinergic interneurons in the feeding system of the pond snail *Lymnaea stagnalis*. II. N1 interneurons make cholinergic synapses with feeding motoneurons. *Philos Trans R Soc Lond B Biol Sci,* 336**,** 167-80.

Esch, T., Mesce, K. A. & Kristan, W. B. 2002. Evidence for sequential decision making in the medicinal leech. *J Neurosci,* 22**,** 11045-54.

Evans, C. G. & Cropper, E. C. 1998. Proprioceptive input to feeding motor programs in *Aplysia*. *J Neurosci,* 18**,** 8016-31.

Evans, C. G., Ludwar, B. & Cropper, E. C. 2007. Mechanoafferent neuron with an inexcitable somatic region: consequences for the regulation of spike propagation and afferent transmission. *J Neurophysiol,* 97**,** 3126-30.

Flood, T. F., Iguchi, S., Gorczyca, M., White, B., Ito, K. & Yoshihara, M. 2013. A single pair of interneurons commands the *Drosophila* feeding motor program. *Nature,* 499**,** 83-7.

Fortin, D. L., Banghart, M. R., Dunn, T. W., Borges, K., Wagenaar, D. A., Gaudry, Q., Karakossian, M. H., Otis, T. S., Kristan, W. B., Trauner, D. & Kramer, R. H.

2008. Photochemical control of endogenous ion channels and cellular excitability. *Nat Methods,* 5**,** 331-8.

Frost, W. N., Hoppe, T. A., Wang, J. & Tian, L. M. 2001. Swim initiation neurons in *Tritonia diomedea*. *American Zoologist,* 41**,** 952-61.

Frost, W. N. & Katz, P. S. 1996. Single neuron control over a complex motor program. *Proc Natl Acad Sci U S A,* 93**,** 422-6.

Gaudry, Q. & Kristan, W. B., JR. 2009. Behavioral choice by presynaptic inhibition of tactile sensory terminals. *Nat Neurosci,* 12**,** 1450-7.

Gillette, R., Huang, R. C., Hatcher, N. & Moroz, L. L. 2000. Cost-benefit analysis potential in feeding behavior of a predatory snail by integration of hunger, taste, and pain. *Proc Natl Acad Sci U S A,* 97**,** 3585-90.

Gold, J. I. & Shadlen, M. N. 2007. The neural basis of decision making. *Annu Rev Neurosci,* 30**,** 535-74.

Goldschmeding, J. T. & de Vlieger, T. A. 1975. Functional anatomy and innervation of the buccal complex of the freshwater snail *Lymnaea stagnalis*. *Proc. K. Ned. Akad. Wet.,* 78**,** 468-476.

Haas, J. S., Zavala, B. & Landisman, C. E. 2011. Activity-dependent long-term depression of electrical synapses. *Science,* 334**,** 389-93.

Harris, C. A., Buckley, C. L., Nowotny, T., Passaro, P. A., Seth, A. K., Kemenes, G. & O'Shea, M. 2012. Multi-neuronal refractory period adapts centrally generated behaviour to reward. *PLoS One,* 7**,** e42493.

Harris, C. A., Passaro, P. A., Kemenes, I., Kemenes, G. & O'Shea, M. 2010. Sensory driven multi-neuronal activity and associative learning monitored in an intact CNS on a multielectrode array. *J Neurosci Methods,* 186**,** 171-8.

Hatakeyama, D., Aonuma, H., Ito, E. & Elekes, K. 2007. Localization of glutamate-like immunoreactive neurons in the central and peripheral nervous system of the adult and developing pond snail, *Lymnaea stagnalis*. *Biol Bull,* 213**,** 172-86.

Hatakeyama, D. & Ito, E. 2000. Distribution and developmental changes in GABA-like immunoreactive neurons in the central nervous system of pond snail, *Lymnaea stagnalis*. *J Comp Neurol,* 418**,** 310-22.

Hawkins, R. D., Castellucci, V. F. & Kandel, E. R. 1981. Interneurons involved in mediation and modulation of gill-withdrawal reflex in *Aplysia*. II. Identified neurons produce heterosynaptic facilitation contributing to behavioral sensitization. *J Neurophysiol,* 45**,** 315-28.

Hernandez, A., Zainos, A. & Romo, R. 2002. Temporal evolution of a decision-making process in medial premotor cortex. *Neuron,* 33**,** 959-72.

Hirayama, K. & Gillette, R. 2012. A neuronal network switch for approach/avoidance toggled by appetitive state. *Curr Biol,* 22**,** 118-23.

Horn, C. C. & Kupfermann, I. 2002. Egestive feeding responses in *Aplysia* persist after sectioning of the cerebral-buccal connectives: evidence for multiple sites of control of motor programs. *Neurosci Lett,* 323**,** 175-8.

Hurwitz, I., Kupfermann, I. & Weiss, K. R. 2003. Fast synaptic connections from CBIs to pattern-generating neurons in *Aplysia*: initiation and modification of motor programs. *J Neurophysiol,* 89**,** 2120-36.

Hurwitz, I. & Susswein, A. J. 1996. B64, a newly identified central pattern generator element producing a phase switch from protraction to retraction in buccal motor programs of *Aplysia californica*. *J Neurophysiol,* 75**,** 1327-44.

Inoue, T., Takasaki, M., Lukowiak, K. & Syed, N. 1996. Inhibition of the respiratory pattern-generating neurons by an identified whole-body withdrawal interneuron of *Lymnaea stagnalis*. *J Exp Biol,* 199**,** 1887-98.

Jing, J. & Gillette, R. 1995. Neuronal elements that mediate escape swimming and suppress feeding behavior in the predatory sea slug *Pleurobranchaea*. *J Neurophysiol,* 74**,** 1900-10.

Jing, J. & Gillette, R. 2000. Escape swim network interneurons have diverse roles in behavioral switching and putative arousal in *Pleurobranchaea*. *J Neurophysiol,* 83**,** 1346-1355.

Jing, J., Vilim, F. S., Cropper, E. C. & Weiss, K. R. 2008. Neural analog of arousal: persistent conditional activation of a feeding modulator by serotonergic initiators of locomotion. *J Neurosci,* 28**,** 12349-61.

Jing, J. & Weiss, K. R. 2001. Neural mechanisms of motor program switching in *Aplysia*. *J Neurosci,* 21**,** 7349-62.

Jing, J. & Weiss, K. R. 2002. Interneuronal basis of the generation of related but distinct motor programs in *Aplysia*: implications for current neuronal models of vertebrate intralimb coordination. *J Neurosci,* 22**,** 6228-38.

Jing, J., Cropper, E. C., Hurwitz, I. & Weiss, K. R. 2004. The construct of movement with behavior-specific and behavior-independent modules. *J Neurosci,* 24**,** 6315-25.Johnson, B. R., Peck, J. H. & Harris-Warrick, R. M. 1993a. Amine modulation of electrical coupling in the pyloric network of the lobster stomatogastric ganglion. *J Comp Physiol A,* 172**,** 715-32.

Johnson, B. R., Peck, J. H. & Harris-Warrick, R. M. 1993b. Dopamine induces sign reversal at mixed chemical-electrical synapses. *Brain Res,* 625**,** 159-64.

Kabotyanski, E. A., Baxter, D. A. & Byrne, J. H. 1998. Identification and characterization of catecholaminergic neuron B65, which initiates and modifies patterned activity in the buccal ganglia of *Aplysia*. *J Neurophysiol,* 79**,** 605-21.

Katz, P. S. & Frost, W. N. 1995. Intrinsic neuromodulation in the *Tritonia* swim CPG: serotonin mediates both neuromodulation and neurotransmission by the dorsal swim interneurons. *J Neurophysiol,* 74**,** 2281-94.

Kawahara, S., Yano, M. & Shimizu, H. 1994. Radular mechanosensory neuron in the buccal ganglia of the terrestrial slug, *Incilaria fruhstorferi*. *J Comp Physiol A,* 174**,** 111-20.

Kawahara, S., Yano, M. & Shimizu, H. 1995. Modulation of the feeding system by a radular mechanosensory neuron in the terrestrial slug, *Incilaria fruhstorferi*. *J Comp Physiol A,* 176**,** 193-203.

Kawano, T., Po, M. D., Gao, S., Leung, G., Ryu, W. S. & Zhen, M. 2011. An imbalancing act: gap junctions reduce the backward motor circuit activity to bias *C. elegans* for forward locomotion. *Neuron,* 72**,** 572-86.

Kemenes, G., Elekes, K., Hiripi, L. & Benjamin, P. R. 1989. A comparison of four techniques for mapping the distribution of serotonin and serotonin-containing neurons in fixed and living ganglia of the snail, *Lymnaea*. *J Neurocytol,* 18**,** 193-208.

Kemenes, G. & Elliott, C. J. 1994. Analysis of the feeding motor pattern in the pond snail, *Lymnaea stagnalis*: photoinactivation of axonally stained pattern-generating interneurons. *J Neurosci,* 14**,** 153-66.

Kemenes, G., Elliott, C. J. & Benjamin, P. R. 1986. Chemical and Tactile inputs to the *Lymnaea* feeding system: effects on behaviour and neural circuitry. *J Exp Biol,* 122**,** 113-137.

Kemenes, G., Staras, K. & Benjamin, P. R. 2001. Multiple types of control by identified interneurons in a sensory-activated rhythmic motor pattern. *J Neurosci,* 21**,** 2903-11.

Kemenes, I., Straub, V. A., Nikitin, E. S., Staras, K., O'Shea, M., Kemenes, G. & Benjamin, P. R. 2006. Role of delayed nonsynaptic neuronal plasticity in long-term associative memory. *Curr Biol,* 16**,** 1269-79.

Klein, A. N., Weiss, K. R. & Cropper, E. C. 2000. Glutamate is the fast excitatory neurotransmitter of small cardioactive peptide-containing *Aplysia* radula mechanoafferent neuron B21. *Neurosci Lett,* 289**,** 37-40.

Kovac, M. P. & Davis, W. J. 1980. Neural mechanism underlying behavioral choice in *Pleurobranchaea*. *J Neurophysiol,* 43**,** 469-87.

Kristan, W. B. 2008. Neuronal decision-making circuits. *Curr Biol,* 18**,** R928-32.

Kristan, W. B. & Gillette, R. 2007. Behavioral choice. *In:* North, G. & Greenspan, R. J. (eds.) *Invertebrate Neurobiology.* New York: Cold Spring Harbor Laboratory Press.

Kupfermann, I. 1974a. Dissociation of the appetitive and consummatory phases of feeding behavior in *Aplysia*: a lesion study. *Behav Biol,* 10**,** 89-97.

Kupfermann, I. 1974b. Feeding behavior in *Aplysia*: a simple system for the study of motivation. *Behav Biol,* 10**,** 1-26.

Kupfermann, I. & Weiss, K. R. 1978. The command neuron concept. *Behav Brain Sci,* 1**,** 3-39.

Large, C. J., Smith, T., Foulds, G., Currey, J. D. & Elliott, C. J. 2006. Leaf mechanical properties modulate feeding movements and ingestive success of the pond snail, *Lymnaea stagnalis*. *Invert Neurosci,* 6**,** 133-40.

Li, W. C., Sautois, B., Roberts, A. & Soffe, S. R. 2007. Reconfiguration of a vertebrate motor network: specific neuron recruitment and context-dependent synaptic plasticity. *J Neurosci,* 27**,** 12267-76.

Marder, E., Bucher, D., Schulz, D. J. & Taylor, A. L. 2005. Invertebrate central pattern generation moves along. *Curr Biol,* 15**,** R685-99.

McCrohan, C. R. 1984a. Initiation of feeding motor output by an identified interneurone in the snail *Lymnaea stagnalis*. *J Exp Biol,* 113**,** 351-66.

McCrohan, C. R. 1984b. Properties of ventral cerebral neurones involved in the feeding system of the snail, *Lymnaea stagnalis*. *J Exp Biol,* 108**,** 257-272.

McCrohan, C. R. & Audesirk, T. E. 1987. Initiation, maintenance and modification of patterned buccal motor output by the cerebral giant cells of *Lymnaea stagnalis*. *Comp Biochem Physiol,* 87A**,** 969-977.

McCrohan, C. R. & Benjamin, P. R. 1980a. Patterns of activity and axonal projections of the cerebral giant cells of the snail, *Lymnaea stagnalis*. *J Exp Biol,* 85**,** 149-68.

McCrohan, C. R. & Benjamin, P. R. 1980b. Synaptic relationships of the cerebral giant cells with motoneurones in the feeding system of *Lymnaea stagnalis*. *J Exp Biol,* 85**,** 169-86.

McCrohan, C. R. & Croll, R. P. 1997. Characterization of an identified cerebrobuccal neuron containing the neuropeptide APGWamide (Ala-Pro-Gly-Trp-NH2) in the snail *Lymnaea stagnalis*. *Invert Neurosci,* 2**,** 273-82.

McCrohan, C. R. & Kyriakides, M. A. 1989. Cerebral interneurones controlling feeding motor output in the snail *Lymnaea stagnalis*. *J Exp Biol,* 147**,** 361-74.

Merten, K. & Nieder, A. 2012. Active encoding of decisions about stimulus absence in primate prefrontal cortex neurons. *Proc Natl Acad Sci U S A,* 109**,** 6289-94.

Meyrand, P., Simmers, J. & Moulins, M. 1994. Dynamic construction of a neural network from multiple pattern generators in the lobster stomatogastric nervous system. *J Neurosci,* 14**,** 630-44.

Miller, M. W., Rosen, S. C., Schissel, S. L., Cropper, E. C., Kupfermann, I. & Weiss, K. R. 1994. A population of SCP-containing neurons in the buccal ganglion of *Aplysia* are radula mechanoafferents and receive excitation of central origin. *J Neurosci,* 14**,** 7008-23.

Morgan, P. T., Jing, J., Vilim, F. S. & Weiss, K. R. 2002. Interneuronal and peptidergic control of motor pattern switching in *Aplysia*. *J Neurophysiol,* 87**,** 49-61.

Morton, D. W. & Chiel, H. J. 1993a. In vivo buccal nerve activity that distinguishes ingestion from rejection can be used to predict behavioral transitions in *Aplysia*. *J Comp Physiol A,* 172**,** 17-32.

Morton, D. W. & Chiel, H. J. 1993b. The timing of activity in motor neurons that produce radula movements distinguishes ingestion from rejection in *Aplysia*. *J Comp Physiol A,* 173**,** 519-36.

Murphy, A. D., Lukowiak, K. & Stell, W. K. 1985. Peptidergic modulation of patterned motor activity in identified neurons of *Helisoma*. *Proc Natl Acad Sci U S A,* 82**,** 7140-4.

Nagy, F. & Dickinson, P. S. 1983. Control of a central pattern generator by an identified modulatory interneurone in crustacea. I. Modulation of the pyloric motor output. *J Exp Biol,* 105**,** 33-58.

Nargeot, R., Baxter, D. A. & Byrne, J. H. 1999. In vitro analog of operant conditioning in aplysia. II. Modifications of the functional dynamics of an identified neuron contribute to motor pattern selection. *J Neurosci,* 19**,** 2261-72.

Nargeot, R., Baxter, D. A. & Byrne, J. H. 2002. Correlation between activity in neuron B52 and two features of fictive feeding in *Aplysia*. *Neurosci Lett,* 328**,** 85-8.

Nargeot, R., Le Bon-Jego, M. & Simmers, J. 2009. Cellular and network mechanisms of operant learning-induced compulsive behavior in *Aplysia*. *Curr Biol,* 19**,** 975-84.

Norekian, T. P. & Satterlie, R. A. 1996. Whole body withdrawal circuit and its involvement in the behavioral hierarchy of the mollusk *Clione limacina*. *J Neurophysiol,* 75**,** 529-37.

O'Gara, B. A. & Friesen, W. O. 1995. Termination of leech swimming activity by a previously identified swim trigger neuron. *J Comp Physiol A,* 177**,** 627-36.

Patel, B. A., Arundell, M., Allen, M. C., Gard, P., O'Hare, D., Parker, K. & Yeoman, M. S. 2006. Changes in the properties of the modulatory cerebral giant cells

contribute to aging in the feeding system of *Lymnaea*. *Neurobiol Aging,* 27**,** 1892-901.

Perrins, R., Walford, A. & Roberts, A. 2002. Sensory activation and role of inhibitory reticulospinal neurons that stop swimming in hatchling frog tadpoles. *J Neurosci,* 22**,** 4229-40.

Perry, S. J., Dobbins, A. C., Schofield, M. G., Piper, M. R. & Benjamin, P. R. 1999. Small cardioactive peptide gene: structure, expression and mass spectrometric analysis reveals a complex pattern of co-transmitters in a snail feeding neuron. *Eur J Neurosci,* 11**,** 655-62.

Perry, S. J., Straub, V. A., Kemenes, G., Santama, N., Worster, B. M., Burke, J. F. & Benjamin, P. R. 1998. Neural modulation of gut motility by myomodulin peptides and acetylcholine in the snail *Lymnaea*. *J Neurophysiol,* 79**,** 2460-74.

Plummer, M. R. & Kirk, M. D. 1990. Premotor neurons B51 and B52 in the buccal ganglia of *Aplysia californica*: synaptic connections, effects on ongoing motor rhythms, and peptide modulation. *J Neurophysiol,* 63**,** 539-58.

Proekt, A., Jing, J. & Weiss, K. R. 2007. Multiple contributions of an input-representing neuron to the dynamics of the *Aplysia* feeding network. *J Neurophysiol,* 97**,** 3046-56.

Romo, R., Hernandez, A. & Zainos, A. 2004. Neuronal correlates of a perceptual decision in ventral premotor cortex. *Neuron,* 41**,** 165-73.

Rose, R. M. & Benjamin, P. R. 1979. The relationship of the central motor pattern to the feeding cycle of *Lymnaea stagnalis*. *J Exp Biol,* 80**,** 137-163.

Rose, R. M. & Benjamin, P. R. 1981a. Interneuronal control of feeding in the pond snail *Lymnaea stagnalis*. I. Initiation of feeding cycles by a single buccal interneurone. *J Exp Biol,* 92**,** 187-201.

Rose, R. M. & Benjamin, P. R. 1981b. Interneuronal control of feeding in the pond snail *Lymnaea stagnalis*. II. The interneuronal mechanism generating feeding cycles. *J Exp Biol,* 92**,** 203-228.

Rosen, S. C., Miller, M. W., Evans, C. G., Cropper, E. C. & Kupfermann, I. 2000. Diverse synaptic connections between peptidergic radula mechanoafferent neurons and neurons in the feeding system of *Aplysia*. *J Neurophysiol,* 83**,** 1605-20.

Rosen, S. C., Teyke, T., Miller, M. W., Weiss, K. R. & Kupfermann, I. 1991. Identification and characterization of cerebral-to-buccal interneurons implicated in the control of motor programs associated with feeding in *Aplysia*. *J Neurosci,* 11**,** 3630-55.

Rosen, S. C., Weiss, K. R., Cohen, J. L. & Kupfermann, I. 1982. Interganglionic cerebral-buccal mechanoafferents of *Aplysia*: receptive fields and synaptic connections to different classes of neurons involved in feeding behavior. *J Neurophysiol,* 48**,** 271-88.

Runham, N. W. 1975. Alimentary canal. *In:* Fretter, V. & Peaks, J. (eds.) *Pulmonates.* London: Academic Press Inc.

Santama, N., Brierley, M., Burke, J. F. & Benjamin, P. R. 1994. Neural network controlling feeding in *Lymnaea stagnalis*: immunocytochemical localization of myomodulin, small cardioactive peptide, buccalin, and FMRFamide-related peptides. *J Comp Neurol,* 342**,** 352-65.

Sasaki, K., Cropper, E. C., Weiss, K. R. & Jing, J. 2013. Functional differentiation of a population of electrically coupled heterogeneous elements in a microcircuit. *J Neurosci,* 33**,** 93-105.

Shaw, B. K. & Kristan, W. B., JR. 1997. The neuronal basis of the behavioral choice between swimming and shortening in the leech: control is not selectively exercised at higher circuit levels. *J Neurosci,* 17**,** 786-95.

Shetreat-Klein, A. N. & Cropper, E. C. 2004. Afferent-induced changes in rhythmic motor programs in the feeding circuitry of *Aplysia*. *J Neurophysiol,* 92**,** 2312-22.

Shinkai, Y., Yamamoto, Y., Fujiwara, M., Tabata, T., Murayama, T., Hirotsu, T., Ikeda, D. D., Tsunozaki, M., Iino, Y., Bargmann, C. I., Katsura, I. & Ishihara, T. 2011. Behavioral choice between conflicting alternatives is regulated by a receptor guanylyl cyclase, GCY-28, and a receptor tyrosine kinase, SCD-2, in AIA interneurons of *Caenorhabditis elegans*. *J Neurosci,* 31**,** 3007-15.

Smith, D. A. 1988. Radular kinetics during grazing in *Helisoma trivolvis* (Gastropoda: Pulmonata). *J Exp Biol,* 136**,** 89-102.

Soffe, S. R. 1997. The pattern of sensory discharge can determine the motor response in young *Xenopus* tadpoles. *J Comp Physiol A,* 180**,** 711-5.

Staras, K. 1997. Neuronal mechanisms underlying appetitive learning in the pond snail *Lymnaea stagnalis.* DPhil, University of Sussex.

Staras, K., Kemenes, G. & Benjamin, P. R. 1998a. Neurophysiological correlates of unconditioned and conditioned feeding behavior in the pond snail *Lymnaea stagnalis*. *J Neurophysiol,* 79**,** 3030-40.

Staras, K., Kemenes, G. & Benjamin, P. R. 1998b. Pattern-generating role for motoneurons in a rhythmically active neuronal network. *J Neurosci,* 18**,** 3669-88.

Staras, K., Kemenes, I., Benjamin, P. R. & Kemenes, G. 2003. Loss of self-inhibition is a cellular mechanism for episodic rhythmic behavior. *Curr Biol,* 13**,** 116-24.

Stein, P. S. G. 1978. Motor systems, with specific reference to the control of locomotion. *Annu Rev Neurosci,* 1**,** 61-81.

Straub, V. A. & Benjamin, P. R. 2001. Extrinsic modulation and motor pattern generation in a feeding network: a cellular study. *J Neurosci,* 21**,** 1767-78.

Straub, V. A., Kemenes, I., O'Shea, M. & Benjamin, P. R. 2006. Associative memory stored by functional novel pathway rather than modifications of preexisting neuronal pathways. *J Neurosci,* 26**,** 4139-46.

Straub, V. A., Staras, K., Kemenes, G. & Benjamin, P. R. 2002. Endogenous and network properties of *Lymnaea* feeding central pattern generator interneurons. *J Neurophysiol,* 88**,** 1569-83.

Straub, V. A., Styles, B. J., Ireland, J. S., O'Shea, M. & Benjamin, P. R. 2004. Central localization of plasticity involved in appetitive conditioning in *Lymnaea*. *Learn Mem,* 11**,** 787-93.

Styles, B. J. 2004. Learning and sensory processing in a simple brain. DPhil, University of sussex.

Syed, N., Harrison, D. & Winlow, W. 1991. Respiratory behavior in the pond snail *Lymnaea stagnalis* I : behavioral analysis and the identification of motor neurons. *J. Comp Physiol,* 169**,** 541-555.

Syed, N. & Winlow, W. 1991a. Respiratory behavior in the pond snail *Lymnaea stagnalis* II: Neural elements of the central pattern generator (CPG). *J Comp Physiol,* 169**,** 557-568.

Syed, N. I. & Winlow, W. 1991b. Coordination of locomotor and cardiorespiratory networks of *Lymnaea stagnalis* by a pair of identified interneurones. *J Exp Biol,* 158**,** 37-62.

Taylor, A. L., Cottrell, G. W., Kleinfeld, D. & Kristan, W. B., JR. 2003. Imaging reveals synaptic targets of a swim-terminating neuron in the leech CNS. *J Neurosci,* 23**,** 11402-10.

Teyke, T., Rosen, S. C., Weiss, K. R. & Kupfermann, I. 1993. Dopaminergic neuron B20 generates rhythmic neuronal activity in the feeding motor circuitry of *Aplysia*. *Brain Res,* 630**,** 226-37.

Teyke, T., Weiss, K. R. & Kupfermann, I. 1990. Appetitive feeding behavior of *Aplysia*: behavioral and neural analysis of directed head turning. *J Neurosci,* 10**,** 3922-34.

Teyke, T., Xin, Y., Weiss, K. R. & Kupfermann, I. 1997. Ganglionic distribution of inputs and outputs of C-PR, a neuron involved in the generation of a food-induced arousal state in *Aplysia*. *Invert Neurosci,* 2**,** 235-44.

Tuersley, M. D. 1989. How is food arousal manifested in the pond snail *Lymnaea stagnalis*?: An overview. *J Moll Stud,* 55**,** 209-216.

Tuersley, M. D. & McCrohan, C. R. 1987. Food arousal in the pond snail, *Lymnaea stagnalis*. *Behav Neural Biol,* 48**,** 222-36.

Vavoulis, D. V., Straub, V. A., Kemenes, I., Kemenes, G., Feng, J. & Benjamin, P. R. 2007. Dynamic control of a central pattern generator circuit: a computational model of the snail feeding network. *Eur J Neurosci,* 25**,** 2805-18.

Vehovszky, A. & Elliott, C. J. 1995. The hybrid modulatory/pattern generating N1L interneuron in the buccal feeding system of *Lymnaea* is cholinergic. *Invert Neurosci,* 1**,** 67-74.

Vehovszky, A. & Elliott, C. J. 2001. Activation and reconfiguration of fictive feeding by the octopamine-containing modulatory OC interneurons in the snail *Lymnaea*. *J Neurophysiol,* 86**,** 792-808.

Vehovszky, A. & Elliott, C. J. 2002. Heterosynaptic modulation by the octopaminergic OC interneurons increases the synaptic outputs of protraction phase interneurons (SO, N1L) in the feeding system of *Lymnaea stagnalis*. *Neuroscience,* 115**,** 483-94.

Vehovszky, A., Elliott, C. J., Voronezhskaya, E. E., Hiripi, L. & Elekes, K. 1998. Octopamine: a new feeding modulator in *Lymnaea*. *Philos Trans R Soc Lond B Biol Sci,* 353**,** 1631-1643.

Vehovszky, A., Hiripi, L. & Elliott, C. J. 2000. Octopamine is the synaptic transmitter between identified neurons in the buccal feeding network of the pond snail *Lymnaea stagnalis*. *Brain Res,* 867**,** 188-99.

Vehovszky, A., Szabo, H. & Elliott, C. J. 2004. Octopamine-containing (OC) interneurons enhance central pattern generator activity in sucrose-induced feeding in the snail *Lymnaea*. *J Comp Physiol A,* 190**,** 837-46.

Warman, E. N. & Chiel, H. J. 1995. A new technique for chronic single-unit extracellular recording in freely behaving animals using pipette electrodes. *J Neurosci Methods,* 57**,** 161-9.

Wentzell, M. M., Martinez-Rubio, C., Miller, M. W. & Murphy, A. D. 2009. Comparative neurobiology of feeding in the opisthobranch sea slug, Aplysia, and the pulmonate snail, *Helisoma*: evolutionary considerations. *Brain Behav Evol,* 74**,** 219-30.

Yang, C. H., Belawat, P., Hafen, E., Jan, L. Y. & Jan, Y. N. 2008. *Drosophila* egg-laying site selection as a system to study simple decision-making processes. *Science,* 319**,** 1679-83.

Yeoman, M. S., Brierley, M. J. & Benjamin, P. R. 1996. Central pattern generator interneurons are targets for the modulatory serotonergic cerebral giant cells in the feeding system of *Lymnaea*. *J Neurophysiol,* 75**,** 11-25.

Yeoman, M. S., Kemenes, G., Benjamin, P. R. & Elliott, C. J. 1994a. Modulatory role for the serotonergic cerebral giant cells in the feeding system of the snail, *Lymnaea*. II. Photoinactivation. *J Neurophysiol,* 72**,** 1372-82.

Yeoman, M. S., Parish, D. C. & Benjamin, P. R. 1993. A cholinergic modulatory interneuron in the feeding system of the snail, *Lymnaea*. *J Neurophysiol,* 70**,** 37-50.

Yeoman, M. S., Pieneman, A. W., Ferguson, G. P., Ter Maat, A. & Benjamin, P. R. 1994b. Modulatory role for the serotonergic cerebral giant cells in the feeding system of the snail, *Lymnaea*. I. Fine wire recording in the intact animal and pharmacology. *J Neurophysiol,* 72**,** 1357-71.

Yeoman, M. S., Vehovszky, A., Kemenes, G., Elliott, C. J. & Benjamin, P. R. 1995. Novel interneuron having hybrid modulatory-central pattern generator properties in the feeding system of the snail, *Lymnaea stagnalis*. *J Neurophysiol,* 73**,** 112-24.